

# CIVIL ENGINEERING STUDIES

STRUCTURAL RESEARCH SERIES NO. 417

Illinois Cooperative Highway Research Program

Series No. 157



10  
I29A  
157

## TIME-DEPENDENT PRESTRESS LOSSES IN PRETENSIONED CONCRETE CONSTRUCTION

By

H. D. HERNANDEZ

W. L. GAMBLE

Issued as a Documentation Report on  
The Field Investigation of Prestressed  
Reinforced Concrete Highway Bridges

Project IHR-93

Phase 1

Illinois Cooperative Highway Research Program

Conducted by

THE STRUCTURAL RESEARCH LABORATORY  
DEPARTMENT OF CIVIL ENGINEERING  
ENGINEERING EXPERIMENT STATION  
UNIVERSITY OF ILLINOIS AT URBANA-CHAMPAIGN

in cooperation with the

STATE OF ILLINOIS  
DEPARTMENT OF TRANSPORTATION

and the

U.S. DEPARTMENT OF TRANSPORTATION  
FEDERAL HIGHWAY ADMINISTRATION

UNIVERSITY OF ILLINOIS  
AT URBANA-CHAMPAIGN  
URBANA, ILLINOIS

MAY 1975



1. Report No. UILU-ENG-75-2005		2. Government Accession No.		3. Recipient's Catalog No.	
4. Title and Subtitle Time-Dependent Prestress Losses in Pretensioned Concrete Construction				5. Report Date May 1975	
				6. Performing Organization Code	
7. Author(s) H. D. Hernandez and W. L. Gamble				8. Performing Organization Report No. SRS No. 417 ICHRP No. 157	
9. Performing Organization Name and Address Department of Civil Engineering University of Illinois 2209 Civil Engineering Building Urbana, Illinois 61801				10. Work Unit No.	
				11. Contract or Grant No. IHR-93	
12. Sponsoring Agency Name and Address Illinois Department of Transportation 2300 South Dirksen Parkway Springfield, Illinois 62764				13. Type of Report and Period Covered Interim Progress	
				14. Sponsoring Agency Code	
15. Supplementary Notes Prepared in Cooperation with the U. S. Department of Transportation, Federal Highway Administration					
16. Abstract <p>Theoretical time-dependent deformations and prestress losses in pretensioned, prestressed simply supported concrete girders, based on the revised rate of creep method, are presented. The effects of age of precast girders at the time of casting of the deck concrete, time of transfer of prestress, deck dead load, type of prestressing strands (stress-relieved or low-relaxation strands), initial level of stress in the concrete, and the effects of varying environmental conditions on the behavior of concrete structures are studied.</p> <p>Predicted unit creep and shrinkage strains versus time relationships are based on the 1970 C.E.B. recommendations and relaxation losses for stress-relieved strands are estimated using the expressions developed by Magura, Sozen, and Siess. A similar expression is used for the case of low-relaxation strands.</p> <p>Predicted deformations are compared with long-term measurements made on full-sized bridge structures located in Illinois. Annual cyclic variations of the total strains and total prestress force occur in all structures located outdoors.</p> <p>Two recommended sets of factors for the estimation of prestress losses are given, one for the case of stress-relieved strands and the other for the case of low-relaxation strands.</p>					
17. Key Words Prestressed concrete, Prestress losses, creep, shrinkage, relaxation of steel, bridges, composite beams, long-term behavior, computer simulation				18. Distribution Statement Release Unlimited	
19. Security Classif. (of this report) Unclassified		20. Security Classif. (of this page) Unclassified		21. No. of Pages 171	22. Price



## ACKNOWLEDGMENTS

This report was prepared as a part of the Illinois Cooperative Highway Research Program, Project IHR-93, "Field Investigation of Prestressed Reinforced Concrete Highway Bridges," by the Department of Civil Engineering, in the Engineering Experiment Station, University of Illinois at Urbana-Champaign, in cooperation with the Illinois Department of Transportation and the U. S. Department of Transportation, Federal Highway Administration.

The contents of this report reflect the views of the authors who are responsible for the facts and the accuracy of the data presented herein. The contents do not necessarily reflect the official views or policies of the Illinois Department of Transportation or the Federal Highway Administration. This report does not constitute a standard, specification, or regulation.



## TABLE OF CONTENTS

Chapter		Page
1	INTRODUCTION . . . . .	1
	1.1 General Remarks . . . . .	1
	1.2 Object and Scope of Investigation . . . . .	1
2	METHOD OF ANALYSIS . . . . .	3
	2.1 Introduction . . . . .	3
	2.2 Revised Rate of Creep Method . . . . .	4
	2.3 Prediction of Creep and Shrinkage Values According to European Con- crete Committee (C.E.B.) Recommendations . . . . .	10
	2.4 Stress Relaxation in Prestressing Steel . . . . .	14
	2.5 Basic Assumptions. . . . .	17
3	PRESENTATION AND DISCUSSION OF FACTORS AFFECTING PRESTRESS LOSSES . . . . .	20
	3.1 Introduction . . . . .	20
	3.2 Effect of Time of Releasing of Prestress . . . . .	22
	3.3 Effect of Age of Precast Girders at the Time of Casting of the Deck Concrete . . . . .	26
	3.4 Effect of Type of Prestressing Strands. . . . .	29
	3.5 Effect of Initial Stresses in Concrete. . . . .	34
	3.6 Effect of Deck Dead Load . . . . .	38
	3.7 Effect of Storage Conditions . . . . .	39
	3.8 Comparison of Measured and Computed Results . . . . .	43
4	FACTORS FOR THE ESTIMATION OF PRESTRESS LOSSES. . . . .	54
	4.1 Introduction . . . . .	54
	4.2 Proposed Set of Loss Factors . . . . .	57
	4.3 Discussion of the Set of Loss Factors . . . . .	63
5	COMPARISON OF PROPOSED SET OF FACTORS WITH OTHER PREDICTION METHODS . . . . .	67
6	CONCLUSIONS AND RECOMMENDATIONS. . . . .	72
7	SUMMARY. . . . .	77
	LIST OF REFERENCES . . . . .	79





APPENDIX

A	PRESTRESSED CONCRETE GIRDERS SELECTED IN THE STUDY . . . . .	163
B	NOTATION . . . . .	168



## LIST OF TABLES

Table		Page
3.1	Deck Section Properties Used in the Analysis . . . . .	81
3.2	Chronology of Girder Construction, Champaign County Bridge . . . . .	82
3.3	Bridge Construction and Locations of Girders at Various Time, Champaign County Bridge . . . . .	82
4.1	Prestress Losses Due to Shrinkage of the Concrete, 1973 AASHO Standard Specifications . . . . .	83
4.2	Prestress Losses Due to Shrinkage of the Concrete, 1973 Proposed Revision to the AASHO Standard Specifications, Section 1.6.7(B). . . . .	83
4.3	Prestress Losses Due to Shrinkage of the Concrete, Proposed Shrinkage Loss Value. . . . .	84
4.4	Summary of Loss Factors for the Estimation of Prestress Losses . . . . .	85
5.1	Comparison of Theoretical and Estimated Prestress Losses, Stress-Relieved Strands . . . . .	86
5.2	Comparison of Theoretical and Estimated Prestress Losses, Low-Relaxation Strands. . . . .	87



## LIST OF FIGURES

Figure		Page
2.1	European Concrete Committee Creep Prediction Factor Coefficient $K_c$ vs. Relative Humidity . . . . .	88
2.2	European Concrete Committee Creep Prediction Factor Coefficient $K_d$ vs. Age at Loading . . . . .	88
2.3	European Concrete Committee Creep Prediction Factor Coefficient $K_b$ vs. Mix Properties . . . . .	89
2.4	European Concrete Committee Creep Prediction Factor Coefficient $K_e$ vs. Theoretical Thickness. . . . .	89
2.5	European Concrete Committee Creep Prediction Factor Coefficient $K_t$ vs. Time . . . . .	90
2.6	European Concrete Committee Shrinkage Prediction Factor Coefficient $\epsilon_c$ vs. Relative Humidity . . . . .	90
2.7	European Concrete Committee Shrinkage Prediction Factor Coefficient $K_e$ vs. Theoretical Thickness . . . . .	91
2.8	Relaxation Loss When Including Stress Reduction at Time $t$ . . . . .	91
3.1	Effect of Time of Transfer of Prestress on Total Prestress Losses and Relaxation Losses, AASHO-III Beam, Stress-Relieved Strands, $f_{si} = 189$ ksi. . . . .	92
3.2	Effect of Time of Transfer of Prestress on Total Prestress Losses and Relaxation Losses, AASHO-III Beam, Low-Relaxation Strands, $f_{si} = 205$ ksi. . . . .	93
3.3	Effect of Time of Transfer of Prestress on Total Prestress Losses and Relaxation Losses, AASHO-III Beam, Low-Relaxation Strands, $f_{si} = 189$ ksi. . . . .	94

	Page
3.4 Elastic Plus Creep Strain Versus Time Under Reducing Stress Conditions . . . . .	95
3.5 Effect of Age of Girders at the Time of Casting of Deck on Total Prestress Losses and Relaxation Losses, AASHO-III Beam . . . . .	96
3.6 Pure Relaxation of Steel Stress . . . . .	97
3.7 Effect of Type of Prestressing Strand on Total Prestress Losses, Relaxation Losses and Creep Losses, AASHO-III Beam. . . . .	98
3.8 Effect of Steel Yield Stress on Pure Relaxation Losses, $f_{si} = 189$ ksi . . . . .	100
3.9 Effect of Steel Yield Stress on Total Prestress Losses, Relaxation Losses and Creep Losses, AASHO-III Beam, Stress-Relieved Strands, $f_{si} = 189$ ksi . . . . .	101
3.10 Effect of Steel Yield Stress on the Components of Prestress Losses, AASHO-III Beam, Stress-Relieved Strands, $f_{si} = 189$ ksi . . . . .	103
3.11 Effect of Initial Stresses in Concrete on Total Prestress Losses and Relaxation Losses, Prestressed Concrete Cylinder . . . . .	104
3.12 Effect of Initial Stresses in Concrete on Total Prestress Losses and Relaxation Losses, AASHO-III Beam, Stress-Relieved Strands . . . . .	105
3.13 Effect of Initial Stresses in Concrete on Total Prestress Losses and Relaxation Losses, Single-Tee Beam, Stress-Relieved Strands. . . . .	106
3.14 Effect of Initial Stresses in Concrete on Total Prestress Losses and Relaxation Losses, Single-Tee Beam, Low-Relaxation Strands . . . . .	107
3.15 Relaxation Losses as Affected by the Creep and Shrinkage Losses . . . . .	108
3.16 Relaxation Losses as Affected by the Elastic Loss of Stress at Transfer . . . . .	109

	Page
3.17 Creep Losses as Affected by Concrete Stress at the Level of the Steel at Transfer . . . . .	110
3.18 Creep Versus Time Under Reducing Stress Condition at 90 Days, European Concrete Committee Creep-Time Relationships. . . . .	111
3.19 Effect of Deck Dead Load on Total Prestress Losses and Relaxation Losses, AASHO-III Beam . . . . .	112
3.20 Effect of Deck Dead Load on Total Prestress Losses and Relaxation Losses, Single-Tee Beam . . . . .	113
3.21 Effect of Concrete Stress Reduction at the Level of Steel on Total Prestress Losses. . . . .	114
3.22 Effect of Relative Humidity on Total Prestress Losses and Relaxation Losses, AASHO-III Beam . . . . .	115
3.23 Measured Creep Strains of Douglas County Bridge Girder Concrete Under Field Conditions and Predicted Creep Strains from European Concrete Committee Method. . . . .	116
3.24 Measured Creep Strains of the Beam Concrete Under Laboratory Storage Conditions, Douglas County Bridge. . . . .	117
3.25 Measured Creep Strains of Douglas County Bridge Deck Concrete and Predicted Creep Strains from European Concrete Committee Method . . . . .	118
3.26 Measured Shrinkage Strains of Douglas County Bridge Girder Concrete Under Field Conditions and Predicted Shrinkage Strains from European Concrete Committee Method . . . . .	119
3.27 Measured Shrinkage Strains of the Beam Concrete Under Laboratory Storage Condition, Douglas County Bridge . . . . .	120
3.28 Measured Shrinkage Strains of Douglas County Bridge Deck Concrete and Predicted Shrinkage Strains from European Concrete Committee Method . . . . .	121

	Page	
3.29	Creep of the Beam Concrete Under Field Storage Conditions, Champaign County Bridge . . . . .	122
3.30	Creep of the Beam Concrete Under Laboratory Storage Conditions, Champaign County Bridge. . . . .	123
3.31	Shrinkage of the Beam Concrete Under Field Conditions, Champaign County Bridge . . . . .	124
3.32	Shrinkage of the Beam Concrete Under Laboratory Storage Conditions, Champaign County Bridge . . . . .	125
3.33	Creep of the Deck Concrete Under Field and Laboratory Storage Conditions, Champaign County Bridge . . . . .	126
3.34	Shrinkage of the Deck Concrete Under Field and Laboratory Conditions, Champaign County Bridge . . . . .	127
3.35	Comparisons of Calculated Total Prestress Losses and Relaxation Losses Using the Douglas County Field Values and the C.E.B. Values, AASHO-III Beam. . . . .	128
3.36	Comparisons of Calculated Total Prestress Losses and Relaxation Losses Using the Douglas County Laboratory Values and the 50 Percent Relative Humidity C.E.B. Values, AASHO-III Beam . . . . .	129
3.37	Comparison of Calculated Total Prestress Losses and Relaxation Losses Using the Champaign County Field Values and the C.E.B. Values. . . . .	130
3.38	Comparisons of Calculated Total Prestress Losses and Relaxation Losses Using the Champaign County Laboratory Values and the 50 Percent Relative Humidity C.E.B. Values . . . . .	131
3.39	Measured and Calculated Total Strains at Midspan vs. Time, Beam BX-3, Douglas County Bridge, Values Computed Using Field Creep and Shrinkage Values . . . . .	132



	Page
3.40 Measured and Calculated Total Strains at Midspan vs. Time, Beam BX-3, Douglas County Bridge, Values Computed Using Lower Bound Laboratory Creep and Shrinkage Values . . . . .	133
3.41 Measured and Calculated Total Strains at Midspan vs. Time, Beam BX-3, Douglas County Bridge, Values Computed Using C.E.B. 50 Percent R.H. Creep and Shrinkage Values . . . . .	134
3.42 Measured and Calculated Total Strains at Midspan vs. Time, Beam BX-3, Douglas County Bridge, Values Computed Using C.E.B. 80 Percent Creep and Shrinkage Values. . . . .	135
3.43 Measured and Calculated Total Strains at Midspan vs. Time, Beam BX-3, Douglas County Bridge, Values Computed Using C.E.B. Values for 50 Percent R.H. Creep and 80 Percent R.H. Shrinkage. . . . .	136
3.44 Calculated Prestressing Force at Midspan vs. Time, Beam BX-3, Douglas County Bridge . . . . .	137
3.45 Measured Total Strains at Midspan of Beam BX-1 and Calculated Total Strains at Midspan of Simply Supported Beam vs. Time, Jefferson County Bridge, Values Computed Using C.E.B. Values for 50 Percent R.H. Creep and 80 Percent R.H. Shrinkage. . . . .	138
3.46 Calculated Total Prestress Loss vs. Time, Beam BX-1, Jefferson County Bridge . . . . .	139
3.47 Plan of Bridge Showing Girder and Diaphragm Placement, Champaign County Bridge . . . . .	140
3.48 Locations of Beam Supports at Various Times, Champaign County Bridge. . . . .	141
3.49 Details of Girders, Champaign County Bridge . . . . .	142
3.50 Elevation of Bridge, Champaign County Bridge. . . . .	143
3.51 Girder Cross Section, Champaign County Bridge . . . . .	144

	Page
3.52 Measured and Calculated Total Strains at Midspan vs. Time, Beam BX-6, Champaign County Bridge, Values Computed Using Field Creep and Shrinkage Values . . . . .	145
3.53 Measured and Calculated Total Strains at Midspan vs. Time, Beam BX-6, Champaign County Bridge, Values Computed Using C.E.B. 50 Percent R.H. Creep and 80 Percent R.H. Shrinkage Values . . . . .	146
3.54 Calculated Prestressing Force vs. Time, Beam BX-6, Champaign County Bridge . . . . .	147
4.1 Prestress Loss Due to Shrinkage of the Concrete as a Function of the Relative Humidity in the Field and Theoretical Thickness of the Member . . . . .	148
4.2 Creep Factor as a Function of the Relative Humidity in the Field and Time of Release of Prestress. . . . .	148
4.3 Creep Factor as a Function of the Relative Humidity in the Field. . . . .	149
4.4 Creep Factor as a Function of the Time of Release of Prestress . . . . .	149
4.5 Prestress Losses Due to Shrinkage of the Concrete Estimated According to Several Proposed Shrinkage Loss Values. . . . .	150
5.1a Comparison of Total Prestress Losses Calculated Using the Proposed Set of Loss Factors and the Theoretical Values. . . . .	151
5.1b Comparison of Total Prestress Losses Calculated Using the 1973 AASHTO Proposal and the Theoretical Values . . . . .	152
5.1c Comparison of Total Prestress Losses Calculated Using the 1970 AASHTO Interim Specifications and the Theoretical Values . . . . .	153
5.2a Comparison of Creep Losses Calculated Using the Proposed Set of Loss Factors and the Theoretical Values. . . . .	154

	Page	
5.2b	Comparison of the Creep Losses Calculated Using the 1973 AASHO Proposal and the Theoretical Values . . . . .	155
5.2c	Comparison of Creep Losses Calculated Using the 1970 AASHO Interim Specifications and the Theoretical Values. . . . .	156
5.3a	Comparison of Relaxation Losses Calculated Using the Proposed Set of Loss Factors and the Theoretical Values. . . . .	157
5.3b	Comparison of Relaxation Losses Calculated Using the 1973 AASHO Proposal and the Theoretical Values . . . . .	158
5.3c	Comparison of Relaxation Losses Calculated Using the 1970 AASHO Interim Specifications and the Theoretical Values . . . . .	159
5.4	Comparison of Total Prestress Losses Calculated Using the Proposed Set of Loss Factors and the Theoretical Values, Low-Relaxation Strands. . . . .	160
5.5	Comparison of Creep Losses Calculated Using the Proposed Set of Loss Factors and the Theoretical Values, Low-Relaxation Strands . . . . .	161
5.6	Comparison of Relaxation Losses Calculated Using the Proposed Set of Loss Factors and the Theoretical Values, Low-Relaxation Strands. . . . .	162
A.1	AASHO-Type III Section. . . . .	164
A.2	Single-Tee Section--8ST28. . . . .	165
A.3	Double-Tee Section--8DT24B . . . . .	165
A.4	Illinois Standard Cross Section for Precast Prestressed Concrete I-Beams, 42 and 48 in. Depths . . . . .	166
A.5	Illinois Standard 54 in.-I Beam. . . . .	167



## 1. INTRODUCTION

### 1.1 General Remarks

Prestressed concrete members undergo time-dependent deformations as a result of creep and shrinkage of the concrete and relaxation of the prestressing reinforcement. The rates of creep and shrinkage and of relaxation of the prestressing steel are greatest during the early ages, and decrease continuously with time (when under constant environmental conditions). The rate of long-time deformations of members also diminishes with time, but measurable deformations may occur for many years.

During the past several years, there has been considerable renewed interest in the amount of prestress losses which occur during the lifetime of prestressed concrete structures (11,14,22). As a result, some long-term investigations of the behavior of prestressed concrete bridges have been carried out under field conditions where the varying environment is an important factor affecting the behavior of the structure (10,13). Now that some experience has been gained, under both laboratory and field conditions, the next step is to use this experience by incorporating it in finding a new set of factors for the prediction of prestress losses, recognizing the complex interrelationships which exist between shrinkage, creep, relaxation of the prestressing steel, and elastic losses at release.

### 1.2 Object and Scope of Investigation

The main purpose of this investigation is to provide a better understanding of the time-dependent prestress losses in composite and

noncomposite pretensioned, prestressed concrete bridges under sustained loads and which are subjected to either fluctuating temperature and humidity under field conditions or constant environmental storage conditions.

The scope of this study is:

1. Analytical study of the time-dependent prestress losses.
2. To develop simple expressions for the prediction of prestress losses in prestressed concrete structures.

The analytical study includes:

1. A reexamination of the revised rate of creep method as a method of analysis for the prediction of time-dependent deflections, stresses, strains, curvatures, and prestress losses. The method of analysis is treated as a step by step numerical procedure which takes into account all the variables having influence on the long-time deformations and prestress losses.

The major variables investigated in this study were: age of precast girders at the time of casting of the deck concrete, time of transfer of prestress, deck dead load, type of prestressing strands (stress-relieved strands and low-relaxation strands), level of prestress, and the effects of varying environmental conditions on the behavior of concrete structures.

## 2. METHOD OF ANALYSIS

### 2.1 Introduction

The prestress force applied to prestressed concrete beams continuously decreases during the lifetime of the structure. Immediately after release of the strands, the initial prestress force decreases due to the elastic shortening of the concrete at the level of the steel. From then on, it continues to decrease due to the combined effects of creep and shrinkage strains of the concrete and relaxation of the steel.

Different methods have been developed for the estimation of the time-dependent deformations of concrete (9,17,21). Among them, the rate of creep and the superposition methods are the most widely recognized methods for calculating creep strains under variable stress in concrete structures. In a previous study, Mossiosian and Gamble (17) came to the conclusion that the rate of creep method gives good results as long as changes in stresses are small but when major changes in stresses occur, such as those taking place at the time of casting of the deck, the revised rate of creep method seems to be the most suitable method of analysis for predicting time-dependent deformations of prestressed concrete structures subjected to different environmental conditions.

They also came to the conclusion that the final prestress losses in simply supported and continuous composite structures were comparable; i.e., that the effects of continuity on prestress losses are not of great importance and in most cases they can be safely neglected.

In this investigation, the method of analysis chosen is the

revised rate of creep method. Prestress losses are calculated for simply supported beams.

## 2.2 Revised Rate of Creep Method

The revised rate of creep method is essentially a small modification of the rate of creep method, made by Mossiosian and Gamble (17), which tries to eliminate part of the errors inherent in the rate of creep method.

Some of the deficiencies of the rate of creep method come from the fact that the method assumes that the concrete at a given stress will creep at the same rate, regardless of previous increases or reductions of stress, i.e., that the rate of creep is independent of the stress history of the member. In addition, the method cannot predict creep recovery after complete removal of stress. The result of these problems is that the rate of creep method overestimates creep strains under decreasing concrete stress and underestimates creep strains under increasing concrete stress conditions.

The difference between the rate of creep and revised rate of creep methods comes in the analysis of a prestressed concrete structure at the time of casting of the deck concrete, a time at which substantial changes occur in the concrete stresses over the depth of the cross section of the member, throughout the length of the girder. Part of the theoretical deficiencies involved in the use of the rate of creep method are diminished if a new beam unit creep versus time relationship is used, specifically for beam concrete loaded at the time of casting of the deck, for the estimation of the creep strains in the precast girder due to the deck dead load.



The revised rate of creep method, like the rate of creep method, makes use of known relationships for the time-dependent shrinkage and creep strains under constant stress for predicting strains and curvatures under variable stress. The method as applied to prestressed concrete beams also takes into account changes in stress due to relaxation of the prestressing steel.

In this study, the revised rate of creep method is treated as a step by step numerical procedure which converts these known relationships into steps functions having constants values over short time intervals. During each time interval, a numerical integration is carried out taking into account all factors having an influence on the long-time deformations and on the prestress losses. Because the rate of creep and shrinkage of the concrete and relaxation of the steel are greatest during the early ages, time intervals should be taken smaller at early ages and bigger at later ages. Also, if major changes occur in the concrete stresses at certain time, time intervals should be taken smaller immediately after that time in order to better observe the effects of the stress changes.

The computer program used in the analysis of prestress losses is basically the one developed by Mossiosian and Gamble (17). However, it was necessary to make some changes because the program contained an error in the method of taking into account the elastic recovery of the concrete, with the result that equilibrium between tension in the steel and compression in the concrete did not quite exist, particularly after casting of the deck concrete. In addition, the changes in stress due to relaxation of the prestressing steel were taking into account in the updated program.

The numerical integration, starting at the time of pulling of the strands up to the time just before casting of the deck, can be carried out in the following steps:

1. Compute the prestress losses due to relaxation of the steel taking place between the time of pulling of the strands and the time their force is transferred to the concrete.
2. Compute the prestress losses taking place immediately after transfer of prestress due to the elastic shortening of the concrete at the level of the steel.
3. Compute total stresses and strains in the concrete immediately after release of prestress, including those due to dead load forces.

For the first and each later time interval:

4. Compute incremental creep and shrinkage strains at the level of the steel due to stresses caused by prestressing force and girder dead load, assuming constant stress during each time interval.
5. Compute prestress losses due to creep and shrinkage of the concrete as the product of the change of concrete strain at the level of the steel found in step 4 times the modulus of elasticity of the steel.
6. Compute prestress losses due to relaxation of the steel, assuming constant strain during each time interval.
7. Compute the total change in prestress losses by adding the prestress losses due to creep and shrinkage of the concrete found in step 5 to the prestress losses due to relaxation of the steel found in step 6.

8. Compute the elastic change of concrete stress by considering the total change of prestress losses found in step 7 as a load equal to the stress found in step 7 multiplied by the steel area applied at the center of gravity of the steel.
9. Compute the elastic change in strain by dividing the elastic change of stress found in step 8 by the modulus of elasticity of the concrete. This change is often termed elastic recovery.
10. Compute the net change in strain by subtracting the elastic change in strain found in step 9 from the incremental creep and shrinkage strains found in step 4.
11. Compute the total strains at the end of time interval by adding, with due regard for signs, the net change in strains found in step 10 to the total strains corresponding to the beginning of time interval.
12. Compute the total stresses at the end of time interval by subtracting the elastic change of stress found in step 8 from the total stresses existing at the beginning of time interval.
13. Consider next time interval and proceed as before, beginning from step 4.

When casting of the deck concrete takes place, major changes in concrete stresses occur. Deformations and prestress changes due to deck dead load and due to concrete stress changes due to creep, shrinkage, differential shrinkage, differential creep, differential curvature, and relaxation of the steel which take place after casting of the deck are computed by using

a new unit curve for beam concrete loaded at the time of casting of the deck. Additional deformations and prestress changes due to the prestressing force existing immediately before casting of the deck and due to girder dead load are still calculated by considering the original unit creep curve for beam concrete loaded at the time of transfer of prestress.

The numerical integration after casting of the deck concrete is carried out in a way similar to that before casting, but the effects of composite action are also considered. The shearing forces and moments at the interface of the slab and girder concrete due to differential shrinkage, differential creep, and differential curvature between the slab and girder concrete, in addition to the direct effects of creep and shrinkage of the girder concrete and steel relaxation, all affect deformations and stresses in the precast beam.

The numerical procedure continues as follows:

14. Compute the elastic prestress loss (or gain) occurring due to casting of the deck.
15. Compute total stresses, total strains, and change in elastic strains immediately after casting of the deck.

For the first time interval after casting of the deck and each later interval:

16. Compute incremental creep and shrinkage strains of the slab and beam concretes due to prestressing force, girder dead load, and deck dead load. For the later time intervals, the stresses caused by differential creep and shrinkage are also included.

17. Compute differential shrinkage strains between the bottom of the slab concrete and top of beam concrete.
18. Compute stresses in the beam and slab due to differential shrinkage strain. (Restore compatibility.)
19. Compute change in steel stresses due to differential shrinkage strain.
20. Adjust concrete stresses due to change in steel stress found in step 19. The change in steel force is applied to the composite section.
21. Compute change in elastic strain due to differential shrinkage strain by dividing the adjusted concrete stress found in step 20 by the modulus of elasticity of the concrete.
22. Compute the differential creep strain and differential creep curvature between the top of the beam concrete and bottom of the slab concrete.
23. Compute changes in concrete stresses due to differential creep strain and differential creep curvature found in step 22. (Restore compatibility.)
24. Compute change in steel stress due to differential creep strain and differential creep curvature found in step 22.
25. Compute the prestress losses due to relaxation of the steel.
26. Adjust concrete stresses due to change in steel stress found in steps 24 and 25. The changes in steel stress are applied to the composite section.

27. Compute the change in elastic strains due to differential creep strain, differential creep curvature and relaxation of the steel by dividing the adjusted concrete stresses found in step 26 by the modulus of elasticity of the concrete.
28. Compute the total change in prestress loss due to creep and shrinkage of the concrete, differential shrinkage strain, differential creep strain, differential creep curvature, and relaxation of the steel.
29. Compute the total concrete stresses at the end of time interval by subtracting the changes in concrete stresses found in steps 20 and 26 from the total concrete stresses existing at the beginning of time interval.
30. Compute the total strains at the end of time interval by adding the changes in strains found in steps 16, 21 and 27 to the total strains existing at the beginning of time interval.
31. Consider next time interval and proceed as before, beginning from step 16.

Once the strains and curvatures have been found, deflections and slopes of the beam are easily found.

### 2.3 Prediction of Creep and Shrinkage Values According to European Concrete Committee (C.E.B.) Recommendations

In all methods of analysis for the prediction of long-time deformations, stresses, strains and prestress losses, it is assumed that the unit creep strain, shrinkage strain, and relaxation of the steel versus time relationships are known.

Mossiossian and Gamble (17) studied the behavior of the Douglas County Bridge beam and deck concrete specimens stored under different environmental conditions. Some of the concrete specimens were stored in a humidity control room where the relative humidity (R.H.) and temperature were maintained at 50 percent and 70°F, respectively. The rest of the concrete specimens were left with the beams and consequently were subjected to the same environmental conditions as the precast beams. Comparisons were made between the creep and shrinkage values recorded in the lab and in the field and the creep and shrinkage values predicted making use of the C.E.B. recommendations. The authors concluded that a fair estimate of final creep and shrinkage values can be made by making use of the C.E.B. recommendations. For field specimens, the higher and lower bounds of the expected creep values can be obtained by using lower and higher monthly average values of the relative humidity and maximum and minimum annual values of the temperature in the field. The expected final shrinkage values can be obtained by assuming the specimens are stored at a constant relative humidity equal to the average annual relative humidity in the field.

In this investigation, prediction of the unit creep and shrinkage strains versus time relationships are based on the 1970 C.E.B. recommendations (8). The notation used here is that of the C.E.B.

According to the C.E.B. recommendations, Section R 12.31, creep of concrete under service loads is predicted in terms of a set of factors depending on the relative humidity of storage, composition of the concrete mix, age of the concrete at the time of loading, size and shape of the cross section of the member, and time after loading.

Creep of the concrete is estimated as:

$$\varepsilon_{cr}(t) = \frac{\sigma_{co}}{E_{co}} \phi_t \quad (2.1)$$

or

$$\varepsilon_{cr}(t) = \varepsilon_{co} \phi_t \quad (2.2)$$

where:

$E_{co}$  = secant modulus of the concrete at the age of 28 days,

$\sigma_{co}$  = constant stress the concrete is subjected to,

$\varepsilon_{co}$  = initial elastic strain of the concrete, equal to  $\frac{\sigma_{co}}{E_{co}}$ , and

$\phi_t$  = creep coefficient expressed as a function of five factors as follows:

$$\phi_t = K_c K_d K_b K_e K_t$$

where:

$K_c$  = creep factor as a function of the relative humidity of storage at a temperature of 20°C (see Fig. 2.1),

$K_d$  = creep factor as a function of the age of the concrete at the time of loading at 20°C (see Fig. 2.2),

$K_b$  = creep factor as a function of the composition of the concrete mix (see Fig. 2.3),

$K_e$  = creep factor as a function of the theoretical thickness of the cross section of the member,  $d_m$  (see Fig. 2.4), and



$K_t$  = time-strain relationship depending on the theoretical thickness of the cross section of the member (see Fig. 2.5).

If the hardening of the concrete prior to loading takes place at a temperature other than 20°C, the equivalent age of concrete at time of loading should be changed by the corresponding degree of hardening as follows:

$$D = \sum \Delta t (T + 10^\circ)$$

where:

$D$  = degree of hardening of the concrete at the moment of loading, an equivalent age in days,

$\Delta t$  = number of days during which hardening has taken place at  $T^\circ \text{C}$ .

$D$  is plotted along the lower edge of Fig. 2.2.

The effect of size and shape of the member on the creep and shrinkage of the concrete has been considered in terms of a theoretical thickness of the cross section of the member,  $d_m$ , which is computed as follows:

$$d_m = \frac{\text{Area of cross section}}{\frac{1}{2} (\text{Perimeter exposed to the atmosphere})}$$

The theoretical thickness is twice the volume-surface ratio used by Hansen and Mattock (12) and others.

In a similar way, the C.E.B. made recommendations for the estimation of the shrinkage strains occurring in the concrete under constant environmental

conditions (Section R 12.32). Shrinkage deformations are expressed as a function of five factors as follows:

$$\epsilon_{sh}(t) = \epsilon_c K_b K_e K_p K_t$$

where:

$\epsilon_c$  = shrinkage factor as a function of the relative humidity at 20° C (see Fig. 2.6),

$K_b$  = shrinkage factor as a function of the composition of the concrete mix. Same as  $K_b$  creep factor (see Fig. 2.3),

$K_e$  = shrinkage factor as a function of the theoretical thickness of the cross section of the member,  $d_m$  (see Fig. 2.7),

$K_p$  = shrinkage factor as a function of the geometric percentage ( $p$ ) of longitudinal reinforcement ( $A_{st}$ ) with respect to the cross sectional area of the member ( $A_c$ )

$$p = 100 \frac{A_{st}}{A_c}, \text{ and}$$

$$K_p = \frac{100}{100 + np}$$

$n = 20$  with regard to the effects of creep,

$K_t$  = time-strain relationship, taken to be the same as  $K_t$ , the creep factor (see Fig. 2.5).

## 2.4 Stress Relaxation in Prestressing Steel

Relaxation is defined as the time-dependent loss of stress in a tendon held at a constant strain. In general, stress relaxation is affected

by the following factors: Ratio of initial stress to yield stress, type of prestressing strand, time, and temperature. Even though most prestressing steel is in service under conditions of continuously decreasing strain, the conditions of the prestressing steel are nearly comparable to those under constant strain since the changes in strain are small compared to the initial strain.

In this investigation, relaxation losses for stress-relieved strands are estimated by making use of the equation developed by Magura, Sozen and Siess (15). The equation was derived from tests conducted under constant strain conditions. This equation has attempted to express relaxation losses in a mathematical form including both time and initial stress level as variables and assuming a relatively constant temperature of about 70°F. The equation has the following form:

$$f_s = f_{si} \left[ 1 - \frac{\log t}{10} \left( \frac{f_{si}}{f_y} - 0.55 \right) \right] \quad (2.3)$$

where:

$f_s$  = stress at time  $t$ ,

$f_{si}$  = initial stress immediately after stressing,

$f_y$  = steel stress at an off-set strain of 0.001,

$t$  = time in hours after stressing, and

$\log t$  = base 10 logarithm of time.

The decay is exponential with time and the greatest losses occur soon after stressing. If the initial steel stress is less than  $0.55 f_y$ ,

relaxation losses would be expected to be very small and for practical purposes they can be safely neglected.

Relaxation may not remain an important source of loss of prestress, as the steel industry is presently manufacturing a new kind of prestressing strand exhibiting relaxation losses significantly lower than those obtained by using Magura's equation. The strand manufacturers claim that the stress-time curve for this new type of strand is (19):

$$f_s = f_{si} \left[ 1 - \frac{\log t}{45} \left( \frac{f_{si}}{f_y} - 0.55 \right) \right] \quad (2.4)$$

During the lifetime of the structure, reduction of prestressing force is continuously taking place. Sometimes such stress reductions occur instantaneously, such as is the case when transfer of prestress takes place. There is an instantaneous increase in steel stress at the time of placement of the deck concrete. These stress changes must be taken into account for a better estimation of the long-time relaxation losses. Figure 2.8 illustrates a way of doing this. In this figure, the upper curve represents the stress-time curve for a steel stressed at an initial stress of 189 ksi and maintained at constant strain thereafter; whereas, the lower stress-time curve has been obtained for the same steel but stressed at a lower initial stress of 175 ksi. Suppose now that at the time of 48 hours a steel stress reduction of about 11.5 ksi occurs in the steel initially stressed at 189 ksi. This stress reduction makes the stress-time curve fall from the upper curve to the lower curve, i.e., before time of 48 hours the stress-time curve is expected to follow the upper curve and after 48 hours is expected to follow the lower curve. In other words, if a steel stress reduction takes place at the

beginning of some time interval I, in order to find the relaxation losses taking place during that time interval, one should first find a hypothetical initial stress at time  $t = 0$  by using the steel stress at the beginning of time interval I and then find the relaxation losses, occurring during that time interval, by using as the initial stress the hypothetical initial stress just found.

A second method for predicting relaxation losses after some strain changes have taken place is suggested by Glodowski and Lorenzetti (11). According to the authors, relaxation losses after stress changes are computed on the basis of an effective initial stress, which is defined as the algebraic sum of the initial applied stress and any later changes due to factors other than relaxation, and an equivalent starting time on the new relaxation curve defined by the previous relaxation loss.

Up to date there have not been enough experimental tests on this problem to allow one to choose one of the methods as being most accurate. However, when comparing both prediction methods, the differences between them is very small. In this investigation, the first method was chosen as the method for predicting relaxation losses under stress changes.

## 2.5 Basic Assumptions

The basic assumptions for the analysis used in this investigation are as follows:

1. Creep strains are proportional to stress (this is true as long as the concrete stress is no more than about  $0.4 f'_c$ ).
2. Strains are linearly distributed over the depth of the cross section of the member.

3. Concrete has a linear stress-strain relationship under short-time loading at the stress levels of interest.
4. Steel has a linear stress-strain relationship under short-time loading.
5. Shrinkage strains are distributed uniformly over the depth of the cross section of the member.
6. The modulus of elasticity of the concrete versus time relationships is known and can be considered as step function.
7. The unit creep strain versus time relationship for constant stress, for the beam concrete loaded at the time of releasing of prestress, is known and can be considered as step function.
8. The unit creep strain versus time relationship for constant stress, for the beam concrete loaded at the time of casting of the deck concrete, is known and can be considered as step function.
9. The unit creep strain versus time relationship for constant stress, for the deck concrete loaded 7 days after casting of the deck, is known and can be considered as step function.  
The final answers are not very sensitive to the age of loading of deck concrete (17).
10. The shrinkage strain versus time relationships, for the beam concrete since release of prestress and for the deck concrete since ending of curing and removal of the deck formwork, are known and can be considered as step functions.

11. The relaxation versus time relationship for the prestressing steel is known and can be considered as step function.
12. Strain in steel is constant during each time interval.
13. Stress in concrete is constant during each time interval.
14. The effects of nontensioned reinforcement on creep and shrinkage of the deck and the beam concrete are neglected.
15. Sequence of stressing, casting and curing of the beam concrete, casting and curing of the deck concrete, and concrete stresses due to prestressing are known.

### 3. PRESENTATION AND DISCUSSION OF FACTORS AFFECTING PRESTRESS LOSSES

#### 3.1 Introduction

Prestress losses occurring in composite and noncomposite prestressed concrete structures are affected by many factors in a variety of ways. Creep and shrinkage of the concrete have long been known to be the main contributors of the time-dependent prestress losses, even though relaxation of the prestressing steel also influences the magnitude of the prestress losses.

Losses begin as soon as the prestressing strands are anchored in the prestressing bed. During the short period of time elapsing between the pulling of the strands and the transferring of their force to the concrete, the only source of prestress losses is stress relaxation of the strands. In fact, a large portion of the prestress losses due to relaxation of the steel occurs before release of prestress.

Immediately after release of prestress, instantaneous prestress losses take place due to the elastic shortening of the concrete at the level of the center of gravity of the strands. The amount of these elastic losses will depend mainly on the magnitude of the concrete stress at the level of the steel at the time of release and the modular ratio,  $E_s/E_{ci}$ . From then on, prestress losses are affected by the creep and shrinkage of the concrete and relaxation of the steel, with these phenomena occurring simultaneously and affecting each other continuously throughout the life of the structure.

Even though the main parameters influencing prestress losses are creep and shrinkage of the concrete and relaxation of the steel, there are also certain important construction and environmental factors which one should always keep in mind because they will determine, to a greater or lesser degree, the magnitudes and rates of the creep and shrinkage of the concrete and



relaxation of the steel; consequently, they will influence the complete behavior of the prestressed concrete structure and the magnitude of the prestress losses.

Environmental factors such as humidity and temperature have been shown to have profound influence on the magnitude and rate of creep and shrinkage of the concrete. At constant temperature, creep and shrinkage of the concrete increase with a decrease in the humidity of the environment.

Construction factors influencing greatly the magnitude of the creep and shrinkage of the concrete are the type and duration of curing of the concrete, age of concrete at time of transferring the prestressing force to the concrete, and age of the girders at the time of casting of the deck concrete. The conditions and sequence of construction of the bridge structure will determine the importance of these factors.

In order to get a better understanding of the general behavior of a prestressed concrete girder, it is therefore essential to know how each of these factors contribute to the magnitude of the prestress losses.

Since it has been found that the time of releasing of prestress, age of the girders at the time of casting of the deck concrete, deck dead load stresses, initial level of stress in the concrete, type of prestressing strands, and effects of varying environmental conditions can play important roles on the time-dependent prestress losses, these effects will be studied and discussed in this chapter. When "final" loss figures are quoted, these are for 2000 days after release. At this age, any subsequent changes will be very small and unimportant.

For purpose of analysis, it will be assumed that the principle of superposition is valid and the single effects can be treated individually.

This is a realistic approach as long as all time-dependent variables are included, with one at a time being treated as a variable. Superposition is not valid if, for example, creep and shrinkage are taken as zero and the variations in relaxation studied as an isolated phenomenon.

### 3.2 Effect of Time of Releasing of Prestress

In prestressed concrete construction, the manufacturing schedule of precast prestressed girders varies from one prestressing plant to another. Usually, the prestressing beds are set up in a way that makes it possible to cast two or more girders during one cycle of casting. After placement of the girder concrete, the girders are cured in a suitable environment during the early stages of concrete hardening, for a certain period of time prior to the release of the prestressing force. Steam cured and moist cured concrete are both conventionally used in the curing of precast elements. From the point of view of the manufacturer, it is desirable to release the pretensioning force as soon as possible after the concrete is cast, so that the girders can be removed and the prestressing beds reused again. Thus, for reasons of economical use of forms as well as prestressing beds, most of the prestressing plants have adopted the technique of using the steam curing because of the rapid development of the strength of the concrete, making it possible to release the prestressing force within 16 to 36 hours after casting. Also, beneficial reductions in the magnitudes of the creep and shrinkage of the concrete have been attributed to the use of steam curing, under both a controlled environment and the alternating temperature and humidity conditions in the field (17,18). These creep and shrinkage strain reductions will be directly

reflected in lower prestress losses, a fact which is important in the design of prestressed concrete girders. Daily turnover of the stressing beds is also obtained by taking advantage of a pretensioned and post-tensioned technique, i.e., transfer of prestress could be done at a lower release concrete strength and post-tension applied when concrete matures to full strength, obtaining in this way higher transfer stresses (7).

Depending on the type of curing of the concrete, construction schedules and specifications, release of the prestressing strands usually takes place in about one to two days when the girders are steam cured and about 2 to 4 days when they are moist cured. This is the general practice for bridge girders. It may be found that building members are often released at earlier ages because lower prestress levels are often used and consequently lower release strengths may be adequate.

In order to have a better understanding of the effects of time of transfer of prestress on the time-dependent prestress losses, four different times of release of prestress have been considered in the analysis of a simply supported prestressed composite girder. For that purpose, an AASHTO-Type III girder has been chosen for the analysis. Casting of the deck concrete has been assumed to be taken place at 90 days after transfer of prestress, creep and shrinkage values for the beam and deck concrete have been obtained by making use of the C.E.B. recommendations for 80 percent relative humidity and 70°F temperature, and the compressive strength for the beam and deck concrete have been taken as 5000 and 3000 psi respectively. Young's modulus of the beam concrete has been assumed constant and equal to  $5.05 \times 10^6$  psi from the time of release of prestress up to the time of casting of the

deck concrete and to be  $5.55 \times 10^6$  psi thereafter, and Young's modulus of the deck concrete has been assumed constant and equal to  $3.93 \times 10^6$  psi.

The results of the analysis for the time of release of prestress at 1, 2-1/2, 4 and 7 days are shown in Figs. 3.1 to 3.3. Figure 3.1 was obtained by using 22-1/2" Grade 270 K stress-relieved strands initially stressed at 189 ksi, while Figs. 3.2 and 3.3 were obtained by using 20-1/2" low-relaxation strands, Fig. 3.2 corresponding to an initial prestress level of 205 ksi and Fig. 3.3 to 189 ksi. In all cases, girders were spaced at 8 ft centers, and the thickness of the normal weight deck concrete was 8 in.

One of the main parameters involved in these cases is creep of the prestressed girders. It is well known that creep varies somewhat with the age of the concrete at the time of loading (18,23). Under the same level of prestress, concrete members loaded at early ages undergo more creep than those loaded at later ages. According to the C.E.B. recommendations, the ratios of the unit creep of a concrete loaded at 1, 2-1/2, 4 and 7 days, with respect to the unit creep of concrete loaded at 28 days, are 1.8, 1.64, 1.53 and 1.4 respectively. The more creep of the concrete, the larger the decrease in the prestressing force; therefore, one could expect higher prestress losses for earlier release of prestress.

In addition, the concrete stresses across the depth of the beam at the time of release of prestress are higher for earlier release times, assuming the same initial prestressing force for all four cases and the same value for Young's modulus. The prestressing force corresponding to earlier release is higher because of the smaller stress relaxation before release.

For the particular case of the bridge structure prestressed using stress-relieved strands, the ratio, in percent, of the level of prestress

at the time of release of prestress with respect to the initial level of prestress for the four different times of release of 1, 2-1/2, 4 and 7 days are 95.99, 94.84, 94.25 and 93.25 percent, respectively. When low-relaxation strands are used as prestressing reinforcement, and initially prestressed to a level of 205 ksi, the ratios are 99.10, 98.84, 98.71, and 98.55 percent, respectively; higher ratios are obtained for an initial prestress level of 189 ksi. Here, the difference in concrete stresses at the time of transfer of prestress between releasing at 7 days and releasing at 1 day is not as great as when stress-relieved strands are used.

Time of releasing of prestress obviously makes some difference in the time-dependent prestress losses. Figure 3.1 illustrates its effect on the total time-dependent prestress losses. It can be observed that the earlier the release, the higher the total prestress losses. Releasing the prestressing force at 1 day gave prestress losses, after 2000 days, of 25.2 percent and releasing at 7 days gave prestress losses of 23.3 percent, i.e., releasing at 1 day gave total prestress losses about 2 percent, or 3 to 4 ksi, higher than those obtained by releasing at 7 days. Intermediate results were obtained by releasing at 2-1/2 and 4 days. It can be observed that during the first couple of months after release of prestress the total prestress losses are larger for later release, but by the time of casting of the deck concrete the total prestress losses are larger for earlier release, a trend which continues thereafter throughout the lifetime of the bridge structure. Also, after about 2 or 3 years after release of prestress, the differences in prestress losses for two different times of release seems to remain constant. Figure 3.1 also shows the effect on the relaxation losses. Here, the earlier

the release takes place, the lower the relaxation losses. Releasing at 7 days gave final relaxation losses about one percent (of the initial stress) higher than those obtained by releasing at 1 day.

Similar results are obtained by using low-relaxation strands, even though in this case the effect of stress relaxation of the steel is not as important and the main parameter involved is essentially just creep of the concrete. It can be seen from Fig. 3.2 that releasing at 1 day gave total prestress losses about 2-1/2 percent (4 to 5 ksi) higher than those obtained by releasing at 7 days. During the first month after release of prestress, the total prestress losses are larger for later release but by the time of casting of the deck, the total prestress losses are larger for earlier release. Also, after 2 or 3 years, the difference in total prestress losses between two different times of release is constant. Figure 3.2 also shows the effect on the total relaxation loss, and it can be observed that the earlier the release, the lower the relaxation losses, though the differences are insignificant. Similar trends are observed for the case of low-relaxation strands initially stressed to a level of 189 ksi, as can be seen in Fig. 3.3.

### 3.3 Effect of Age of Precast Girders at the Time of Casting of the Deck Concrete

The sequence of construction of a prestressed composite bridge structure beginning from the time of manufacturing of the precast prestressed concrete girders up to the time of casting of the deck concrete varies from one job to another. Usually, the girders, after being cast and cured, are moved to a storage area located in the same prestressing plant and left there until they are shipped to the bridge site. Casting of the deck may occur as

early as 28 days after casting of the girders, according to the usual specifications, but for one reason or another it might be done at 2 or 3 months or even be delayed more. Therefore, at the time of casting of the deck concrete, the precast girders might be very young or quite old.

Creep of the precast girders plays an important part in the behavior of the bridge structure. Concrete loaded at an early age yields larger creep strains for a given time under sustained load compared to the same concrete loaded at later age.

In a composite bridge structure, in addition to the continuously decreasing concrete stresses at the level of the prestressing steel due to time-dependent effects, there is a large decrease in stress when casting of the deck concrete takes place due to moments caused by the deck dead load. These stress reductions have a large influence on the continued creep of the concrete. This can be best illustrated by examining the creep curves of Fig. 3.4 for concrete specimens subjected to several variable and constant stress states. These curves have been obtained by using the revised rate of creep method (17) which states that when substantial stress reductions occur in a concrete specimen at any time  $t_1$ , the resulting creep recovery accompanying the reduction in stress will be the same as the creep a similar specimen subjected to a compressive stress equal to the stress reduction at the age  $t_1$ . That is, a new unit creep versus time curve is used for a concrete loaded at the time  $t_1$  when the stress reductions take place. For this special case, when just one stress reduction is considered, same results would have been obtained by using McHenry's principle of superposition of strains (16), which states that the strains produced in a concrete specimen

at any time  $t$  by a stress increment applied at any time  $t_0$  are independent of the effects of any stress applied either earlier or later than  $t_0$ . It is necessary to point out that the creep recovery measured in tests usually is not as great as that predicted using McHenry's directly, especially for mature concretes. The Young's modulus of the concrete considered in Fig. 3.4 has been assumed constant and equal to  $5.05 \times 10^6$  psi up to 90 days and to be  $5.55 \times 10^6$  psi thereafter.

On Fig. 3.4, the upper strain-time curve corresponds to a concrete specimen subjected to a sustained stress of 2 ksi and the lower strain-time curve corresponds to the same specimen under a sustained stress of 1 ksi. Unloading the specimen initially stressed at 2 ksi to a stress level of 1 ksi at different times will not bring the lower curve and the new curve together. Reducing the stress at an early time would make the difference smaller but it would still be significant as long as the stress reduction takes place more than even a day after first stressing.

In order to study the effects of the age of the girders at the time of casting of the deck concrete on the time-dependent prestress losses and relaxation losses, an AASHTO-Type III beam has been analyzed with casting of the deck concrete taking place at various different times. Initial prestressing force and other material properties were assumed to be the same for all cases.

The results of the analysis with casting of the deck concrete occurring at 28, 56, and 90 days after release of prestress are shown in Fig. 3.5. The time of casting of the deck makes some difference, with the total prestress losses being smaller for earlier placement of the deck concrete, as illustrated in Fig. 3.5. Placement of the deck concrete at any age later than



90 days gives total prestress losses only slightly higher than those obtained for casting of the deck at 90 days. For practical purposes, one can consider 90 days as a limiting time beyond which the age at deck casting is no longer a meaningful variable.

It is also obvious from Fig. 3.5 that the prestress losses are larger than those computed assuming the deck is always present and smaller than those computed ignoring the deck dead load.

Figure 3.5 also shows the effect of time of casting of the deck concrete on the time-dependent relaxation losses. It can be observed that the earlier the placement of the deck concrete, the higher the relaxation losses, though the differences between relaxation losses for different times of casting of the deck are negligible.

#### 3.4 Effect of Type of Prestressing Strands

In the design of prestressed concrete bridge structures it is important to know, at least approximately, the magnitude of the prestress losses that will occur during the lifetime of the structure.

In addition to creep and shrinkage of the concrete, relaxation of the prestressing strands is also an important parameter having an influence on the time-dependent changes in prestressing force which one should take into consideration for predicting long-time prestress losses.

As said before, in this investigation only two types of prestressing strands have been considered in the analysis of prestress losses: stress-relieved strands and low-relaxation strands. Most of the cases considered have used 270 K strand.

At the present, the most common type of prestressing strand in use by the prestressed concrete industry is the stress-relieved strand type. According to Magura, et al. (15), stress relaxation losses for this type of strand can be estimated by Eq. 3.1, which tries to take into consideration the main factors affecting stress relaxation. The equation has the following form:

$$f_s = f_{si} \left[ 1 - \frac{\log t}{10} \left( \frac{f_{si}}{f_y} - 0.55 \right) \right] \quad (3.1)$$

where:

$f_y$  = steel stress at 0.001 offset strain,

$f_{si}$  = initial stress immediately after stressing,

$t$  = time in hours after stressing, and

$\log t$  = base 10 logarithm of time.

Low-relaxation strands are a new type of prestressing strand exhibiting relaxation losses significantly lower than those obtained by using Magura's equation. The steel manufacturers (19) claim that this type of strand has a stress relaxation curve of the form:

$$f_s = f_{si} \left[ 1 - \frac{\log t}{45} \left( \frac{f_{si}}{f_y} - 0.55 \right) \right] \quad (3.2)$$

This expression is quite similar to the one proposed by Magura, et al., for stress-relieved strands. Both equations are based on the results of constant-strain relaxation tests.

Stress relaxation characteristics for these two types of strands can be better seen by plotting Eqs. 3.1 and 3.2 in a semi-logarithmic plot. Both

straight line semi-log curves are shown in Fig. 3.6, in which, for purposes of comparison, it has been assumed that both strands have been stressed to the same stress level of 189 ksi and from then on left free to relax. By about 500 days after initial stressing, the stress-relieved strand has exhibited a stress loss of about 22 ksi, a stress relaxation loss of about 11.5 percent; while the low-relaxation strand only a loss of about 4 ksi, i.e., a loss of about 2 percent. The advantages of the low-relaxation strands are quite obvious. In addition, low-relaxation strand has a yield stress, at 1 percent strain, of about 90 percent of the ultimate strength, a fact that makes it possible to prestress up to a stress level of about 205 ksi. Stress-relieved strands, Grade 270 K, with yield stresses of 85 percent of the ultimate strength, are allowed to be prestressed up to a stress level of about 189 ksi.

The complex interrelationship between creep and shrinkage of the concrete and relaxation of the steel in a prestressed concrete structure exists for both types of strands, although, for the case of a structure with low-relaxation strands, the effects of relaxation are going to be less than those of a similar structure prestressed using stress-relieved strands. The total prestress losses are expected to be greater when stress-relieved strands are used.

During the manufacturing of a prestressed concrete girder, the strands are first stressed between abutments for a period of time of about one to four days before release of prestress takes place. The time period, as mentioned before, depends on the type of curing of the concrete and on the work schedules of the prestressing plant. This time period is very significant in relation to the stress relaxation losses, since approximately 30

to 45 percent of the total relaxation losses may be expected to occur during this period. For the case of a girder, prestressed at 189 ksi with stress-relieved strands, the total relaxation losses expected to occur are in the order of 8 to 12 percent of the initial stress. The precise magnitude depends on many factors including the type of cross section, position of the strands with respect to center of gravity of the cross section of the girder, creep and shrinkage of the concrete, initial prestressing force, and yield stress of the prestressing strands. This means, that if the strands are initially stressed to 189 ksi, relaxation losses before release would be in the order of 8000 to 11,000 psi, making then, the actual prestress level at the time of transfer of prestress of about 180 ksi.

If instead of using stress-relieved strands, low-relaxation strands are used as prestressing reinforcement, the total relaxation losses would be in the order of 2 to 3 percent of the initial prestressing. If the strands are initially stressed up to a stress level of 205 ksi, the relaxation losses taking place before release would be of the order of 2000 to 3000 psi, so that the actual prestress level at the time of release of prestress about 202 ksi.

Higher prestress level implies larger creep losses; therefore, creep losses are expected to be higher when low-relaxation strands are used. To illustrate this, an AASHO-Type III girder has been analyzed using the two types of prestressing strands. The prestressing force, 189 ksi, as well as other material properties have been assumed the same for both cases. It can be observed from Fig. 3.7 that the total prestress losses are greater for the case of stress-relieved strands. The difference in total prestress losses is

about 6.5 percent. Obviously the main factor involved in these cases is relaxation of the strands, as can be seen in Fig. 3.7, where relaxation losses for the case of low-relaxation strands are about 2 percent, and about 10 percent for stress-relieved strands. Creep losses, on the other hand, are smaller for the case of stress-relieved strands, as can be seen in Fig. 3.7. Creep losses for the case of stress-relieved strands are more than one percent (of the initial stress) smaller than those obtained for the case of low-relaxation strands.

In the preceding paragraphs, the behavior of prestressed concrete girders were studied for two types of prestressing strands. However, stress-relieved strands of grades 250 K and 270 K are both widely used. According to present specifications (3,5,6), the maximum allowable prestress level is up to 0.70 of the ultimate strength of the prestressing steel, stress levels which corresponds to 175 and 189 ksi for the 250 K and 270 K strands respectively. Very often the ultimate strength of those steels are greater than the specified ultimate strength (13), and in addition, the initial prestress level may be lower than the maximum allowable.

Time-dependent prestress losses are going to be different for prestressed girders with different initial prestressing forces and strands exhibiting different yield stress. The main parameter involved is relaxation of the prestressing strands. It is known that relaxation is affected by steel yield stress and initial stress. To illustrate this, relaxation losses which have been obtained using Magura's equation for strands having different yield stresses and the same initial stress of 189 ksi are shown in Fig. 3.8. After 10,000 hours, relaxation losses for a strand with a yield stress of 265 ksi is about 6.5 percent of the initial stress and for a strand with a yield

stress of 225 ksi is about 11.5 percent. Intermediate values are obtained for strands with yield stresses of 255, 245, and 235 ksi.

In order to understand the influence of these variables on the time-dependent behavior of a prestressed concrete girder, the same AASHTO-Type III beam has been analyzed using different steel yield stress values. All other material properties have been assumed constant, including the initial prestressing force. Yield stresses of 225, 235, 245, 255, and 265 ksi have been considered in the analyses. Figure 3.9 shows the result of such analyses. It can be observed that the main influenced of yield stresses is on relaxation losses and only indirectly and to much less degree on the creep losses. The greater the yield stress, the less the total prestress losses, the less the relaxation losses, and the greater the creep losses. For the case of the girder studied, the net difference in total prestress losses between strands having yield stresses of 265 and 225 ksi is about 4 percent of the initial stress. If the relaxation loss increases about 5 percent, the creep loss decreases about 1 percent. Figure 3.10 shows that, for the range of yield stresses studied, creep and relaxation losses are nearly linearly related to yield stress. Changes in elastic losses due to changes of yield stresses are insignificant and shrinkage losses are independent of stresses.

### 3.5 Effect of Initial Stresses in Concrete

The design of a prestressed concrete girder is usually made having as one set of criteria the allowable stresses at the concrete under service loads, as well as minimum strength requirements. The concrete stresses immediately after release of prestress are also specified and are very important

to the long-time behavior of the girder, because of the dominance of creep in the complex interaction of creep, shrinkage, and relaxation as related to the prestress loss problem.

Creep strains are dependent on the distribution of stresses across the depth of the beam. A decrease in prestressing force due to creep of the concrete at the level of the steel causes changes in the rates of creep all across the depth of the cross section of the beam.

Shrinkage strains have been assumed to be distributed uniformly over the depth of the cross section of the beam and to be independent of the level of prestress, but the decrease in prestressing force due to shrinkage strains also causes a change in the rate of creep of the concrete.

Relaxation of the steel causes loss of prestress and is directly dependent on the actual level of steel stress, which it is strongly dependent on the creep and shrinkage of the concrete.

The effect of magnitude of the prestressing force can be seen by examining the curves shown in Fig. 3.11. These curves have been obtained for a prestressed concrete cylinder, 6 x 12 in., subjected to three different initial prestress values. For these particular illustrative examples only creep of the concrete and relaxation of the steel have been considered in the analysis, i.e., this concrete does not shrink. (This represents the case of piles driven in saturated soils.) The following trends can be observed: the greater the initial concrete stress level, the greater the total prestress losses but the lower the total relaxation losses.

A better understanding of the effects of the initial prestress level on the total prestress losses and relaxation losses of a precast prestressed

concrete girder can be attained by observing the results of the analyses of a simply supported concrete bridge structure subjected to different initial prestress levels as shown in Figs. 3.12 to 3.14. Two types of beam cross sections have been considered: AASHO-Type III and Single-Tee cross sections (see Appendix A). For both beams, release of prestress and casting of the deck concrete have been assumed to be taken place at 2-1/2 and 90 days, respectively.

Figure 3.12 was obtained for an AASHO-Type III beam. The initial prestress level was varied by increasing or decreasing the number of strands. In this case the number of strands selected were 20, 22, 24, and 26. All strands were initially prestressed to 189 ksi. It can be observed that the greater the initial prestress level, the greater the total prestress losses and the lower the relaxation losses.

Figure 3.13 was obtained for a Single-Tee beam. Stress-relieved strand was selected and 12, 14, or 16 strands were used in the analysis, all initially prestressed to 189 ksi. Similar trends were observed for this type of section.

The differences in the trends of loss with time in the period soon after casting of the composite concrete which are shown in Figs. 3.12 and 3.13 are the result of a number of factors. The deck dead load is much greater, relative to the dead load of the precast section, for the I-beam than for the T-beam. The centroidal axis position for the precast sections are quite different relative to member depth. These two factors appear to combine their effects in such a way to make the initial response after placing of the deck concrete different even though this operation produces about the same stress change in the concrete at the level of the prestressing steel.



Figure 3.14 was also obtained for a Single-Tee beam but low-relaxation strands were used instead. The 12, 14, and 16 strands selected were initially prestressed to 205 ksi. Similar trends were observed, though the relaxation losses were small.

Another way of looking the interrelationship between creep and shrinkage of the concrete, relaxation of the steel, and elastic losses at release is shown in Figs. 3.15 to 3.17 which were obtained considering different beam cross sections (see Appendix A). These beams were subjected to different initial prestress values, different times of transfer of prestress, and different relative humidities.

Plotting the prestress losses due to creep and shrinkage of the concrete versus the prestress losses due to relaxation of the steel gave the straight line relationships shown in Fig. 3.15 from which it is obvious that losses due to relaxation of the steel and losses due to creep and shrinkage of the concrete are inversely related, i.e., the greater the losses due to creep and shrinkage of the concrete, the lower the prestress losses due to relaxation and vice versa. Finding that all lines are essentially parallel is helpful; it will aid in developing guides for prediction of losses for design purposes.

Figure 3.16 shows a similar inverse relationship between relaxation and the elastic shortening loss accompanying release. Again, all lines are essentially parallel in the range shown, although they must converge toward some common value when the elastic loss becomes very small. The slopes are steeper than in Fig. 3.15 (note the different horizontal scales), as is reasonable since the elastic shortening is an instantaneous event early in the

life of the structure while creep and shrinkage shortening occur slowly over many years.

Prestress losses due to creep of the concrete as a function of the concrete stress at the level of the center of gravity of the steel at the time immediately after release of prestress are plotted in Fig. 3.17. The straight line relationships show the direct proportionality between prestress losses due to creep and concrete stress at the level of the steel at the time of transfer of prestress, i.e., the greater the initial concrete stress at the level of the steel at release, the greater the prestress losses due to creep of the concrete. For the special case of a girder without deck such lines must converge toward the origin, as can be seen for the cases of the AASHO-Type III and Single-Tee sections.

### 3.6 Effect of Deck Dead Load

In composite prestressed concrete structures, both the stresses during the period following the release of prestress and the change in concrete stresses due to placement of the deck concrete influence the creep of the concrete. The stresses both before and after placement of the deck concrete must be considered for the prediction of prestress losses.

The effects of stress reduction can be seen by observing the creep curves of Fig. 3.18, which have been obtained by using the revised rate of creep method (or superposition method for this special case) and the creep-time relationships given in the C.E.B. recommendations. In that figure, the upper curve corresponds to a concrete specimen subjected to a constant stress of 2 ksi. The lower curves correspond to the similar specimens subjected to

the same constant stress of 2 ksi up to the time of 90 days, when various stress reductions have taken place.

In order to get a better insight of the effects of deck weight on the time-dependent prestress and relaxation losses, AASHO-Type III and Single-Tee beams have been analyzed, considering different deck sections. Casting of the deck was assumed to take place at 90 days after release of prestress, and all other variables have been assumed the same for all cases. Table 3.1 shows the deck sections properties considered in the analysis.

The results of the analysis are shown in Figs. 3.19 and 3.20. It can be observed that the prestress losses are smaller for the heaviest deck and greater for the case of no deck. The effect of deck dead load on relaxation losses is insignificant as can be seen in such figures.

From Figs. 3.19 and 3.20, it is obvious that the concrete stress reductions due to the weight of the deck directly influence the creep of the concrete, and therefore the prestress losses, in some fairly direct proportion to the concrete stress reduction at the level of the steel. This is demonstrated in Fig. 3.21, in which a linear relationship between the concrete stress reduction at the level of the steel and the total prestress losses is shown for several different prestressed girders. The slopes of the various lines are reasonably close to the same values.

### 3.7 Effect of Storage Conditions

Fluctuating temperature and humidity of the surrounding environment are known to have significant influences on the magnitudes and rates of creep and shrinkage of the concrete; therefore, their effects on the long-time deformations and prestress losses are important.

Creep, according to the C.E.B. recommendations, is obtained by multiplying the creep strain at a relative humidity of 100 percent by a coefficient which depends on the relative humidity of the surrounding atmosphere (see Fig. 2.1). Thus, for example, for a 50 and 80 percent relative humidity, the coefficients are 2.85 and 1.92, respectively. These strains are for constant environmental conditions, and not for variable environments such as exist outdoors.

Investigations of the effects of alternating relative humidity on the creep of the concrete have shown that if the variations take place slowly, creep values tend toward the magnitudes that a similar concrete would have at a constant relative humidity equal to the lower limit of the fluctuating humidity. If rapid variations occur, creep values tend to magnitudes that a similar concrete would have at a constant relative humidity of magnitude somewhere between the higher and lower limits of relative humidity.

Mossiosian and Gamble (17) came to the conclusion that a fair estimate of the creep strains of the concrete can be made by making use of the C.E.B. recommendations. For field specimens, higher and lower bounds to the expected creep values can be obtained by using the lowest monthly average and the annual average values of the relative humidity in the field.

The expected shrinkage values can be obtained by assuming the specimens are stored at a constant relative humidity equal to the average annual relative humidity in the field, realizing that there will be seasonal fluctuations in the shrinkage strain.

In most of this investigation, the study of the time-dependent prestress losses has been made assuming that the prestressed concrete structure

is under constant relative humidity and temperature conditions. Different values of relative humidity have been considered to give information on the influence of this important variable. A few cases using creep and shrinkage data obtained in a variable environment are also presented and discussed.

The results of the analysis of AASHO-Type III beams under constant relative humidities of values of 100, 80 and 50 percent are shown in Fig. 3.22. It can be seen that the lower the relative humidity, the greater the total prestress losses and the lower the relaxation losses. The actual loss of prestress in a beam located anywhere in the midwest would be expected to lie within the bounds established by the 50 and 80 percent relative humidity curves.

In order to examine the effects of alternating humidity and temperature on the time-dependent prestress losses, the same AASHO-Type III beam has been analyzed using the Douglas County (13,17) and the Champaign County creep and shrinkage values obtained under both field and laboratory storage conditions. The results have been compared with the prestress loss values obtained by using the 80 and 50 percent relative humidity creep and shrinkage curves recommended by the 1970 C.E.B. recommendations.

The data from field stored cylinders are for 6 by 12 in. specimens subjected to a constant 1,000 psi stress. The data from the girder were obtained from strain measurements at the centroid of the precast girder, and are for a stress of 1,000 psi. The stress in the girder varied with time, but this was taken into account in finding an equivalent curve for constant stress (17).

In Figs. 3.23 to 3.28 the Douglas County creep and shrinkage curves, for the beam and slab concretes under both field and laboratory storage

conditions are shown. Creep and shrinkage curves recommended by the European Concrete Committee for 50 and 80 percent relative humidity are also shown. In Figs. 3.29 to 3.34 the Champaign County creep and shrinkage curves are shown.

In Figs. 3.35 and 3.36 the computed prestress losses obtained using the Douglas County creep and shrinkage values are compared with the C.E.B. prestress loss values. It can be observed from Fig. 3.35 that the total prestress losses obtained by using the Douglas County field values lie in between the 50 and 80 percent C.E.B. relative humidity curves, with the Douglas County values much closer to 50 percent humidity curve. This phenomenon can be explained by comparing the creep and shrinkage curves of the Douglas County field specimens and the C.E.B. values shown in Figs. 3.23 and 3.26. It can be seen that the Douglas County field creep values, for concrete specimens loaded 2-1/2 days after casting, are comparable with the creep strains of the corresponding 50 percent C.E.B. relative humidity curve, although there are sometimes large differences between shrinkage strains. Due to variation in the humidity and temperature in the field, the Douglas County specimens were subjected to shrinkage and swelling as can be seen in Fig. 3.26. Consequently, the main differences in prestress losses between the Douglas County and the C.E.B. values come from the shrinkage strains and not from differences in creep strains.

Figure 3.35 also shows the variation of relaxation losses obtained from the Douglas County field stored values and the C.E.B. values. The differences in relaxation losses between the two Douglas County bridge values and the 50 percent relative humidity C.E.B. values are insignificant, and all are slightly smaller than those found using the 80 percent relative humidity C.E.B. values.

Figure 3.36 shows the computed variation in total prestress and relaxation losses obtained using creep and shrinkage values from the Douglas County laboratory stored 6 by 12 in. cylinder specimens and the 50 percent relative humidity C.E.B. values. It can be seen that the total prestress losses are greater for the case of the Douglas County bridge values. This can be explained by observing the creep and shrinkage curves shown in Figs. 3.23, 3.24, 3.26 and 3.27. The creep values are comparable with the 50 percent C.E.B. relative humidity values but major differences are observed in the corresponding shrinkage values. The final shrinkage strain (782 days) for the lab specimens reached a maximum value of  $600 \times 10^{-6}$  while the corresponding C.E.B. shrinkage strain is  $235 \times 10^{-6}$ . Hence, the major differences in total prestress losses come from differences in the shrinkage strain values. Differences in total relaxation losses are in the order of one percent, as can be seen in Fig. 3.36.

Similar observations are found when comparing the computed losses for the Champaign County Bridge values obtained using measured and C.E.B. values of creep and shrinkage. The comparisons are shown in Figs. 3.37 and 3.38.

### 3.8 Comparison of Measured and Computed Results

In order to study the correlations between the results of analyses, and the actual behavior of bridge structures under field conditions, analyses were carried out for the Jefferson County bridge structure (see Gamble, 1970), the Douglas County bridge structure (see Houdeshell, et al., 1972), and the Champaign County bridge structure.\* In such analyses initial prestressing

---

\* No report has yet been published, but is expected in a few months.

force and other material properties were assumed to be the same as in the actual structure. For purposes of comparison, different sets of creep and shrinkage data were used in the analyses. The 1970 European Concrete Committee recommendations were used for predicting the creep and shrinkage strains of the girder and deck concrete. Values of 80 and 50 percent relative humidity storage conditions were considered, and also values for the combination of 50 percent relative humidity creep strains and 80 percent relative humidity shrinkage strains. In addition, the data obtained from the creep and shrinkage measurements under field and laboratory storage conditions on the various test specimens which accompanied the bridge girders were also used, taking into account the effects of size and shape of the specimens (8,12,17).

### 3.8.1 Douglas County Bridge Structure

A description of the bridge structure, its construction, materials, and observations of the long-term deformations are presented in detail in previous reports (see Houdeshell et al., 1972 and Mossiosian and Gamble, 1972).

Figure 3.39 shows measured and computed total strains at the top, centroid, and bottom gage lines versus time at midspan section for the interior test girder BX-3. The creep and shrinkage values of the corresponding girder and deck concrete under field storage conditions were used. The modulus of elasticity of the strands was taken as  $28.2 \times 10^6$  psi, as was obtained from the strand tests. The measured total prestressing force after all 38-7/16 in. Grade 250 K strands were stressed was 695 kips. Variation of Young's modulus



of the beam concrete with time, the variation of the beam span length during storage time is presented in Mossiosian's thesis. Young's modulus of the deck concrete was assumed constant and equal to the average value of the Young's modulus obtained from the field stored deck concrete cylinder tests ( $5.0 \times 10^6$  psi).

From Fig. 3.39, it can be seen that computed total strains are in good agreement with the measured total strains in the field. Better agreement is observed for the bottom and centroid gage lines than for the top line. In general, the calculated total strains follow the cyclic variation of the measured strains, which occur due to the continuous variation of humidity and temperature in the field. The differences between the curves may lie in that the assumed variation of creep and shrinkage strains of the beam and deck concrete under field conditions was probably not exactly the same as the actual values of the bridge structure, because of the differences in volume, exposed surface, and possibly exposure conditions of test specimens and bridge structure. The cross sections of the shrinkage specimens were identical to those of the bridge structure, but they were not as long or wide. Also, the effects of the nontensioned reinforcement on the shrinkage or swelling of the concrete was not taken into account, which must affect the time-dependent behavior in some small degree.

The calculated total strains shown in Fig. 3.40 were obtained by using the lower bound of creep and shrinkage values of the corresponding girder and deck concrete under laboratory storage conditions, 50 percent relative humidity and 70°F temperature. The creep and shrinkage strains were based on measured values from cylinders, but corrected for size effects using the C.E.B. coefficients. Young's modulus of the beam and deck concrete were assumed

constant and equal to the average values of Young's modulus ( $3.40 \times 10^6$  and  $4.60 \times 10^6$  psi respectively) obtained from the beam and deck concrete cylinder tests. All other material properties as well as initial prestressing force were assumed to be the same as those of the actual structure.

From Fig. 3.40, it can be observed that the computed total strains are generally in good agreement in the early stages before casting of the deck and for later ages they represent an upper bound of the measured total strains, even though they do not follow the cyclic variation of the measured values.

After casting of the deck concrete there are substantial differences between calculated and measured strains. During the summer, measured total strains in the field were found to increase, whereas during winter they decreased. This is not the case in the laboratory, where strains increase continuously at a decreasing rate because of the nearly constant atmospheric conditions.

On Fig. 3.41, calculated total strains were obtained using creep and shrinkage values according to C.E.B. recommendations for 50 percent relative humidity and 70°F temperature. Young's modulus of the beam and deck concrete were also assumed constant and equal to the recommended value given by the C.E.B.

All other material properties and initial prestressing force were considered to be the same as those of the actual structure.

Figure 3.41 indicates that the calculated total strains are also in good agreement with measured values for times before casting of the deck and that they represent an upper bound of the measured total strains at later ages. Substantial differences are also observed after casting of the

deck because of the effects of changes in the atmospheric conditions in the field.

Figure 3.42 shows the comparison between measured total strains and calculated values which were obtained using the C.E.B. recommendations for 80 percent relative humidity and 70°F temperature. It can be seen that the calculated total strains are not in agreement with measured values at any time. However, such values represent a lower bound of the measured total strains.

Actual strains in a beam located in the midwest are expected to lie within the bounds established by the 50 and 80 percent relative humidity curves. However, up to date, there are certain unknowns related to the prediction of the behavior of concrete structures under conditions of alternating humidity and temperature in the field, due to the fact that such variations do not affect creep in concrete in the same manner as they influence the magnitude of shrinkage. Then, the question arises when trying to estimate deformations, stresses, and prestress losses about what would be the most appropriate method of prediction of creep relative to the value of shrinkage.

In order to get an insight of this problem, the Douglas County Bridge structure was analyzed for the combination of creep values obtained for 50 percent relative humidity and shrinkage values for 80 percent relative humidity. Figure 3.43 shows the comparison between measured and calculated total strains. It can be seen that the calculated values are in much better agreement than for the cases of 80 and 50 percent relative humidity treated separately. Even though the cyclic variation could not be predicted because of the constant environmental conditions assumed in the analysis, the calculated

values give an average of the cyclic measured values after casting of the deck.

#### Loss of Prestress

The changes in strand force after release of prestress, used for purpose of comparison, were obtained from the creep and shrinkage data of the corresponding girder and deck concrete under field conditions.

Relaxation of the prestressing strands are included in the analysis. However, the relaxation losses of 3 to 4 percent are very small since the yield stress for the strand was very high relative to the applied stress level.

The estimated prestressing loss plotted versus time is shown in Fig. 3.44. After 782 days after release, the prestress loss was about 22.7 percent. The assumed loss was 24.4 percent. As in the case of strains, environmental conditions in the field caused cyclic variations in prestressing force after casting of the deck.

On the same Fig. 3.44, estimated prestressing force obtained by using the lower bound of creep and shrinkage values under laboratory storage conditions, C.E.B. creep and shrinkage values for 80 and 50 percent relative humidity, and for the combination of 50 percent relative humidity creep values and 80 percent relative humidity shrinkage values are also presented. It can be seen that the C.E.B. values for 80 and 50 percent represent a lower and upper bound of the time-dependent prestress losses and that the estimated values obtained from the combination 50 percent creep-80 percent shrinkage represent a good estimate of the cyclic variation of prestressing force.

### 3.8.2 Jefferson County Bridge Structure

Description of the bridge structure, its construction, materials, and observation deformations are presented in a previous report (see Gamble, 1970).

The test structure is a four-span bridge, with interior girders of 72 ft 3 in. long and end girders of 43 ft 8 in. long.

Mossiossian and Gamble (17) studied the effect of continuity on the time-dependent strains and prestress losses. The study indicated that the effects of continuity on the strain-time values for centroid and top fibers are insignificant, while its effect on bottom fibers is small at early ages after casting of the deck and at later ages its effect becomes insignificant. For practical purposes, strains of a continuous composite structure can be predicted considering the structure as a series of simply supported spans.

For purposes of comparison, analyses of the Jefferson County bridge structure were carried out considering the bridge structure as simply supported. The span length was assumed to be the same as the interior span of the actual structure.

Figure 3.45 shows the measured and computed total strains at the top, centroid, and bottom gage lines versus time at the midspan section of the interior test girder BX-1. The calculated strains were obtained for the combination of C.E.B. values for 50 percent R.H. creep and 80 percent R.H. shrinkage. It can be seen that the computed values are in good agreement with measured values after casting of the deck. Cyclic variation could not be predicted but calculated values give a sort of average of the cyclic

variation of strains at later times after casting of the deck. Reliable creep and shrinkage data for the concrete used in the girders are not available.

#### Loss of Prestress

For the Jefferson County bridge structure, there was no way to compare predicted losses based on the C.E.B. recommendations with the predicted losses based on the creep and shrinkage data of the corresponding girder and deck concrete specimens under field conditions. The field data appears to be reasonable except for the field-stored beam concrete creep data. Because of a series of experimental difficulties, its reliability is very low. Gamble (10) compared total deformations in the creep specimens with the deformations at the centroidal fiber at midspan of beam BX-1 and concluded that the creep measurements for the set of specimens were meaningless.

The variation of the prestress loss with time in Beam BX-1 is shown in Fig. 3.46. Such figures have been obtained for the combination of C.E.B. values for 50 percent R.H. creep and 80 percent R.H. shrinkage. Relaxation of the prestressing strands are included in the analysis although its contribution to the total prestress loss is small because of the low initial stress level ratio.

One thousand days after release of prestress, total computed prestress losses amount to 24.7 percent of the initial prestress, of which relaxation losses contributed just 4.7 percent.

### 3.8.3 Champaign County Bridge Structure

#### Description of the Test Structure

The test structure located in Champaign County, Illinois, is a three-span bridge with six precast prestressed concrete girders in each span and cast-in-place deck concrete which provides continuity over three spans.

The plan of the bridge is shown in Fig. 3.47. The bridge is oriented in the east-west direction. Support locations for the two test girders, BX-5 and BX-6, at different times, are shown in Fig. 3.48. All girders were 46 ft 2 in. long and 42 in. deep.

The elevation of a typical girder and the profile of the 7/16 in. prestressing strands are shown in Fig. 3.49. The stirrups and other mild steel reinforcement are not shown. An elevation of the structure is shown in Fig. 3.50.

The cross section of the girder is shown in Fig. 3.51. The girders were spaced at 8 ft centers, and the composite deck was 8 in. thick. The deck was reinforced continuously both top and bottom and in both directions, and in conjunction with cast-in-place diaphragms over the piers provided continuity for live load negative moments.

The girders of the test bridge were manufactured in Centralia, Illinois, during March of 1972 and were placed on the piers during March and April of 1972. The deck and diaphragms were cast 3 May 1972.

The chronology of the bridge construction is presented in Tables 3.2 and 3.3.

The prestressed reinforcement was 7/16 in. diameter, 7-wire strand

meeting the requirement of ASTM A-416. The specified ultimate strength is 250 ksi, and the minimum elongation is 3.5 percent in a 24 in. gage length.

The strand samples were unfortunately lost before samples were tested. For purpose of analysis, it was assumed that strands had an average failure stress of 250 ksi, an average Young's Modulus of  $E_s = 28,000$  ksi, and an 0.001 offset strain yield stress of  $f_y = 212.5$  ksi.

The measured total prestressing force in the 24 strands immediately after all strands were stressed was 413.6 kips or 158 ksi. The measured total prestressing force before transfer was 418.6 kips or 160 ksi.

The concrete used in the girders had an average cylinder strength in the field of 5630 and 6590 psi at 4 and 32 days after casting, respectively.

The deck concrete had an average cylinder strength in the field of 3360 and 4360 psi at 8 and 31 days after casting, respectively.

#### Predicted and Measured Total Strains

The creep and shrinkage specimens accompanying this bridge structure under field and laboratory storage conditions were 6 by 12 in. cylinders. In addition, deck concrete prisms were cast.

Mossiosian and Gamble (17) found that creep of concrete in the girder under field storage conditions cannot be obtained from the corresponding cylinder creep values by considering the effect of size and shape of the girder section in the same way it is done for laboratory storage conditions (12).

However, for purposes of some comparison, the creep and shrinkage strains under field conditions were obtained by reducing the corresponding cylinder values by the average reduced values obtained from C.E.B. (1970) and Hansen and Mattock.



Figure 3.52 shows the measured and computed total strains at the top, centroid, and bottom gage lines versus time at the midspan section of the test girder BX-6. Measured values were obtained up to 284 days after release of prestress. Calculated strains have been obtained by using the reduced cylinder beam and deck concrete creep and shrinkage data under field conditions. Good agreement is observed between the curves, especially for bottom and top gage line strains. Somehow, the measured centroid strains seems to be quite large. So far no reason for this behavior has been found.

In Fig. 3.53, the predicted total strains have been obtained by using the combination of C.E.B. values for 50 percent R.H. creep and 80 percent R.H. shrinkage.

#### Loss of Prestress

The changes in prestressing force after release of prestress, were computed using the reduced creep and shrinkage data of the corresponding girder and deck concrete under field conditions.

The estimated prestress loss is shown in Fig. 3.54. After 458 days after release of prestress, the estimated loss was about 18 percent of the initial stress. Environmental conditions in the field caused cyclic variations in prestressing force.

Also in Fig. 3.54, the estimated losses computed using the combination of 50 percent R.H. creep and 80 percent R.H. shrinkage are shown. It can be seen that the C.E.B. values represent a reasonable average of the cyclic variation of prestressing force for later times.

#### 4. FACTORS FOR THE ESTIMATION OF PRESTRESS LOSSES

##### 4.1 Introduction

The AASHO 1969 Specifications, Sec. 1.6.8(B), for prestress losses in bridge structures considered the prestress losses to be 35,000 psi for pretensioned members and 25,000 psi for post-tensioned members. The same losses have been used by the 1963 ACI Code (4) and are suggested in the Commentary to the 1971 ACI Code (6).

The AASHO 1970 Interim Specifications, Sec. 1.6.7(B), introduced a new set of loss factors to be considered in the estimation of the prestress losses in prestressed concrete girders. The Interim Specifications, included in the 1973 AASHO Specifications, represented an improvement over the AASHO 1969 Specifications in that the effects of climate on the shrinkage of the concrete are taken into consideration and in addition, the interrelationship between creep and shrinkage of the concrete, relaxation of the steel, and elastic losses at release are recognized to some extent. According to these Interim Specifications, prestress losses are estimated in the following way:

$$\Delta f_s = SH + ES + CR_c + CR_s \quad (4.1)$$

where:

$\Delta f_s$  = total estimated prestress losses in psi,

SH = prestress losses due to shrinkage of the concrete,  
in psi, as a function of the average ambient relative  
humidity for the geographic area (see Table 4.1),

ES =  $7 f_{cr}$  = prestress losses due to elastic shortening of the

concrete at the level of the center of gravity of the prestressing steel, immediately after release of prestress, where  $f_{cr}$  = concrete stress at the level of the center of gravity of the prestressing steel immediately after transfer of prestress and including the stress due to dead load of the girder,

$CR_c = 16 f_{cd}$  = prestress losses due to creep of the concrete where  $f_{cd}$  = concrete stress at the level of the center of gravity of the steel immediately after release of prestress and including the stress due to dead load of the girder and deck. Both  $f_{cr}$  and  $f_{cd}$  are stresses averaged along the length of the beam.

$CR_s = 20,000 - 0.125 (SH + ES + CR_c)$  prestress losses due to relaxation of the prestressing steel.

Losses calculated using these factors are generally much higher than the 35,000 psi lump-sum losses previously included in the AASHTO 1969 Specifications.

Gamble proposed a new set of loss factors to the AASHTO Standard Specifications for Highway Bridges, Sec. 1.6.7(B), which are included, with modifications, in a later proposal to AASHTO (20). The main changes recommended occur in the losses due to creep of the concrete and relaxation of the steel. The following set of factors for use in Eq. 4.1 were proposed for the estimation of the prestress losses:

$SH = 17,000 - 150 R.H.$ , prestress losses due to shrinkage of the concrete where R.H. average annual ambient relative humidity, percent (see Table 4.2)

ES =  $\frac{E_s}{E_c} f_{cir}$ , prestress losses due to elastic shortening of the concrete at the level of the prestressing steel, immediately after release of prestress, where  $f_{cir}$  = concrete stress at the level of the center of gravity of the prestressing steel at the section considered just after release of prestress. Stresses due to the dead load of the girder are included.

$E_s$  = Young's modulus of steel

$E_c$  = Young's modulus of concrete

CR<sub>c</sub> = Prestress losses due to creep of the concrete. It was originally divided in two categories for emphasis of the differences: one for composite and one for noncomposite construction.

For noncomposite construction, the following value was recommended:

$$CR_c = 12 f_{cir}$$

For composite construction, the effect of the deck dead load on the creep of the concrete is taken into account.

The following creep loss value was recommended:

$$CR_c = 12 f_{cir} - 7 f_{cds}$$

where  $f_{cds}$  = change in concrete stress at the level of the center of gravity of the prestressing steel at the section considered due to dead load of the deck concrete and permanent formwork. Since the two equations give the same result when there is no additional dead load, only the second is included in the 1973 proposal.

$CR_s$  = Prestress losses due to stress relaxation of the prestressing steel.

The following value was recommended for members pretensioned with 7-wire stress-relieved strand:

$$CR_s = 20,000 - 0.4 ES - 0.2 (SH + CR_c), \text{ in psi.}$$

The current and proposed AASHO loss values must be considered only as fairly simple approximations of the trends of an extremely complex interaction of the effects of creep and shrinkage of concrete, relaxation of steel stress, and changes in the stresses caused by the casting of the deck concrete. Factors such as possible influence of humidity, and especially variable humidity, on creep, the effects of member size, and the effects of different aggregates on creep and shrinkage are not included. However, it is only fair to point out that the first two problems are not yet completely solved and the third is perhaps somewhat self-limiting because the aggregates leading to the highest creep and shrinkage values are usually not well suited to making the high-strength concretes needed for the quick, economical, reuse of prestressing beds.

#### 4.2 Proposed Set of Loss Factors

In this section a set of loss factors are presented, keeping within the general format of the AASHO Specifications. The same set of four factors are considered, but are given somewhat different values containing more variables, in order to more completely take into account the pertinent factors affecting prestress losses. The following four factors are recommended for use in Eq. 4.1. All losses are in psi units. Values are given first for

stress relieved strands, and then modified values are given where necessary for low-relaxation strands.

SH = Prestress loss due to shrinkage of the concrete, computed as a function of the average annual relative humidity in the field and the theoretical thickness of the member

$$= F (14,000 - 1.4 \text{ R.H.}^2)$$

where, R.H. = average annual relative humidity in the field,

$F = 1.25 - 0.025 d_m$ , a factor depending on the theoretical thickness of the member,  $d_m$ , and

$$d_m = \frac{\text{Area of cross section}}{1/2 (\text{Perimeter exposed to the atmosphere})}, \text{ cm.}$$

If  $d_m$  is measured in inches, the factor becomes  $F = 1.25 - 0.0625 d_m$ .

Values of shrinkage loss for different relative humidities and theoretical thicknesses are tabulated in Table 4.3 and also are plotted in Fig. 4.1.

ES = Prestress losses due to the elastic shortening of the concrete at the level of the prestressing steel accompanying release of prestress.

A precise value can be found by using the following expression, which has been found from compatibility of deformations of the concrete and steel at the level of the center of gravity of the prestressing strands, assuming perfect bond between concrete and steel.

$$P_o = \frac{P_i}{1 + n \frac{A_{st}}{A_c} + \frac{ne^2 A_{st}}{I}} + \frac{\frac{M_{DL}}{I} enA_{st}}{1 + n \frac{A_{st}}{A_c} + \frac{ne^2 A_{st}}{I}} \quad (4.3)$$

where:

$P_o$  = prestressing force immediately after transfer of prestress,

$P_i$  = prestressing force just before transfer of prestress, computed considering relaxation occurring between stressing and transfer,

$n$  = modular ratio,  $E_s/E_c$ ,

$A_{st}$  = area of strands,

$A_c$  = area of cross section of the beam concrete,

$e$  = eccentricity of prestressing strands,

$I$  = moment of inertia of cross section of the beam concrete,  
and

$M_{DL}$  = dead load moment of beam concrete.

The elastic prestress losses immediately after release of prestress will then simply be:

$$E\bar{\epsilon} = \frac{P_i - P_o}{A_{st}} \quad (4.4)$$

An approximate expression for the evaluation of the elastic shortening losses is the following:

$$E\bar{\epsilon} = \frac{E_s}{E_c} f_{cir} \quad (4.4a)$$

where:

$f_{cir}$  = concrete stress at the level of the center of gravity of the steel immediately after release of prestress. The dead load moment of the girder should also be included in the calculation of  $f_{cir}$ ,

$E_s$  = modulus of elasticity of the steel, and

$E_c$  = modulus of elasticity of the concrete at the time of release of prestress.

$CR_c$  = creep losses, which may be divided in two categories, one for composite and one for noncomposite construction. For noncomposite construction, the following value is recommended:

$$CR_c = K (10 f_{cir}) \quad (4.5)$$

where:

$K$  = creep factor as function of the relative humidity and time of transfer of prestress. It can be expressed as:

$$K = K_{RH} \cdot K_R \quad (\text{see Fig. 4.2})$$

$K_{RH}$  = creep factor as a function of the relative humidity (see Fig. 4.3)

$$K_{RH} = 1.0 - 0.0225 (R.H. - 80)$$

$K_R$  = creep factor as a function of the time of releasing of prestress (see Fig. 4.4)

$$K_R = 1.15 - 0.375 \log R$$



R = time from stressing to transfer, days.

For composite construction, the following creep loss value, which converges to the value for noncomposite construction as the deck dead load reduces, is recommended:

$$CR_c = K (10 f_{cir} - 7 f_{cds}) \quad (4.6)$$

where:

$f_{cds}$  = change in concrete stress at the level of the center of gravity of the prestressing steel due to deck dead load and permanent formwork

$CR_s = 25,000 - 0.3 ES - 0.15 (SH + CR_c) =$  prestress losses due to stress relaxation of the prestressing steel

More generally,

$$CR_s = F_R F_I^2 [25,000 - 0.3 ES - 0.15 (CR_c + SH)]$$

where:

$F_R$  = relaxation factor as a function of steel yield stress  
 =  $3.7 - 0.012 f_y$ . If  $f_y = 225$  ksi,  $F_R = 1.0$ .

$F_I$  = relaxation factor as a function of initial prestressing  
 =  $0.011 f_{si} - 1.08$ . If  $f_{si} = 189$  ksi,  $F_I = 1.0$ .

For the usual design problem where  $f_y$  is not known and standard stressing procedures are used, both  $F_R$  and  $F_I$  are taken as 1.0. In no case should  $F_R$  or  $F_I$  be taken as negative numbers.

When low-relaxation strands are used as prestressing reinforcement,

the total prestress losses are significantly reduced and they can be estimated using the following factors in Eq. 4.1.

Shrinkage losses and elastic losses are estimated using the same expressions as in the case of stress-relieved strands.

$CR_c$  = creep losses are again divided into two categories

For noncomposite construction, the following value is recommended:

$$CR_c = K (11 f_{cir})$$

$K$  is the same creep factor as for the case of stress-relieved strands (see Figs. 4.2 to 4.4).

For composite construction, the following value is recommended:

$$CR_c = K (11 f_{cir} - 7 f_{cds})$$

$CR_s$  = prestress losses due to stress relaxation of the prestressing steel

$$CR_s = F_{RL} F_{IL}^2 [7,000 - 0.10 ES - 0.05 (SH + CR_c)]$$

where:

$F_{RL}$  = relaxation factor as a function of steel yield stress  
 =  $3.880 - 0.012 f_y$ . If  $f_y = 240$  ksi,  $F_{RL} = 1.0$ .

$F_{IL}$  = relaxation factor as a function of initial prestressing  
 =  $0.011 f_{si} - 1.255$ . If  $f_{si} = 205$  ksi,  $F_{IL} = 1.0$ .

Table 4.4 shows a summary of the set of factors for the estimation of prestress losses of composite and noncomposite prestressed concrete structures according to the 1970 AASHO Interim Specifications, the 1973 AASHO Proposal, and the Proposed Values given in this chapter.

### 4.3 Discussion of the Set of Loss Factors

In this section, a discussion of the reasons for adopting the proposed set of loss factors is presented.

The prestress losses due to shrinkage of the concrete estimated according to both the 1970 AASHO Interim Specifications, Sec. 1.6.7(B) and the 1973 AASHO Proposal seem to be in the right ranges for relative humidity, and are plotted versus humidity in Fig. 4.5. The values are also in agreement with the values recommended by the European Concrete Committee (C.E.B) for a structural member of theoretical thickness of 10 cm (3.94 in.), although most I-section pretensioned girders have theoretical thicknesses of about 20 cm (8 in.).

The recommended shrinkage loss value,  $SH = F(14,000 - 1.4 R.H.^2)$  matches quite closely the shrinkage loss found using the C.E.B. recommendations, as can be seen in Fig. 4.5. Figure 4.1 shows the shrinkage loss curves for different theoretical thickness of the structural member.

The prestress loss due to creep of the concrete, for the case of noncomposite construction,  $CR_c = K(10 f_{cir})$ , was based on the study of creep loss versus  $f_{cir}$  curves similar to those shown in Fig. 3.17, where linear relationships between creep loss and concrete stress at the level of the steel just after release of prestress are given, for different cross section girders. The greater the concrete stress,  $f_{cir}$ , the greater the total creep loss. Also, the earlier the release of prestress, the greater the total creep loss for two identical structures stressed to the same level of prestress.

The case of composite construction is more complicated because in addition to the continuously decreasing concrete stress at the level of the

center of gravity of the prestressing steel, there is also a large decrease in concrete stress at that level by the time of the placement of the deck concrete. Hence, the stresses both before and after casting of the deck must be considered in the estimation of the prestress losses due to creep of the concrete.

The value of the creep loss, for the case of composite construction,  $CR_C = K(10 f_{cir} - 7 f_{cds})$ , was based on the study of the slopes of curves similar to those shown in Fig. 3.21.

Plotting the total prestress losses versus the concrete stress reduction at the level of the center of gravity of the prestressing steel due to placement of the deck concrete gave the straight line relationships shown in Fig. 3.21. When the concrete stress reduction is zero, one gets the case of noncomposite construction and the creep loss value reduces to the value recommended for noncomposite construction, i.e., noncomposite construction is a special case of composite construction. It should be pointed out that additional noncomposite dead load would have about the same effect on prestress losses, though not on camber (17), and this equation can be used satisfactorily for this additional case.

By studying the effect of time of casting of the deck concrete on the total prestress losses, it can be seen that the earlier the placement of the deck, the smaller the prestress losses. However, for practical purposes one can consider 90 days as a limiting time for casting of the deck, after which age is no longer a significant variable. In this study, prestress losses were estimated assuming the deck is cast between two and three months after the girders were cast.

It is on the basis of this background that the above value for creep loss for the case of composite construction has been recommended.

The proposed relaxation loss value was based on the study of the slopes of curves similar to those shown in Figs. 3.15 and 3.16.

Plotting total relaxation losses as a function of the initial elastic losses gave the straight line relationships shown in Fig. 3.16. It can be observed that the slopes of these lines are approximately 0.6 (total relaxation losses/initial elastic losses). However, it should be pointed out that the total relaxation loss values plotted includes the influence of the creep and shrinkage of the concrete.

Comparing total relaxation losses as a function of the total creep and shrinkage losses gave the straight line relationships shown in Fig. 3.15. Losses due to creep and shrinkage of the concrete occur continuously over an extended period of time, and so would be less effective in reducing relaxation losses than those due to the elastic shortening of the concrete at the level of the steel at the time of release of prestress. This is obvious by observing that the slopes of these lines are approximately 0.3 (total relaxation losses/creep and shrinkage losses). As mentioned above, the total relaxation loss values plotted in these figures include, besides the effects of creep and shrinkage of the concrete on relaxation losses, the effects of the initial elastic losses on the relaxation losses.

From the slopes of the lines in Figs. 3.15 and 3.16, it is obvious that elastic losses are twice as efficient as the creep and shrinkage losses in reducing the relaxation loss. However, these are not the correct slopes for a reduction equation involving both losses, and the coefficients of 0.3

and 0.15 in the expression  $CR_S = 25,000 - 0.3ES - 0.15 (CR_C + SH)$  were determined by trial and error to give the best fit to the completed data. The 25,000 psi term is the relaxation expected at 2,000 days in a constant strain test, and would not have been much larger for very much greater time intervals. The expression is valid only for the case of strands with a  $f_y = 225$  ksi initially stressed up to 189 ksi.

In order to present a more general expression that incorporates the initial prestress value and the yield stress as important factors affecting relaxation losses, the additional relaxation factors  $F_I$  and  $F_R$  were included in the expression for estimating relaxation losses as follows

$$CR_S = F_R F_I^2 [25,000 - 0.3 ES - 0.15 (CR_C + SH)]$$

These factors were found by studying relaxation losses occurring in beams for strands with different yield stresses and initial stresses. Curves for different yield stresses are shown in Figs. 3.8 to 3.10, and similar curves were obtained for different initial stresses.

Similar studies were made for the case of bridge structures prestressed using low-relaxation strands, and it was on the basis of these analyses that the proposed set of prestress loss values were recommended.

## 5. COMPARISON OF PROPOSED SET OF FACTORS WITH OTHER PREDICTION METHODS

This chapter contains a comparison of the prestress loss values obtained from the theoretical method of analysis used in this investigation, the values obtained by using the set of approximate factors proposed in this study, the 1970 AASHO Interim Specifications set of factors, and the 1973 AASHO proposal.

Comparisons have been made for the various components of prestress losses obtained by each one of the methods, even though it is more significant to compare only the total prestress losses.

It is necessary to point out that only the proposed set of factors is capable of estimating the components of prestress loss for the case of structures prestressed with the new type of strands which exhibit low relaxation characteristics. Also, it takes into account different relative humidities of the environment, different time of transfer of prestress, and different member thicknesses. For the case of low-relaxation strands, comparison has been made only with respect to the values obtained from the theoretical method of analysis.

Tabulated values of each of the components of prestress loss as well as total prestress losses are shown in Table 5.1 for stress-relieved strands and in Table 5.2 for low-relaxation strands. A wide variety of example problems has been considered for these comparisons. The variables considered include different cross section girders and decks, time of releasing of prestress, time of casting of the deck, initial stresses in concrete, relative humidity of the environment, and type of prestressing strands. The values are also plotted on Figs. 5.1 to 5.6.

Figure 5.1a shows the total theoretical prestress losses plotted versus the total approximate prestress losses obtained by using the proposed set of factors. The agreement between the approximate procedure proposed in Chapter 4 and the theoretical values is generally quite good. The differences between theoretical and approximate values are rather small, with the differences usually falling between the bounds of  $r$  of 1.05 and 0.95 (where  $r$  is the ratio of approximate to theoretical values).

In Fig. 5.1b, the 1973 AASHO proposal prestress loss values have been plotted versus the theoretical prestress loss values. It can be observed that the AASHO values generally fall below the theoretical values, usually between the bounds of  $r$  of 0.95 and 0.90, for the 80 percent relative humidity cases; however, the AASHO values are found to be too high for the 100 percent relative humidity cases and too low for the 50 percent relative humidity cases, which is to be expected as the creep values were certainly never intended to cover such a high and low, constant relative humidity conditions, but to cover creep values somewhere in the 50-80 percent relative humidity range.

In Fig. 5.1c, the 1970 AASHO prestress loss values have been compared with the theoretical prestress loss values. It can be observed that the 1970 AASHO values fall above the theoretical values, usually between the bounds of  $r$  of 1.05 and 1.15, for the 80 percent relative humidity cases and between the bounds of  $r$  of 1.40 and 1.50 for the 100 percent relative humidity cases. However, good results were obtained for the 50 percent relative humidity cases. These results were expected since the value for creep loss of  $CR_c = 16 f_{cd}$  is considerably too high for most conditions. The



number 16 implies a creep coefficient of  $16/7 = 2.3$ , which is usually too high for a high quality steam cured concrete which is subjected to a continuously decreasing stress. This also explains why good results were obtained for the 50 percent relative humidity cases, as the creep values were never intended to cover such a low, constant relative humidity condition but rather to cover creep values somewhere in the 50 to 80 percent relative humidity range.

Good agreement has also been found when comparing the components of prestress losses (creep and relaxation losses) obtained by using the proposed set of factors with the theoretical loss values as can be seen by observing Figs. 5.2a and 5.3a.

Great differences have been found when comparing the components of prestress losses obtained by using the 1970 and 1973 AASHO Specifications with the theoretical loss values as can be seen in Figs. 5.2b, 5.2c, 5.3b and 5.3c, in spite of getting rather good results when comparing total prestress losses for the case of the 1973 AASHO values.

Considering the wide variety of examples presented, which included a wide range in the main variables known as the main contributors to the magnitude of the prestress losses, the proposed set of factors seems to give good results for the prediction of prestress losses.

Comparisons have been made for the case of low-relaxation strands, but only between the theoretical values and the ones obtained with the proposed procedure since the other prediction methods do not consider low-relaxation strands. Good agreement has also been found for the case of low-relaxation strands, as can be seen in Figs. 5.4 to 5.6.

It is necessary to point out that the proposed set of loss factors are based on the analysis of bridge structures for a period of 2000 days (5.5 years), an age at which the rates of change in prestress losses are extremely low. The theoretical values are those found at 2000 days.

It is necessary to comment on other aspects regarding unknowns not taken into account in the comparison. One problem is the determination of most appropriate value of relative humidity for creep prediction relative to the value for shrinkage. This question comes from the fact that variations of relative humidity and temperature do not affect creep in concrete in the same manner as it influences the magnitude of the shrinkage in concrete. Mossiosian and Gamble (17) came to the conclusion that higher and lower bounds of the expected creep values can be obtained by using lower and higher monthly average values of the relative humidity in the field. Also, "final" shrinkage values can be obtained by using average annual values of the relative humidity in the field, although there are significant cyclic variations in strain during a year.

Secondly, the study carried out in this investigation was mainly based on creep and shrinkage curves obtained by using the 1970 C.E.B. recommendations. Some questions consequently arise concerning the behavior of a bridge structure subjected to field conditions. A few cases were analyzed using creep and shrinkage data of actual structures, such as the Douglas County bridge and Champaign County bridge field data. It was observed that for prestressed concrete bridges located in the Midwest, average values of measured total strains and prestress losses can be computed by using the 50 percent relative humidity creep and 80 percent relative humidity shrinkage

C.E.B. values. Also, upper and lower bounds of total strains and prestress losses are obtained by using the 50 and 80 percent relative humidity creep and shrinkage C.E.B. values respectively.

Finally, the main objective of this study was to get an understanding of the time-dependent prestress losses. However, it is felt that some additional study is needed in the area concerning time-dependent stresses throughout the cross section of a composite girder. Immediately after casting of the deck, stresses are distributed only on the cross section of the girder. With time, some redistribution of stresses is expected in the section due to creep and shrinkage of the concretes and relaxation of the steel, with the result that the concrete deck is subjected to some small stresses and the distribution of stresses over the depth of the cross section of the girder may be quite different from that existing at the time of casting. One result of this redistribution of stresses is that in some members the concrete compression stresses at the bottom of a composite section may remain at approximately the value existing when the deck was cast, in spite of significant reductions in the reinforcement stress which occur after the deck is cast. This information can be computed using the theoretical analysis but needs to be generalized and put into a form which is useful for design purposes.

## 6. CONCLUSIONS AND RECOMMENDATIONS

Based on the results of parametric studies of the time-dependent behavior of various simply supported prestressed concrete members, a set of factors for the estimation of prestress losses for pretensioned concrete bridge girders and other prestressed members were given in Chapter 4. Because the factors take into account the effects of varying environmental conditions, member size, time of transfer of prestress, age of the girders at the time of casting of the deck, deck dead load, initial level of stress at the concrete, and type of prestressing strands (stress-relieved strands or low-relaxation strands), the recommended procedure represents an improvement over the previous methods. The interrelationships which exist between shrinkage, creep, relaxation of the prestressing steel, and elastic losses at release are taken into account.

The conclusions can be summarized as follows:

1. Age at release of prestress obviously makes some difference in the time-dependent prestress losses, with the total prestress losses being greater and the total relaxation losses being smaller for earlier release of prestress.
2. Time of casting of the deck makes some difference in the total prestress losses, with the total prestress losses being slightly smaller for earlier placement of the deck concrete. However, for practical purposes it is conservative to assume that casting of the deck takes place two or three months after the girders are cast; losses for later casting times are not appreciably greater. The differences between

relaxation losses for different times of casting of the deck are negligible. Prestress losses are larger than those computed assuming the deck is always present and smaller than those found ignoring the deck dead load.

3. Prestress losses are affected by the type of prestressing strands, with the losses obviously being greater for the case of stress-relieved strands than for low-relaxation strands under the same conditions. However, the reduction in relaxation losses is partially offset by an increase in creep losses when low-relaxation strands are used. In addition, prestress losses are affected by steel yield stress and initial prestressing. For the same initial steel stress, the greater the yield stress of the steel, the less the total prestress loss, the less the relaxation losses, and the greater the creep losses. For girders prestressed with strands exhibiting the same yield stress, the greater the initial prestressing, the greater the total prestress losses and the greater the relaxation losses.

Due to these facts, two sets of loss factors were recommended, one for the case of stress-relieved strands and the other for low-relaxation strands.

4. The initial stress in the concrete is an important factor influencing prestress losses. The greater the initial prestress level, the greater the total prestress losses and the lower the total relaxation losses.
5. The effects of deck dead load in the total prestress losses

are significant, with the total prestress losses being smallest for the heaviest deck and greatest for the case of no deck.

The effects on the relaxation losses are insignificant.

6. The effects of varying environmental conditions on the total prestress losses are important, with the total prestress losses being greater for the lower average relative humidity. Total strains and total prestress losses of a beam located in the midwest are expected to lie within the bounds established by the 50 and 80 percent relative humidity values. Average values can be found by using a combination of creep at 50 percent R.H. and shrinkage at 80 percent R.H., using C.E.B. values.
7. For the calculation of the concrete stresses immediately after release of prestress, the prestress losses due to relaxation of the steel before release and due to elastic shortening of the concrete at the time of release should be considered.
8. The recommended set of factors is based on the analysis of bridge structures for a period of 2000 days (5.5 years), by which time the rates of change are extremely low.

In summary, the following set of factors for the estimation of prestress losses for pretensioned prestressed concrete members are recommended for design purposes:

For the case of stress-relieved strands:

$$\Delta f_s = SH + ES + CR_C + CR_S \quad (6.1)$$

where:

SH = concrete shrinkage loss

$$= F[14,000 - 1.4(\text{R.H.})^2]$$

$$F = 1.25 - 0.025d_m$$

$d_m$  = theoretical thickness of the member, cm

ES = elastic shortening loss

$$= \frac{E_s}{E_c} f_{cir}, \text{ where } f_{cir} = \text{concrete stress at the level of center of gravity of the prestressing steel immediately after release of prestress, including stress due to dead load of member. The designer could use the more comprehensive procedure given in Sec. 4.2}$$

$CR_c$  = prestress loss due to creep of the concrete

For noncomposite construction

$$CR_c = K (10 f_{cir})$$

where, K = creep factor as a function of the relative humidity and time of transfer of prestress (see Fig. 4.2).

For composite construction

$$CR_c = K (10 f_{cir} - 7 f_{cds})$$

where,  $f_{cds}$  = change in concrete stress at the level of the center of gravity of the prestressing steel due to dead load of the deck concrete and permanent formwork.

$CR_S$  = prestress losses due to stress relaxation of the prestressing steel

$$= F_R \cdot F_I^2 [25,000 - 0.3 ES - 0.15 (SH + CR_C)]$$

where,  $F_R$  = relaxation factor as a function of steel yield

stress.  $F_R = 3.7 - 0.012 f_y$ . If  $f_y = 225$  ksi,  $F_R = 1.0$ ,

and  $F_I$  = relaxation factor as a function of initial pre-

stressing  $F_I = 0.011 f_{si} - 1.08$ . If  $f_{si} = 189$  ksi,  $F_I = 1.0$ .

For the case of low-relaxation strands, Eq. 6.1 is again used, with the following changes in values of terms:

SH and ES as defined for the case of stress-relieved strands.

$CR_C$  = creep loss

For noncomposite construction

$$= K (11 f_{cir})$$

For composite construction

$$= K (11 f_{cir} - 7.0 f_{cds})$$

$CR_S$  = prestress losses due to relaxation of the steel

$$= F_{RL} F_{IL}^2 [7,000 - 0.10 ES - 0.05(SH + CR_C)]$$

where,  $F_{RL}$  = relaxation factor as a function of steel yield

stress,  $F_{RL} = 3.88 - 0.012 f_y$ . If  $f_y = 240$  ksi,  $F_{RL} = 1.0$ .

$F_{IL}$  = relaxation factor as a function of initial prestressing

$F_{IL} = 0.011 f_{si} - 1.255$ . If  $f_{si} = 205$  ksi,  $F_{IL} = 1.0$ .



## 7. SUMMARY

The main purpose of this investigation has been to study the long-time behavior of composite and noncomposite pretensioned prestressed concrete bridge members which are subjected to sustained loads and to either fluctuating temperature and humidity under field conditions or constant environmental conditions. As a result, a much better understanding of the main parameters influencing the time-dependent prestress losses has been gained.

The scope of this investigation was divided in two parts:

1. The analytical study of the main parameters influencing the time-dependent prestress losses.
2. The development of simple expressions for the prediction of prestress losses.

The analytical study included a reexamination of Mossiosian's revised rate of creep method (17) as a method of analysis for the estimation of the time-dependent strains, curvatures, stresses, and prestress losses in simply supported bridges.

The main parameters influencing prestress losses selected in this study were: time of transfer of prestress, age of the girders at the time of casting of the deck, relative humidity, initial stresses in the concrete, deck dead load, type of prestressing strands (stress-relieved strands or low-relaxation strands), creep and shrinkage characteristics of the concrete, and member size (effective thickness or volume/surface ratio).

For purposes of analysis, it was assumed that the principle of superposition was valid and the single effects of each of the main parameters

were treated individually, i.e., in the analysis all variables were included with one at a time being treated as a variable.

Based in this study, two recommended set of factors for the estimation of prestress losses were given, one for the case of stress-relieved strands and the other for the case of low-relaxation strands, as outlined in Chapters 4 and 6.

## LIST OF REFERENCES

1. American Association of State Highway Officials, "Standard Specifications for Highway Bridges," Tenth Edition, 1969.
2. American Association of State Highway Officials, "Standard Specifications for Highway Bridges, Interim Specification--Prestressed Concrete, Section 6," November 1970.
3. American Association of State Highway Officials, "Standard Specifications for Highway Bridges," Eleventh Edition, 1973.
4. ACI Committee 318, "Building Code Requirements for Reinforced Concrete (ACI 318-63)," American Concrete Institute, Detroit, June 1963.
5. ACI Committee 318, "Building Code Requirements for Reinforced Concrete (ACI 318-71)," American Concrete Institute, Detroit, November 1971.
6. ACI Committee 318, "Commentary on Building Code Requirements for Reinforced Concrete (ACI 318-71)," American Concrete Institute, Detroit, November 1971.
7. Anderson, A. R., "Systems Concepts for Precast and Prestressed Concrete Bridge Construction," Highway Research Board, Special Report 132, 1971, pp. 9-21.
8. C.E.B. (European Concrete Committee), "International Recommendations for the Design and Construction of Concrete Structures, Principles and Recommendations," June 1970.
9. Corley, W. G., Sozen, M. A. and Siess, C. P., "Time-Dependent Deflections of Prestressed Concrete Beams," Highway Research Board, Bulletin 307, 1961, pp. 1-25.
10. Gamble, W. L., "Field Investigation of a Continuous Composite Prestressed I-Beam Highway Bridge Located in Jefferson County, Illinois," Structural Research Series No. 360, Civil Engineering Studies, University of Illinois, Urbana, June 1970.
11. Glodowski, R. J. and Lorenzetti, J. J., "A Method for Predicting Prestress Losses in a Prestressed Concrete Structure," PCI Journal, Vol. 17, No. 2, March/April 1972, pp. 17-31.
12. Hansen, T. C. and Mattock, A. H., "Influence of Size and Shape of Member on the Shrinkage and Creep of Concrete," ACI Journal, Proceedings, Vol. 63, No. 2, February 1966, pp. 267-289.
13. Houdeshell, D. M., Anderson, T. C. and Gamble, W. L., "Field Investigation of a Prestressed Concrete Highway Bridge Located in Douglas County, Illinois," Structural Research Series No. 375, Civil Engineering Studies, University of Illinois, Urbana, May 1971.

14. Huang, T., "Prestress Losses in Pretensioned Concrete Structural Members," Fritz Engineering Laboratory Report No. 339.9, Lehigh University, August 1973.
15. Magura, D. D., Sozen, M. A. and Siess, C. P., "A Study of Stress Relaxation in Prestressing Reinforcement," PCI Journal, Vol. 9, No. 2, April 1964, pp. 13-57.
16. McHenry, D., "A New Aspect of Creep in Concrete and its Application to Design," Proceedings, ASTM, Vol. 43, 1943, pp. 1069-1084.
17. Mossiossian, V. and Gamble, W. L., "Time-Dependent Behavior of Non-Composite and Composite Prestressed Concrete Structures Under Field and Laboratory Conditions," Structural Research Series No. 385, Civil Engineering Studies, University of Illinois, Urbana, May 1972.
18. Neville, A. M., "Creep of Concrete: Plain, Reinforced, and Prestressed," North-Holland Publishing Company, Amsterdam, 1970, 622 pp.
19. Preston, H. K., "Private Communication to W. L. Gamble," April 1972.
20. "Proposed Amendment to the AASHTO Standard Specifications for Highway Bridges, Art. 1.6.7(B) Prestress Losses," July 1973.
21. Ross, A. D., "Creep of Concrete Under Variable Stress," ACI Journal, Proceedings, Vol. 54, March 1958, pp. 739-758.
22. Sinno, R. and Furr, H. L., "Hyperbolic Functions of Prestress Losses and Camber," Proceedings of ASCE, Journal of Structural Division, Vol. 96, No. ST4, April 1970, pp. 803-821.
23. Troxell, G. E., Raphael, J. M. and Davis, R. E., "Long-Time Creep and Shrinkage Tests of Plain and Reinforced Concrete," Proceedings, ASTM, Vol. 58, 1958, pp. 1101-1120.

Table 3.1

## Deck Section Properties Used in the Analysis

Section	Deck			$f'_c$ (psi)
	Width (in.)	Thickness (in.)	Weight (plf)	
AASHO-III	0	0	0	-
	60	5	310	3000
	72	7.5	560	3000
	96	8	800	3000
	120	8	1000	3000
Single-Tee	0	0	0	-
	96	1	100	3000
	96	1.5	150	3000
	96	2	200	3000
Double-Tee	0	0	0	-
	96	1	100	3000
	96	1.5	150	3000
	96	2	200	3000
54"-I Beam	60	5	310	3000
	96	8	800	3000
	120	8	1000	3000

Table 3.2  
Chronology of Girder Construction,  
Champaign County Bridge

Date (1972)	Time	Elapsed Time	Task
3 Mar	8:00 am	0:00	Beds clean, bulkheads and holddowns set, all strands place
	8:40	0:40	Start stressing strands
	11:30	3:30	Finish stressing strands
	1:00 pm	5:00	Start placement of deformed bars *
	4:30	8:30	Finish placement of deformed bars *
4 Mar	9:00 am	25:00	Begin to set forms
	10:40	26:40	Finish setting forms
	1:10 pm	28:70	Start placing concrete
	3:00	31:00	Finish casting
	4:00	32:00	Start steam curing
5 Mar	7:00 am	47:00	Start stripping forms
	8:00	48:00	Start installing gage points
6 Mar			Install gage points
7 Mar	8:30 am	96:30	Start zero readings
	10:30	98:30	Finish zero readings
	1:00 pm	101:00	Start cutting strands
	2:00	102:00	Finish cutting strands and move to storage

\* Nonprestressed Reinforcement

Table 3.3  
Bridge Construction and Locations of Girders at Various Times,  
Champaign County Bridge

4 March 1972	Cast Girders BX-5, BX-6
7 March 1972	Release prestress and move beams off beds to storage
28 March 1972	BX-5 arrives at bridge site and is set on piers
4 April 1972	BX-6 arrives at bridge site and is set on piers
3 May 1972	Cast deck

Table 4.1

Prestress Losses Due to Shrinkage of the Concrete,  
1973 AASHO Standard Specifications

Avg. R.H.	SH (psi)
100-75	5000
75-25	10000
25-0	15000

Table 4.2

Prestress Losses Due to Shrinkage of the Concrete,  
1973 Proposed Revision to the AASHO Standard Specifications,  
Section 1.6.7(B)

$$SH = 17000 - 150 \text{ R.H.}$$

Avg. R.H.	SH (psi)
100	2000
90	3500
80	5000
70	6500
60	8000
50	9500
40	11000
30	12500
20	14000
10	15500
0	17000

Table 4.3

Prestress Losses Due to Shrinkage of the Concrete,  
Proposed Shrinkage Loss Value

$$SH = F(14000 - 1.4 R.H.^2)$$

$$F = 1.25 - 0.025 d_m$$

$$d_m = \frac{\text{Area of cross section}}{1/2(\text{Perimeter exposed to atmosphere})}$$

R.H.	100	90	80	70	60	50	40	30	20	10	0
$d_m = 10 \text{ cm}$ $F = 1.0$	0	2660	5040	7140	8960	10500	11760	12740	13440	13860	14000
$d_m = 15 \text{ cm}$ $F = 0.875$	0	2328	4410	6247	7840	9187	10290	11147	11760	12127	12250
$d_m = 20 \text{ cm}$ $F = 0.75$	0	1995	3780	5355	6720	7875	8820	9555	10080	10395	10500



Table 4.4  
Summary of Loss Factors for the Estimation of Prestress Losses

	Shrinkage Loss SH	Elastic Loss ES	Creep Loss CR <sub>C</sub>	Relaxation Loss CR <sub>S</sub>
Proposed Set of Loss Factors (Stress Relieved Strands)	F(14,000 - 1.4R.H. <sup>2</sup> )	$ES = \frac{P_i - P_o}{A_{st}}$ $P_o = \frac{P_i + \frac{M_{DL} e A_{st}^n}{I}}{1 + np + \frac{ne^2 A_{st}}{I}}$ <p>or <math>ES = f_{cir} \frac{E_s}{E_c}</math></p>	K[10f <sub>cir</sub> - 7f <sub>cds</sub> ]	$F_R F_I^2 [25,000 - 0.3ES - 0.15(CR_C + SH)]$
Proposed Set of Loss Factors (Low-Relaxation Strands)	F(14,000 - 1.4R.H. <sup>2</sup> )	Same as above	K[11f <sub>cir</sub> - 7f <sub>cds</sub> ]	$F_{RL} F_{IL}^2 [7,000 - 0.10ES - 0.05 (CR_C + SH)]$
Gamble's Loss Factors	see Table 4.1	$ES = f_{cr} \frac{E_s}{E_c}$	12f <sub>cr</sub> - 7f <sub>cd</sub>	20,000 - 0.4ES - 0.2(CR <sub>C</sub> + SH)
1973 AASHO Proposal	17,000 - 150R.H.	$ES = f_{cir} \frac{E_s}{E_c}$	12f <sub>cir</sub> - 7f <sub>cds</sub>	20,000 - 0.4ES - 0.2(CR <sub>C</sub> + SH)
1973 AASHO Standard Specifications	see Table 4.1	$ES = 7f_{cr}$	16f <sub>cd</sub>	20,000 - 0.125(SH + ES + CR <sub>C</sub> )



Table 5.1  
 Theoretical and Estimated Prestress Losses,  
 Stress-Relieved Strands

Beam Section	Deck* Width x Thickness Weight	Transfer at (days)	Cast Deck (days)	No. of Strands $\phi$ 1/2"	R pe	Elastic Losses (psi)			Relaxation Losses (psi)			
						Proposed	1973 AASHO Proposal	1973 AASHO	Theor.	Proposed	1973 AASHO Proposal	1973 AASHO
AASHO-III	No Deck	2-1/2	--	20		9,057	9,057	10,850	18,699	19,264	11,455	14,918
	No Deck	2-1/2	--	22		10,202	10,202	12,110	18,026	18,612	11,524	14,401
	No Deck	2-1/2	--	22		10,202	10,202	12,110	16,490	16,158	9,603	13,776
	No Deck	2-1/2	--	22		10,364	10,364	12,292	18,085	19,073	11,439	15,420
	96x8-800	1	90	22		9,054	9,054	10,878	18,951	19,831	12,538	16,001
	96x8-800	1	90	20		9,054	9,054	10,878	18,384	19,261	11,877	15,331
	60x5-310	1	90	20		10,364	10,364	11,508	18,504	19,017	11,833	15,740
	96x8-800	1	28	22		10,440			8,760	9,870		
	96x8-800	1	90	22		10,400			10,850	12,160		
	96x8-800	1	90	22		10,320			13,100	14,140		
	96x8-800	1	90	22		10,250			15,530	16,798		
	96x8-800	1	90	22		11,840			30,500	30,580		
	96x8-800	1	90	22		9,750			9,950	11,900		
	96x8-800	1	90	22		10,202	10,202	12,110	18,421	18,922	10,916	14,782
	60x5-310	2-1/2	28	22		10,202	10,202	12,110	18,733	19,415	11,574	15,493
	96x8-800	2-1/2	180	22		10,202	10,202	12,110	18,816	19,415	11,574	15,493
	96x8-800	2-1/2	90	22		10,202	10,202	12,110	18,548	19,174	11,252	15,165
	72x7.5-560	2-1/2	90	22		10,202	10,202	12,110	20,765	20,863	12,175	15,493
	96x8-800	2-1/2	90	22		10,202	10,202	12,110	20,410	20,687	11,519	14,825
	60x5-310	2-1/2	90	22		9,057	9,057	10,843	21,377	21,379	13,133	16,015
	96x8-800	2-1/2	90	20		11,332	11,332	13,370	20,179	20,353	11,227	14,977
	96x8-800	2-1/2	90	24		11,332	11,332	13,370	18,157	18,765	10,625	14,977
	96x8-800	2-1/2	90	24		12,447	12,447	14,602	17,539	18,125	9,691	14,469
	96x8-800	2-1/2	90	26		9,057	9,057	10,843	19,510	20,073	12,533	16,015
	96x8-800	2-1/2	90	20		9,057	9,057	10,843	18,007	18,364	11,633	15,390
	96x8-800	2-1/2	90	20		9,057	9,057	10,843	19,950	20,068	12,526	16,015
	96x8-800	2-1/2	28	20		10,202	10,202	12,110	17,263	17,497	10,674	14,868
	96x8-800	2-1/2	90	22		10,202	10,202	12,110	18,115	18,748	11,267	14,870
	96x8-800	2-1/2	90	22		10,202	10,202	12,110	19,625	20,113	11,867	15,495
	96x8-800	2-1/2	90	22		10,202	10,202	12,110	16,743	16,679	10,019	14,200
	60x5-310	2-1/2	90	22		9,054	9,054	10,843	19,090	19,576	11,871	15,345
	60x5-310	2-1/2	28	20		10,202	10,202	12,110	19,015	19,410	11,567	15,495
	96x8-800	2-1/2	56	22		9,054	9,054	11,508	19,750	20,275	12,803	16,206
	120x8-1000	2-1/2	90	20		11,332	11,332	13,370	16,571	16,640	9,725	14,352
	96x8-800	2-1/2	90	24		9,054	9,054	11,508	18,937	19,578	12,079	15,262
	60x5-310	2-1/2	90	20		10,120	10,120	12,019	19,285	19,609	11,643	15,532
	96x8-800	4	90	22		9,864	9,864	11,781	19,380	19,510	11,200	14,962
	60x5-310	7	90	22		10,965	10,965	13,073	19,370	19,337	10,932	15,124
	96x8-800	7	90	24		9,864	9,864	11,781	19,939	19,920	11,857	15,630
	96x8-800	7	90	22		8,746	8,746	10,528	20,542	20,512	12,794	16,143
	96x8-800	7	90	20		10,202	10,202	12,110	20,001	20,421	11,103	14,401
	No Deck	2-1/2	--	22								
Single-Tee	No Deck	2-1/2	--	12		8,170	8,170	9,562	17,926	19,582	12,194	15,447
	No Deck	2-1/2	--	14		11,020	11,020	12,390	16,121	17,956	9,820	14,286
	No Deck	2-1/2	--	16		13,778	13,778	15,134	14,602	16,383	7,524	13,159
	No Deck	2-1/2	--	16		8,170	8,170	9,562	18,949	20,311	13,167	16,467
	96x2-200	2-1/2	90	12		11,020	11,020	12,390	16,951	18,675	10,779	15,306
	96x2-200	2-1/2	90	14		13,778	13,778	15,134	15,280	17,092	8,471	14,179
	96x2-200	2-1/2	90	16		11,020	11,020	12,390	16,715	18,495	10,540	15,052
	96x1.5-150	2-1/2	90	14		11,020	11,020	12,390	16,484	18,316	10,301	14,796
96x1-100	2-1/2	90	14									
Double-Tee	No Deck	2-1/2	--	18		5,853	5,853	8,379	19,678	20,904	14,124	15,933
	No Deck	2-1/2	--	24		11,264	11,264	14,014	16,151	17,816	9,617	13,619
	96x2-200	2-1/2	90	18		5,853	5,853	8,379	20,844	21,650	15,126	16,979
	96x2-200	2-1/2	90	24		11,264	11,264	14,014	16,840	18,547	10,592	14,665
	96x2-200	2-1/2	90	24		5,853	5,853	8,379	20,533	21,467	14,876	16,717
	96x1.5-150	2-1/2	90	18		7,696	7,696	10,297	17,333	18,564	12,435	15,931
	96x1.5-150	2-1/2	90	20		11,264	11,264	14,014	16,620	18,364	10,348	14,403
	96x1.5-150	2-1/2	90	24		11,264	11,264	14,014	16,401	18,182	10,104	14,143
96x1-100	2-1/2	90	24									
54" I Beam	96x8-800	2-1/2	90	34		11,668	11,668	14,273	18,796	18,563	10,320	14,646
	60x5-310	2-1/2	90	30		9,984	9,984	12,243	18,414	19,060	11,116	14,786
	120x8-1000	2-1/2	90	34		11,668	11,668	14,273	19,030	18,769	10,596	14,930
	60x5-310	2-1/2	90	34		11,668	11,668	14,273	18,255	18,055	9,644	13,952
	96x8-800	2-1/2	90	32		10,824	10,824	13,188	18,501	19,089	11,094	15,090
	96x8-800	2-1/2	90	30		9,984	9,984	12,243	19,003	19,572	11,798	15,480

Table 5.2

Comparison of Theoretical and Estimated Prestress Losses,  
Low-Relaxation Strands

Beam Section	Deck	Release at (days)	Cast Deck (days)	No. of Strands	R.H.	$f_{cir}$	$f_{c ds}$	Total Loss (psi)		$CR_c$ (psi)		SH (psi)		ES (psi)		$CR_s$ (psi)	
								Theor.	Proposed	Theor.	Proposed	Theor.	Proposed	Theor.	Proposed	Theor.	Proposed
Single-Tee		2-1/2	90	12	80	1857	696	36,393	35,830	16,192	15,555	5,348	5,040	10,295	10,295	4,558	4,940
		2-1/2	90	14	80	2427	685	45,931	44,707	22,982	21,902	5,348	5,040	13,458	13,453	4,143	4,307
		2-1/2	90	16	80	2979	676	54,726	53,289	29,075	28,037	5,348	5,040	16,518	16,518	3,784	3,694
AASHO-III	96x8-800	2-1/2	90	24	80	2311	761	40,996	41,214	19,780	20,094	3,835	3,780	12,816	12,816	4,564	4,524
	60x5-800	2-1/2	90	24	80	2311	295	45,105	44,313	23,984	23,356	3,835	3,780	12,816	12,816	4,469	4,361
	96x8-800	2-1/2	90	22	80	1947	765	33,978	33,983	15,912	16,062	3,835	3,780	10,794	10,794	3,436	3,347
	96x8-800	2-1/2	90	20	80	1859	771	34,081	34,168	15,086	15,052	3,835	3,780	10,309	10,309	4,852	5,027
	96x8-800	1	90	20	80	1866	771	35,877	36,428	17,014	17,398	3,835	3,780	10,343	10,343	4,683	4,907
	96x8-800	7	90	20	80	1852	771	30,900	31,683	11,718	12,474	3,835	3,780	10,269	10,269	5,077	5,160
	96x8-800	4	90	20	80	1856	770	32,617	33,043	13,533	13,884	3,835	3,780	10,291	10,291	4,957	5,088
	96x8-800	2-1/2	90	20	80	1731	770	30,635	30,540	13,638	13,651	3,835	3,780	9,599	9,599	3,560	3,510
	96x8-800	1	90	22	80	1678	766	29,600	30,080	14,670	15,060	3,835	3,780	9,300	9,300	1,794	1,940
54"-I-Beam	96x8-800	2-1/2	90	30	80	1903	796	33,910	34,681	15,154	15,361	3,835	3,780	10,552	10,552	4,368	4,988

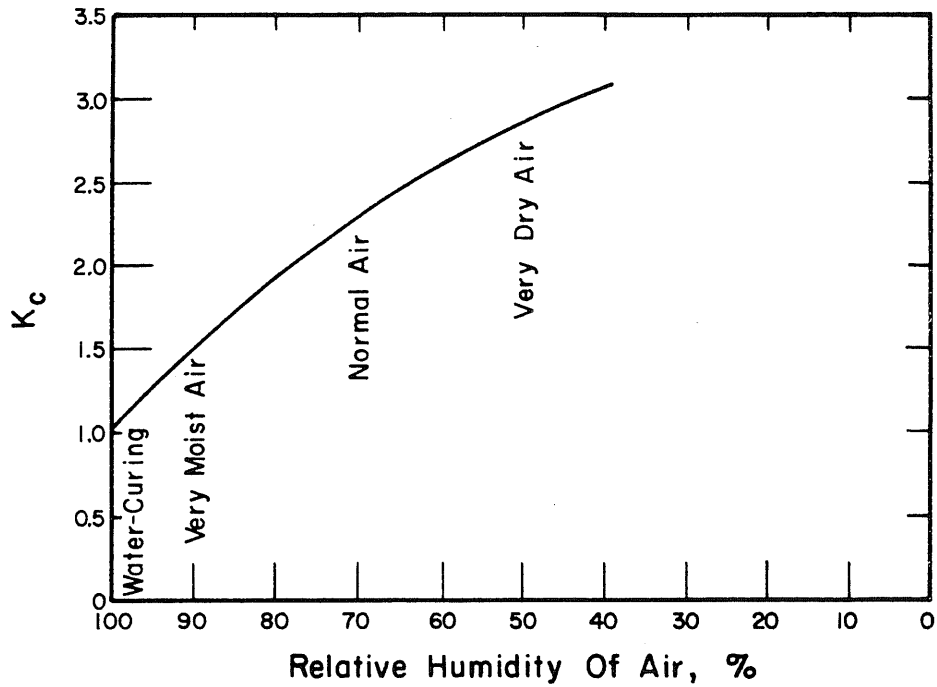


Fig. 2.1 European Concrete Committee Creep Prediction Factor Coefficient  $K_c$  vs. Relative Humidity

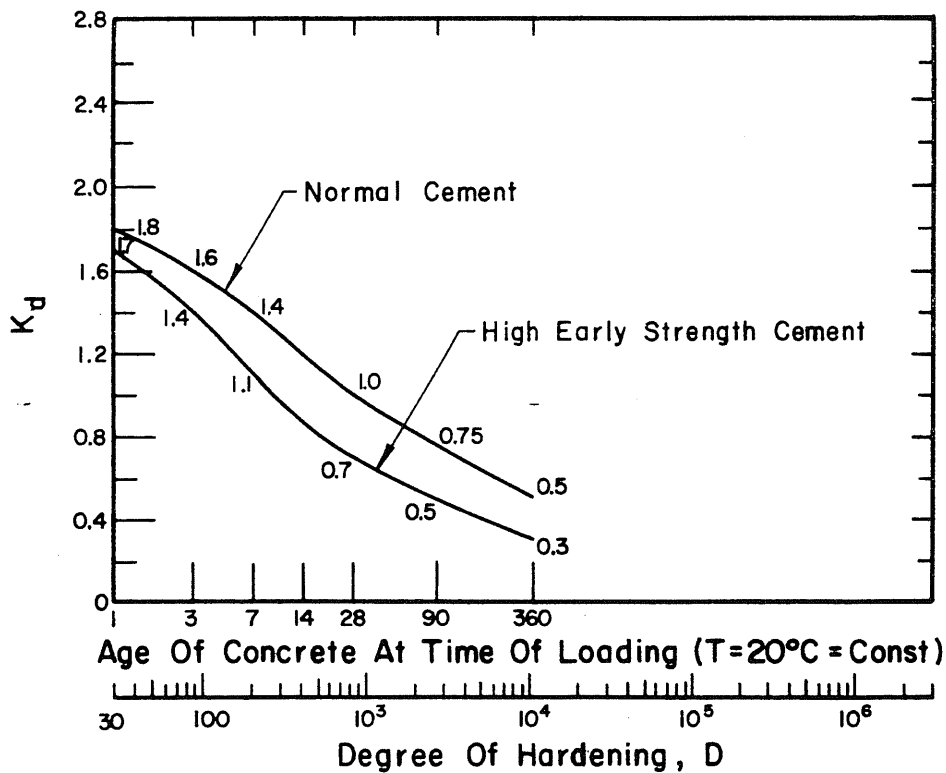


Fig. 2.2 European Concrete Committee Creep Prediction Factor Coefficient  $K_d$  vs. Age at Loading

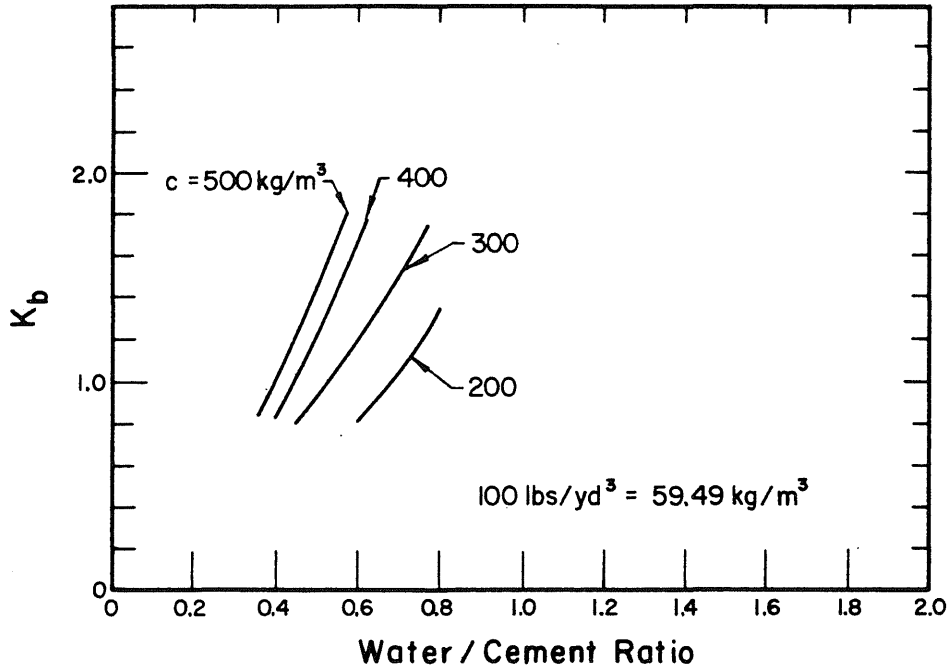


Fig. 2.3 European Concrete Committee Creep Prediction Factor Coefficient  $K_b$  vs. Mix Properties

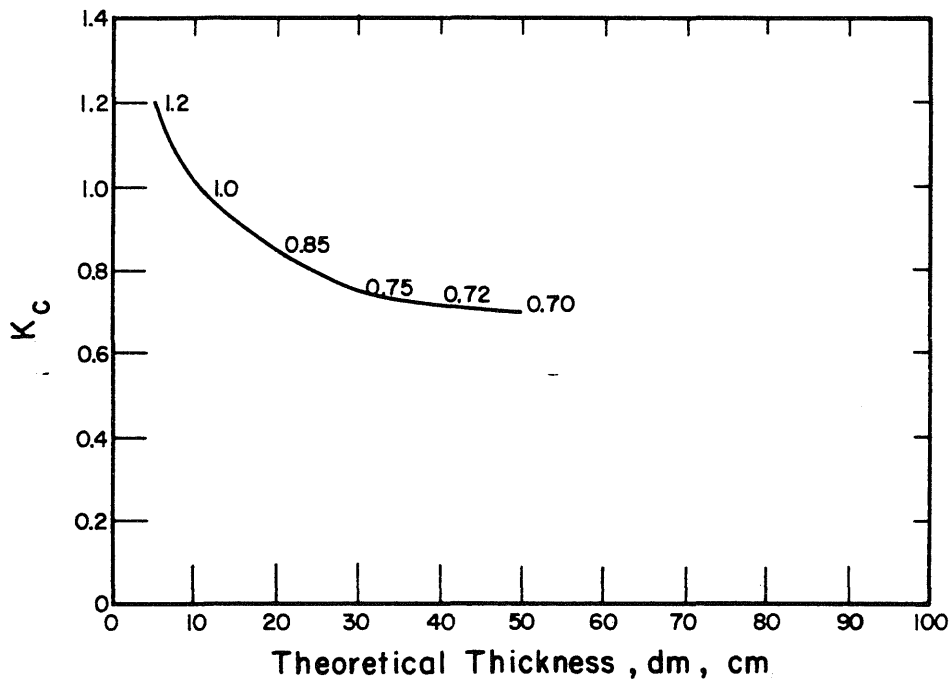


Fig. 2.4 European Concrete Committee Creep Prediction Factor Coefficient  $K_e$  vs. Theoretical Thickness

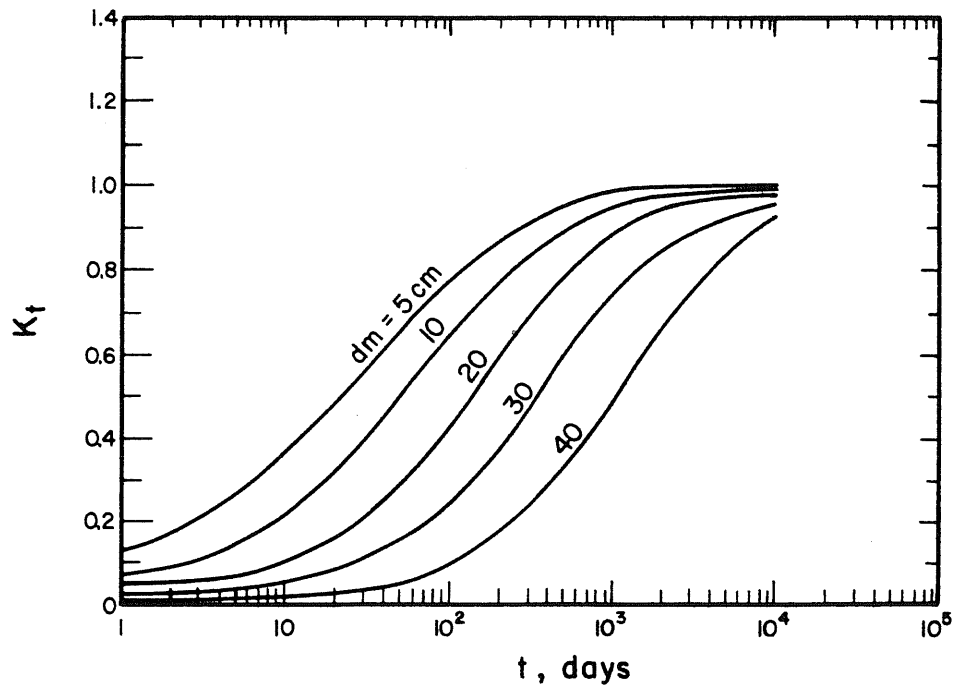


Fig. 2.5 European Concrete Committee Creep Prediction Factor Coefficient  $K_t$  vs. Time

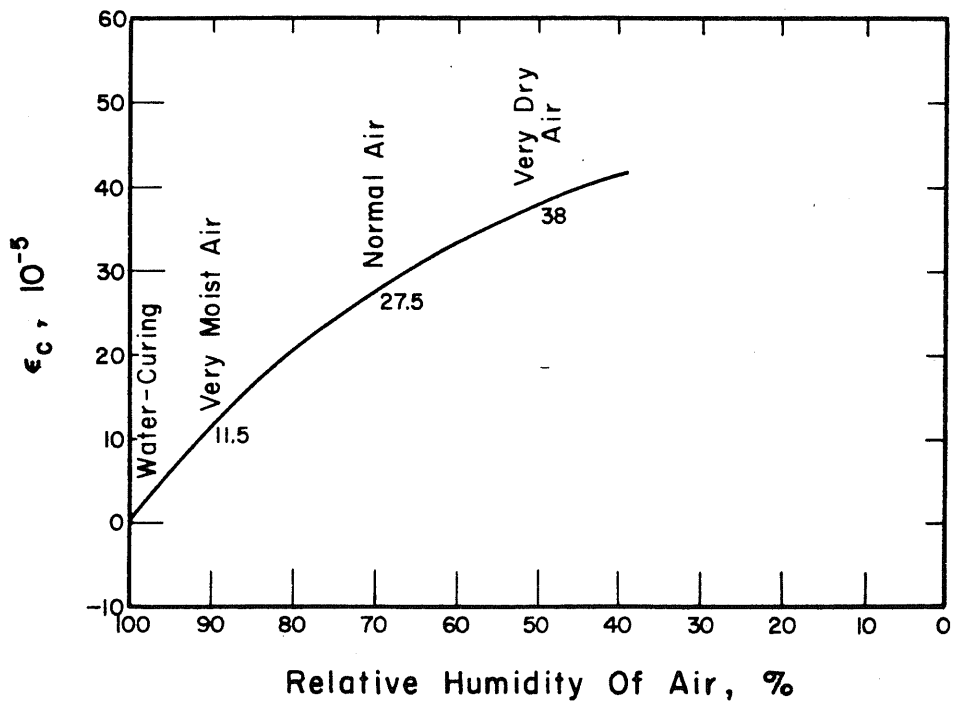


Fig. 2.6 European Concrete Committee Shrinkage Prediction Factor Coefficient  $\epsilon_c$  vs. Relative Humidity

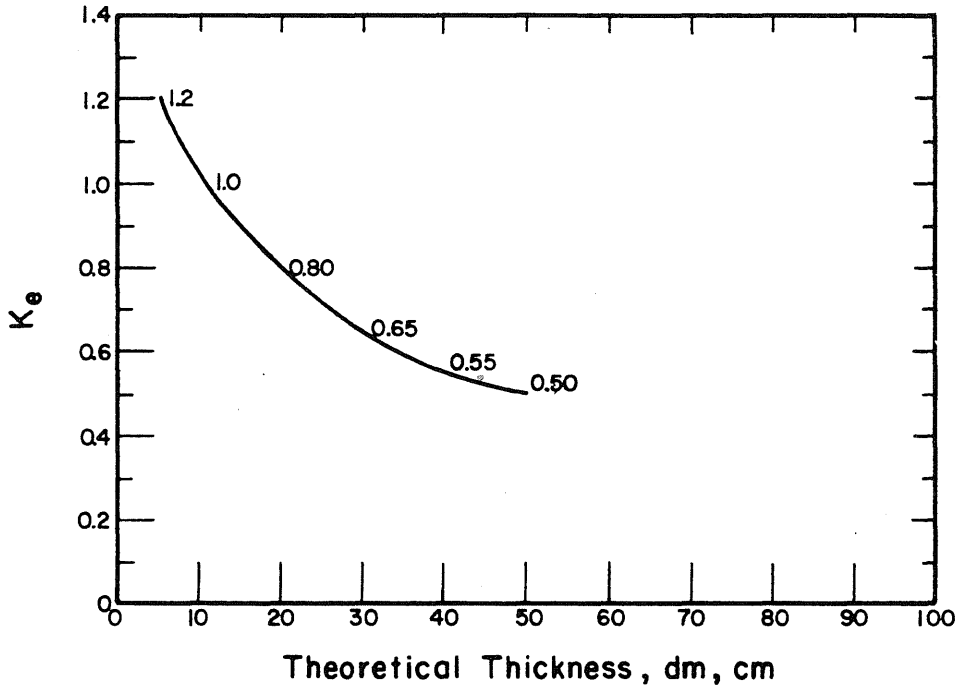


Fig. 2.7 European Concrete Committee Shrinkage Prediction Factor Coefficient  $K_e$  vs. Theoretical Thickness

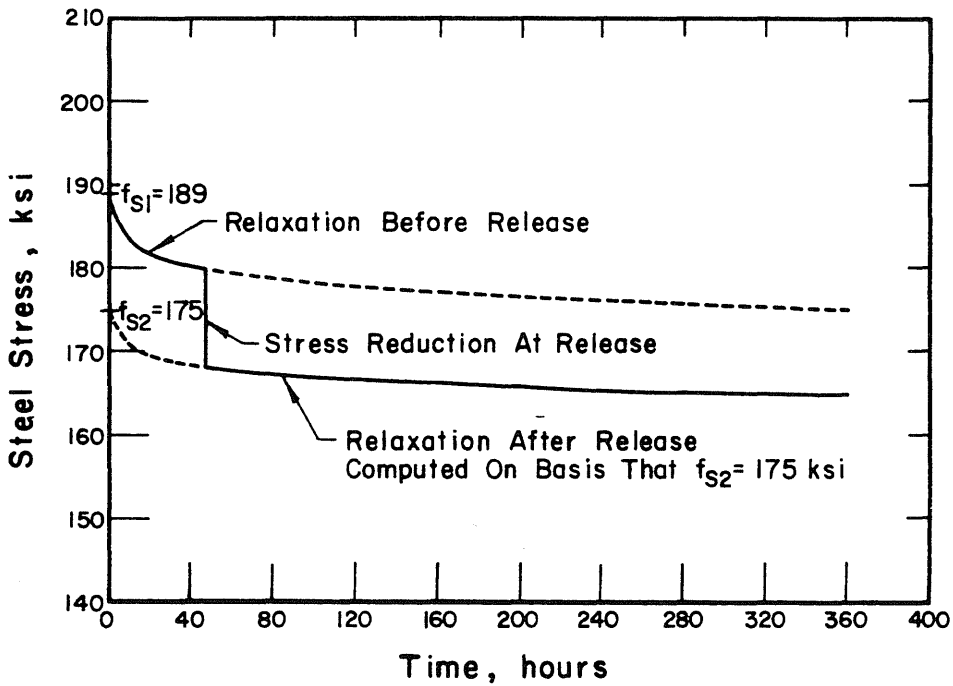


Fig. 2.8 Relaxation Loss When Including Stress Reduction at Time  $t$



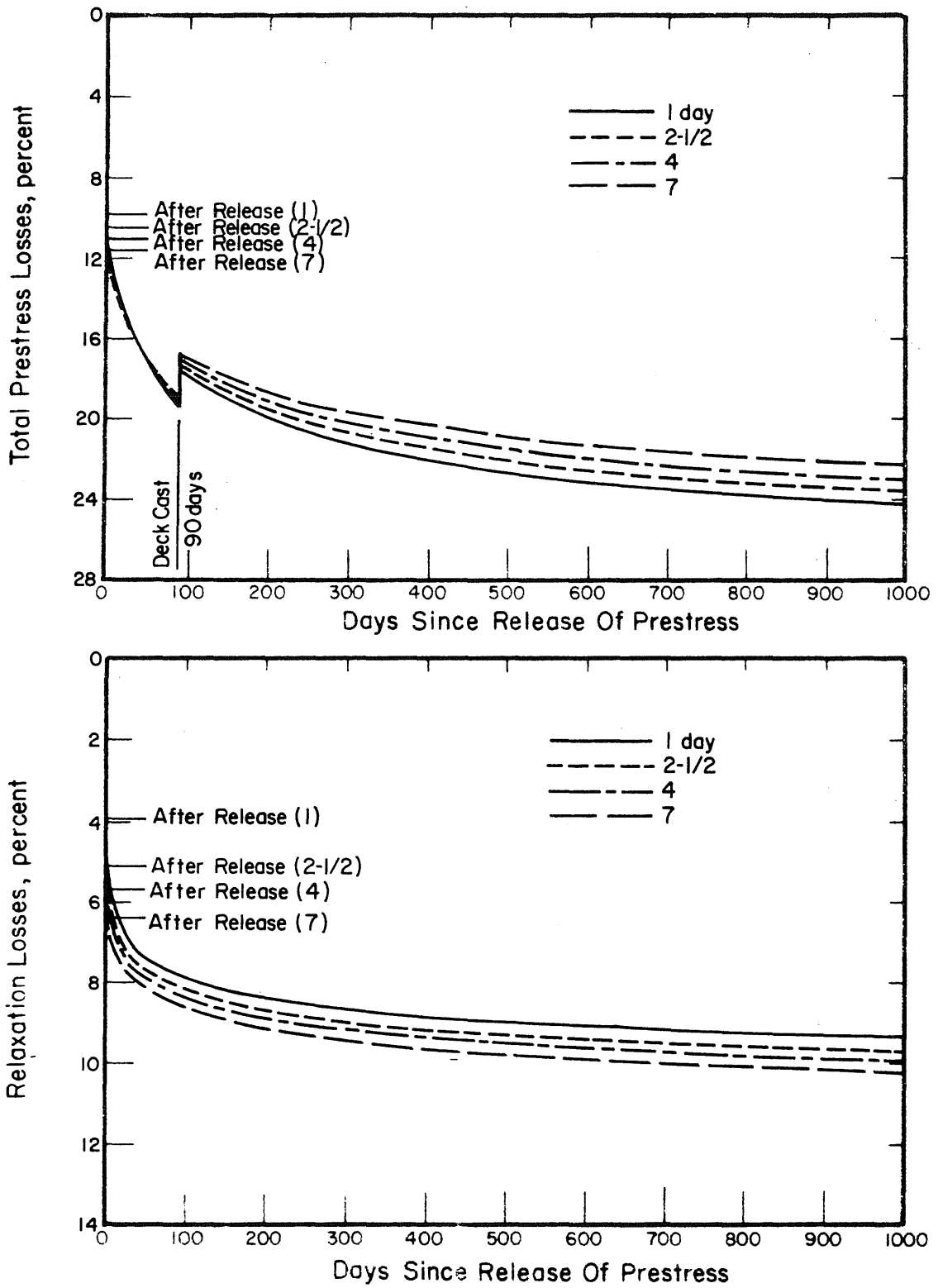


Fig. 3.1 Effect of Time of Transfer of Prestress on Total Prestress Losses and Relaxation Losses, AASHO-III Beam, Stress-Relieved Strands,  $f_{sj} = 189$  ksi

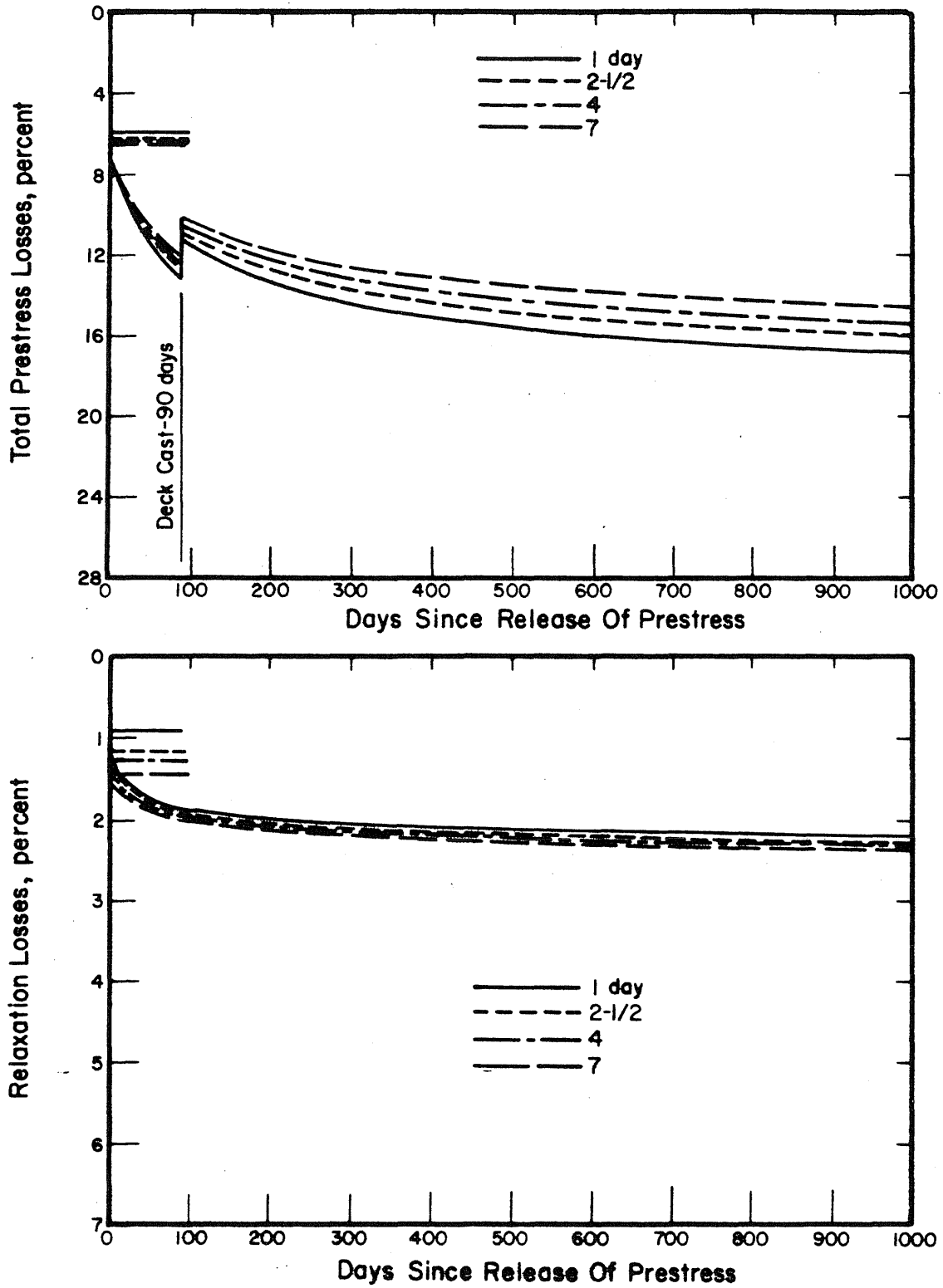


Fig. 3.2 Effect of Time of Transfer of Prestress on Total Prestress Losses and Relaxation Losses, AASHTO-III Beam, Low-Relaxation Strands,  $f_{si} = 205$  ksi

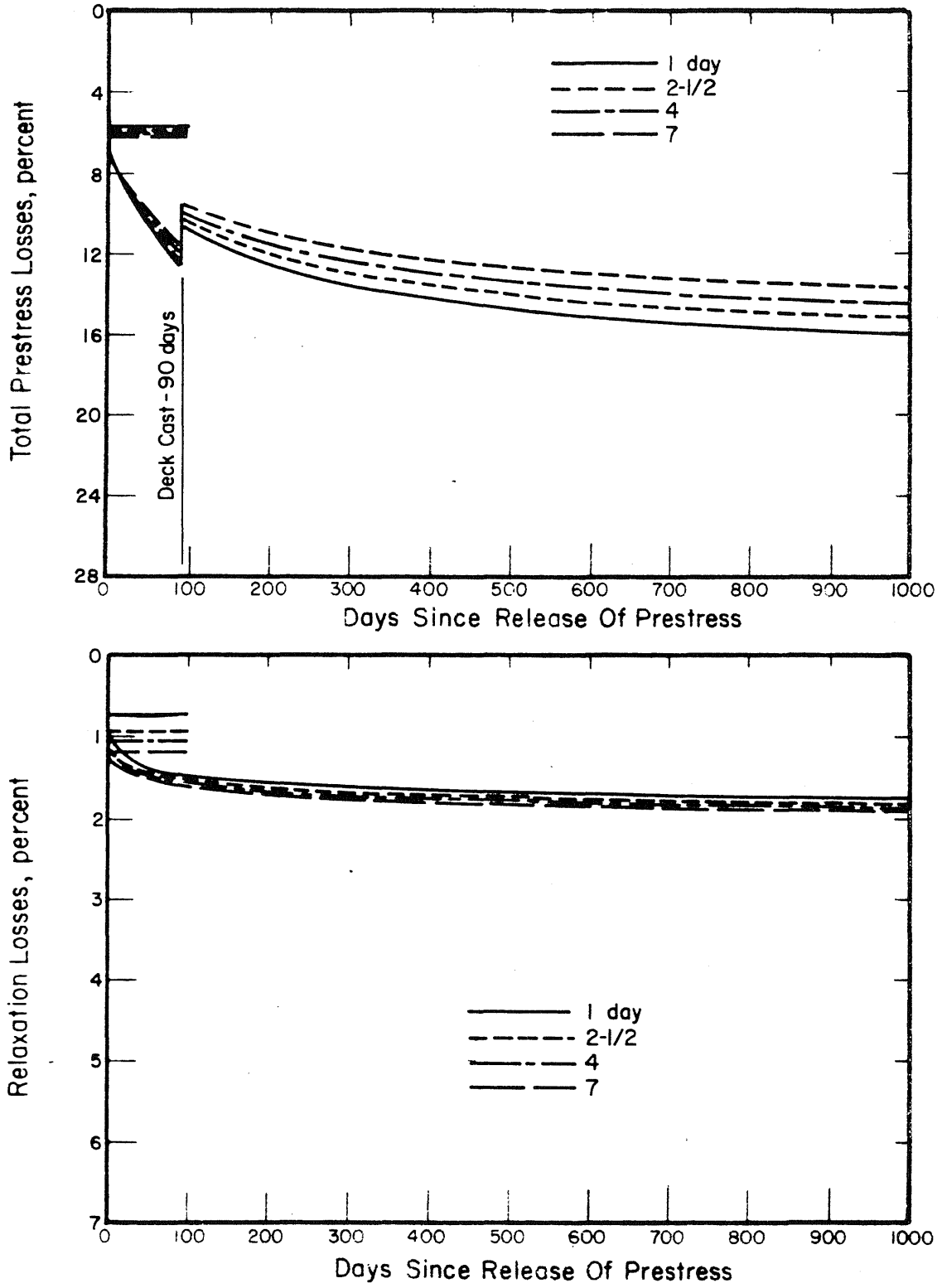


Fig. 3.3 Effect of Time of Transfer of Prestress on Total Prestress Losses and Relaxation Losses, AASHO-III Beam, Low-Relaxation Strands,  $f_{sj} = 189$  ksi

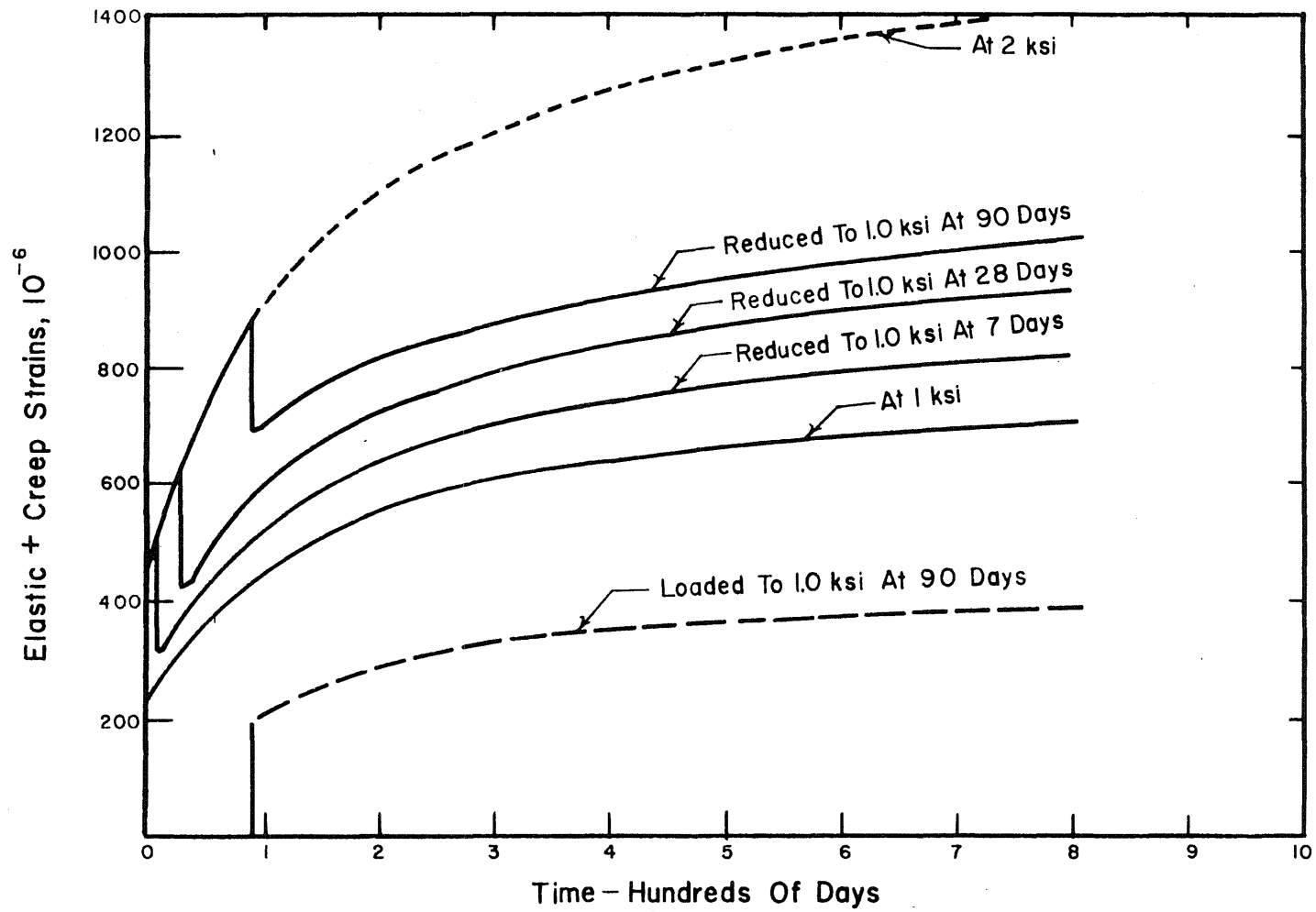


Fig. 3.4 Elastic Plus Creep Strain Versus Time Under Reducing Stress Conditions

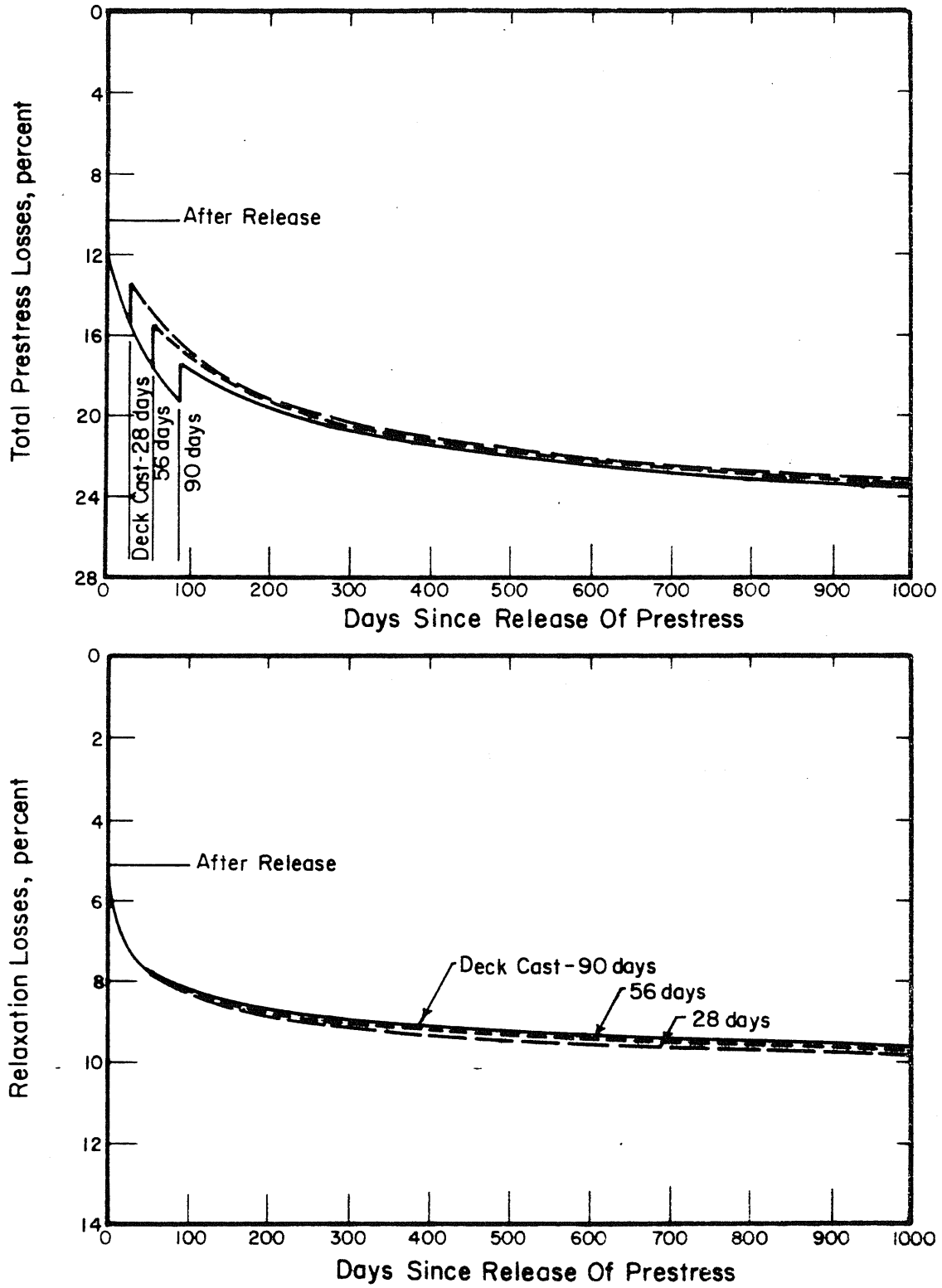


Fig. 3.5 Effect of Age of Girders at the Time of Casting of Deck on Total Prestress Losses and Relaxation Losses, AASHO-III Beam

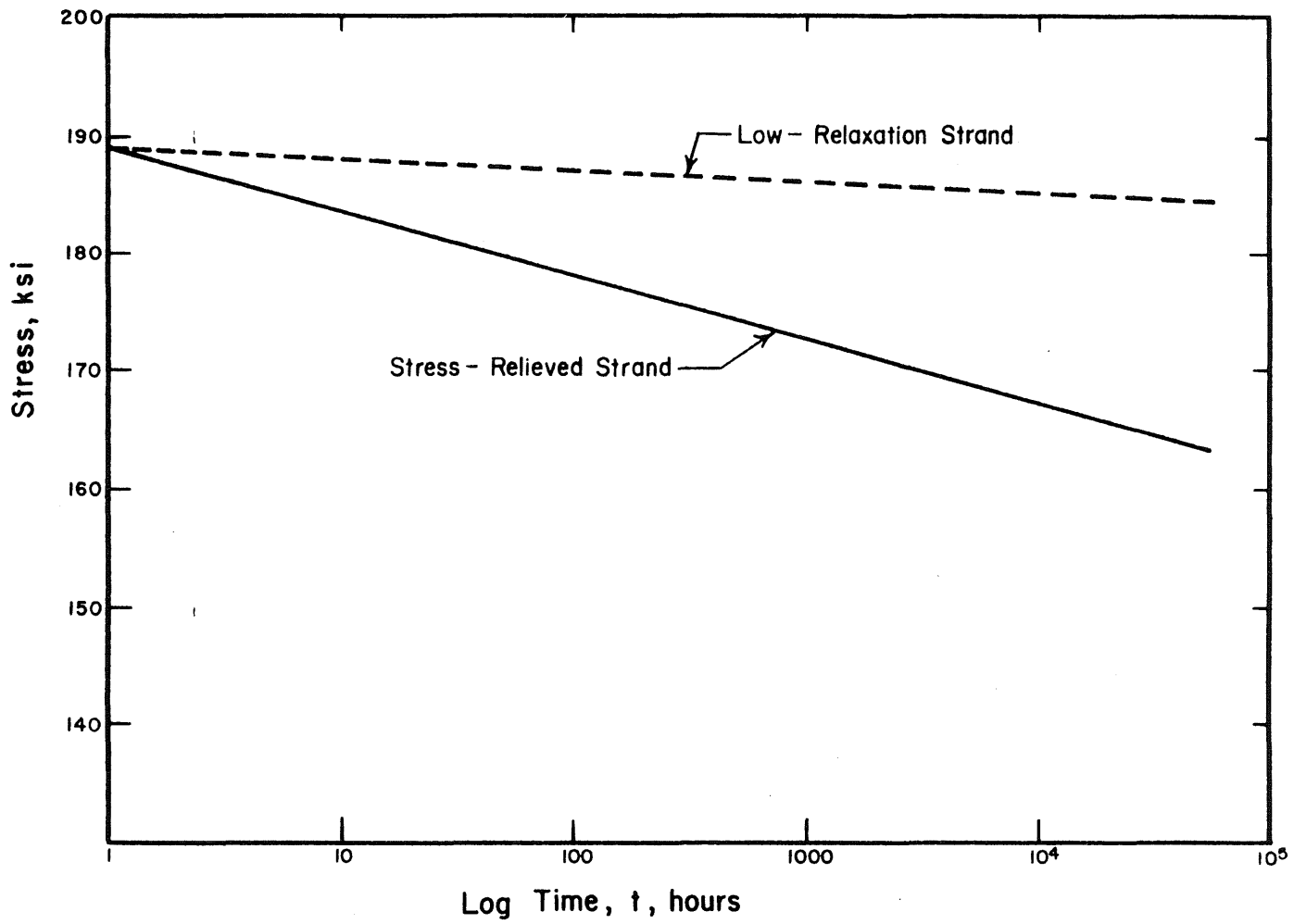


Fig. 3.6 Pure Relaxation of Steel Stress

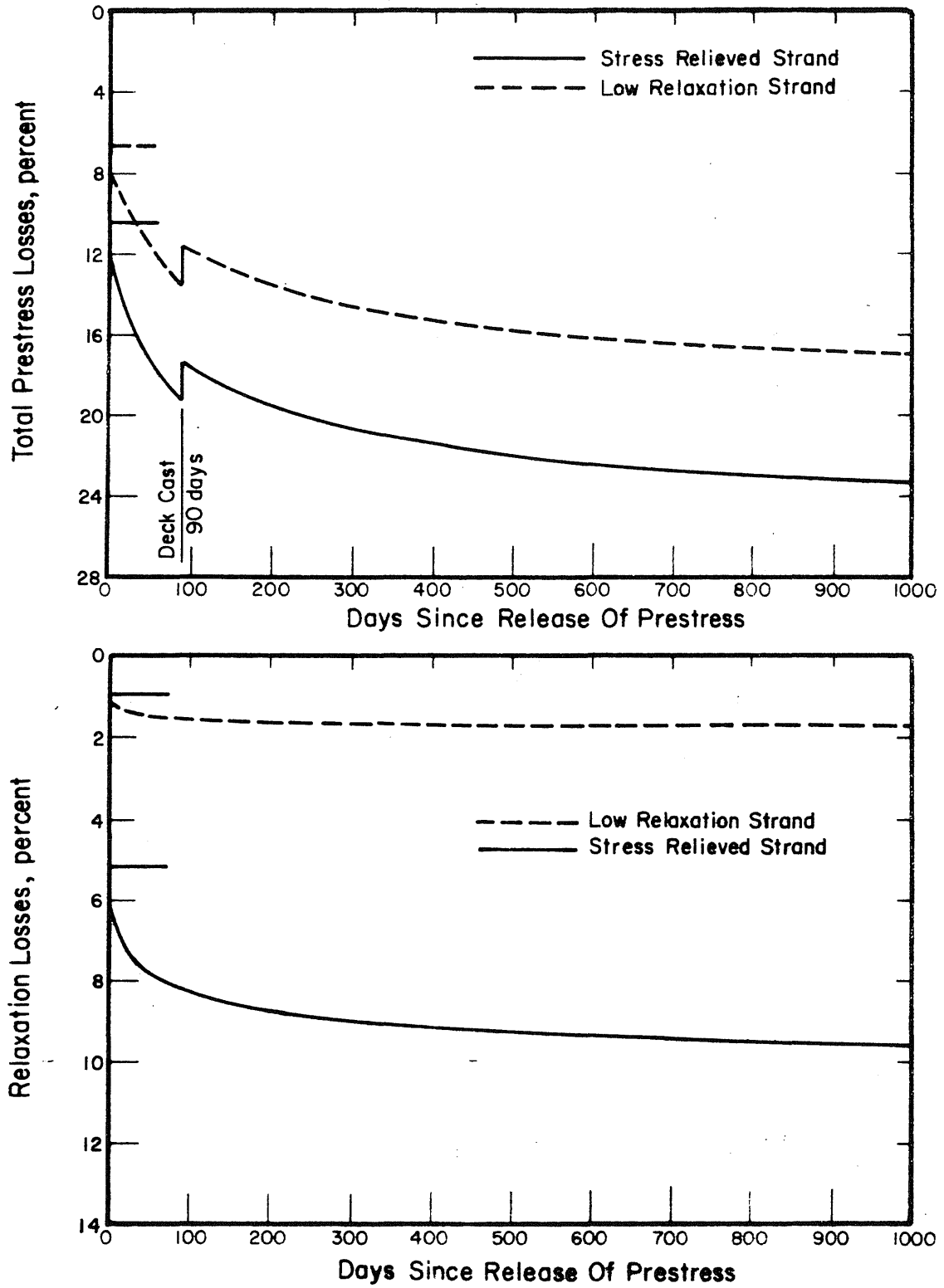


Fig. 3.7 Effect of Type of Prestressing Strand on Total Prestress Losses, Relaxation Losses and Creep Losses, AASHO-III Beam

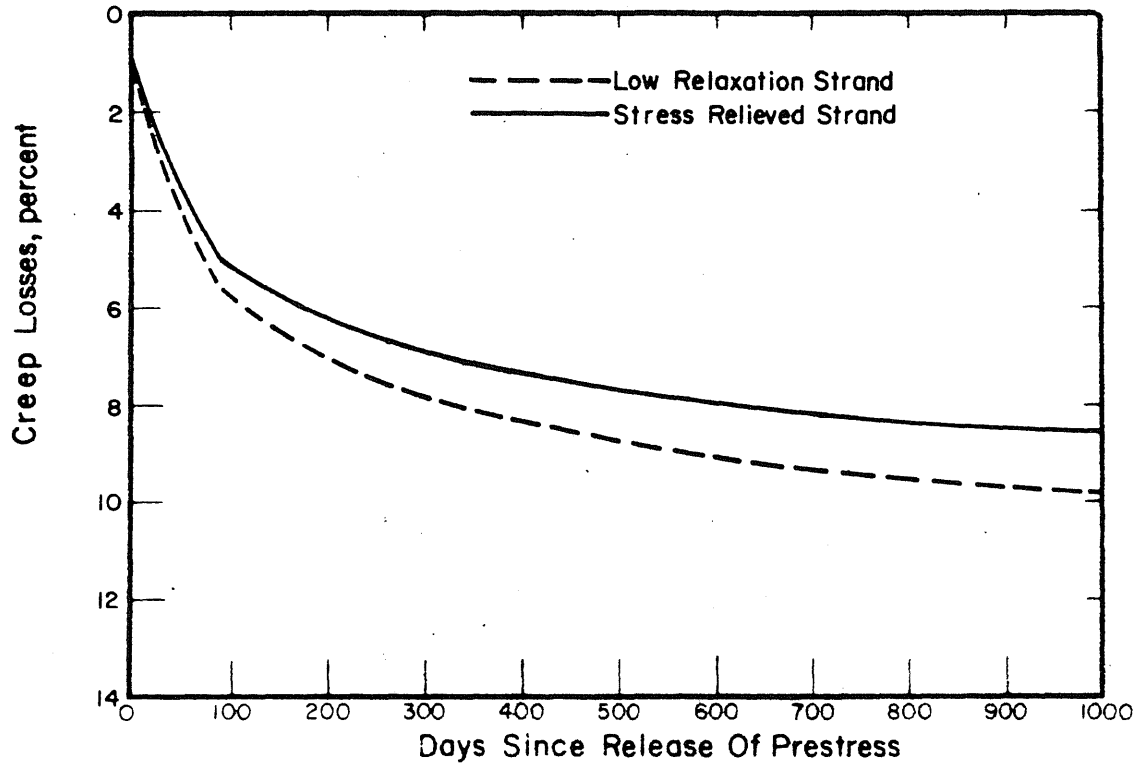


Fig. 3.7 (Continued)



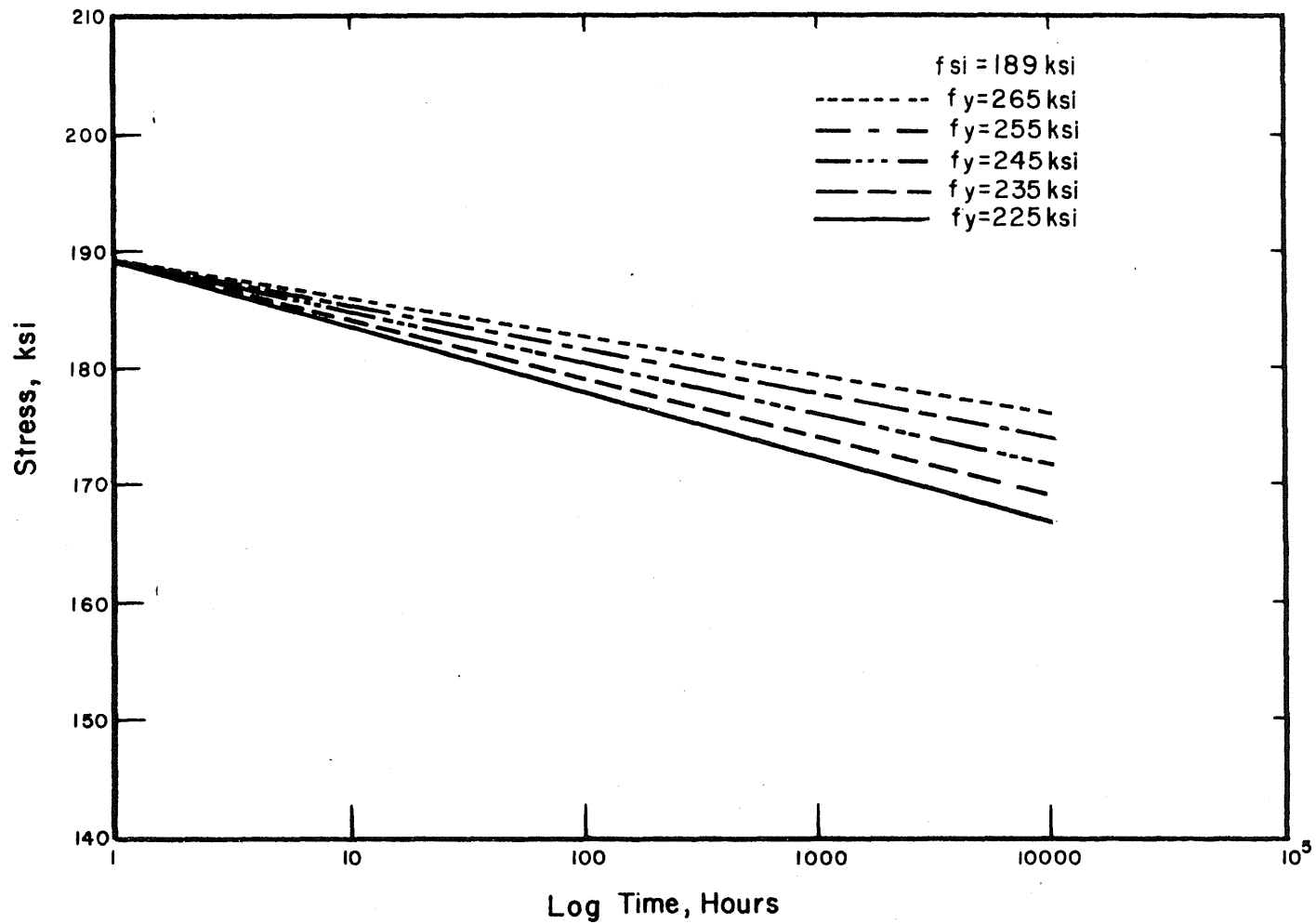


Fig. 3.8 Effect of Steel Yield Stress on Pure Relaxation Losses,  
 $f_{si} = 189$  ksi

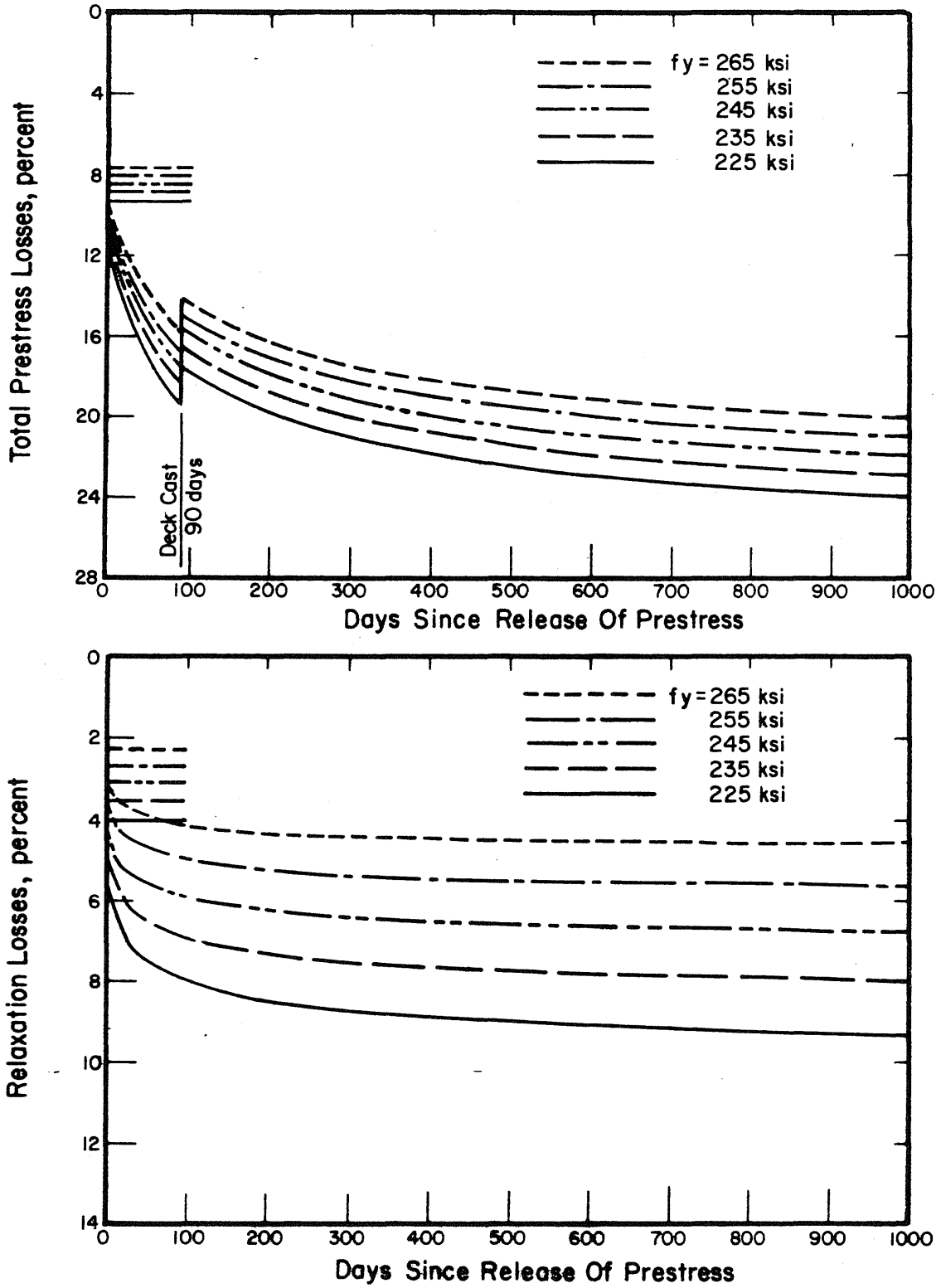


Fig. 3.9 Effect of Steel Yield Stress on Total Prestress Losses, Relaxation Losses and Creep Losses, AASHO-III Beam, Stress-Relieved Strands,  $f_{si} = 189$  ksi

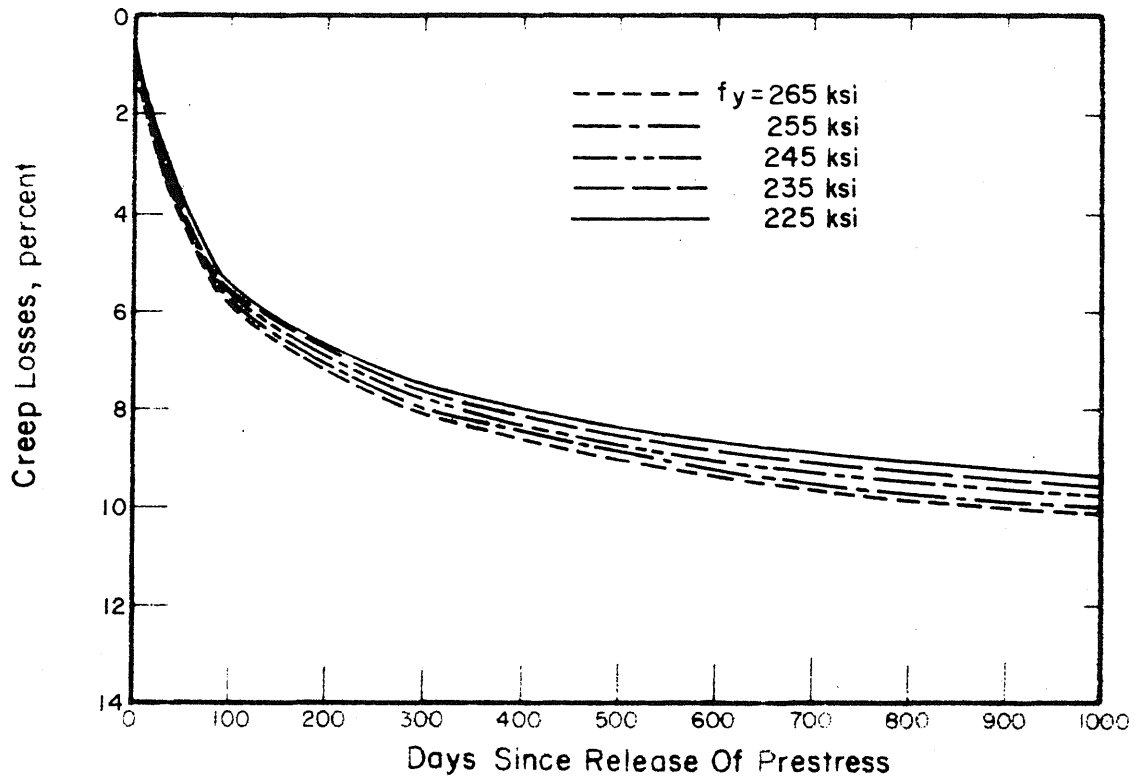


Fig. 3.9 (Continued)

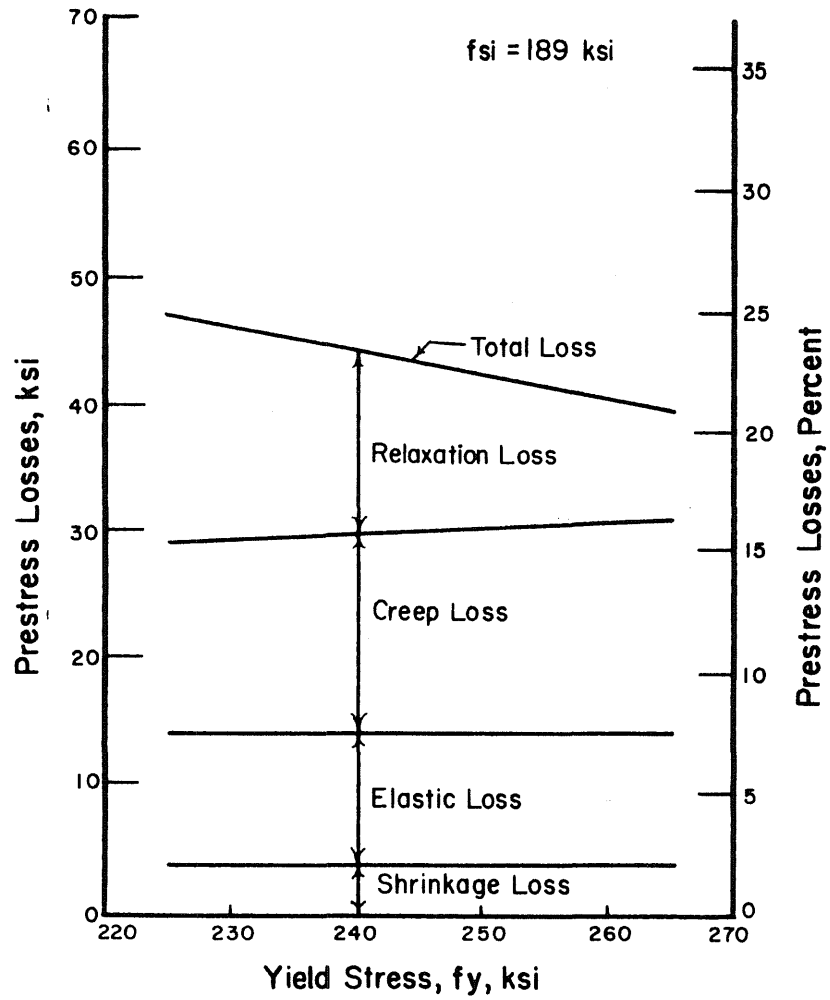


Fig. 3.10 Effect of Steel Yield Stress on the Components of Prestress Losses, AASHO-III Beam, Stress-Relieved Strands,  $f_{si} = 189$  ksi

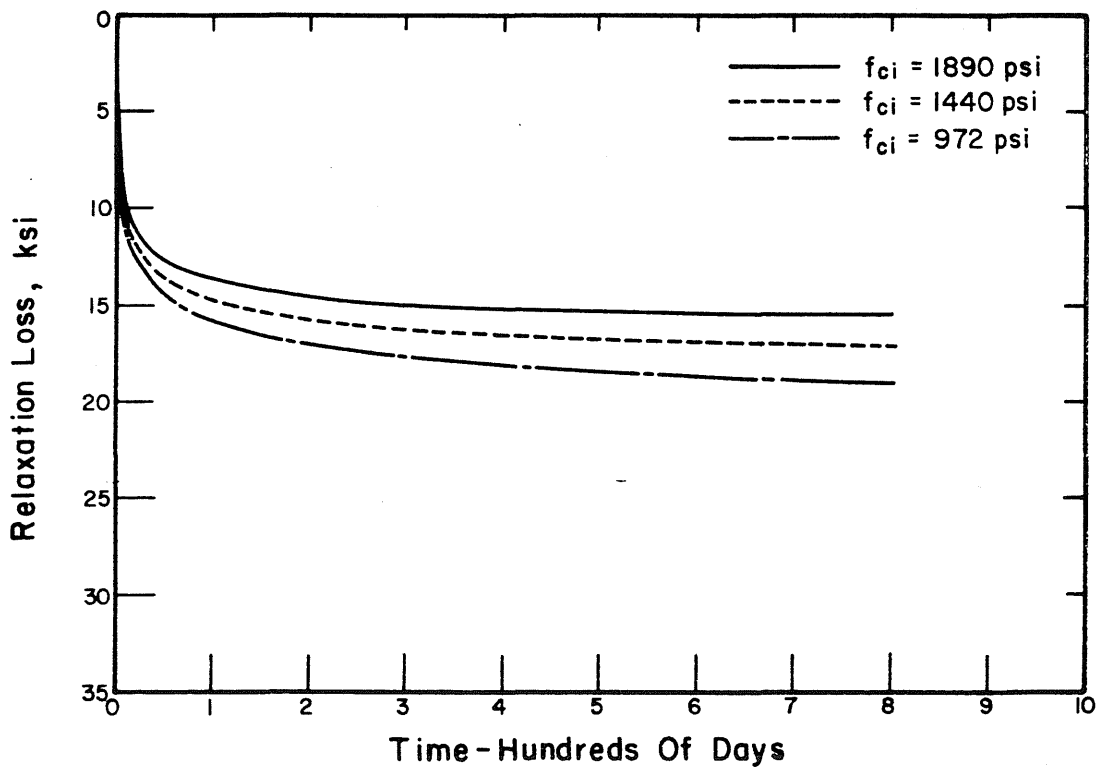
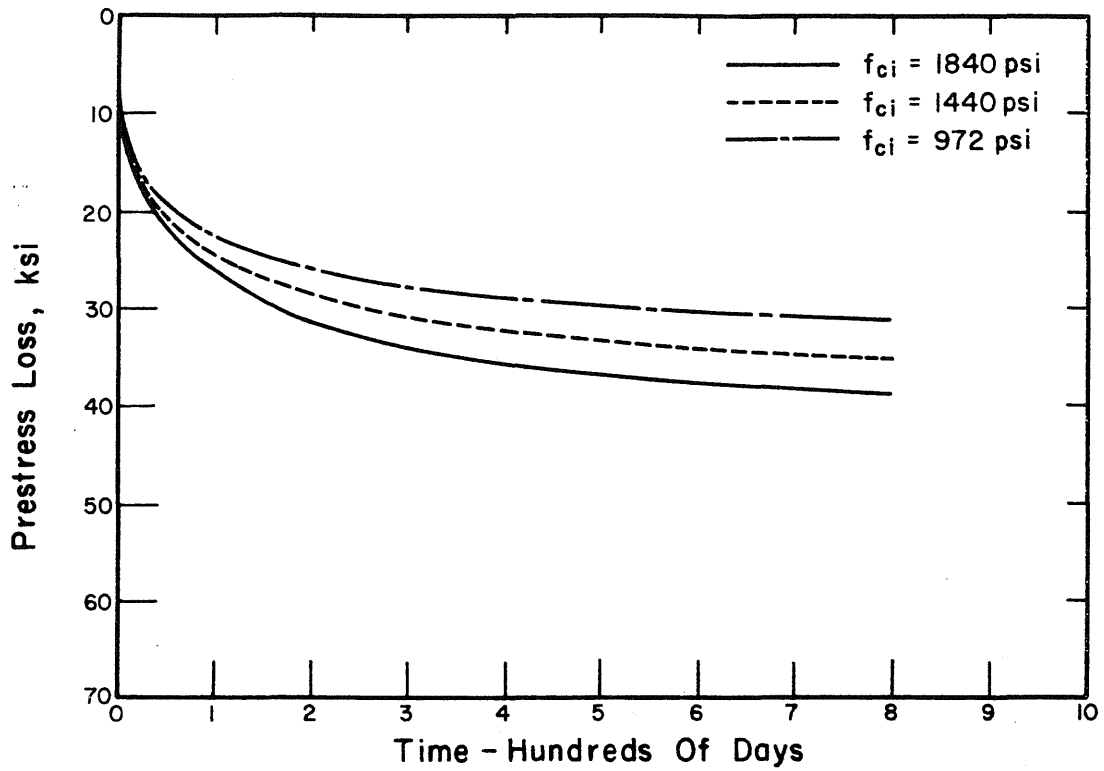


Fig. 3.11 Effect of Initial Stresses in Concrete on Total Prestress Losses and Relaxation Losses, Prestressed Concrete Cylinder

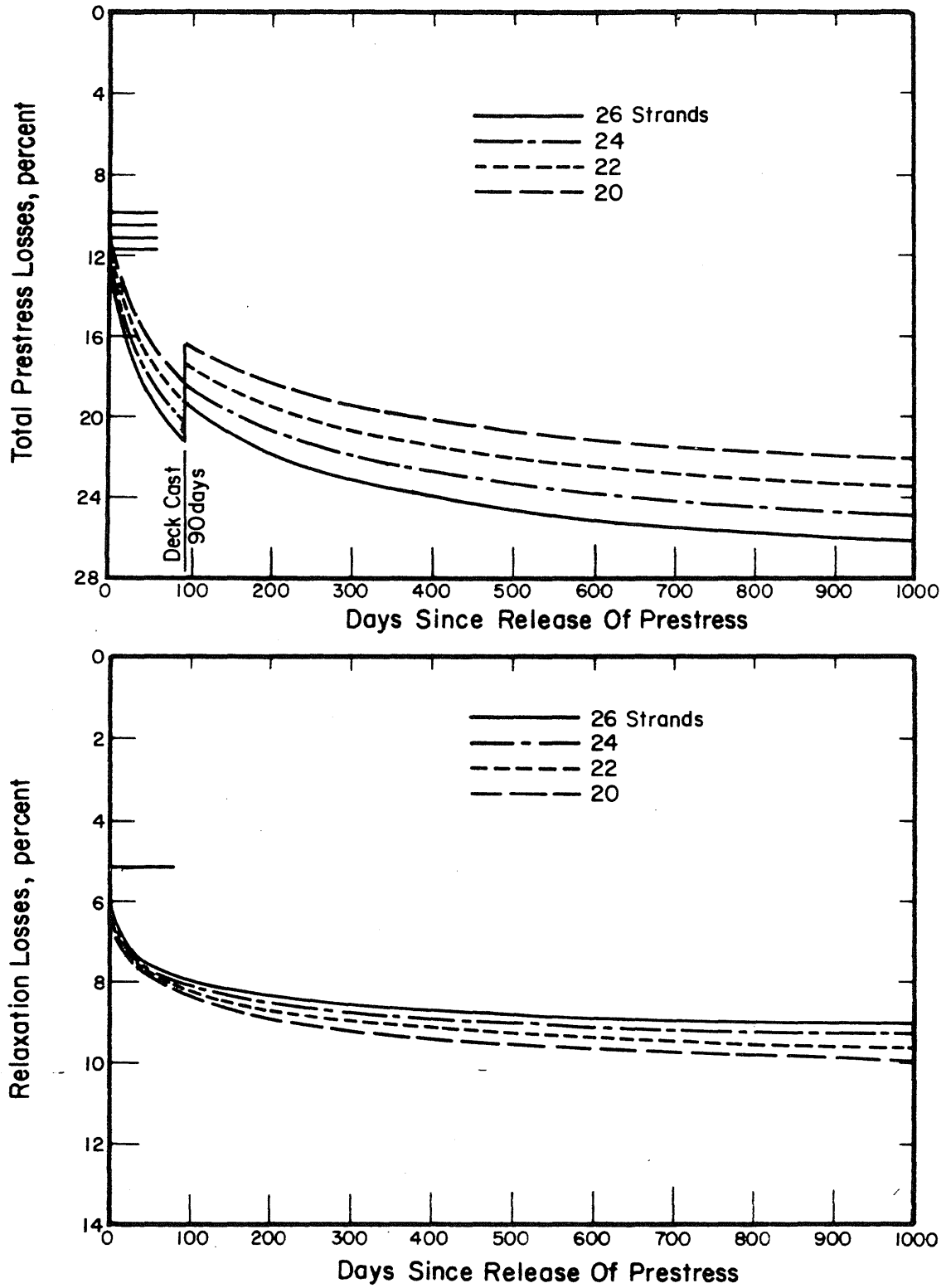


Fig. 3.12 Effect of Initial Stresses in Concrete on Total Prestress Losses and Relaxation Losses, AASHO-III Beam, Stress-Relieved Strands

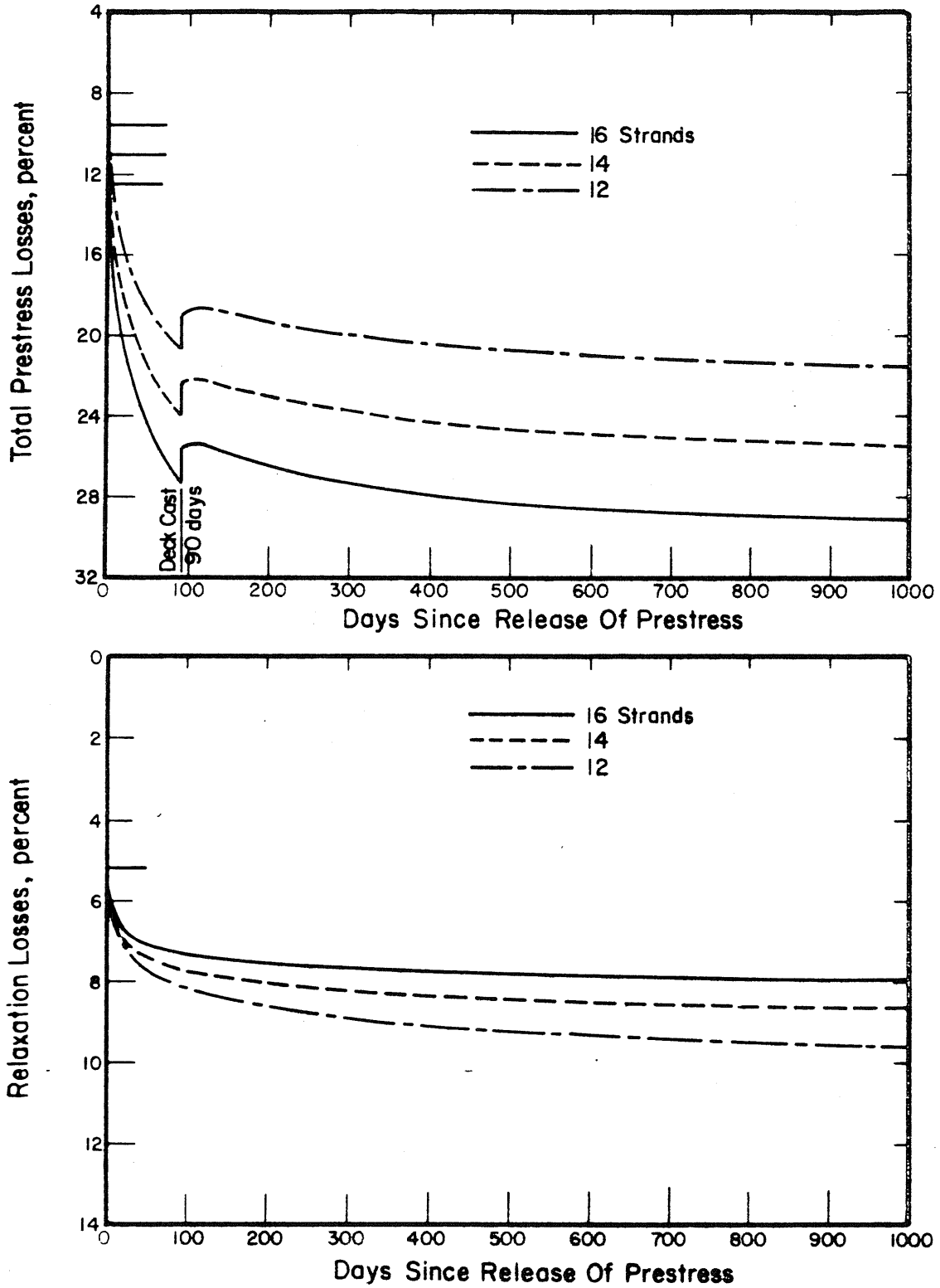


Fig. 3.13 Effect of Initial Stresses in Concrete on Total Prestress Losses and Relaxation Losses, Single-Tee Beam, Stress-Relieved Strands

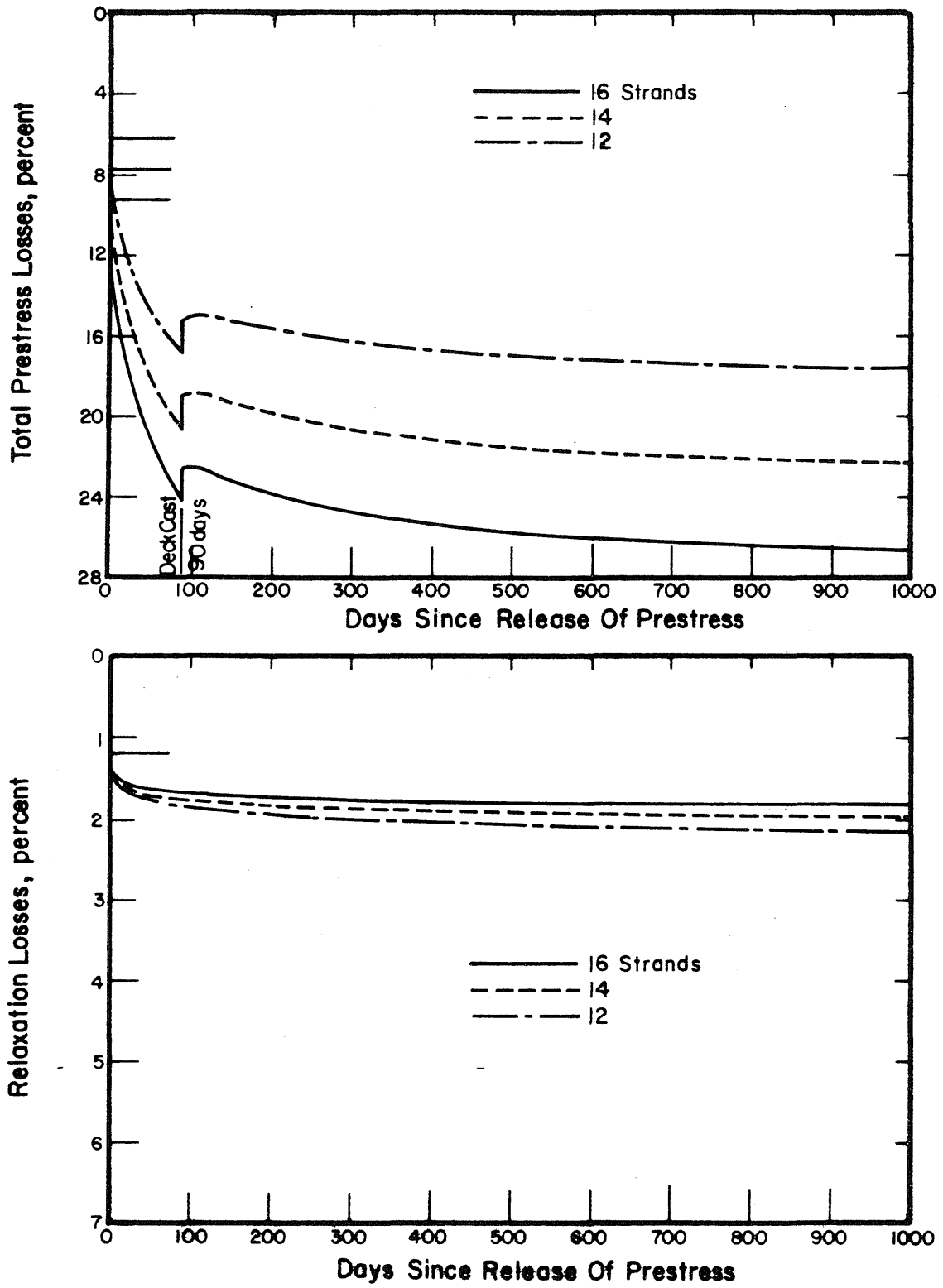


Fig. 3.14 Effect of Initial Stresses in Concrete on Total Prestress Losses and Relaxation Losses, Single-Tee Beam, Low-Relaxation Strands



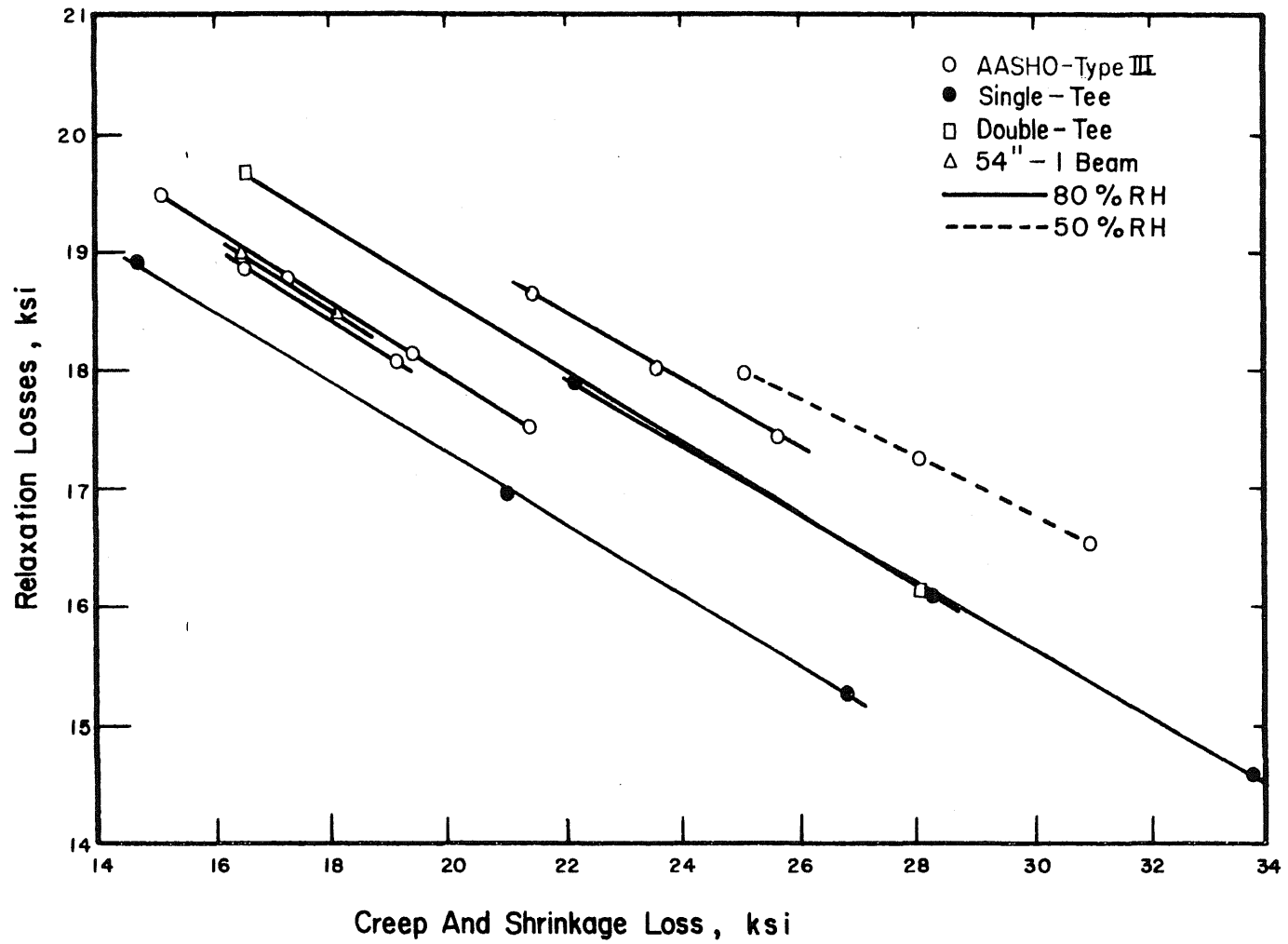


Fig. 3.15 Relaxation Losses as Affected by the Creep and Shrinkage Losses

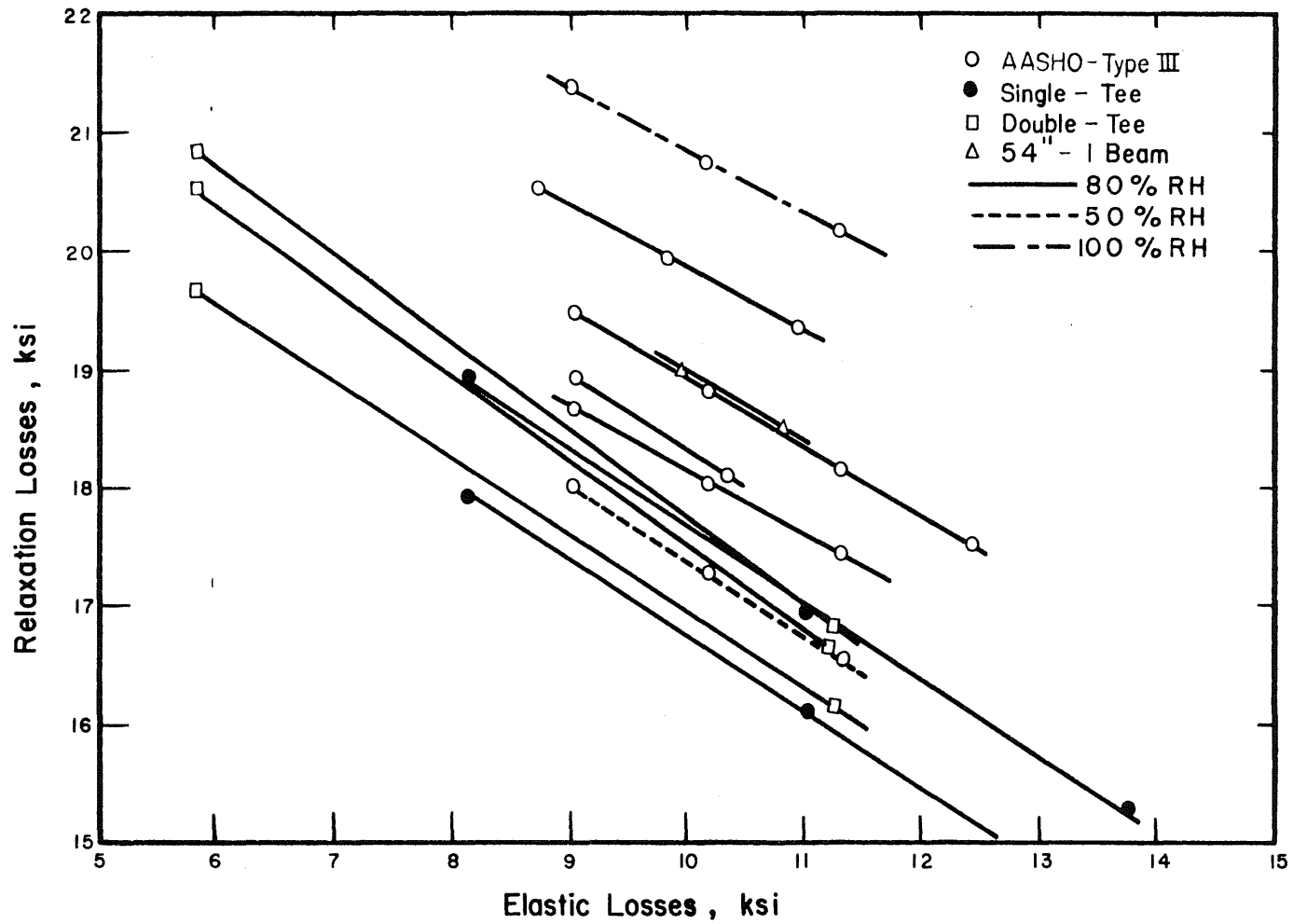


Fig. 3.16 Relaxation Losses as Affected by the Elastic Loss of Stress at Transfer

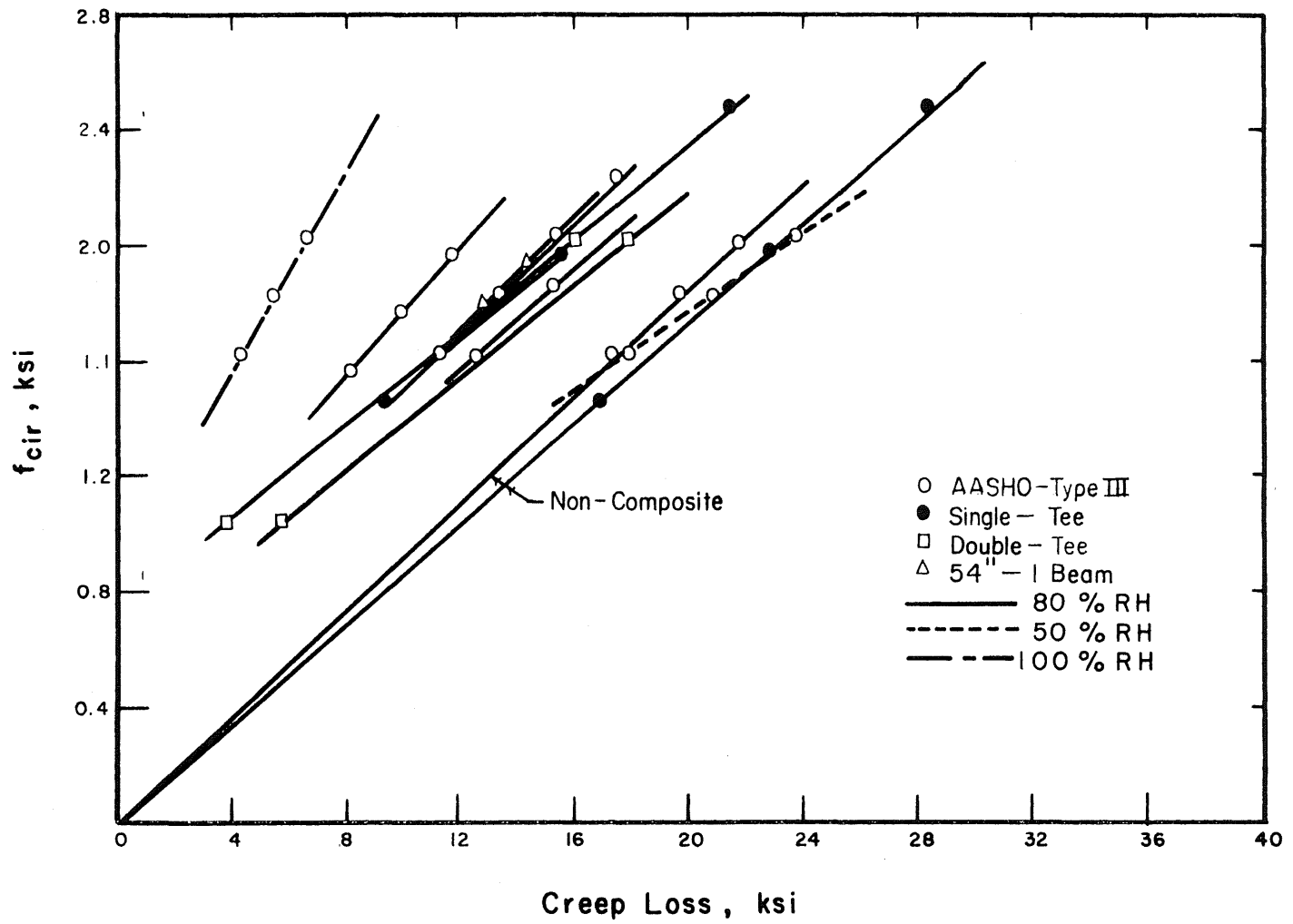


Fig. 3.17 Creep Losses as Affected by Concrete Stress at the Level of the Steel at Transfer

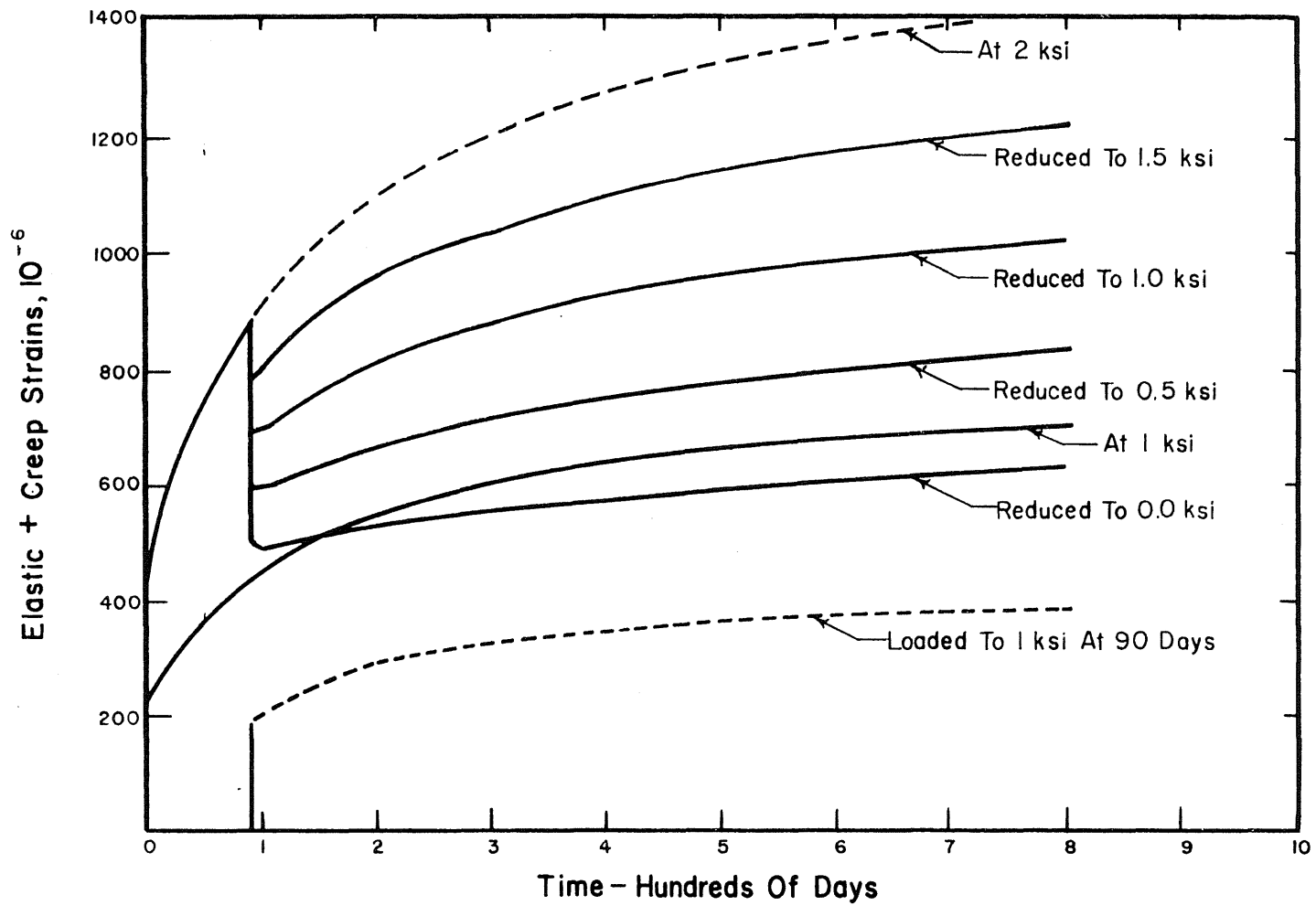


Fig. 3.18 Creep Versus Time Under Reducing Stress Condition at 90 Days, European Concrete Committee Creep-Time Relationships

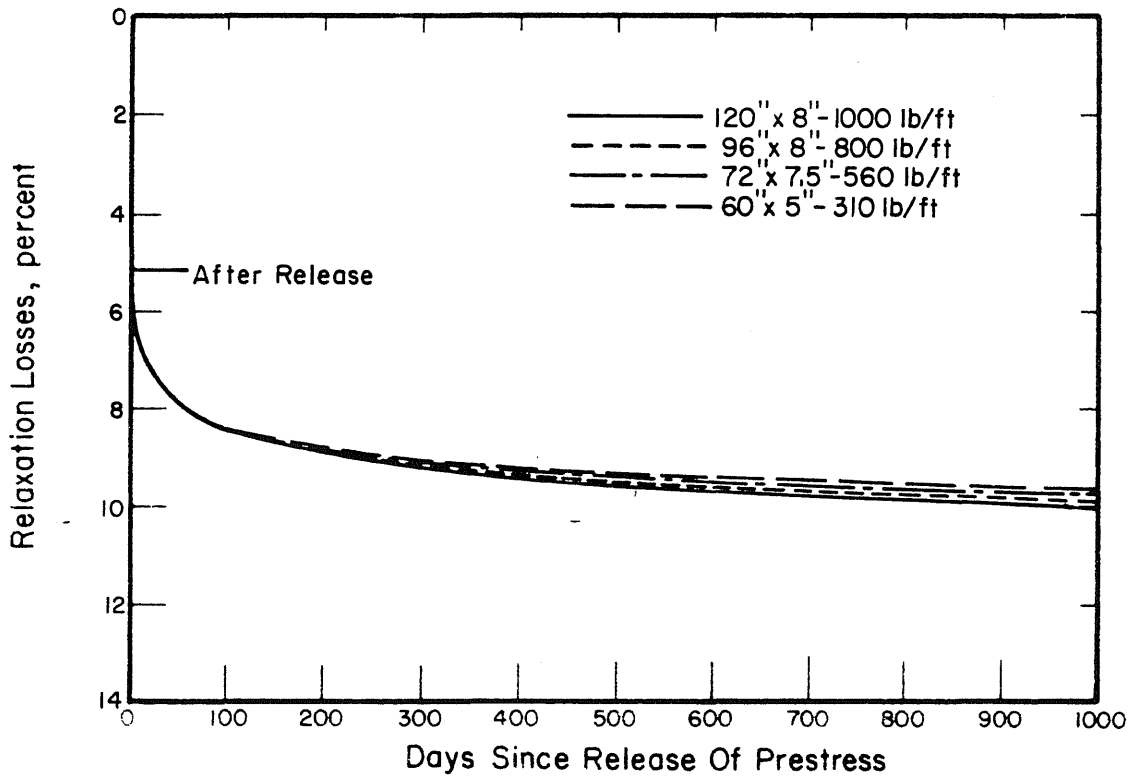
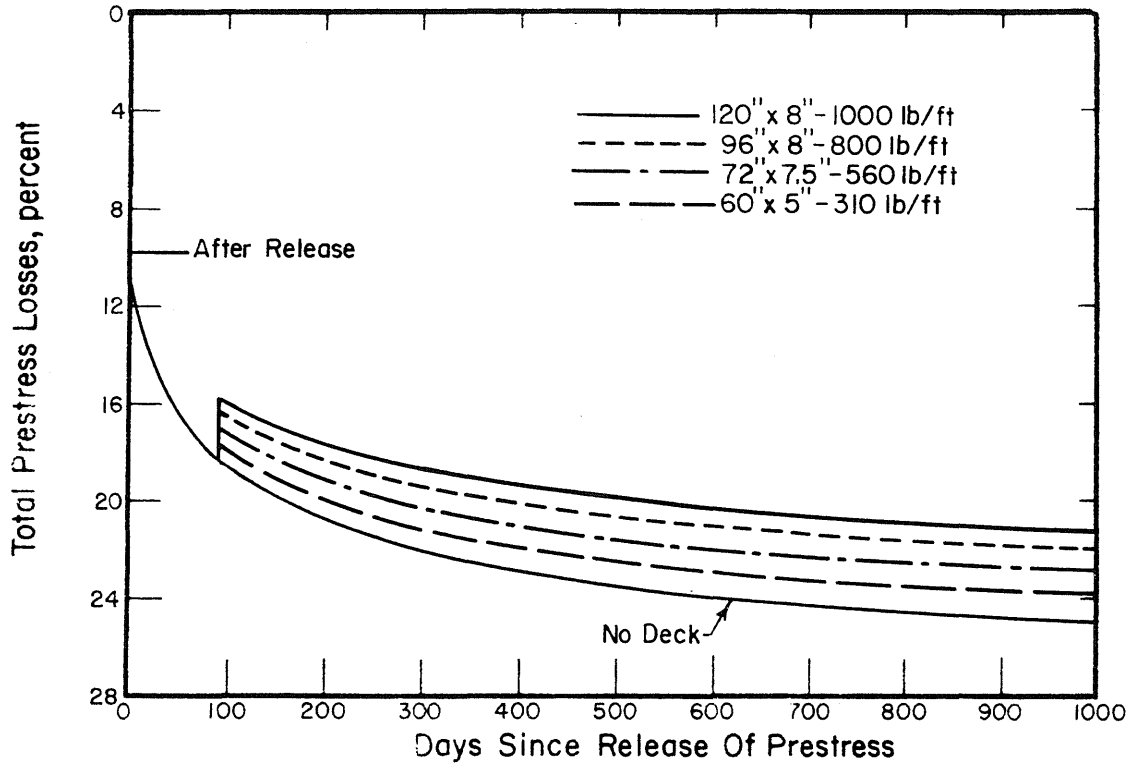


Fig. 3.19 Effect of Deck Dead Load on Total Prestress Losses and Relaxation Losses, AASHO-III Beam

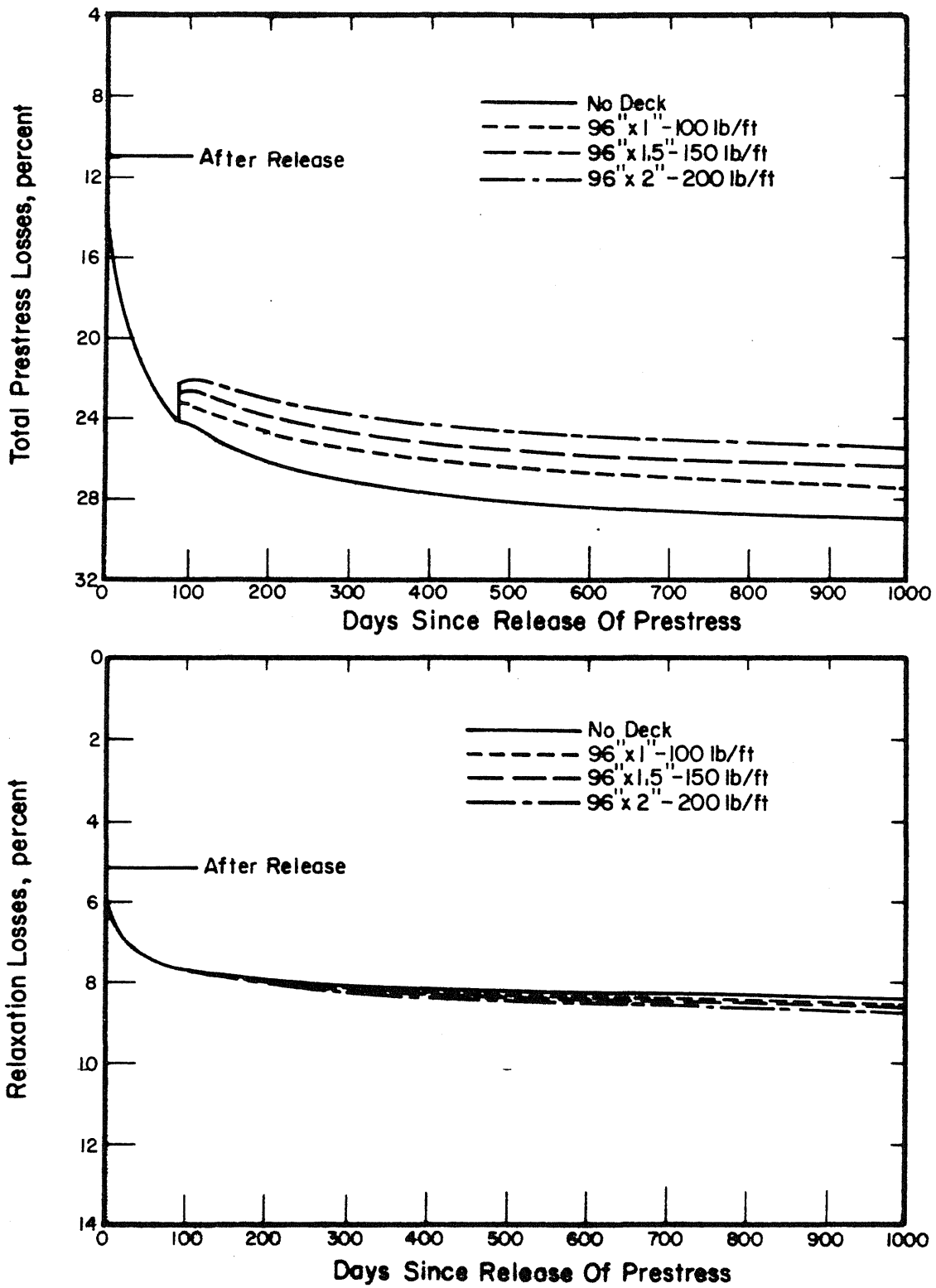


Fig. 3.20 Effect of Deck Dead Load on Total Prestress Losses and Relaxation Losses, Single-Tee Beam

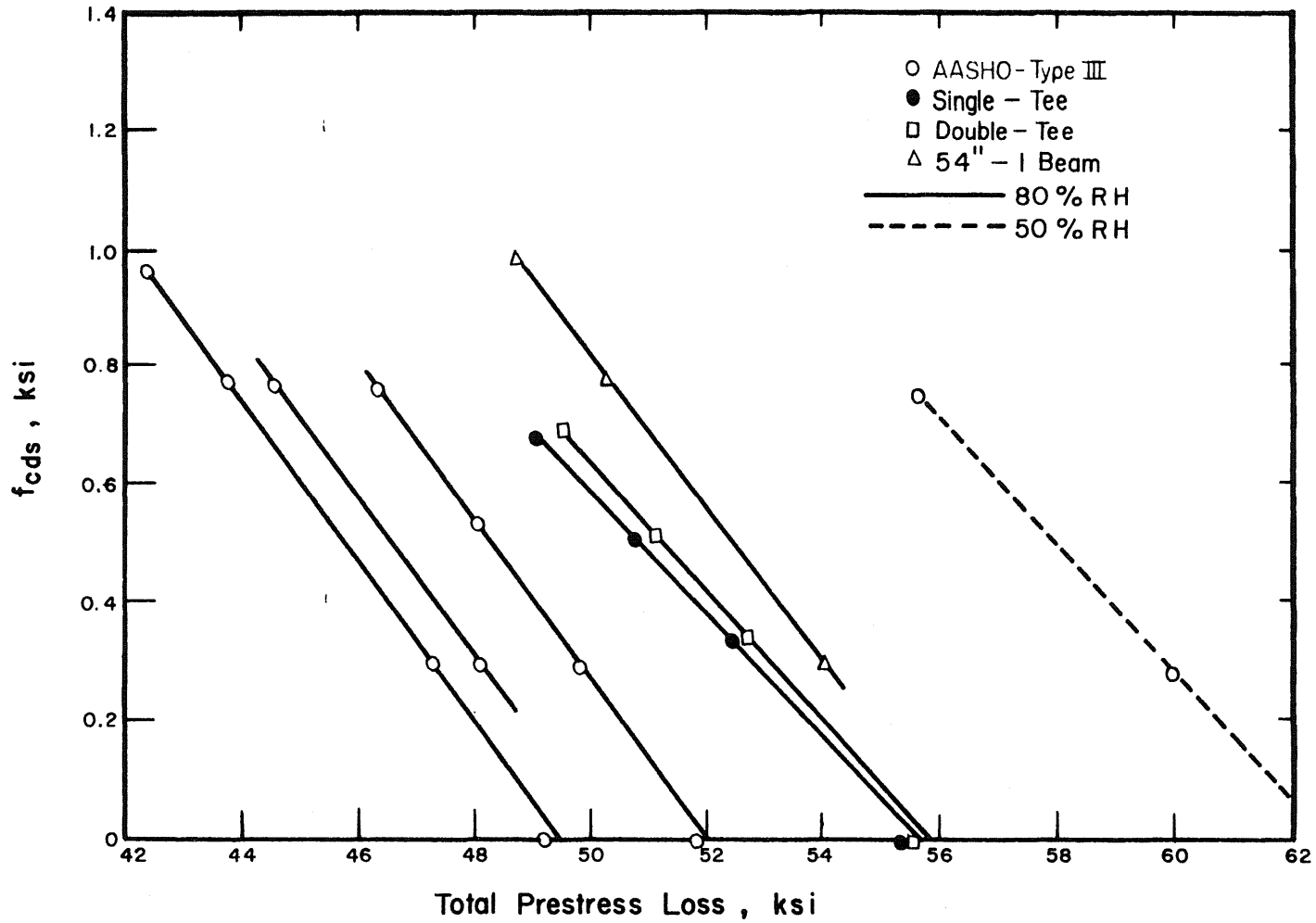


Fig. 3.21 Effect of Concrete Stress Reduction at the Level of Steel on Total Prestress Losses

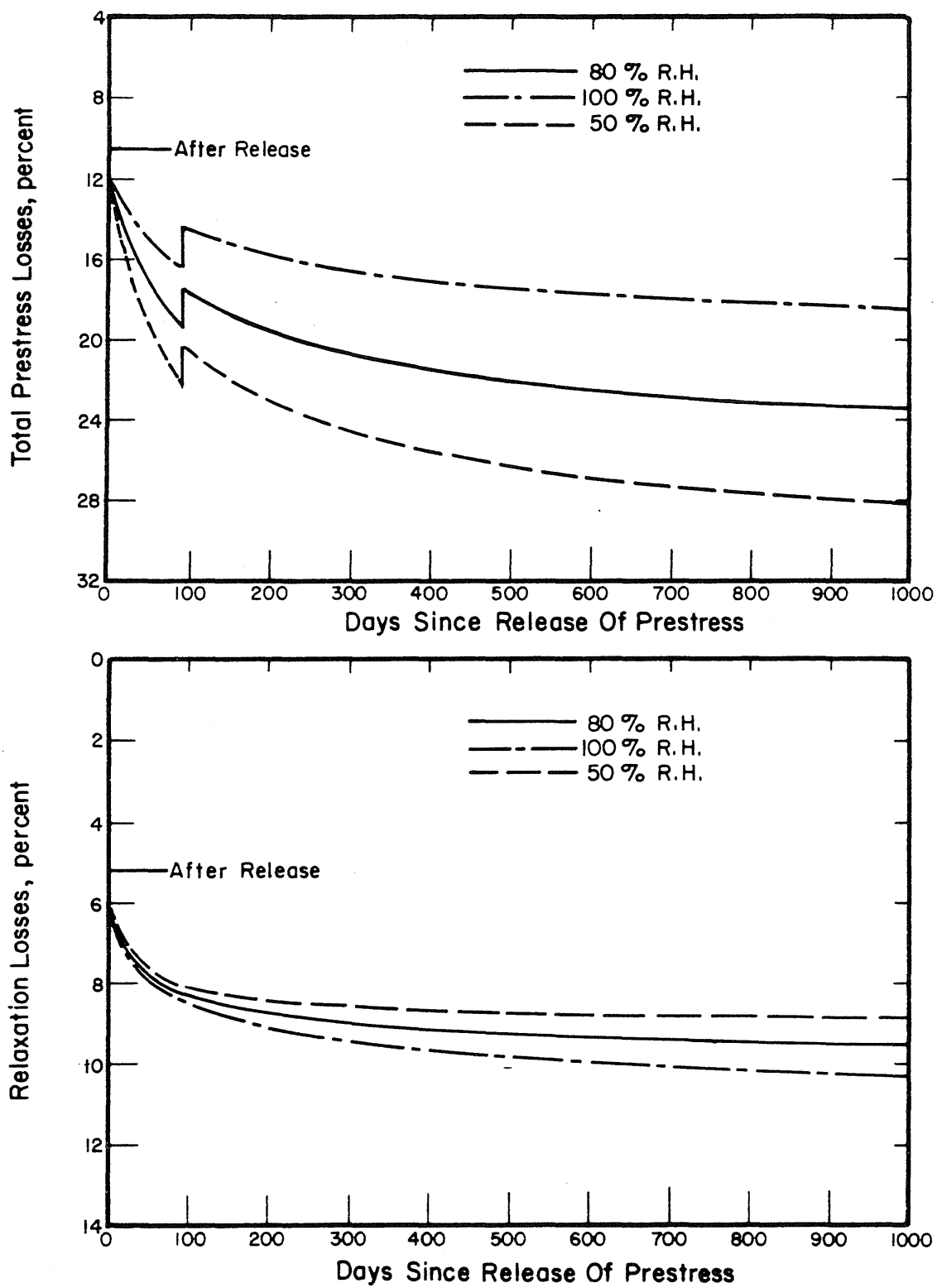


Fig. 3.22 Effect of Relative Humidity on Total Prestress Losses and Relaxation Losses, AASHO-III Beam



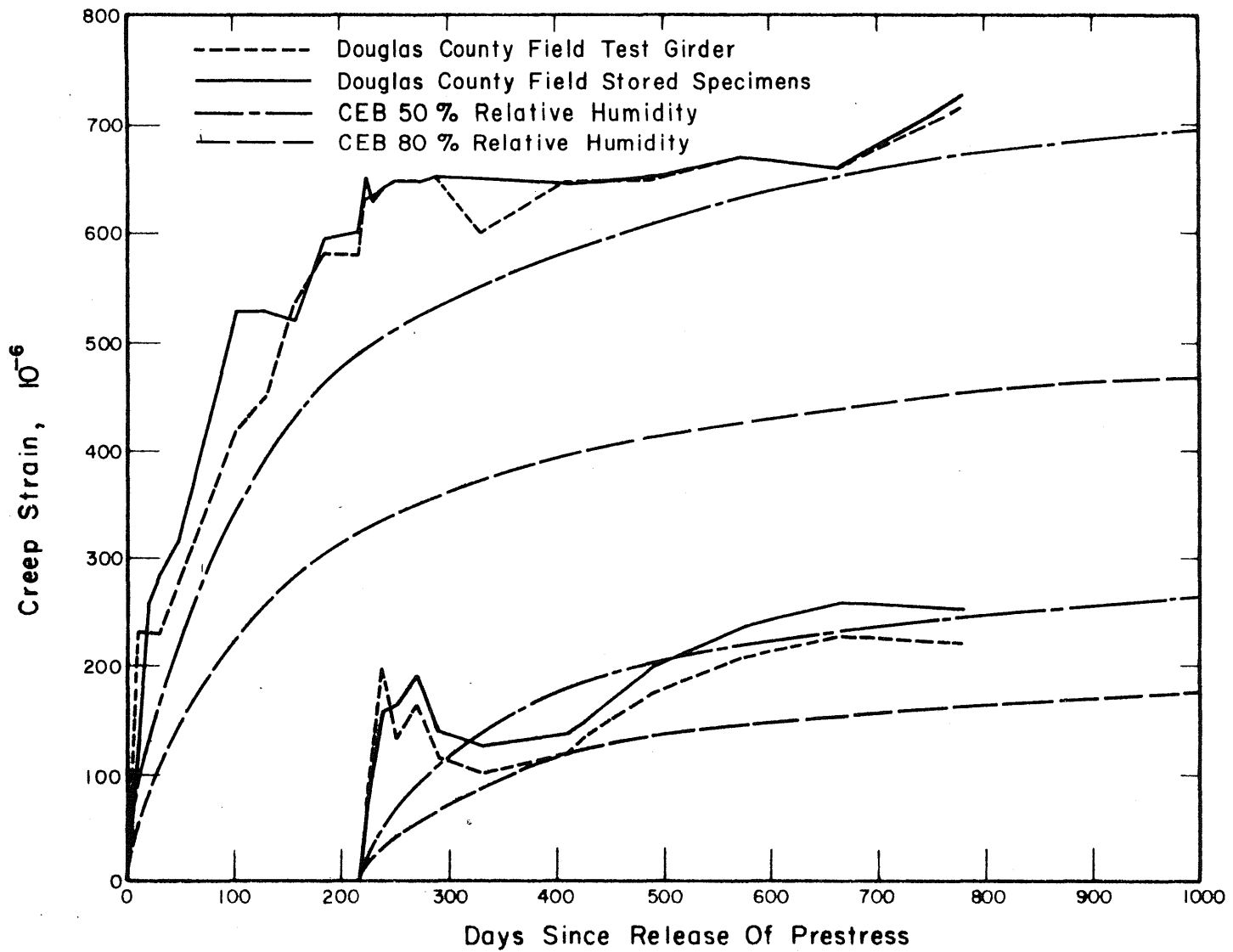


Fig. 3.23 Measured Creep Strains of Douglas County Bridge Girder Concrete Under Field Conditions and Predicted Creep Strains from European Concrete Committee Method

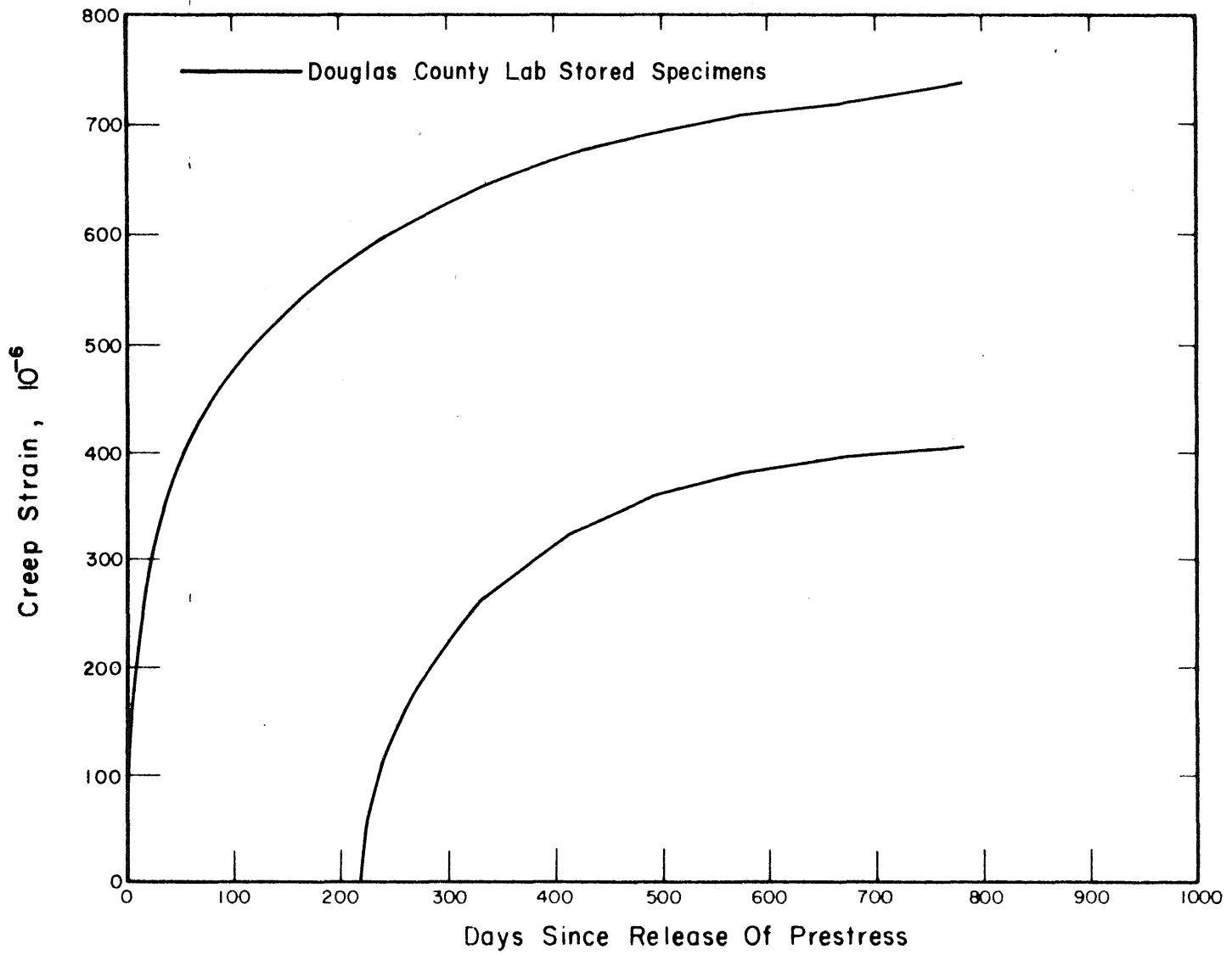


Fig. 3.24 Measured Creep Strains of the Beam Concrete Under Laboratory Storage Conditions, Douglas County Bridge

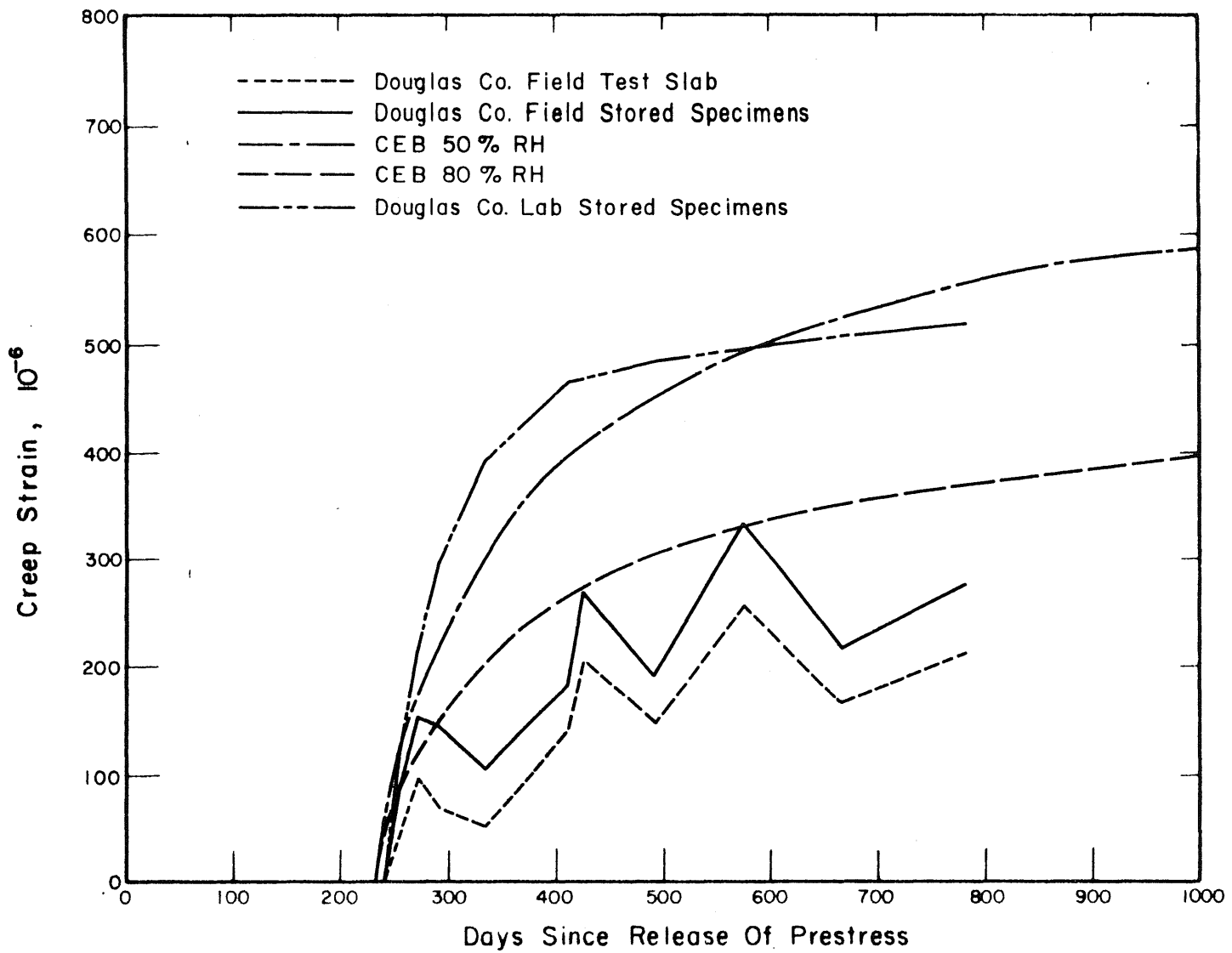


Fig. 3.25 Measured Creep Strains of Douglas County Bridge Deck Concrete and Predicted Creep Strains from European Concrete Committee Method

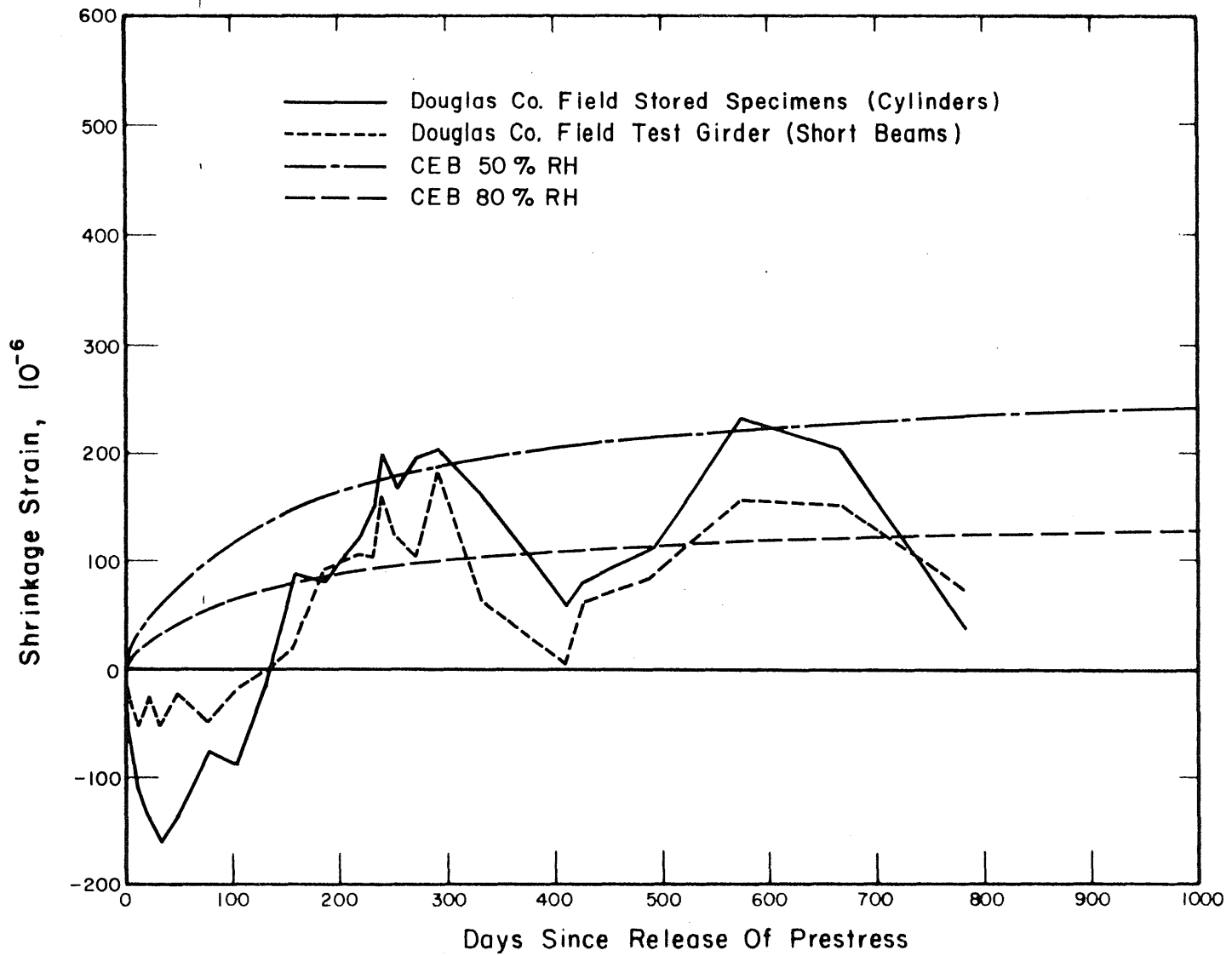


Fig. 3.26 Measured Shrinkage Strains of Douglas County Bridge Girder Concrete Under Field Conditions and Predicted Shrinkage Strains from European Concrete Committee Method

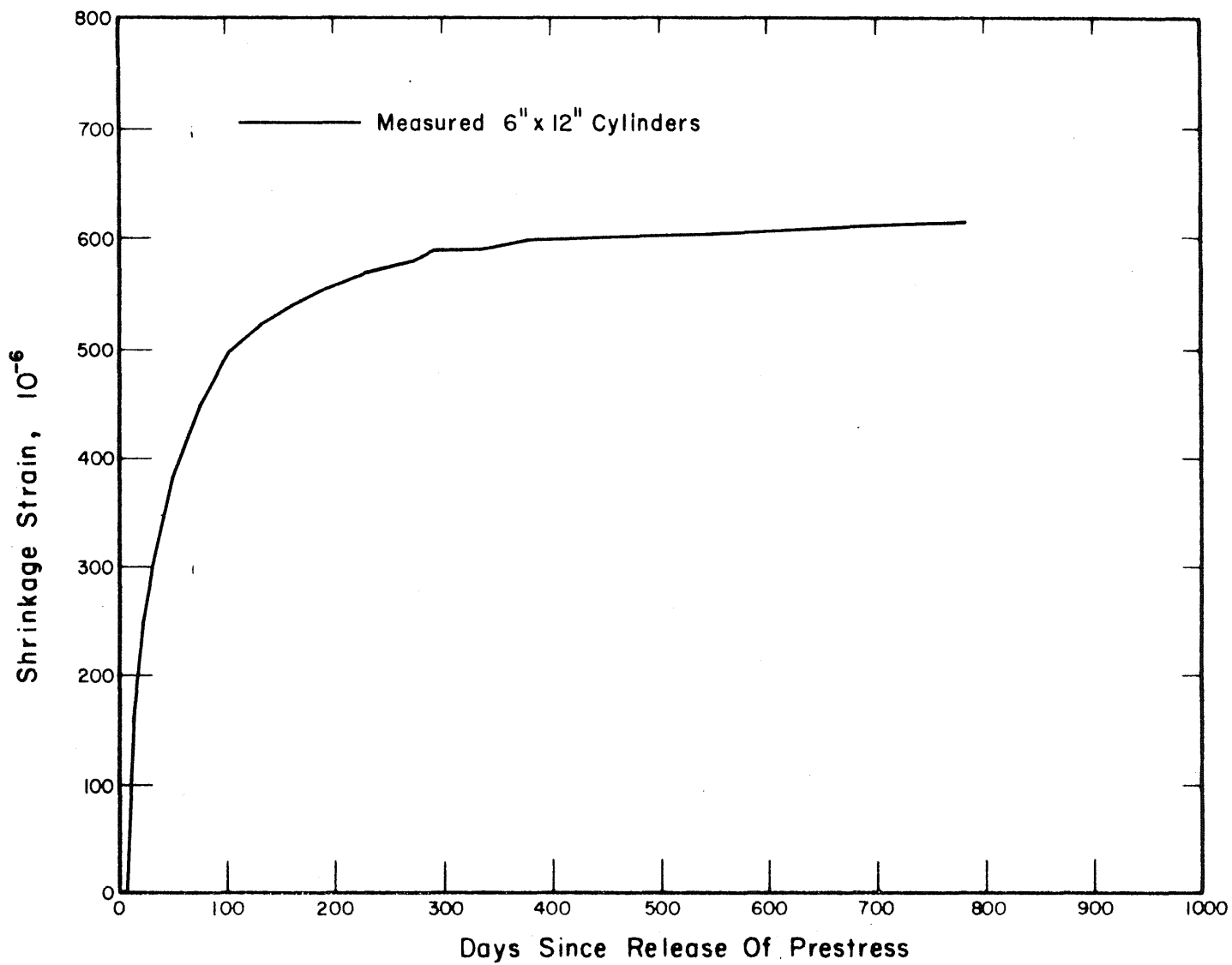


Fig. 3.27 Measured Shrinkage Strains of the Beam Concrete Under Laboratory Storage Condition, Douglas County Bridge

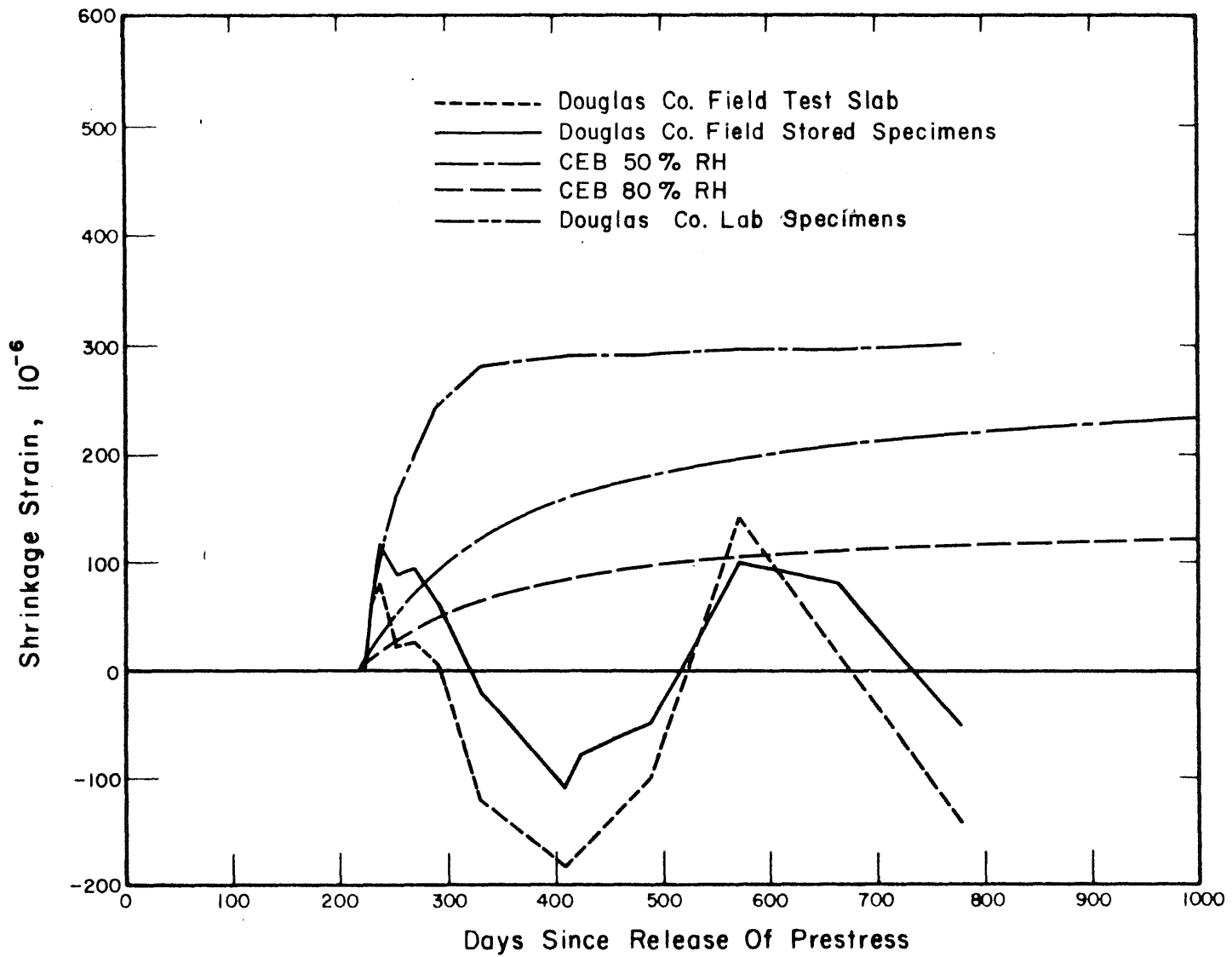


Fig. 3.28 Measured Shrinkage Strains of Douglas County Bridge Deck Concrete and Predicted Shrinkage Strains from European Concrete Committee Method

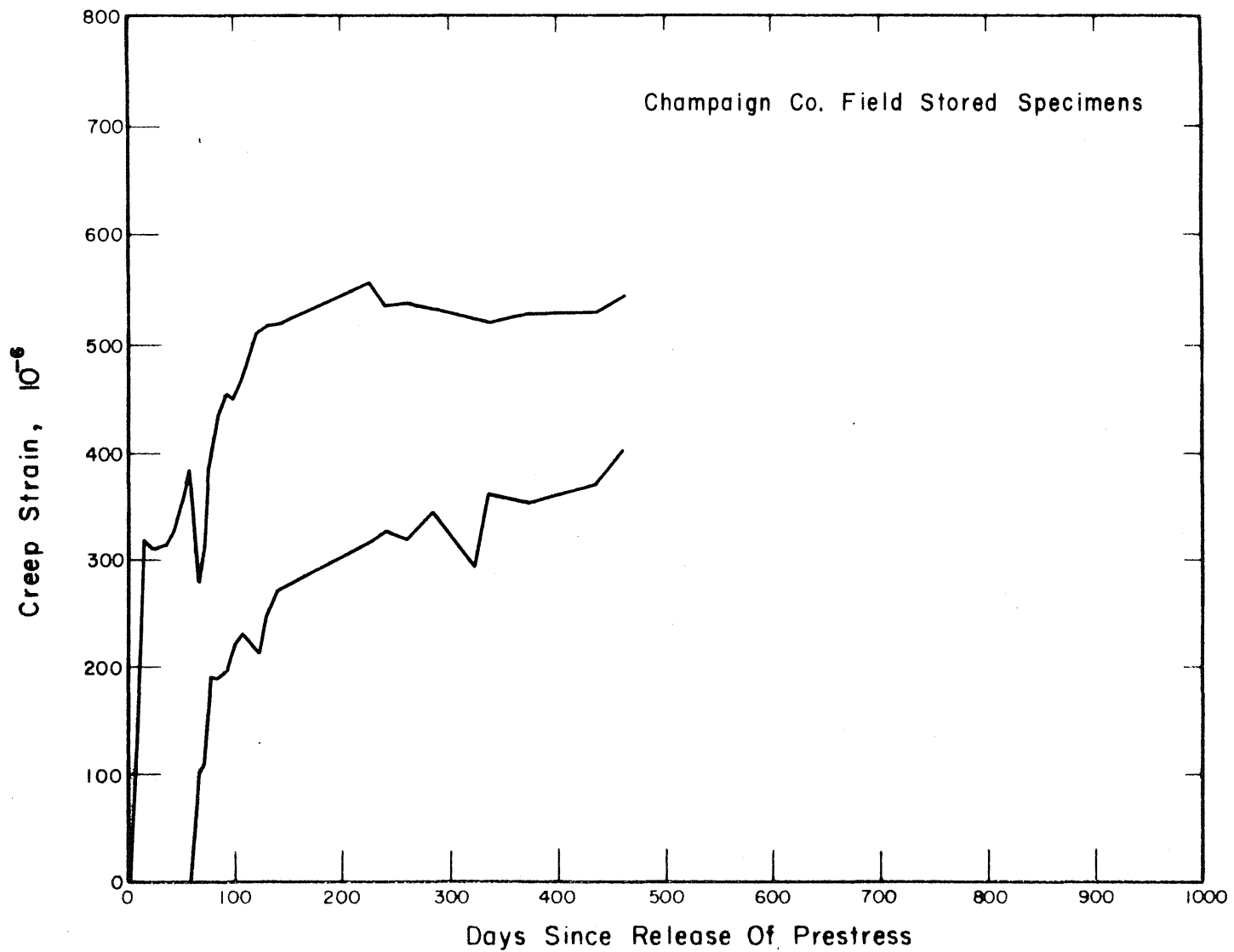


Fig. 3.29 Creep of the Beam Concrete Under Field Storage Conditions, Champaign County Bridge









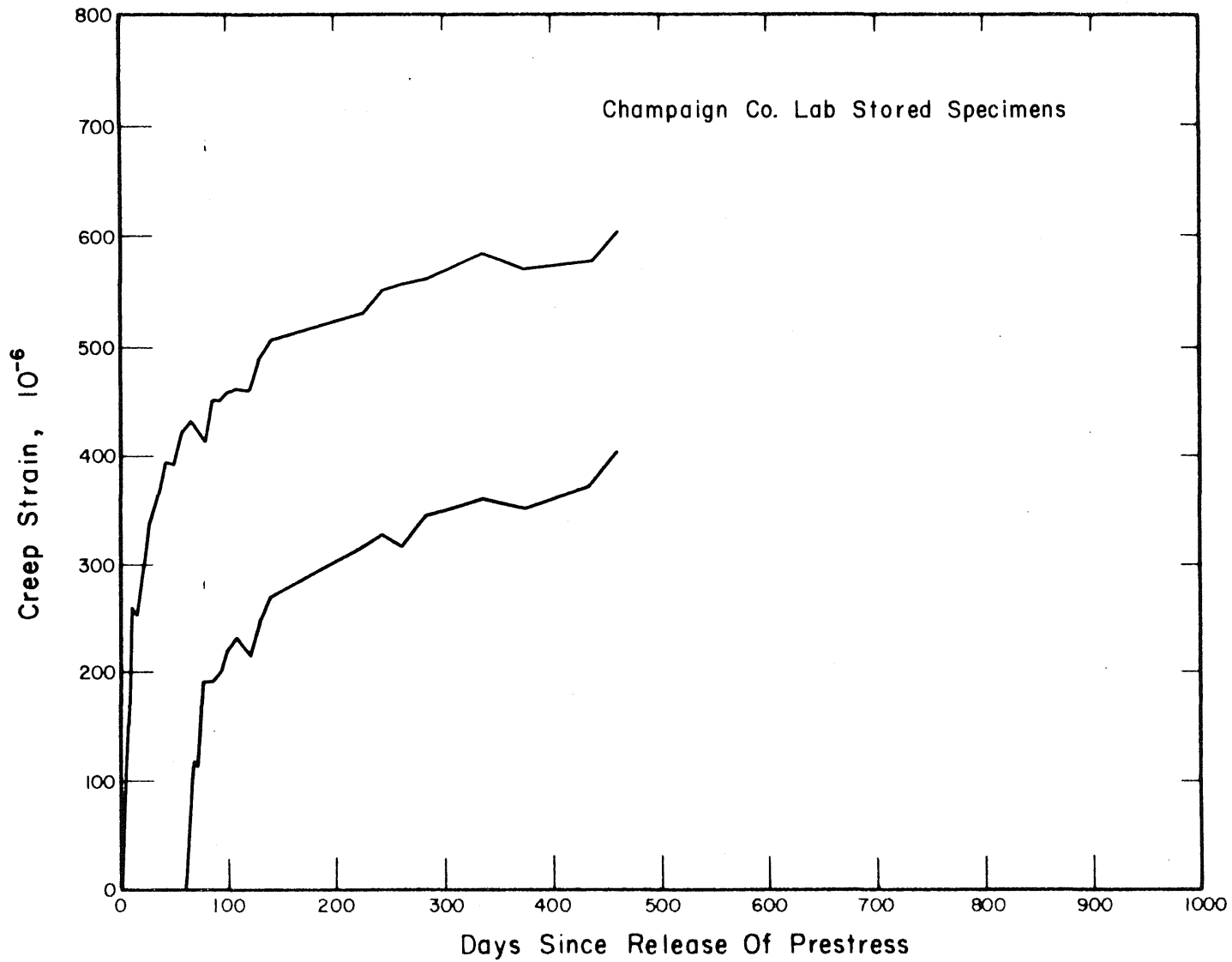


Fig. 3.30 Creep of the Beam Concrete Under Laboratory Storage Conditions, Champaign County Bridge

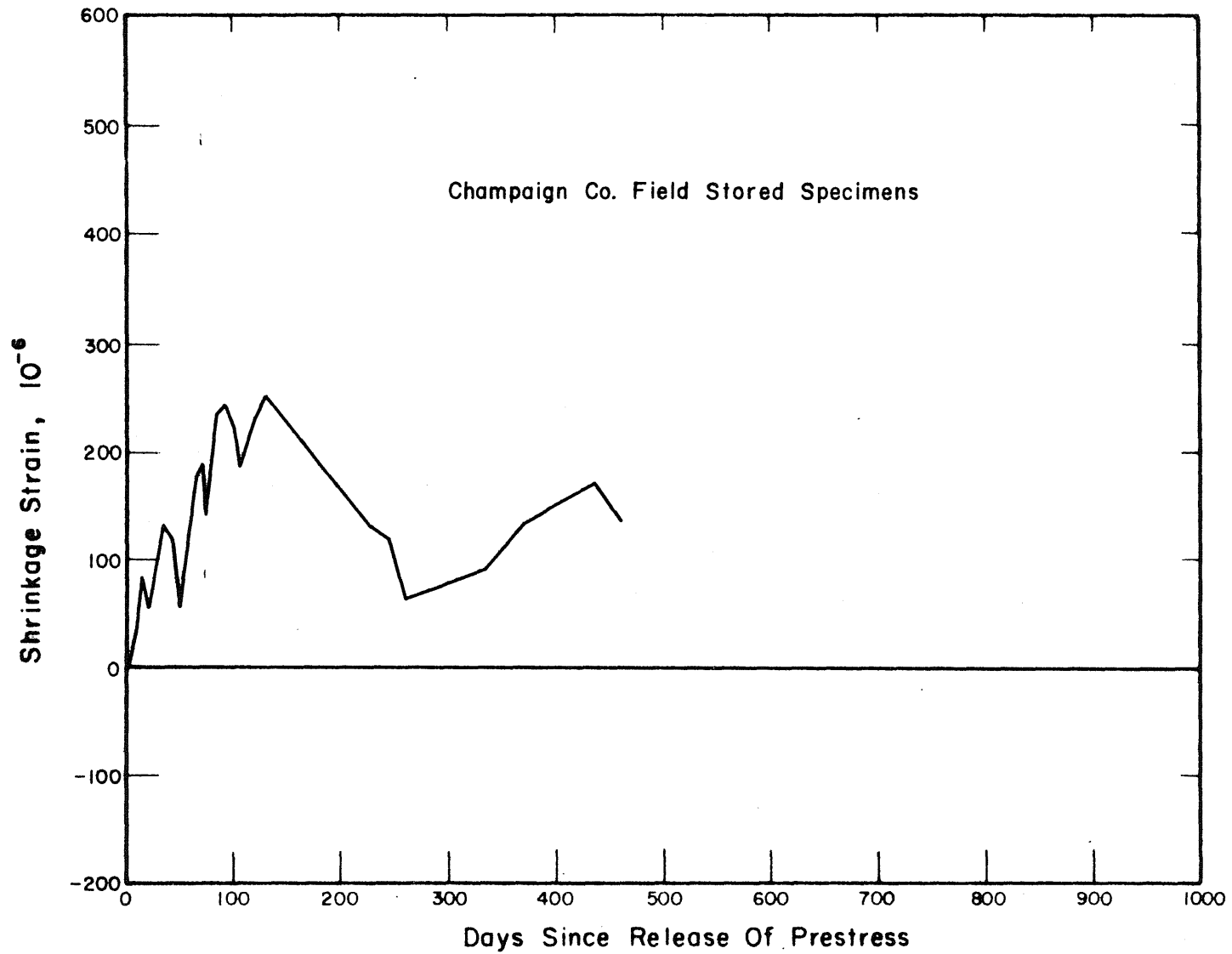


Fig. 3.31 Shrinkage of the Beam Concrete Under Field Storage Conditions, Champaign County Bridge

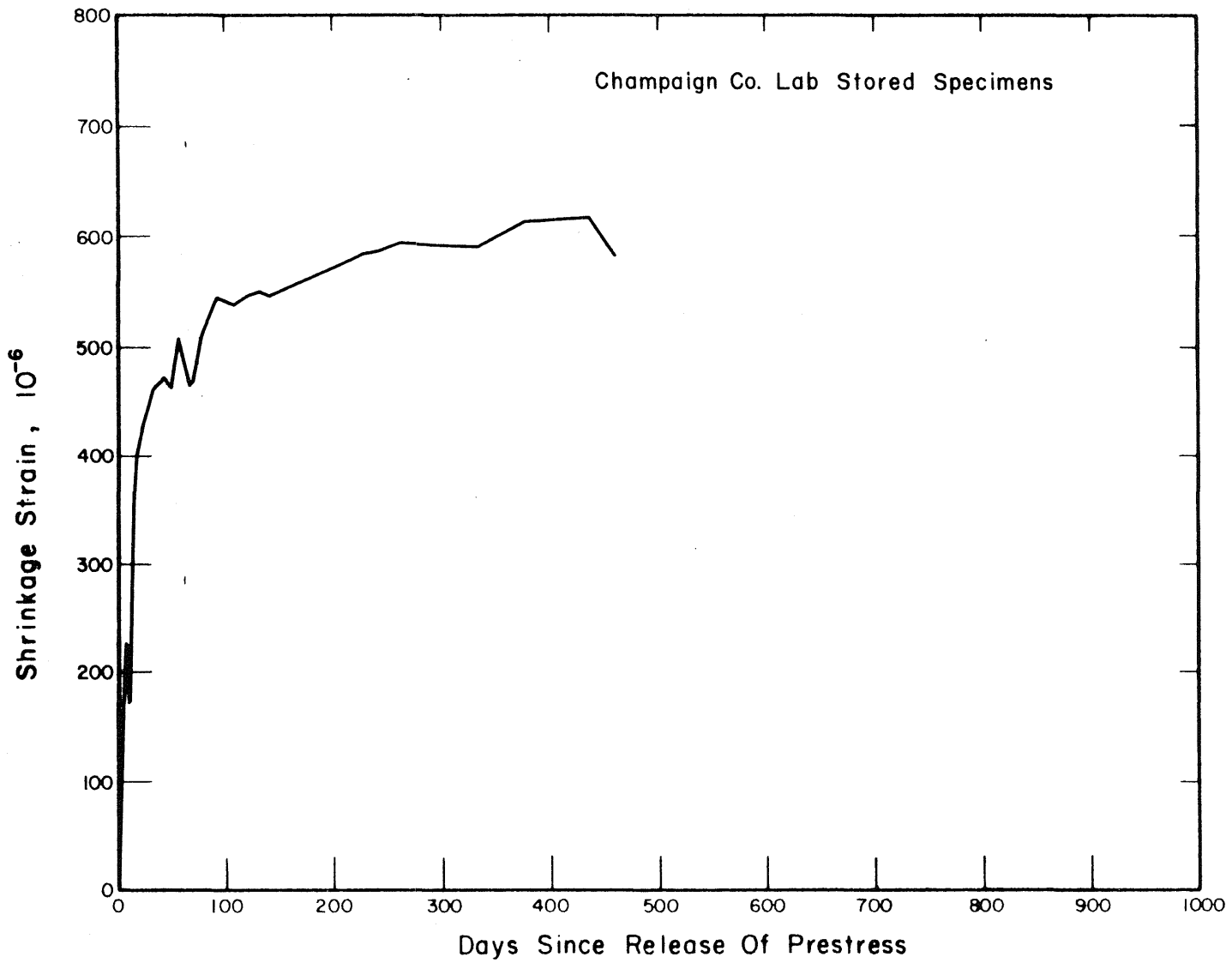


Fig. 3.32 Shrinkage of the Beam Concrete Under Laboratory Storage Conditions, Champaign County Bridge

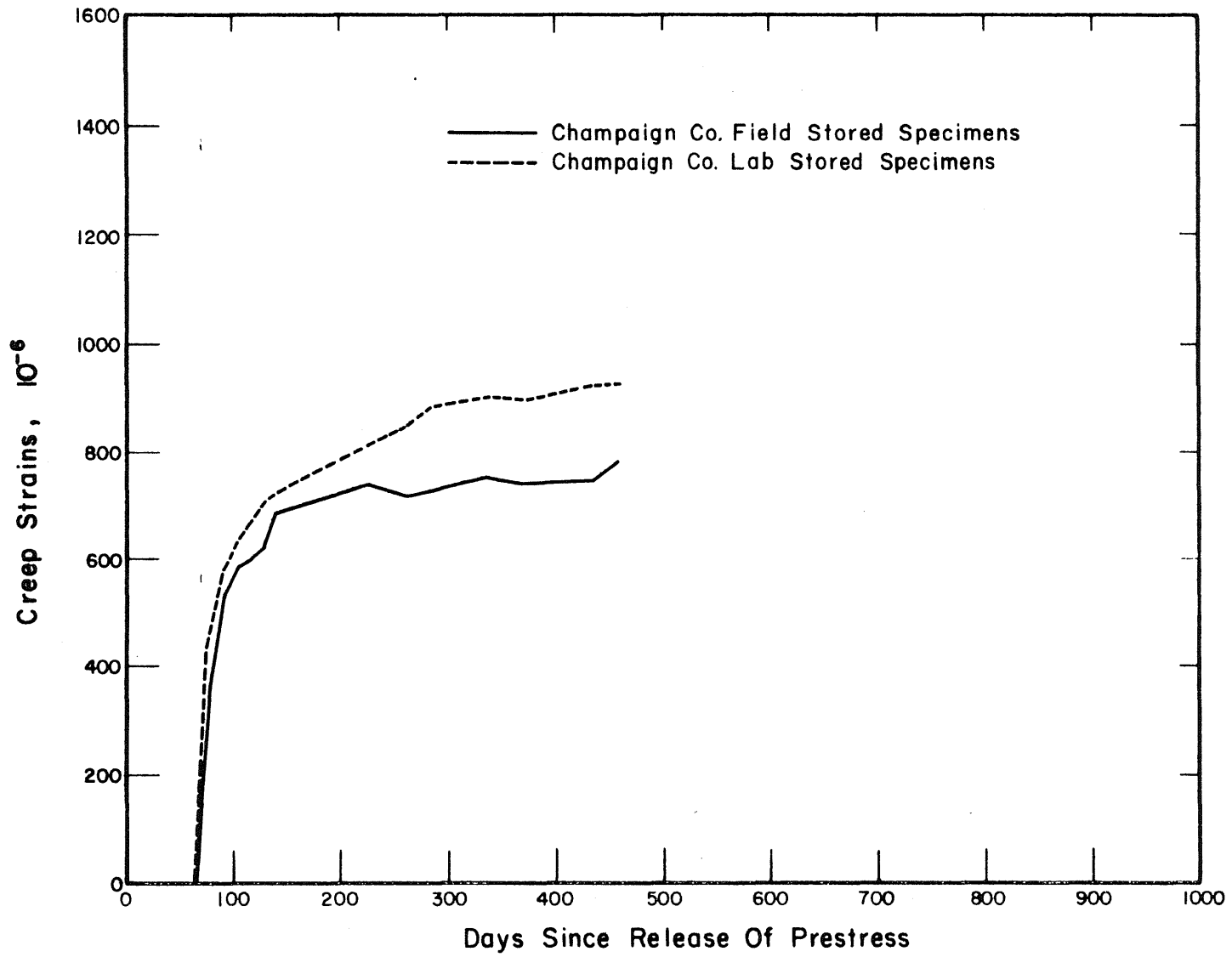


Fig. 3.33 Creep of the Deck Concrete Under Field and Laboratory Storage Conditions, Champaign County Bridge

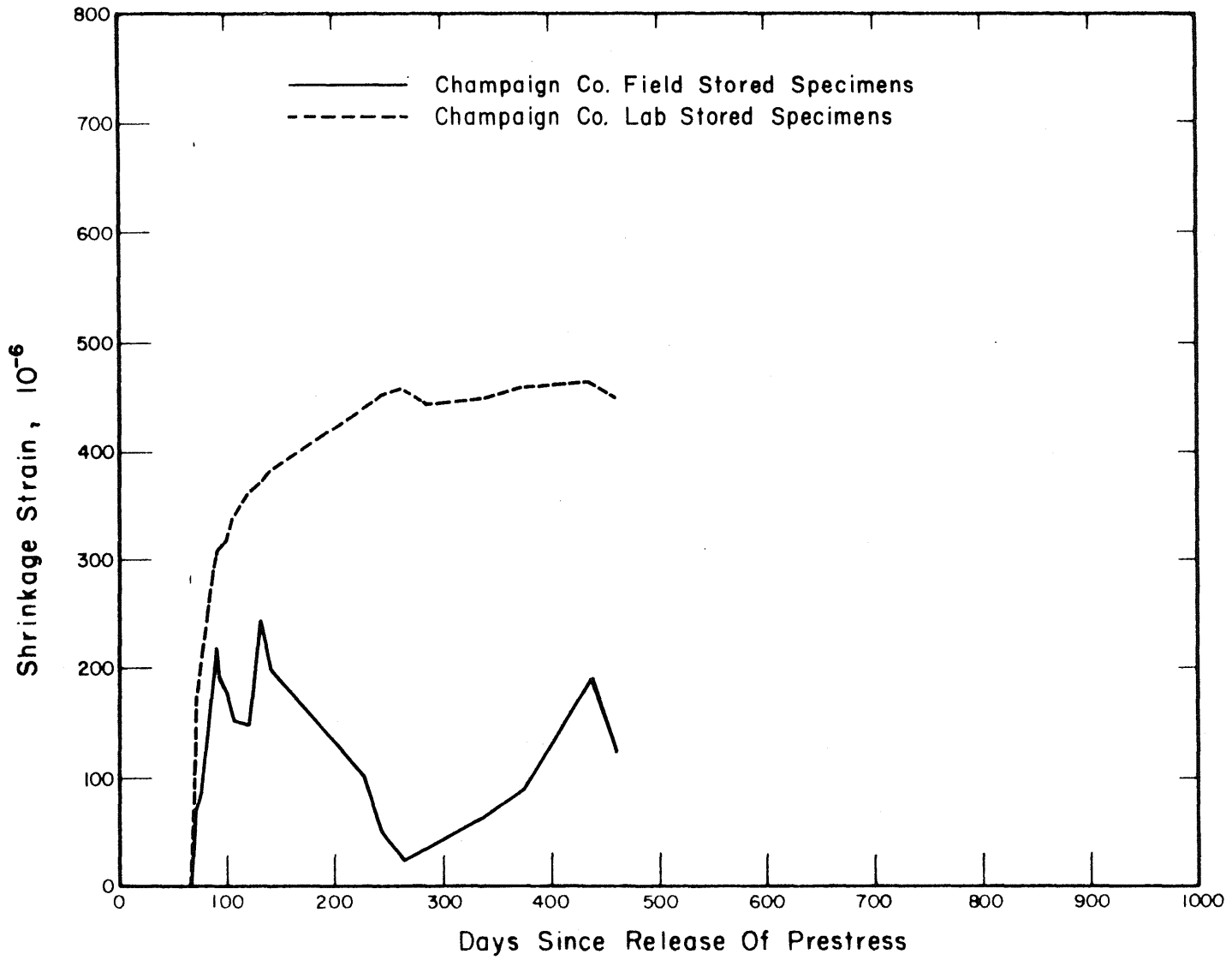


Fig. 3.34 Shrinkage of the Deck Concrete Under Field and Laboratory Conditions, Champaign County Bridge

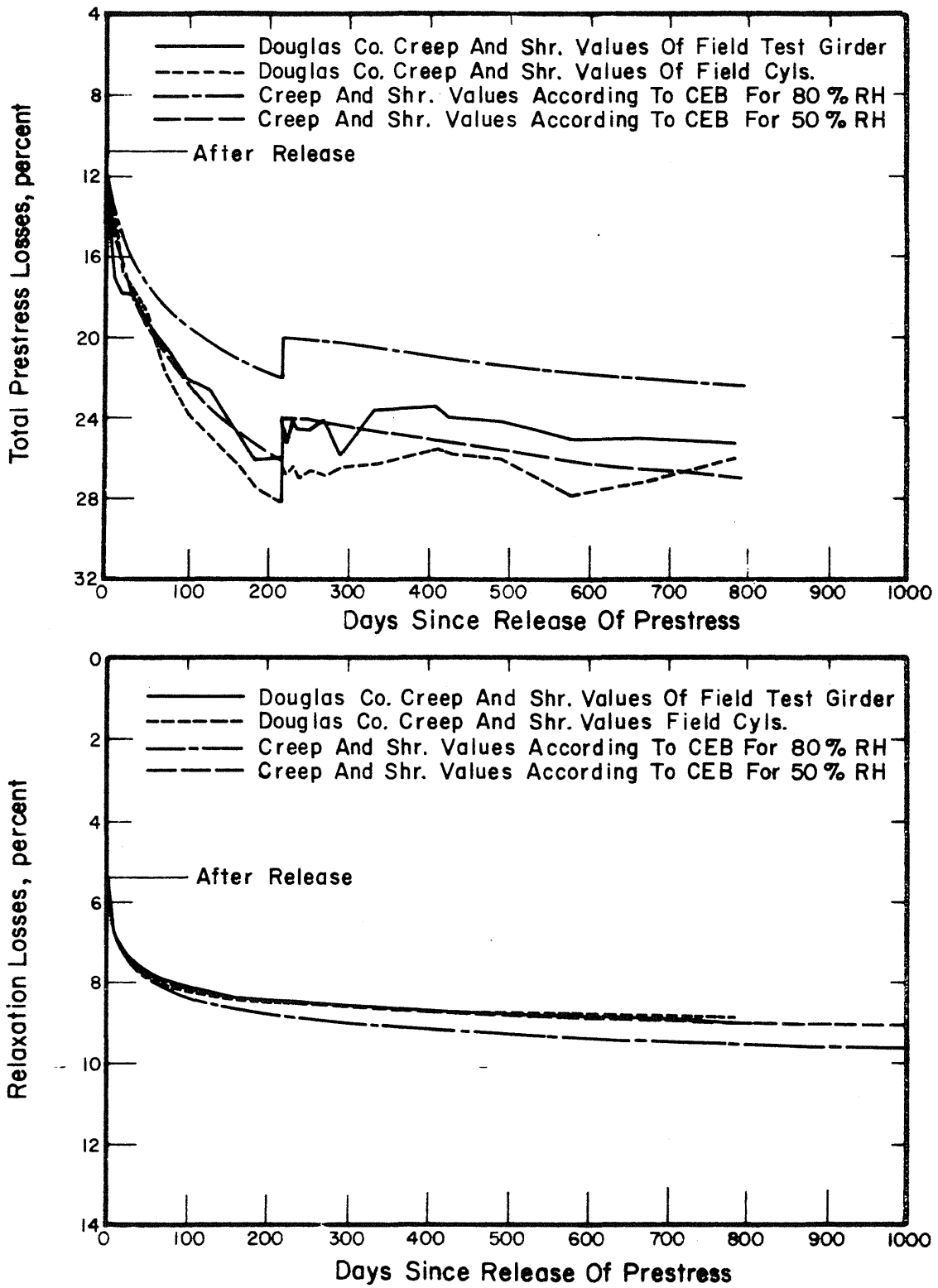


Fig. 3.35 Comparisons of Calculated Total Prestress Losses and Relaxation Losses Using the Douglas County Field Values and the C.E.B. Values, AASHO-III Beam



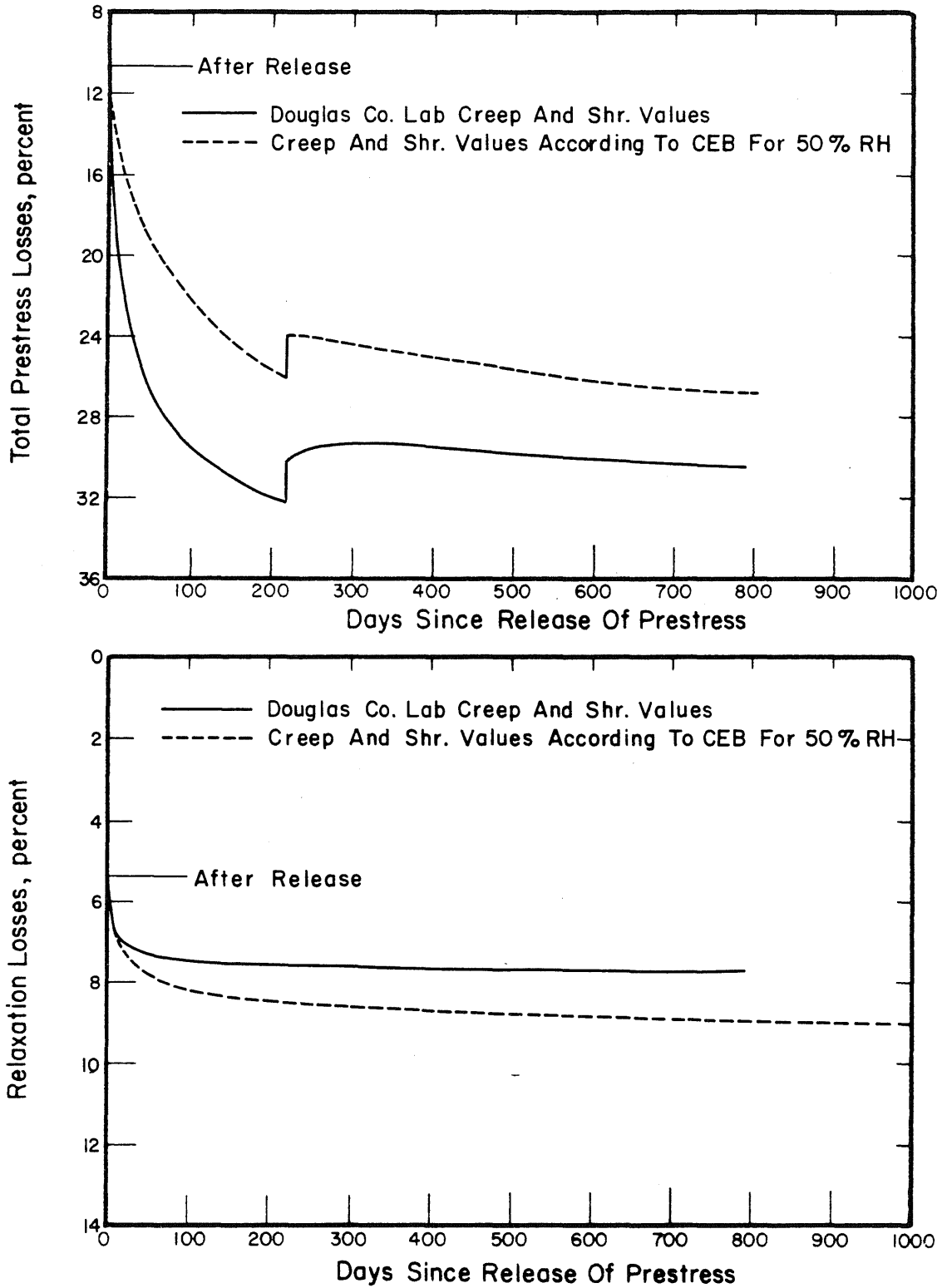


Fig. 3.36 Comparisons of Calculated Total Prestress Losses and Relaxation Losses Using the Douglas County Laboratory Values and the 50 Percent Relative Humidity C.E.B. Values, AASHTO-III Beam

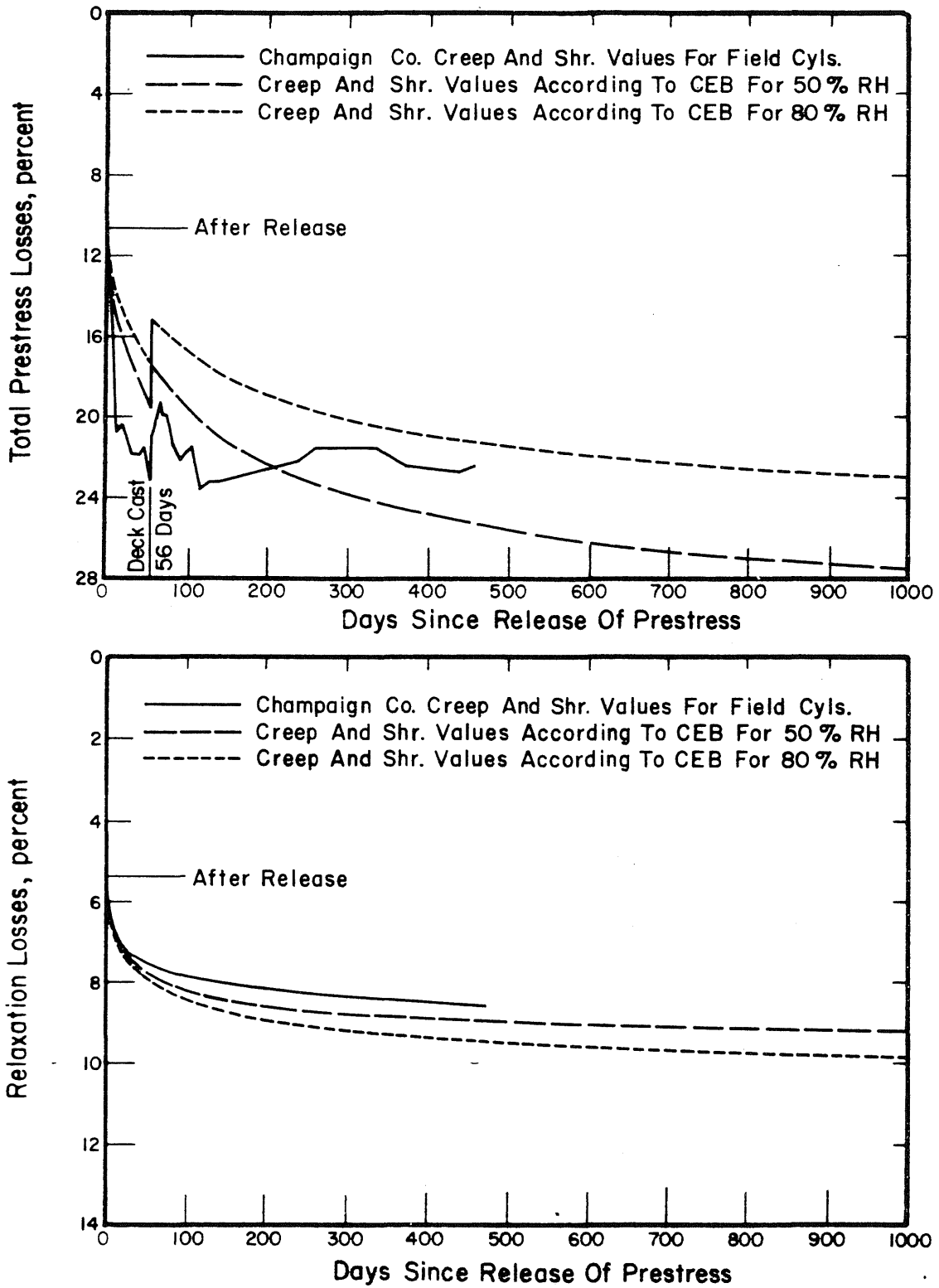


Fig. 3.37 Comparisons of Calculated Total Prestress Losses and Relaxation Losses Using the Champaign County Field Values and the C.E.B. Values

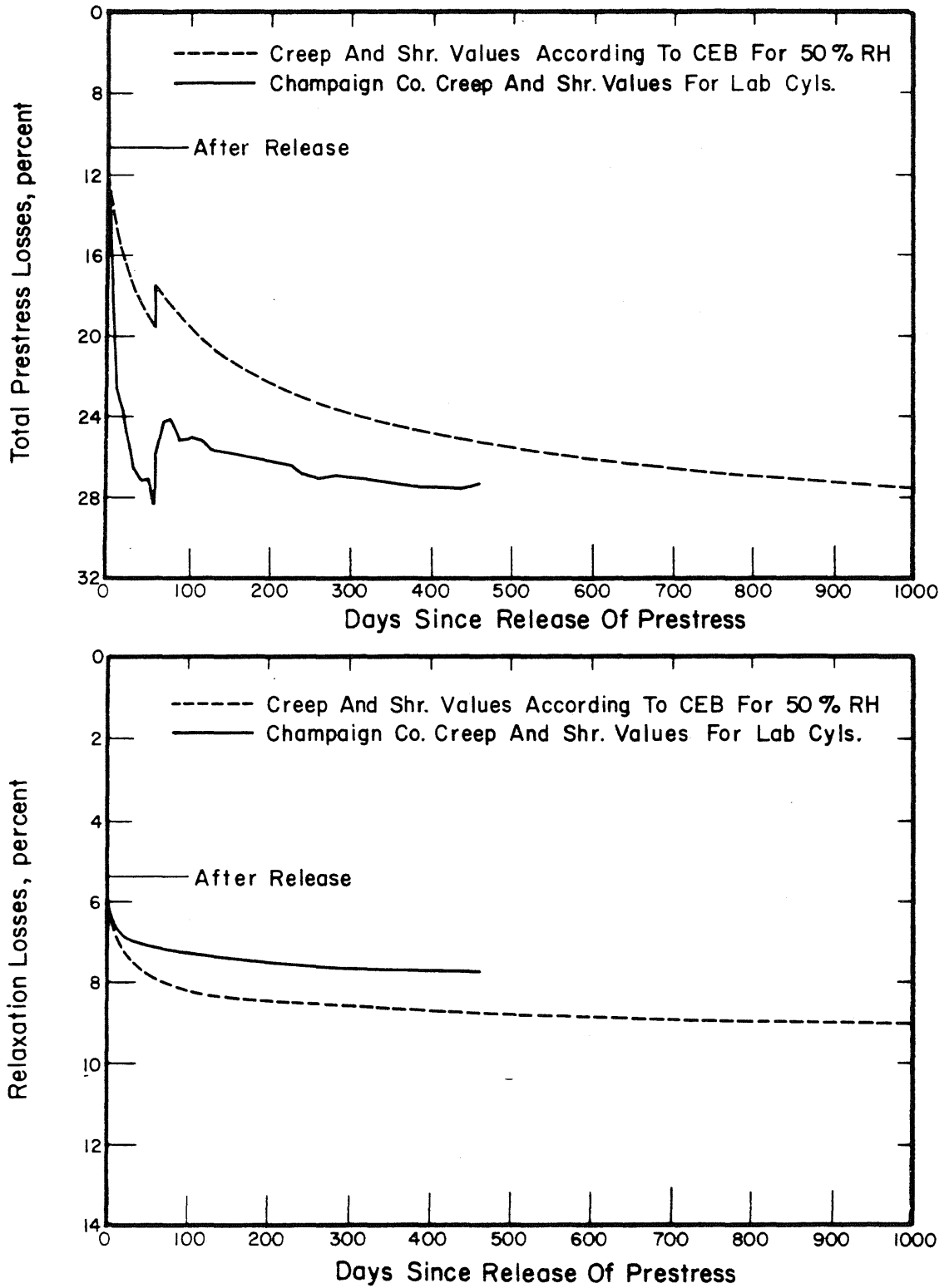


Fig. 3.38 Comparisons of Calculated Total Prestress Losses and Relaxation Losses Using the Champaign County Laboratory Values and the 50 Percent Relative Humidity C.E.B. Values

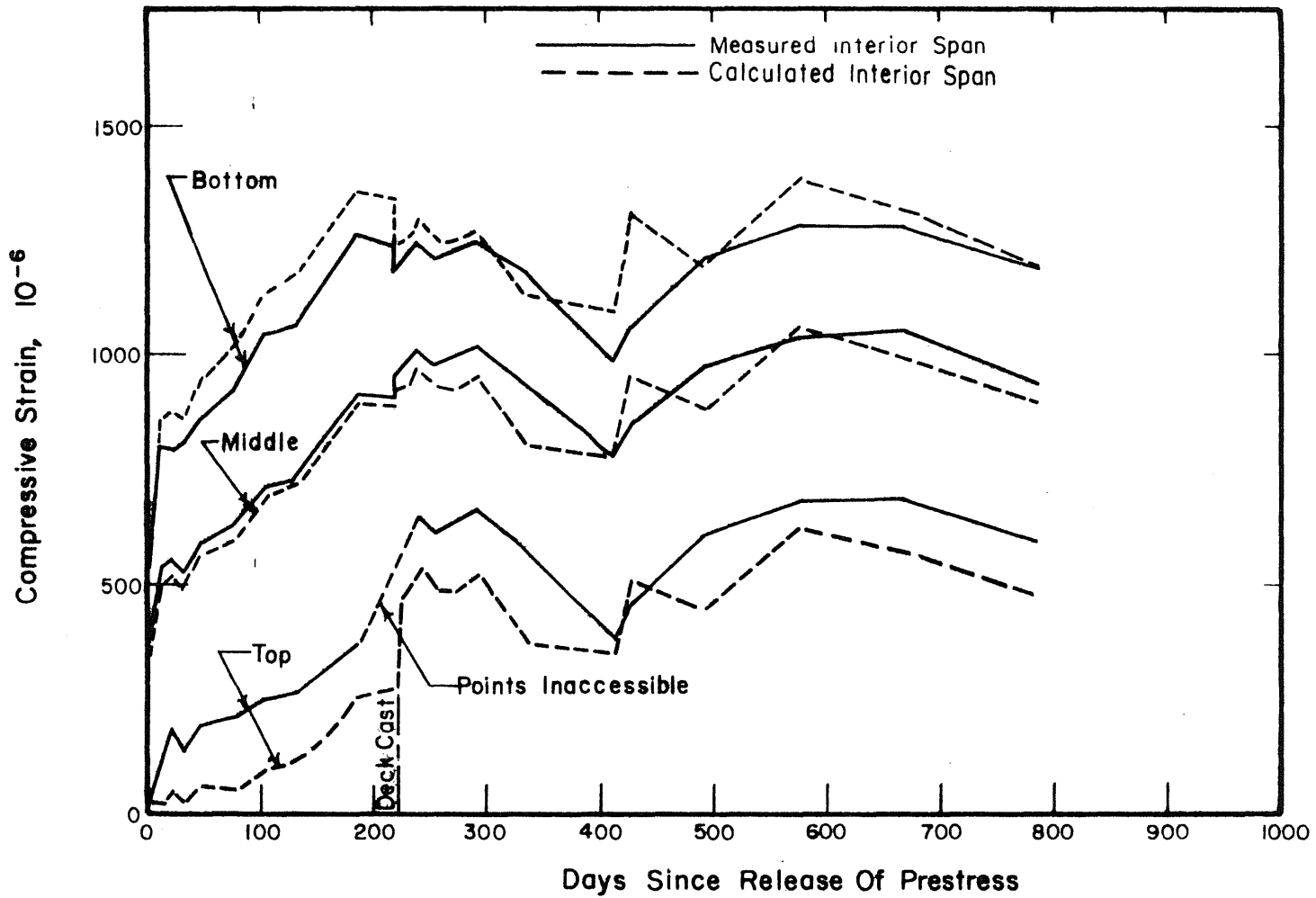


Fig. 3.39 Measured and Calculated Total Strains at Midspan vs. Time, Beam BX-3, Douglas County Bridge, Values Computed Using Field Creep and Shrinkage Values

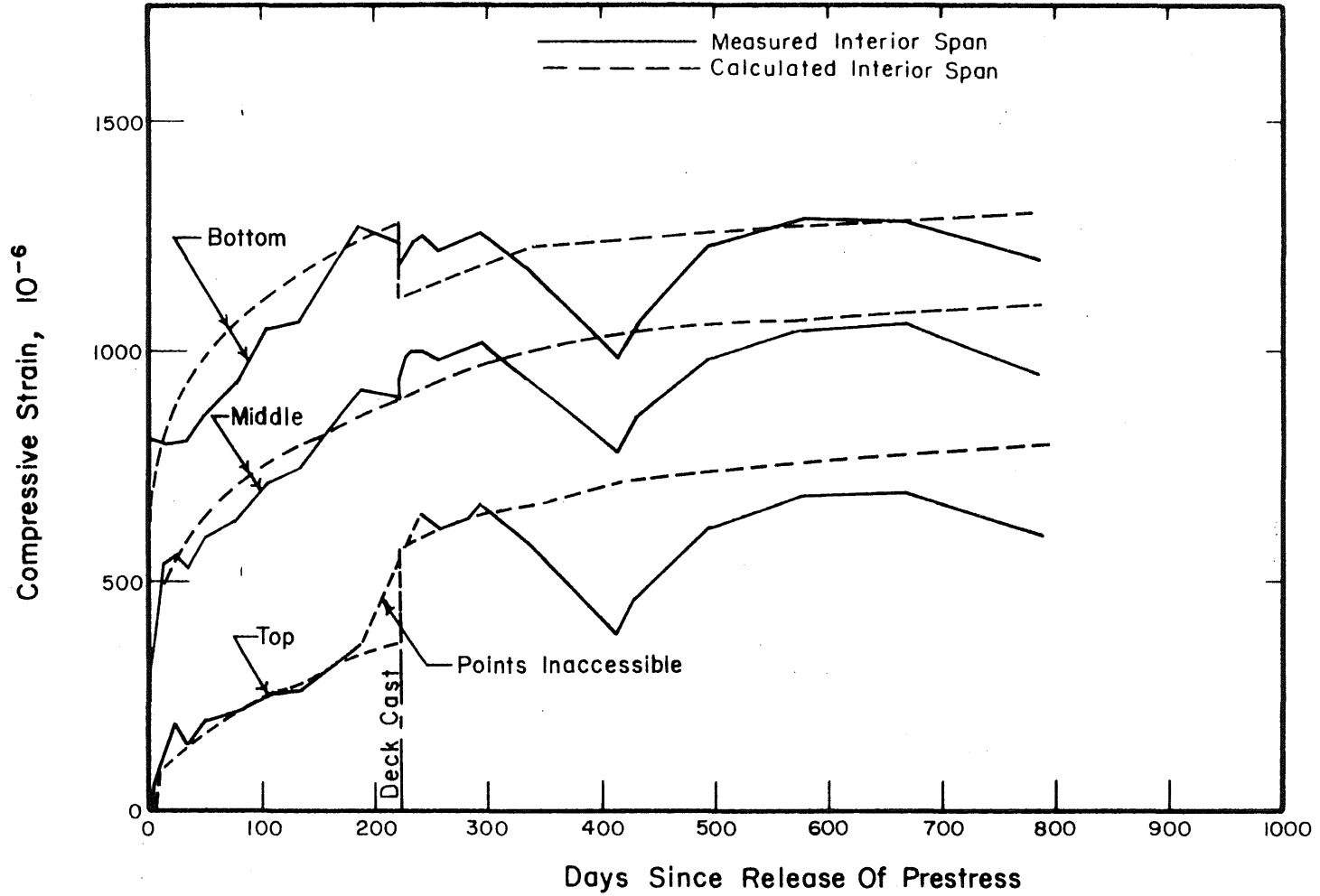


Fig. 3.40 Measured and Calculated Total Strains at Midspan vs. Time, Beam BX-3, Douglas County Bridge, Values Computed Using Lower Bound Laboratory Creep and Shrinkage Values

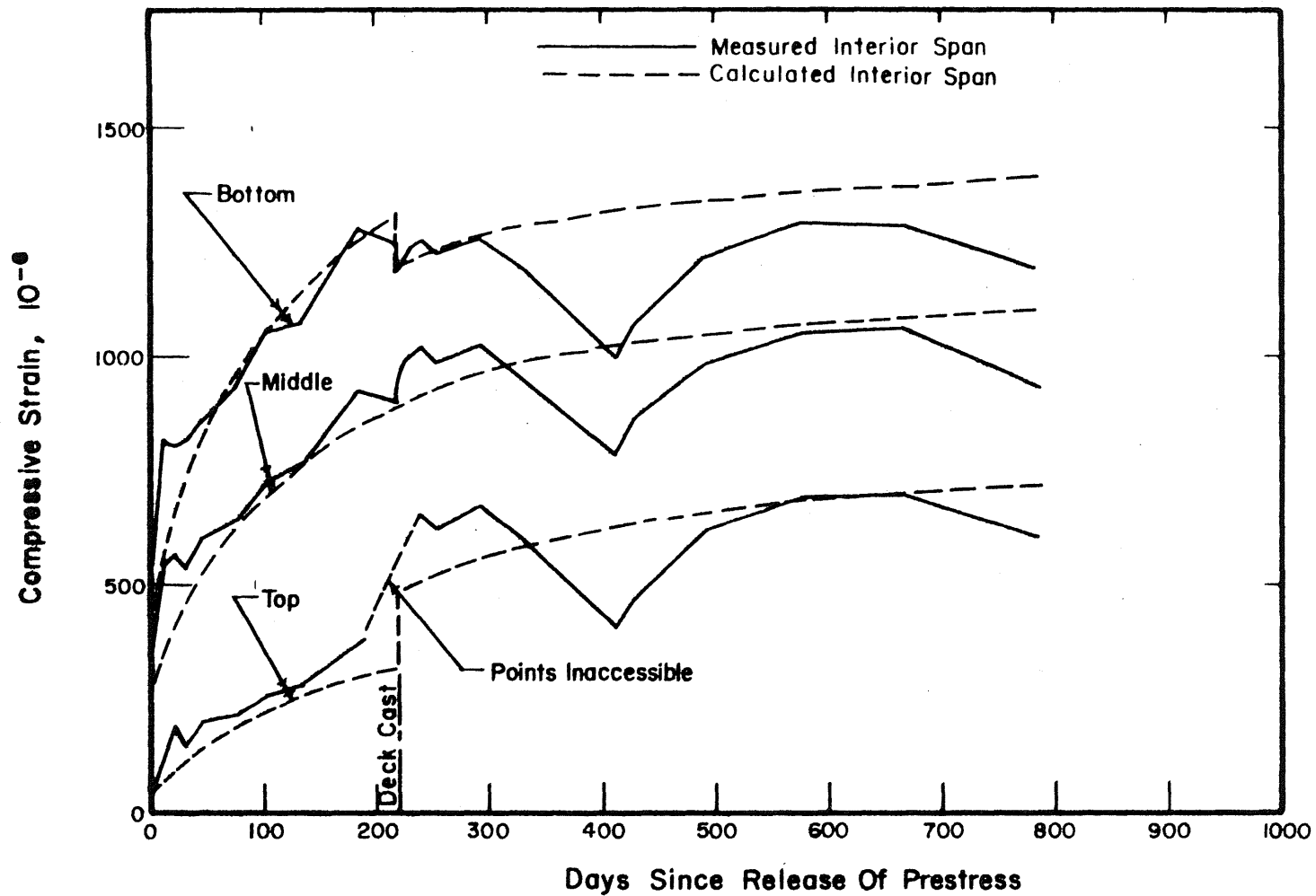


Fig. 3.41 Measured and Calculated Total Strains at Midspan vs. Time, Beam BX-3, Douglas County Bridge, Values Computed Using C.E.B. 50 Percent R.H. Creep and Shrinkage Values

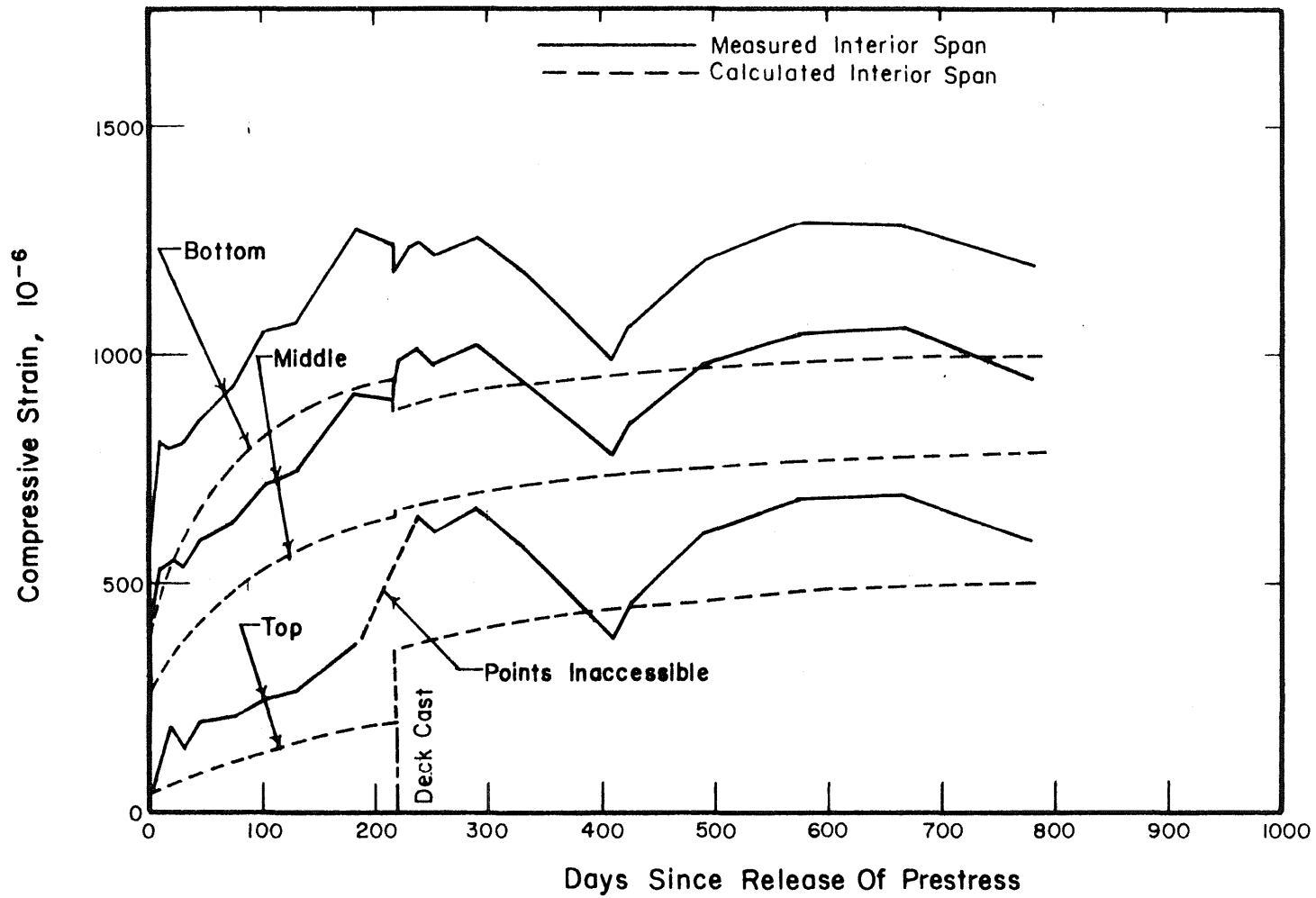


Fig. 3.42 Measured and Calculated Total Strains at Midspan vs. Time, Beam BX-3, Douglas County Bridge, Values Computed Using C.E.B. 80 Percent Creep and Shrinkage Values

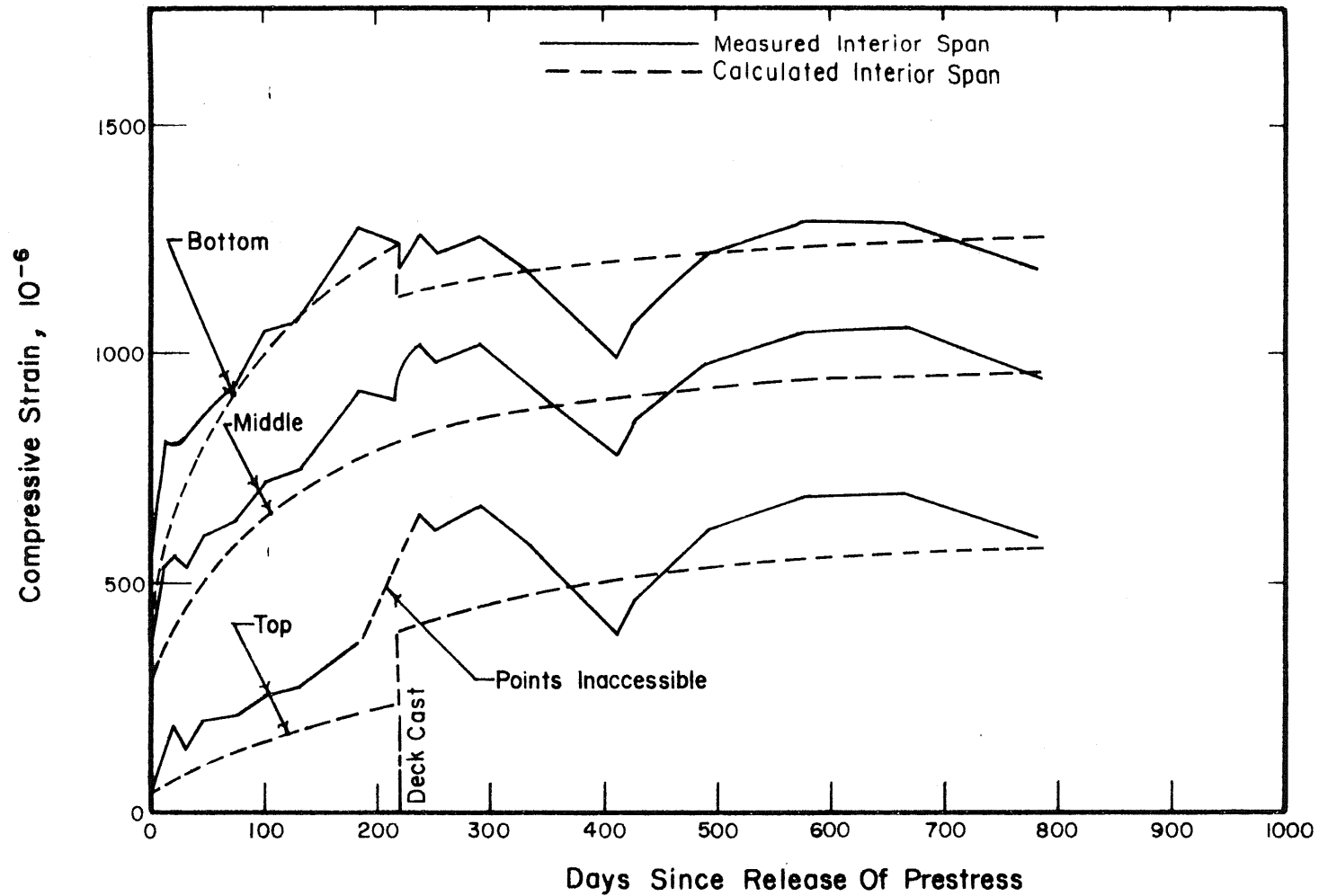


Fig. 3.43 Measured and Calculated Total Strains at Midspan vs. Time, Beam BX-3, Douglas County Bridge, Values Computed Using C.E.R. Values for 50 Percent R.H. Creep and 80 Percent R.H. Shrinkage



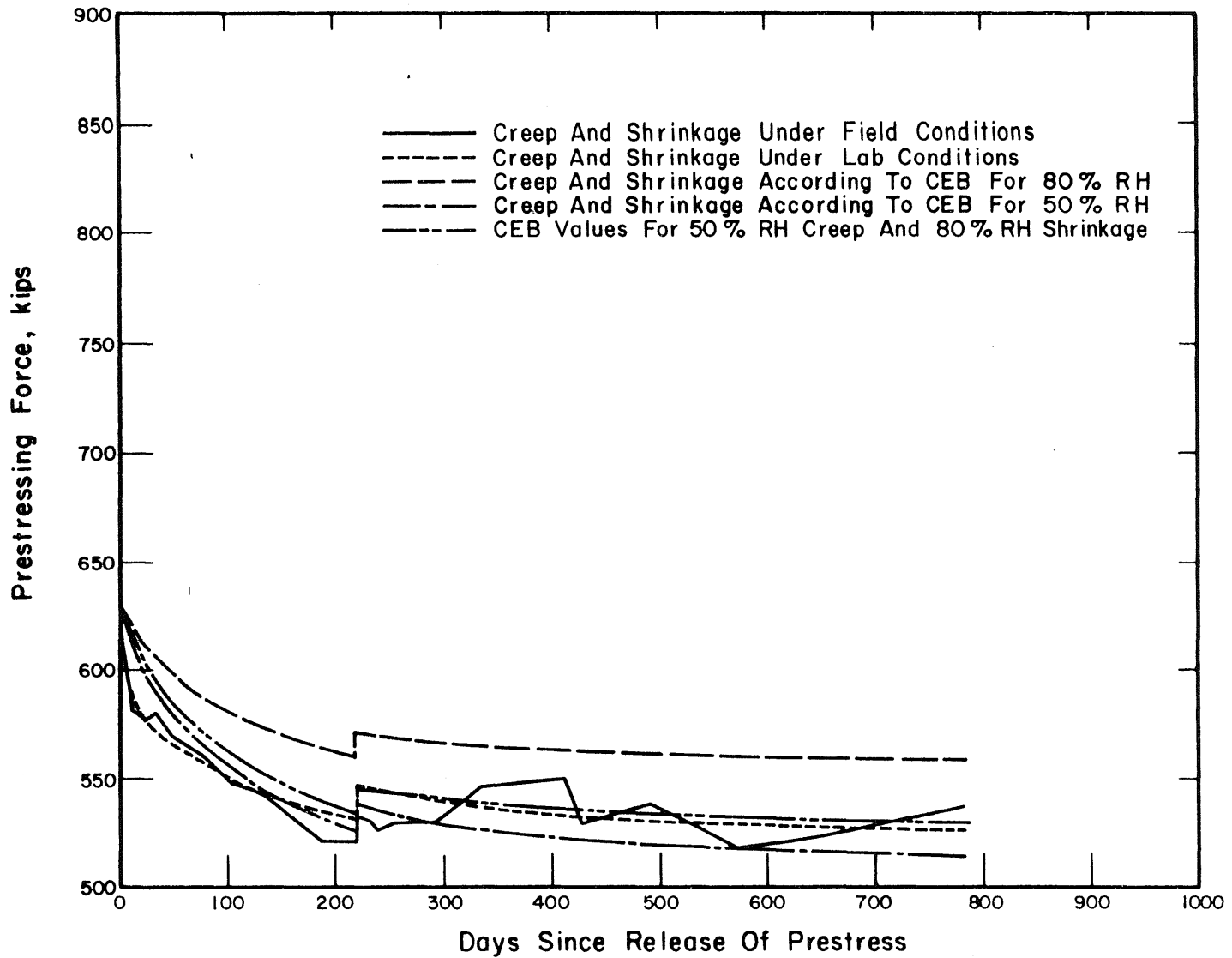


Fig. 3.44 Calculated Prestressing Force at Midspan vs. Time, Beam BX-3, Douglas County Bridge

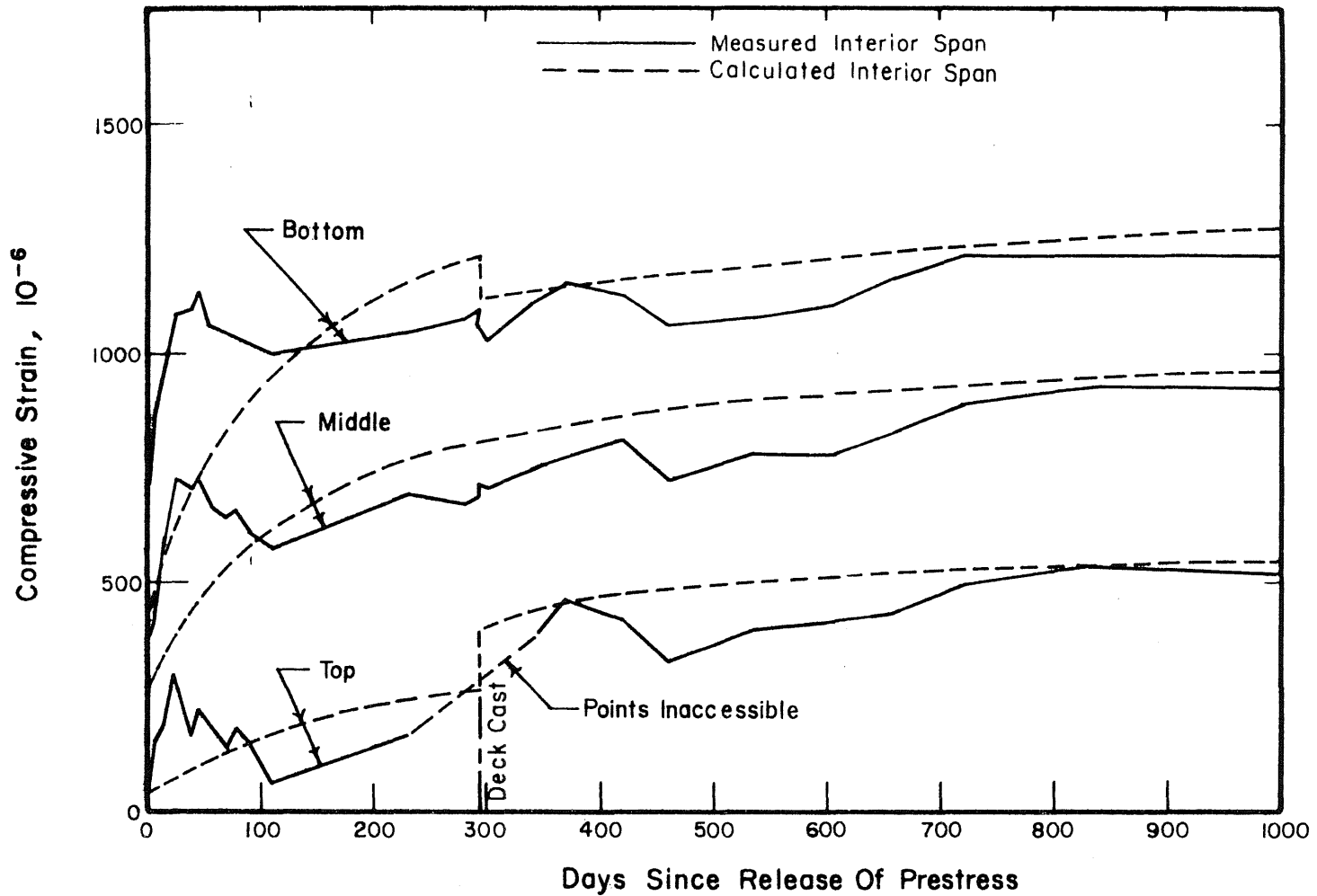


Fig. 3.45 Measured Total Strains at Midspan of Beam BX-1 and Calculated Total Strains at Midspan of Simply Supported Beam vs. Time, Jefferson County Bridge, Values Computed Using C.E.B. Values for 50 Percent R.H. Creep and 80 Percent R.H. Shrinkage

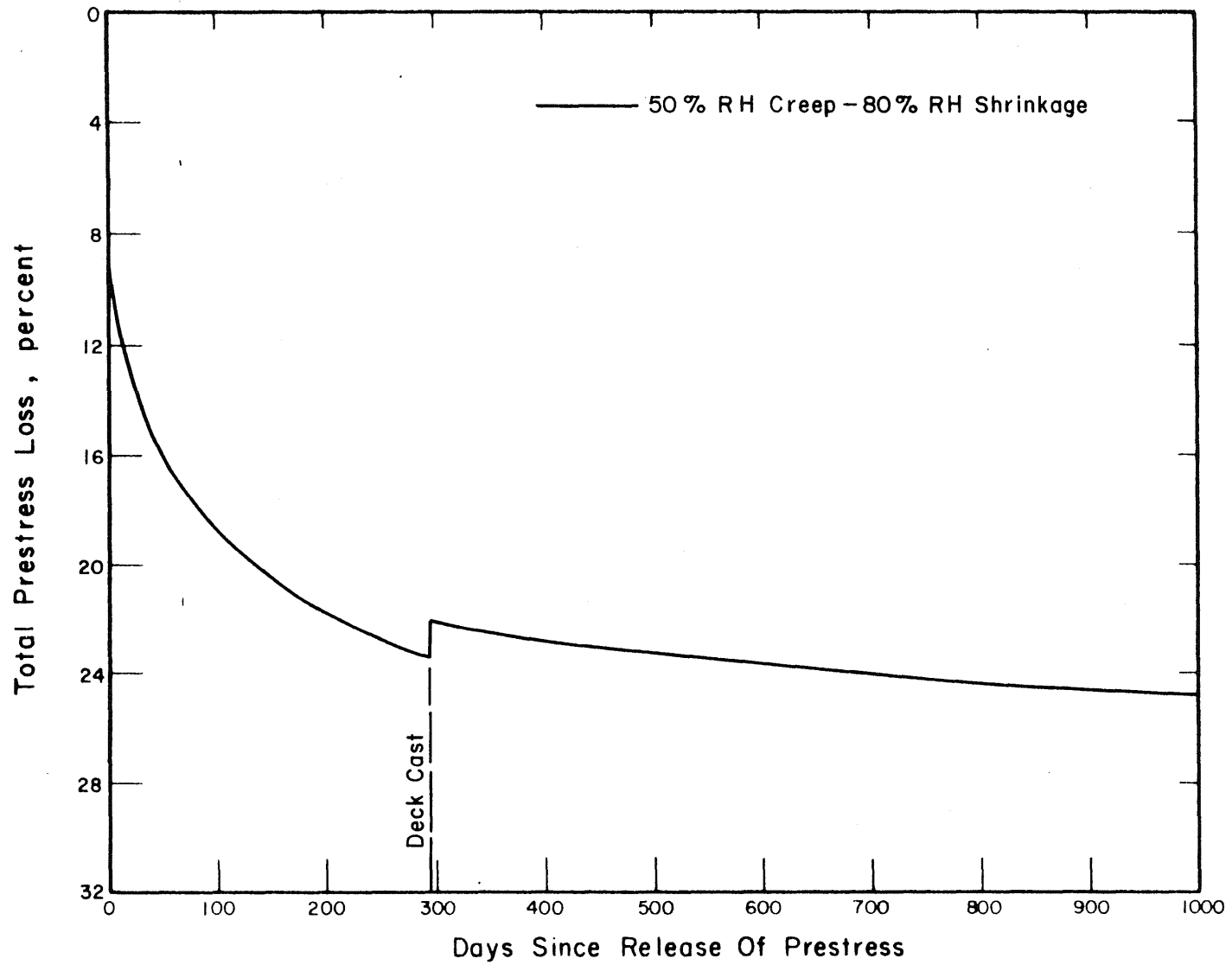


Fig. 3.46 Calculated Total Prestress Loss vs. Time, Beam BX-1, Jefferson County Bridge

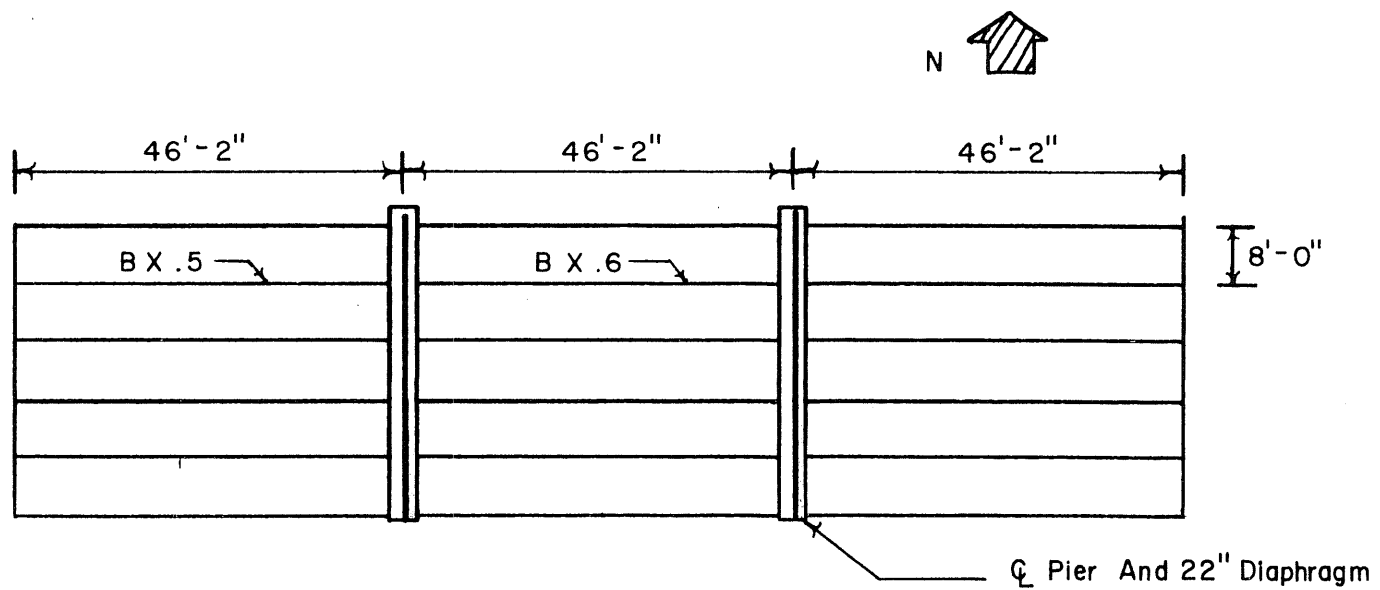


Fig. 3.47 Plan of Bridge Showing Girder and Diaphragm Placement,  
Champaign County Bridge

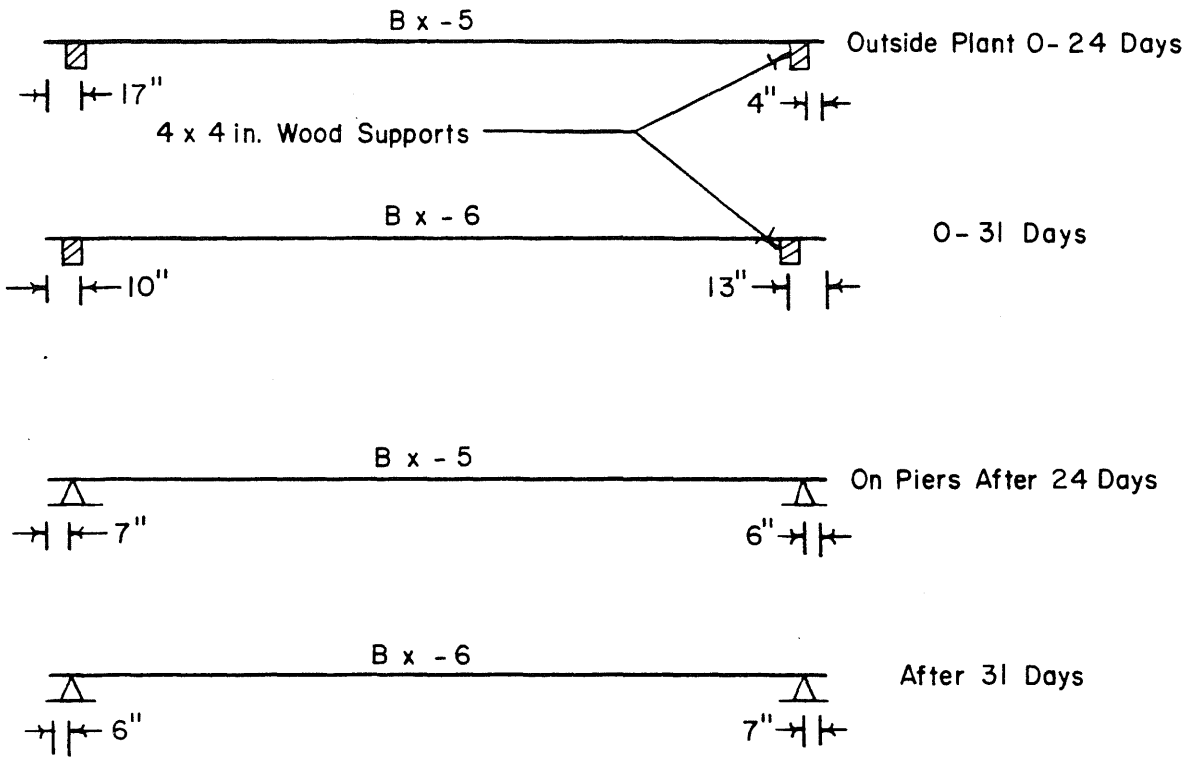
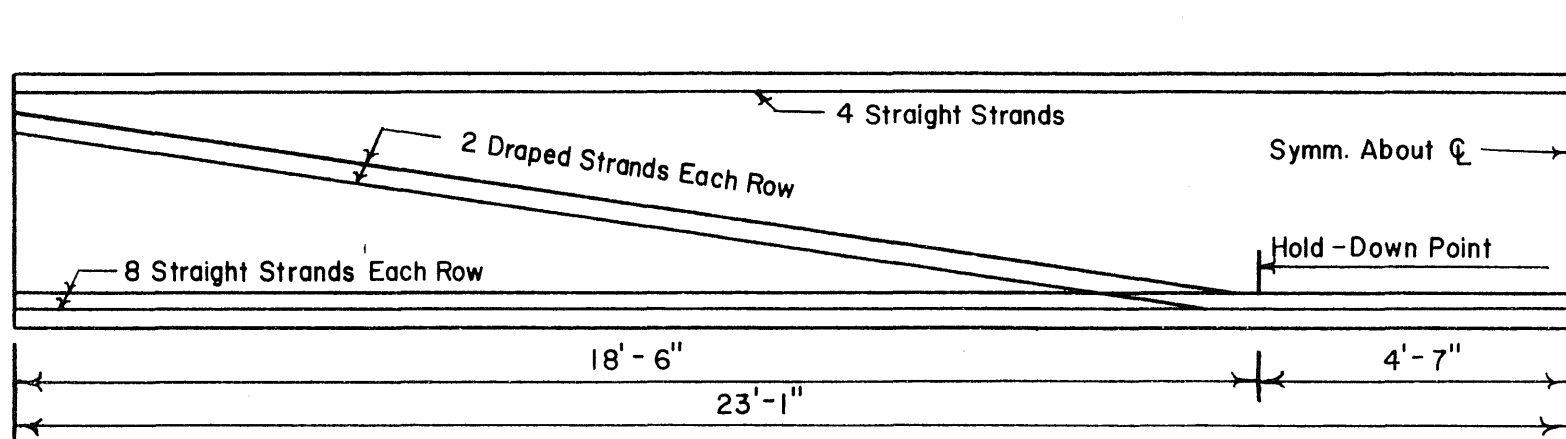
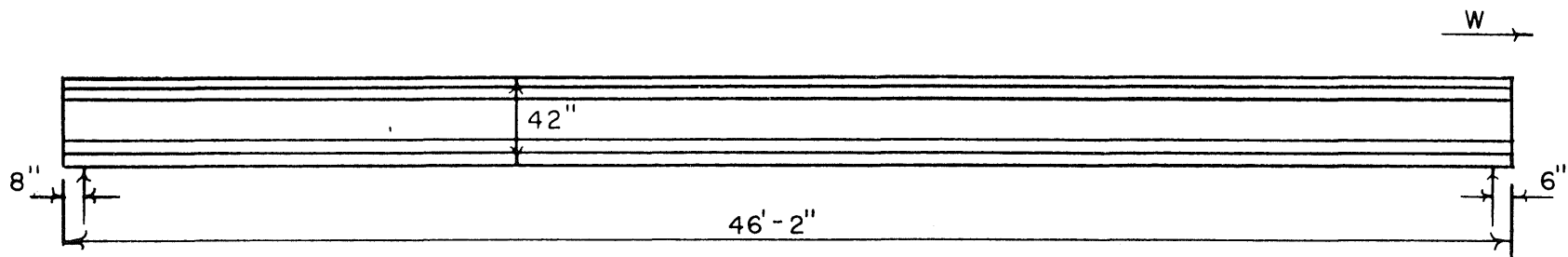


Fig. 3.48 Locations of Beam Supports at Various Times,  
Champaign County Bridge



Profile Of  $7/16$  in. Prestressing Strands

Fig. 3.49 Details of Girders, Champaign County Bridge

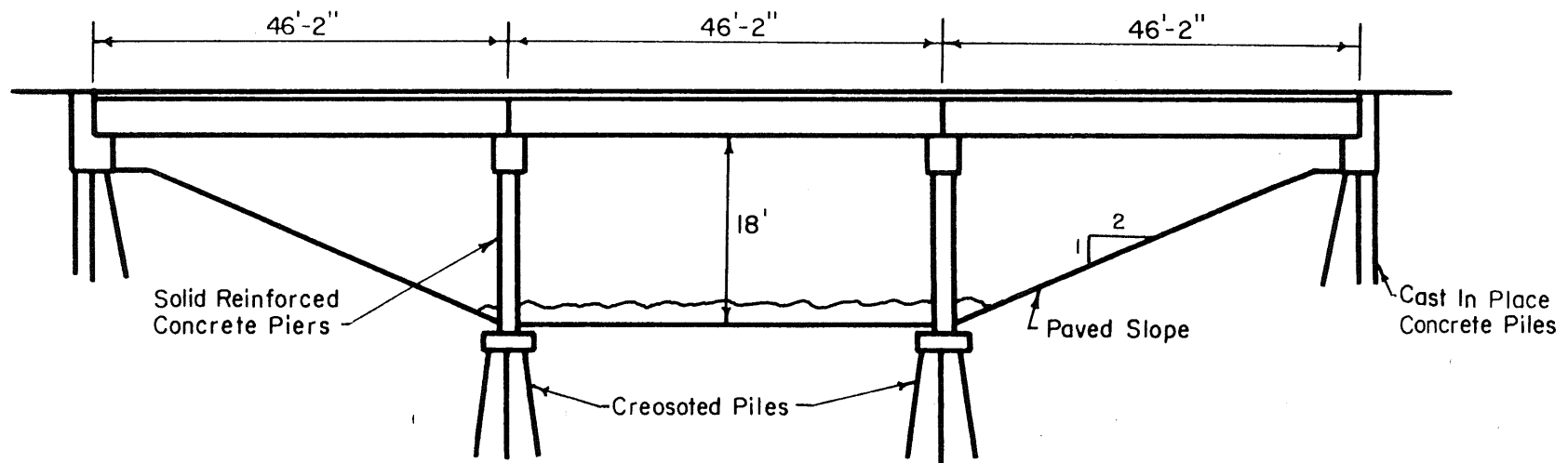
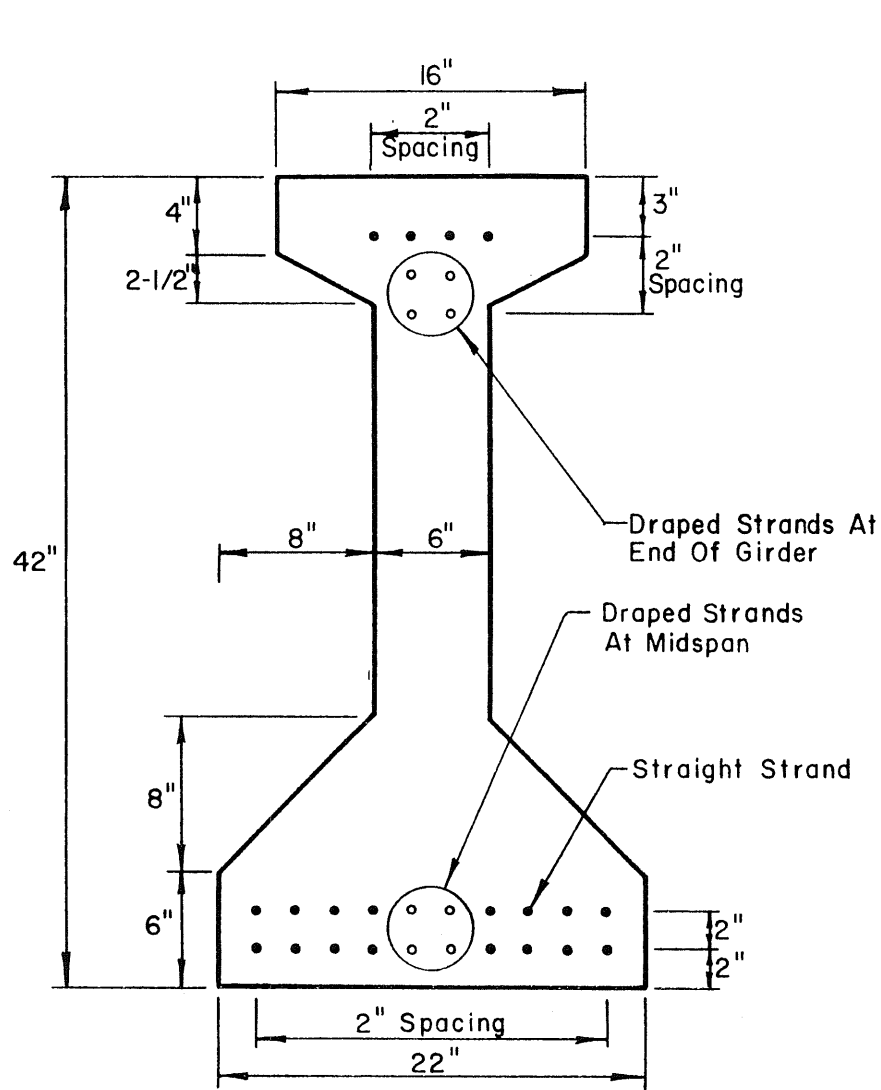
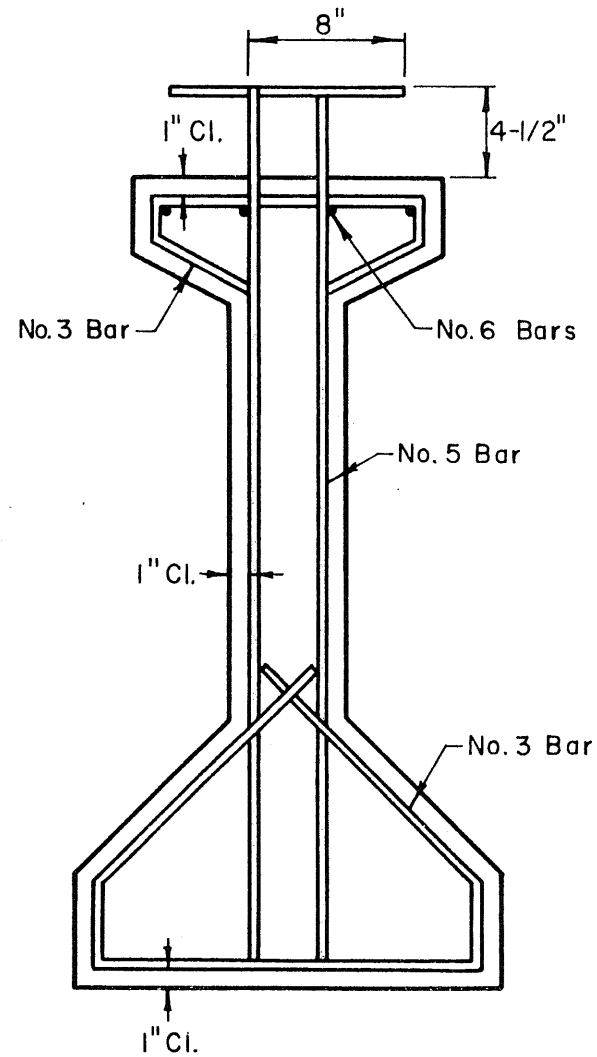


Fig. 3.50 Elevation of Bridge, Champaign County Bridge



(a) Strand Placement



(b) Reinforcement

Fig. 3.51 Girder Cross Section, Champaign County Bridge



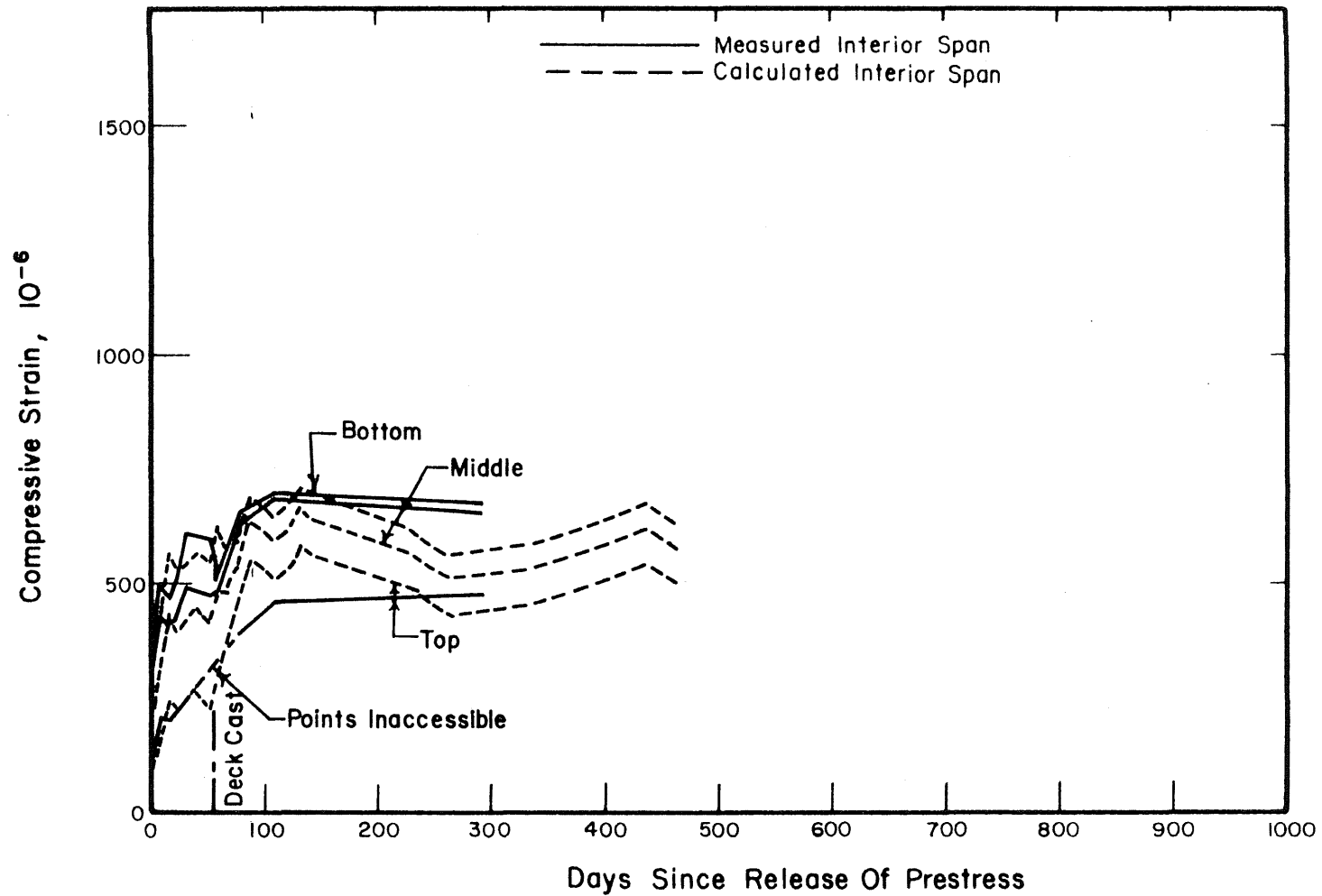


Fig. 3.52 Measured and Calculated Total Strains at Midspan vs. Time, Beam BX-6, Champaign County Bridge, Values Computed Using Field Creep and Shrinkage Values

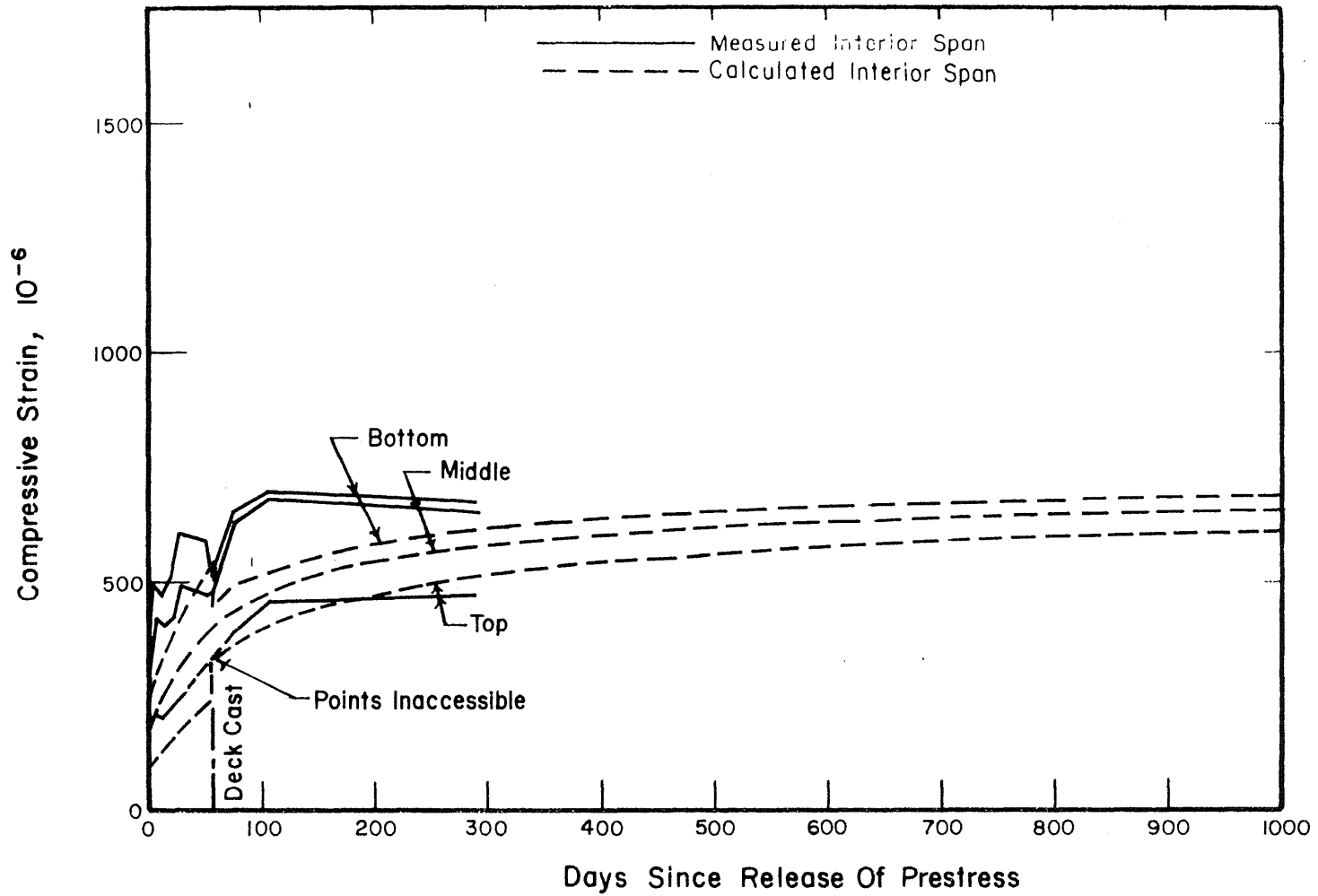


Fig. 3.53 Measured and Calculated Total Strains at Midspan vs. Time, Beam BX-6, Champaign County Bridge, Values Computed Using C.E.B. 50 Percent R.H. Creep and 80 Percent R.H. Shrinkage Values

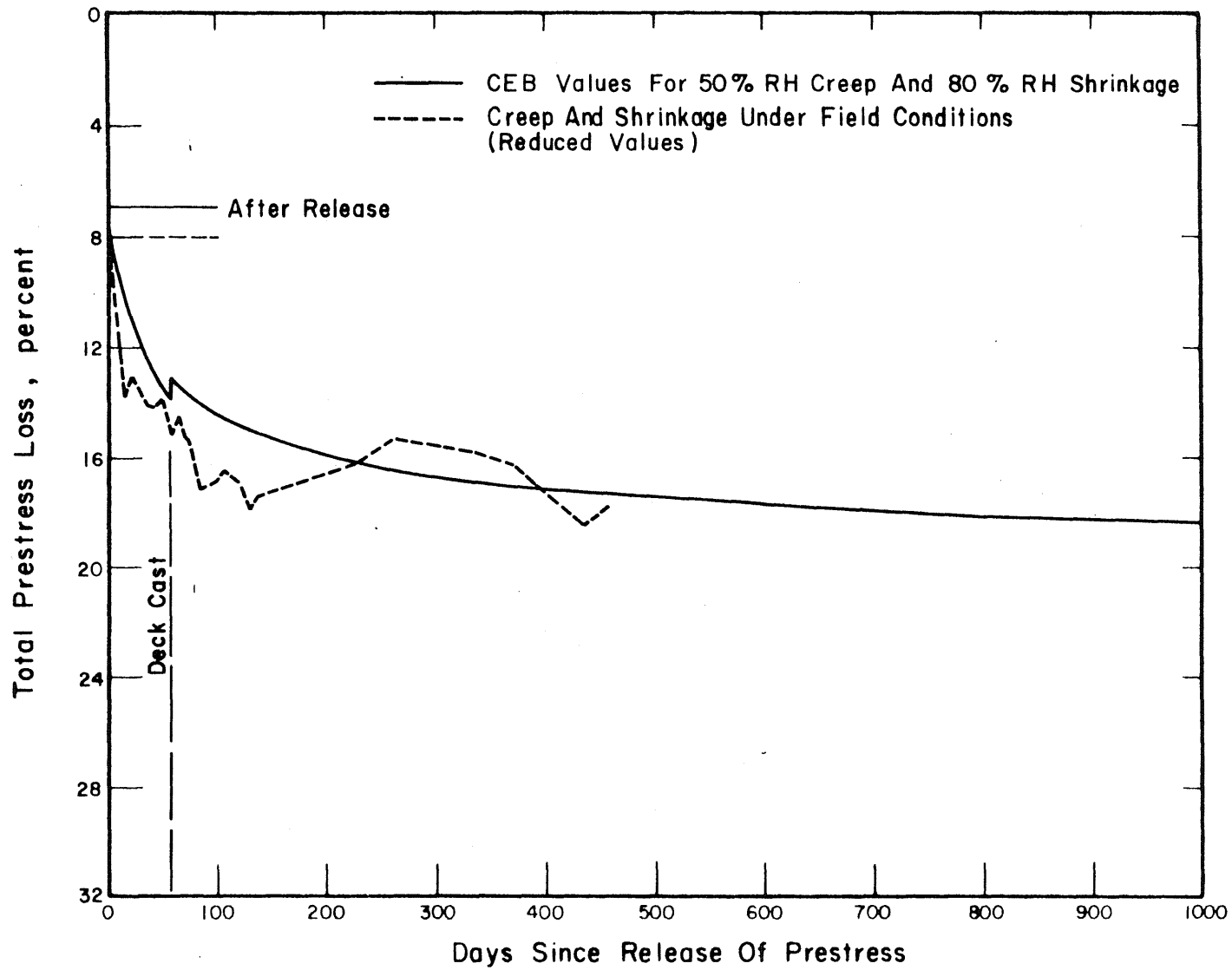


Fig. 3.54 Calculated Prestressing Force vs. Time, Beam BX-6, Champaign County Bridge

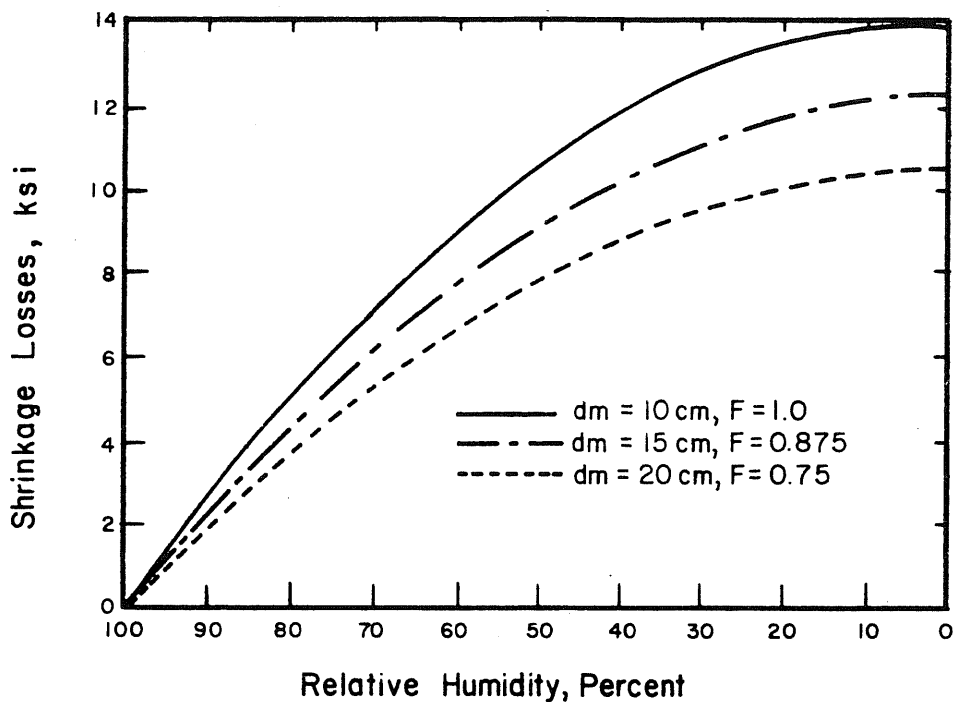


Fig. 4.1 Prestress Loss Due to Shrinkage of the Concrete as a Function of the Relative Humidity in the Field and Theoretical Thickness of the Member

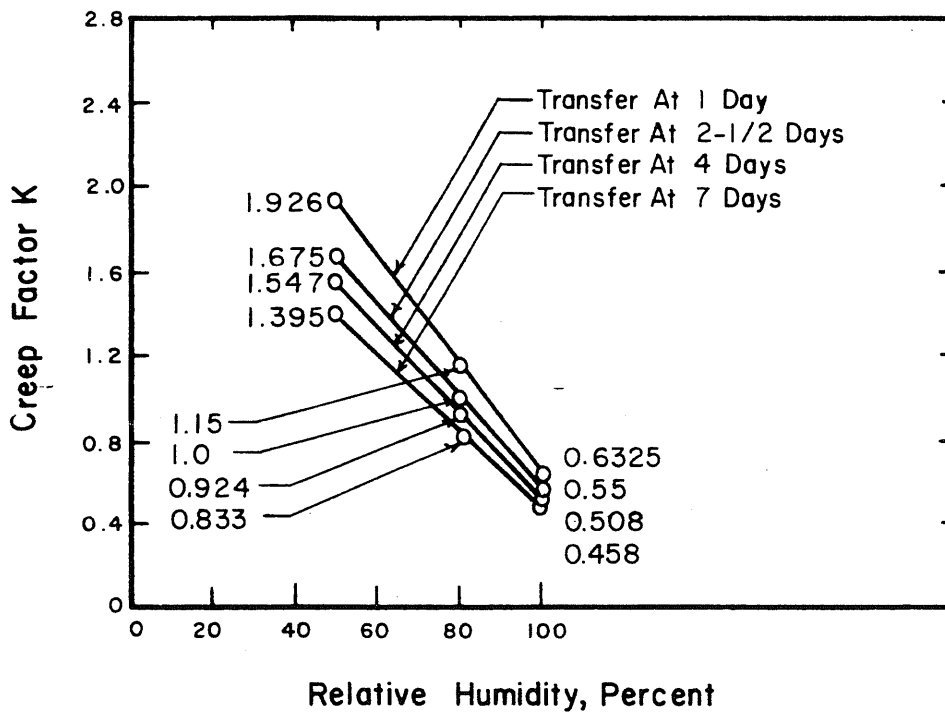


Fig. 4.2 Creep Factor as a Function of the Relative Humidity in the Field and Time of Release of Prestress

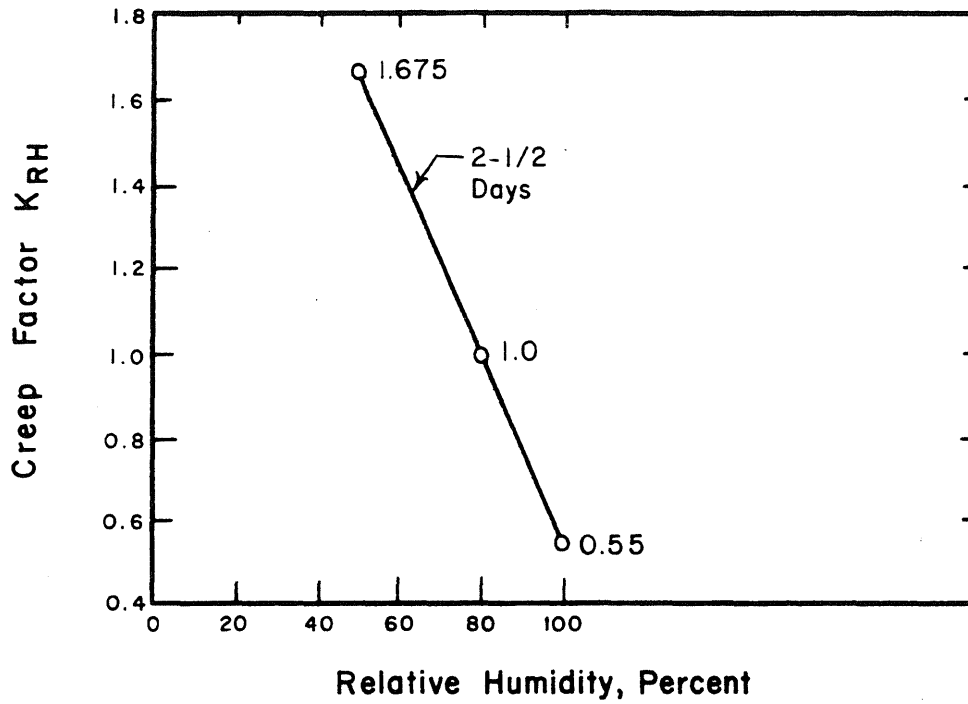


Fig. 4.3 Creep Factor as a Function of the Relative Humidity in the Field

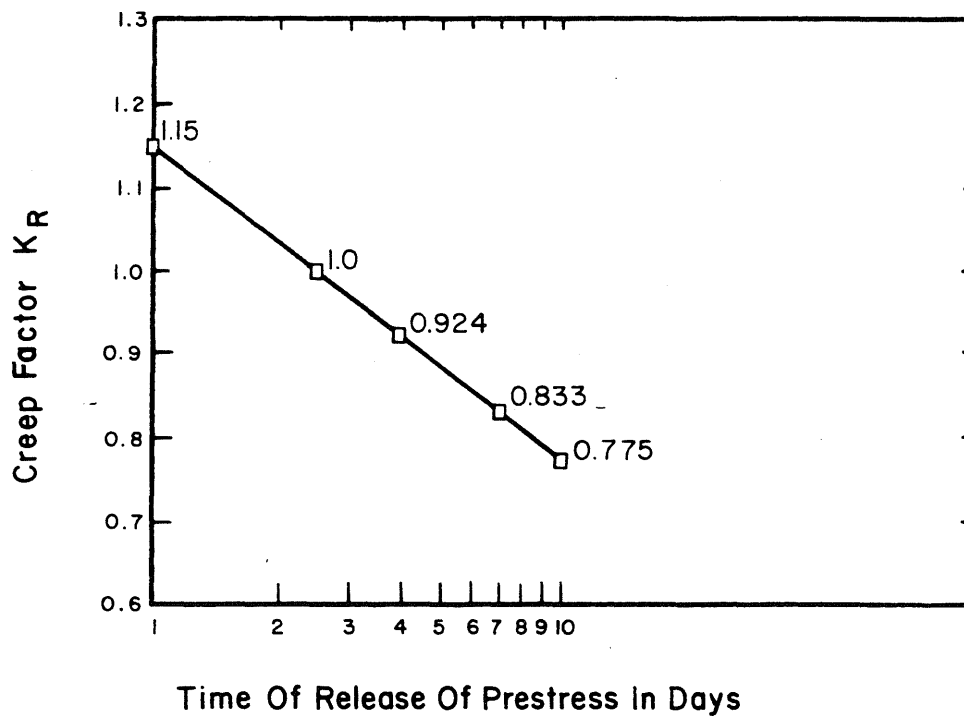


Fig. 4.4 Creep Factor as a Function of the Time of Release of Prestress

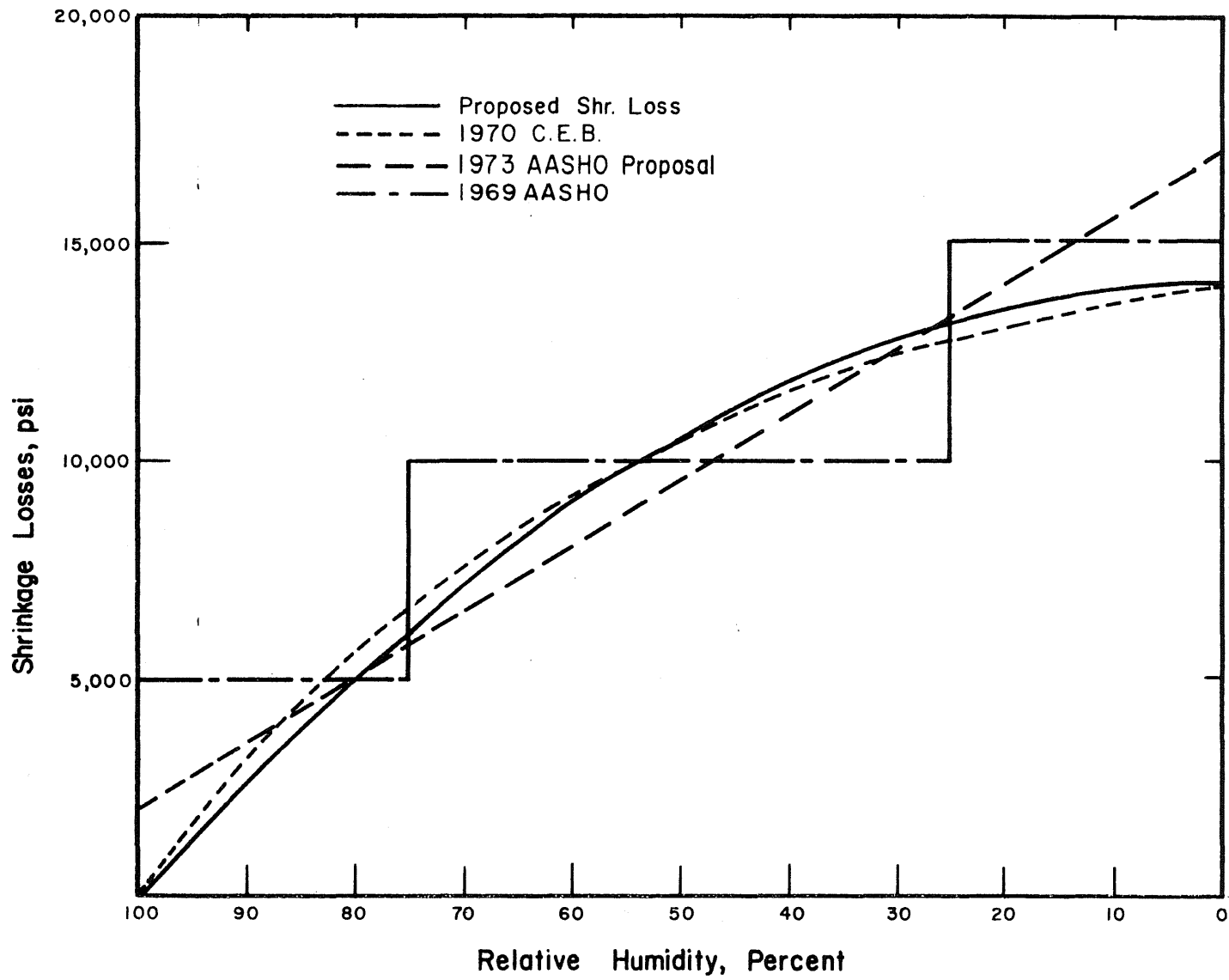


Fig. 4.5 Prestress Losses Due to Shrinkage of the Concrete Estimated According to Several Proposed Shrinkage Loss Values

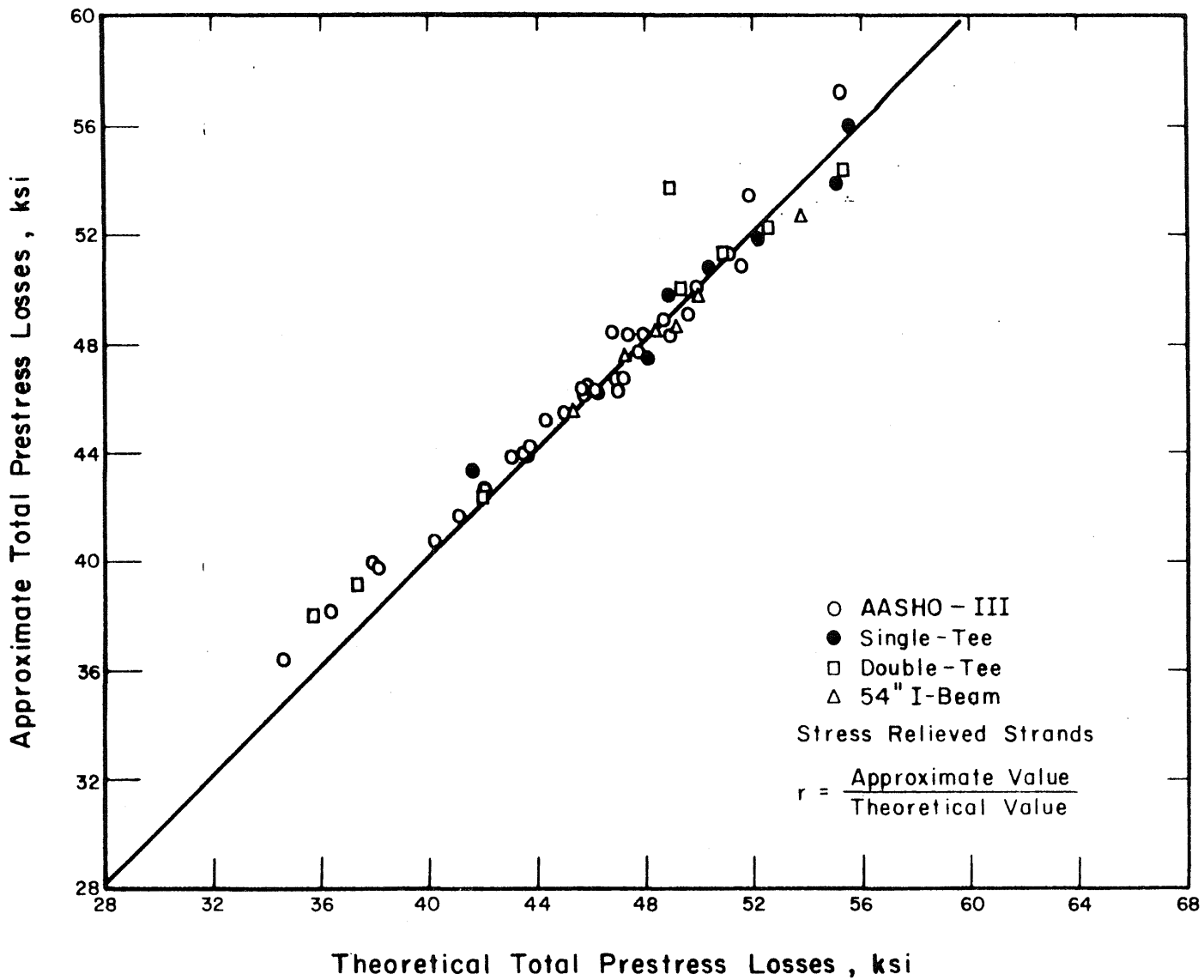


Fig. 5.1a Comparison of Total Prestress Losses Calculated Using the Proposed Set of Loss Factors and the Theoretical Values

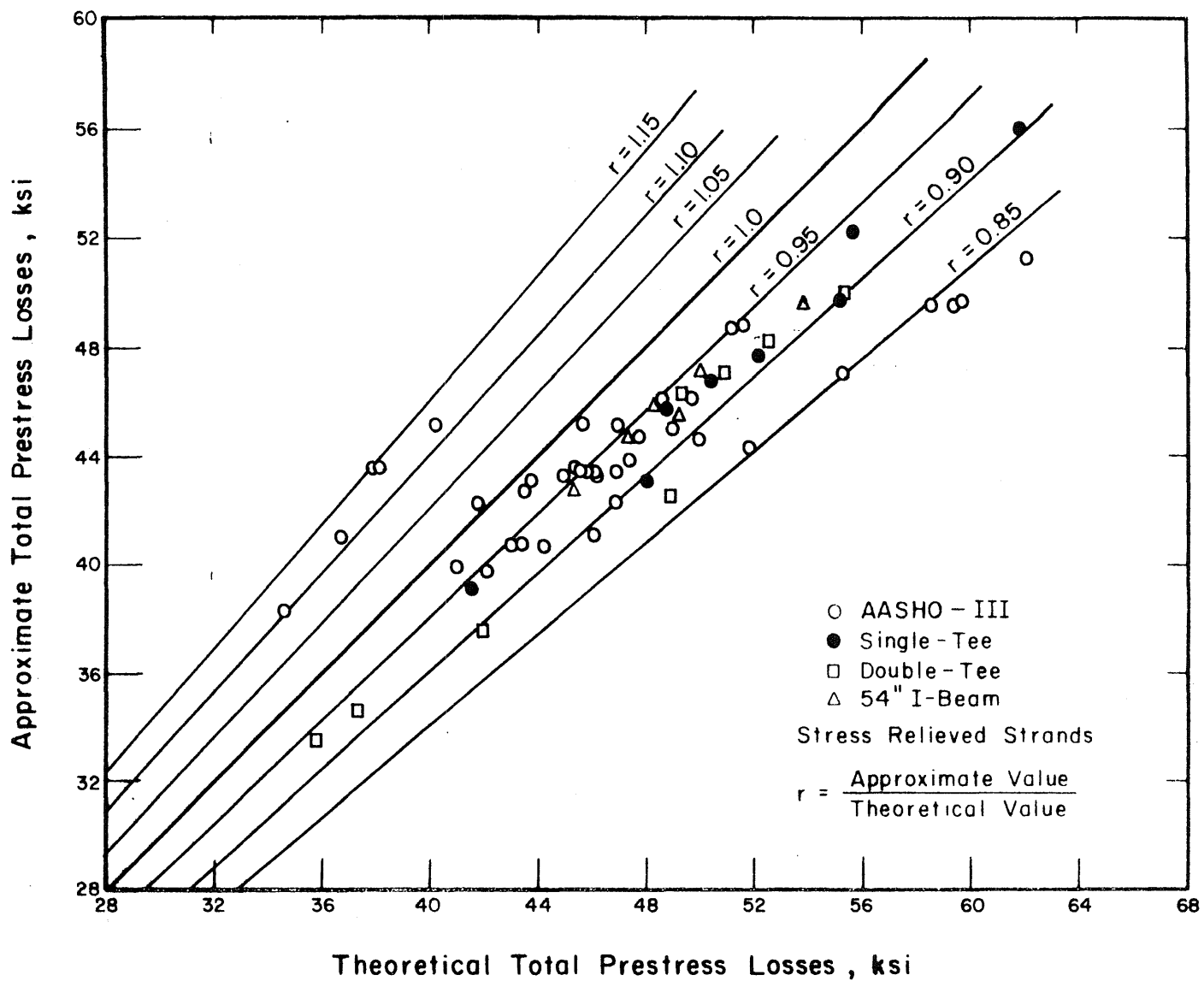


Fig. 5.1b Comparison of Total Prestress Losses Calculated Using the 1973 AASHO Proposal and the Theoretical Values



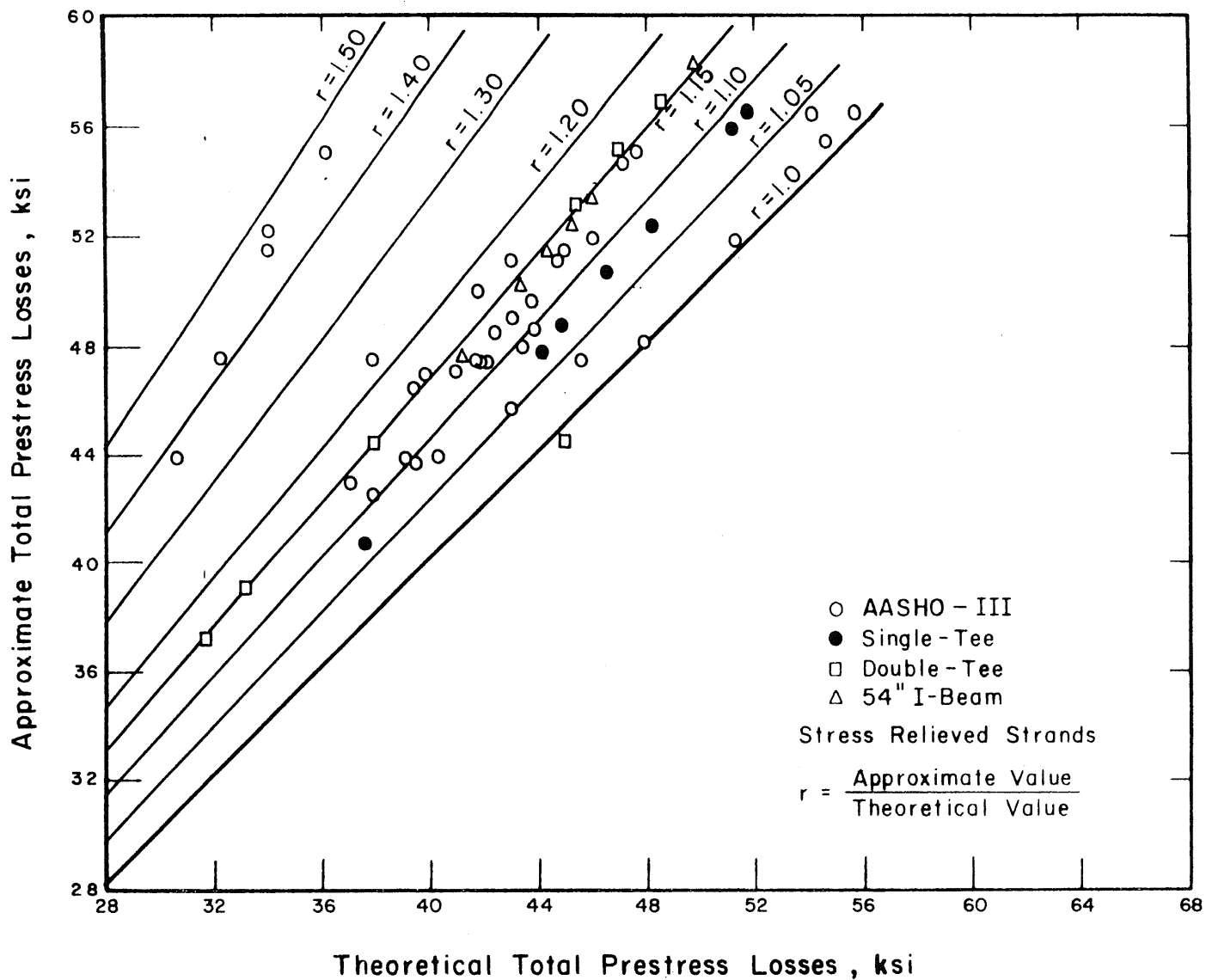


Fig. 5.1c Comparison of Total Prestress Losses Calculated Using the 1970 AASHO Interim Specifications and the Theoretical Values

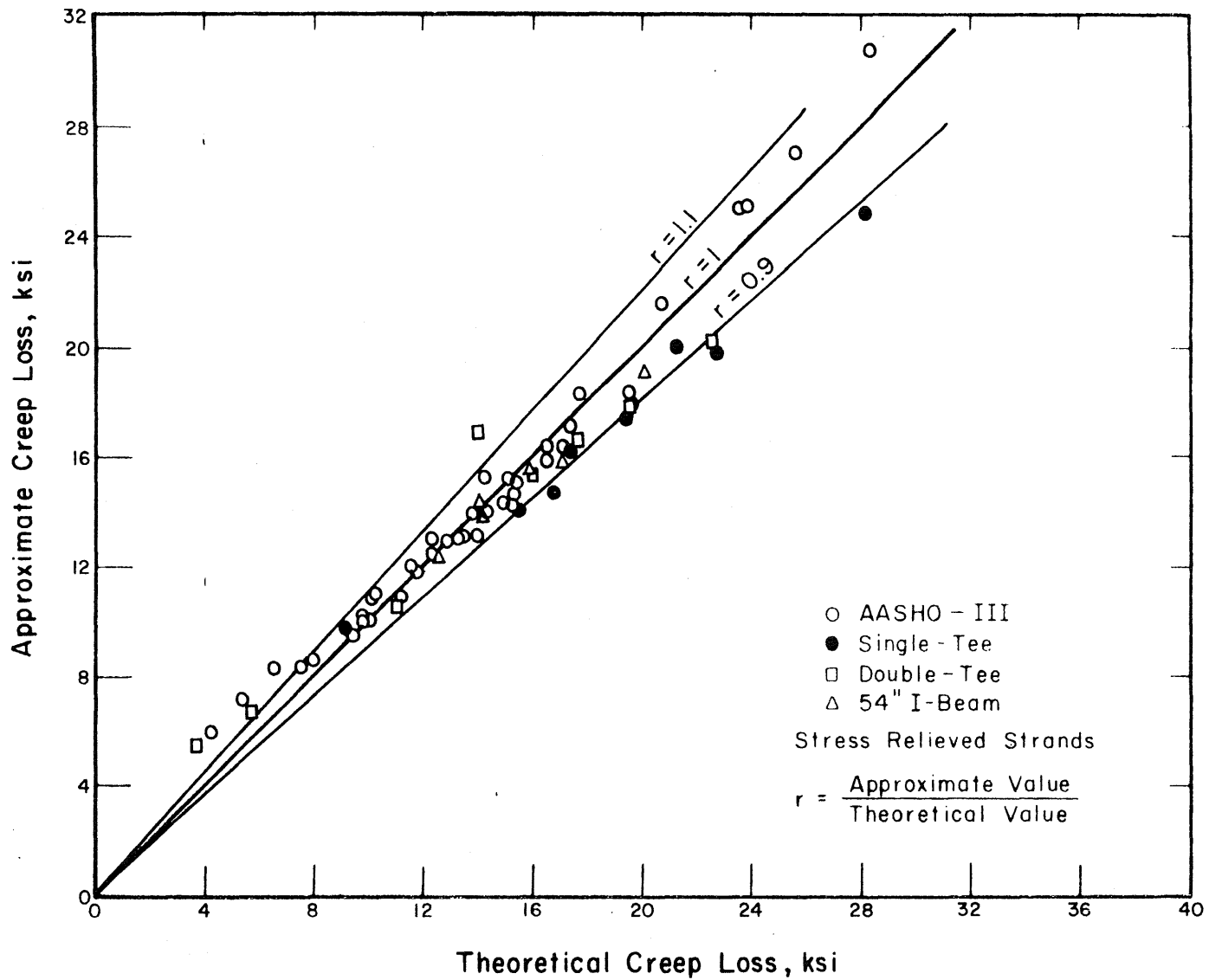


Fig. 5.2a Comparison of Creep Losses Calculated Using the Proposed Set of Loss Factors and the Theoretical Values

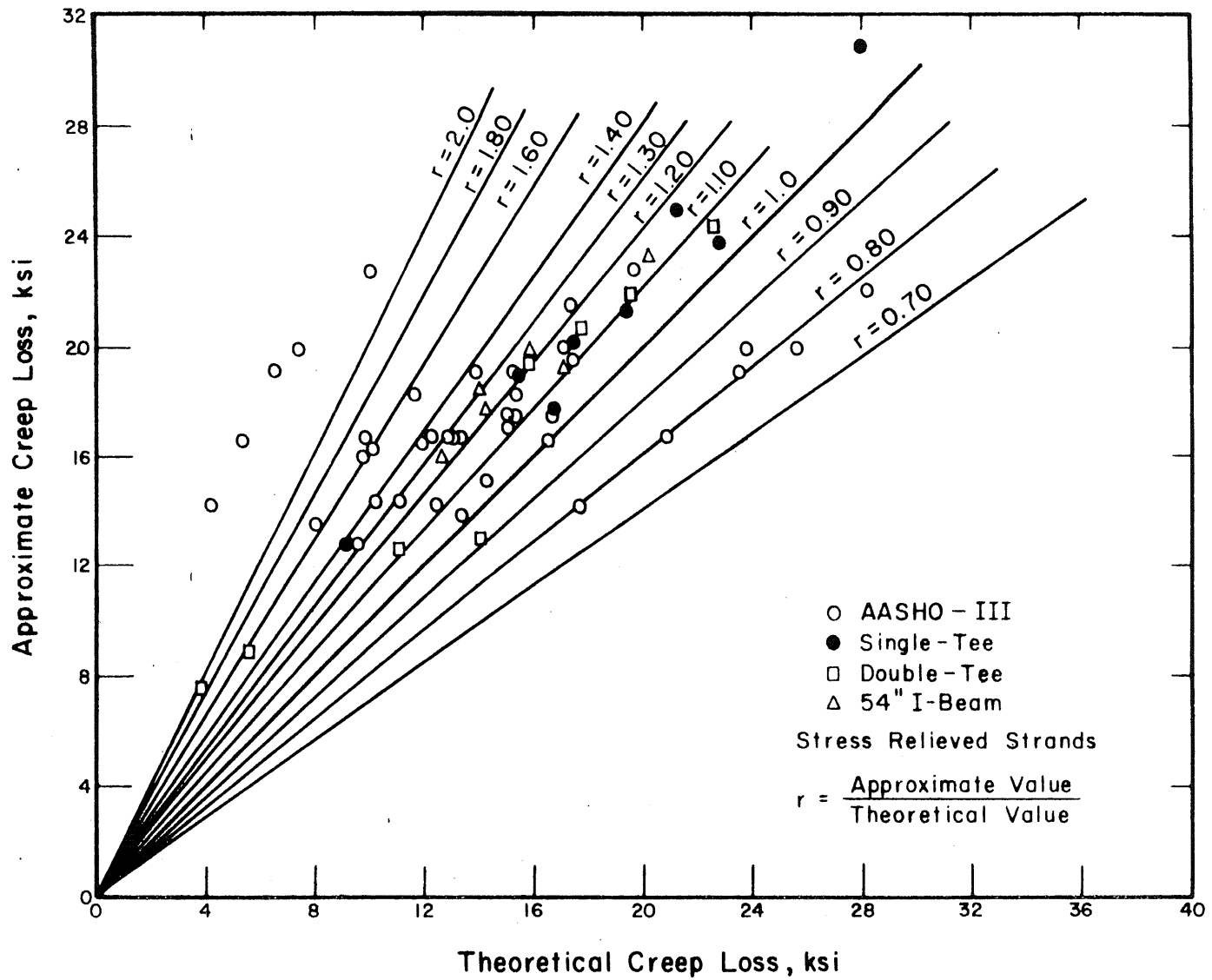


Fig. 5.2b Comparison of the Creep Losses Calculated Using the 1973 AASHO Proposal and the Theoretical Values

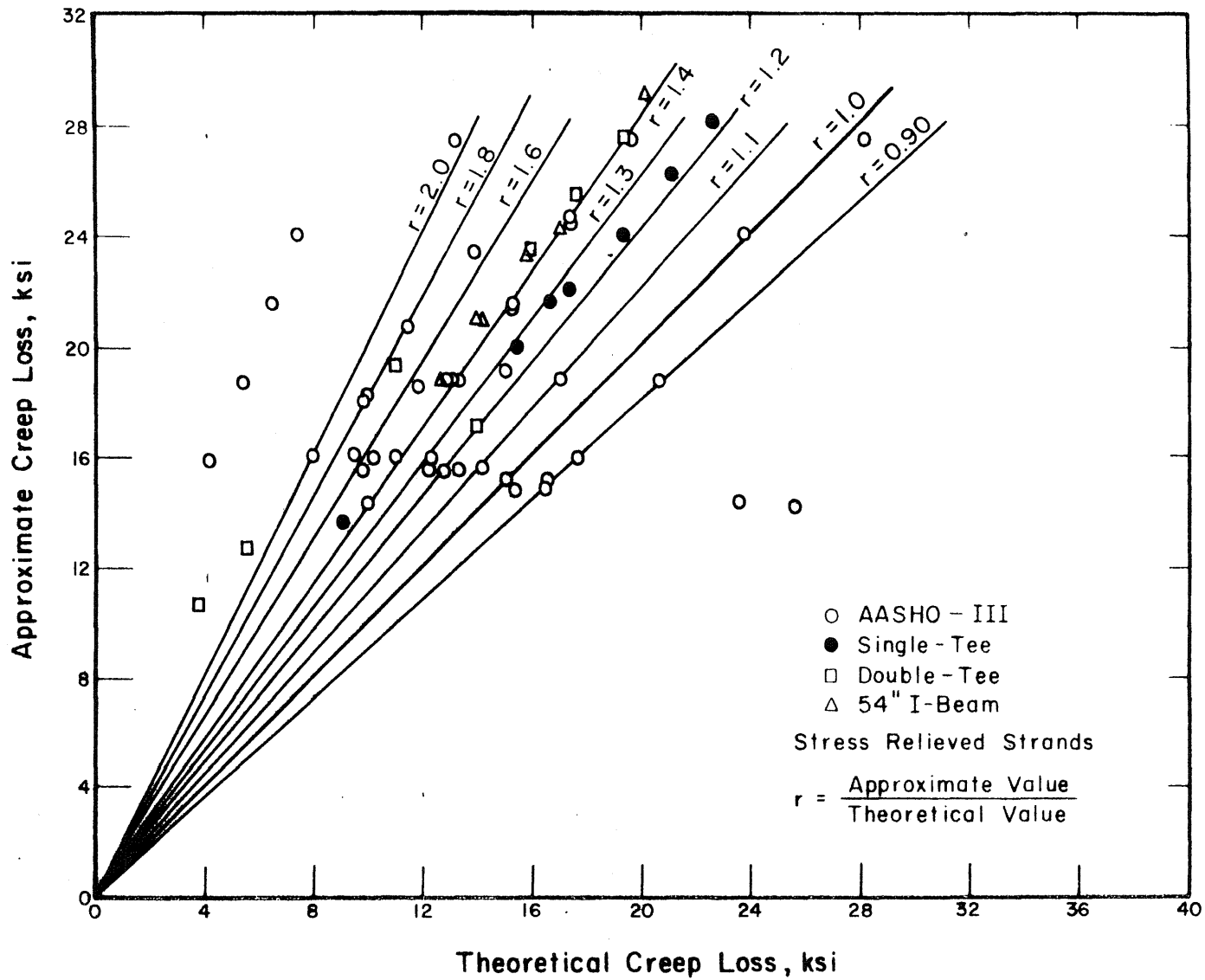


Fig. 5.2c Comparison of Creep Losses Calculated Using the 1970 AASHO Interim Specifications and the Theoretical Values

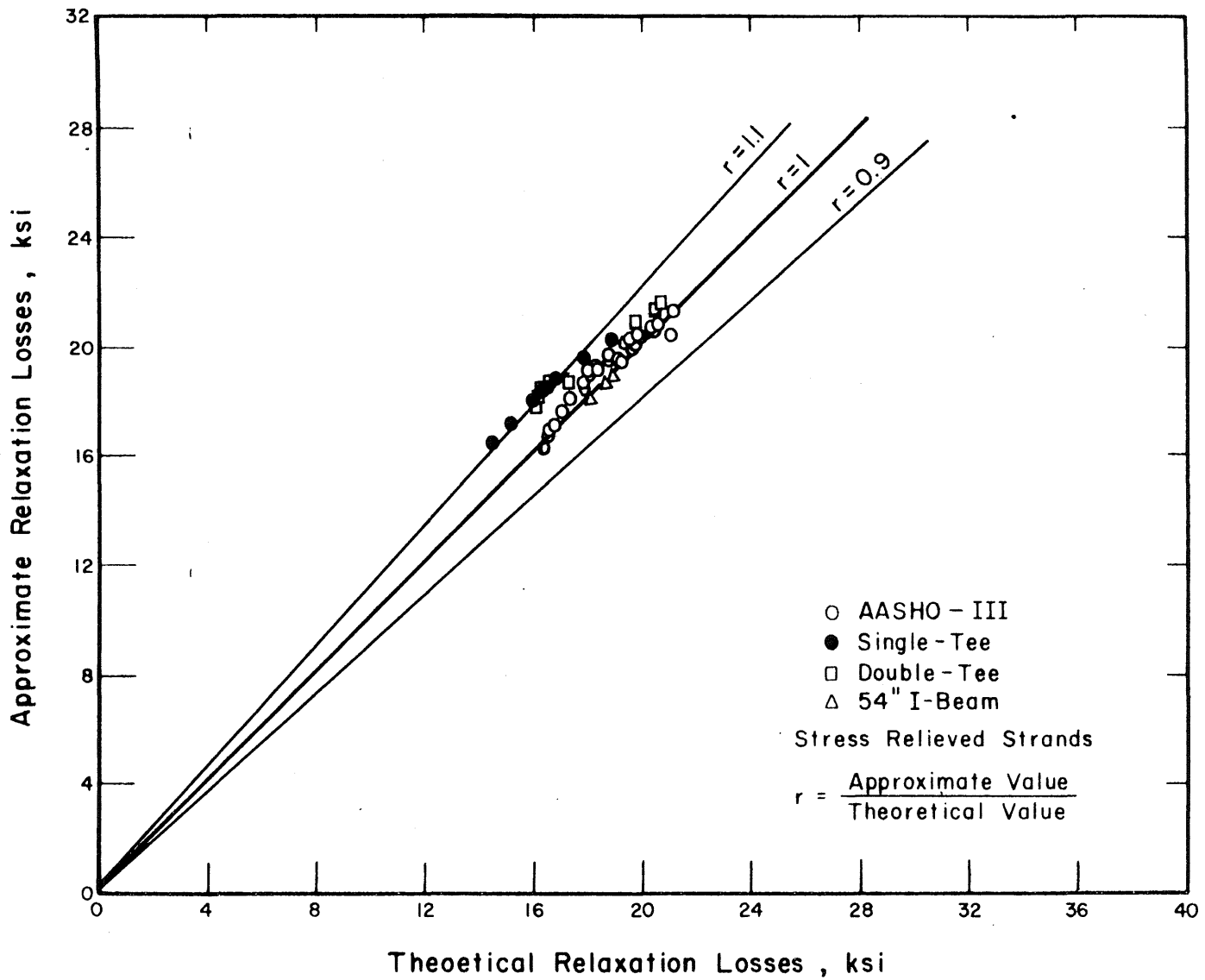


Fig. 5.3a Comparison of Relaxation Losses Calculated Using the Proposed Set of Loss Factors and the Theoretical Values

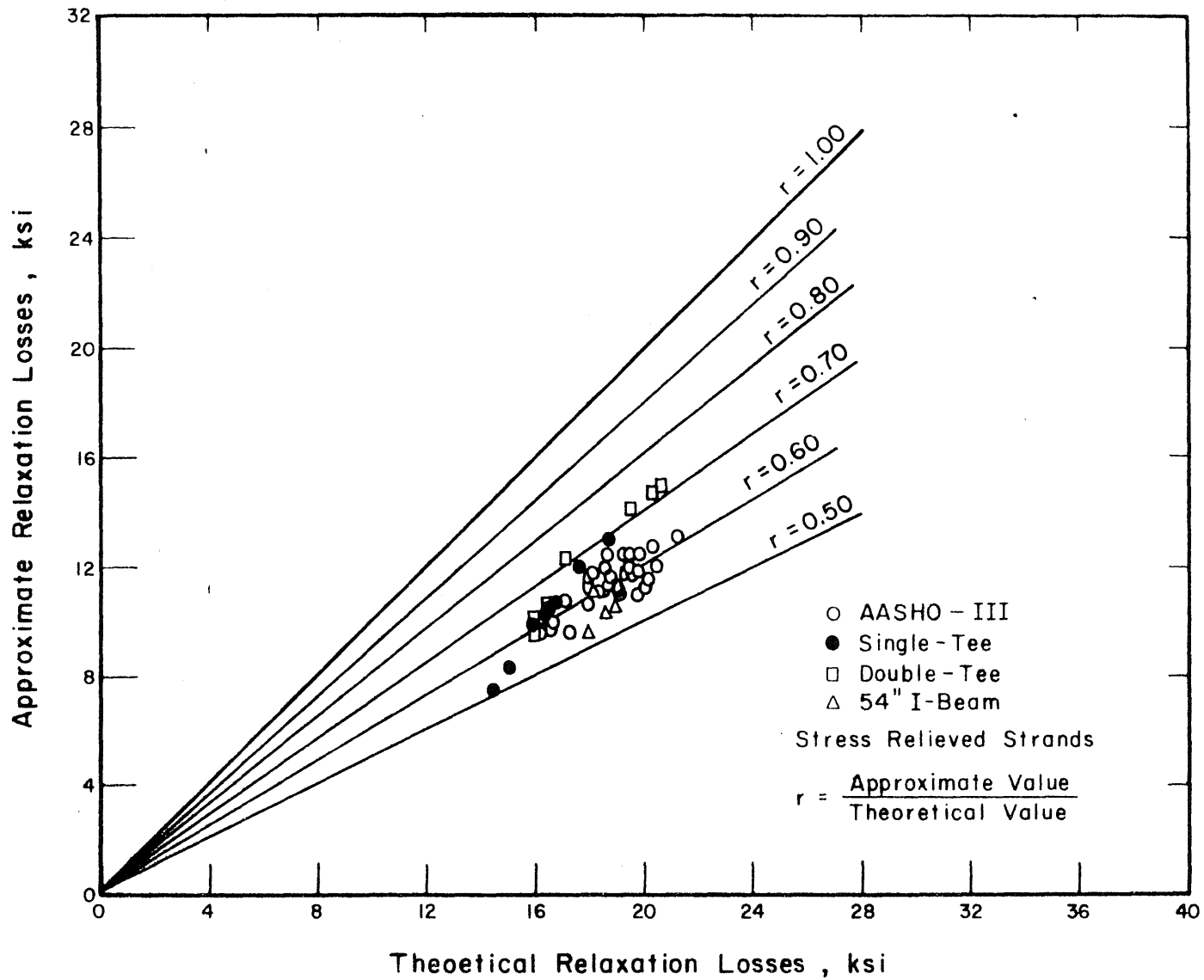


Fig. 5.3b Comparison of Relaxation Losses Calculated Using the 1973 AASHO Proposal and the Theoretical Values

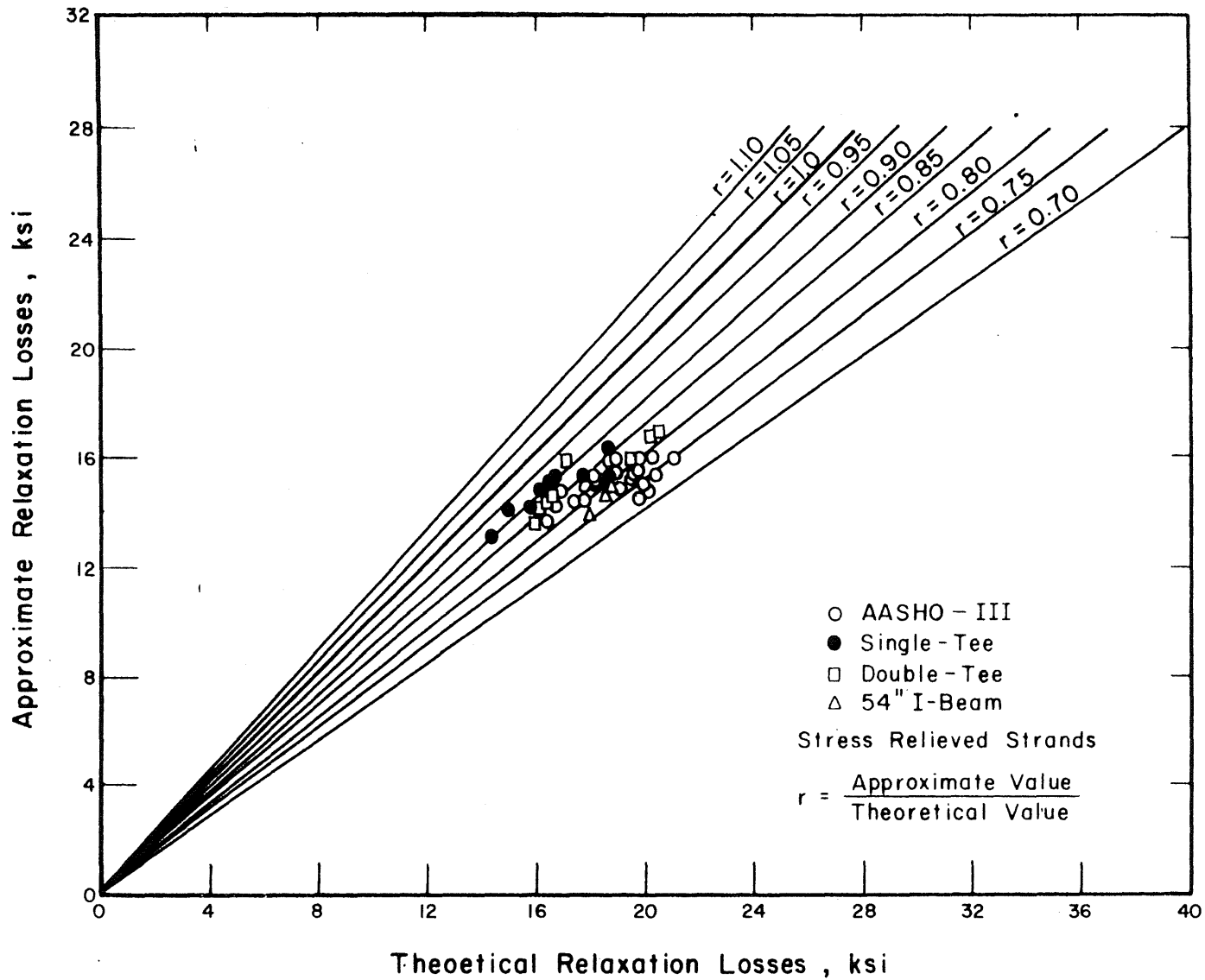


Fig. 5.3c Comparison of Relaxation Losses Calculated Using the 1970 AASHO Interim Specifications and the Theoretical Values

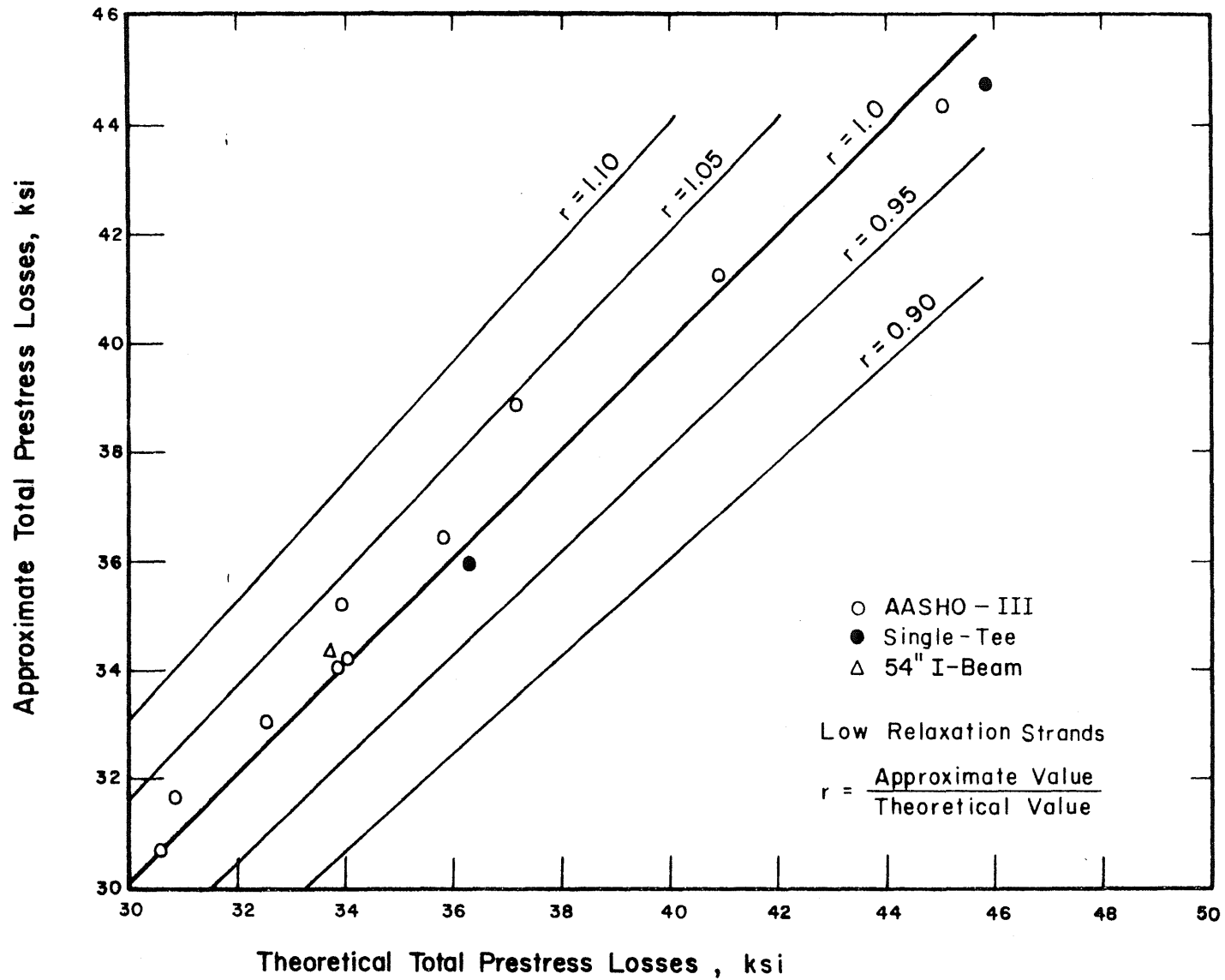


Fig. 5.4 Comparison of Total Prestress Losses Calculated Using the Proposed Set of Loss Factors and the Theoretical Values, Low-Relaxation Strands



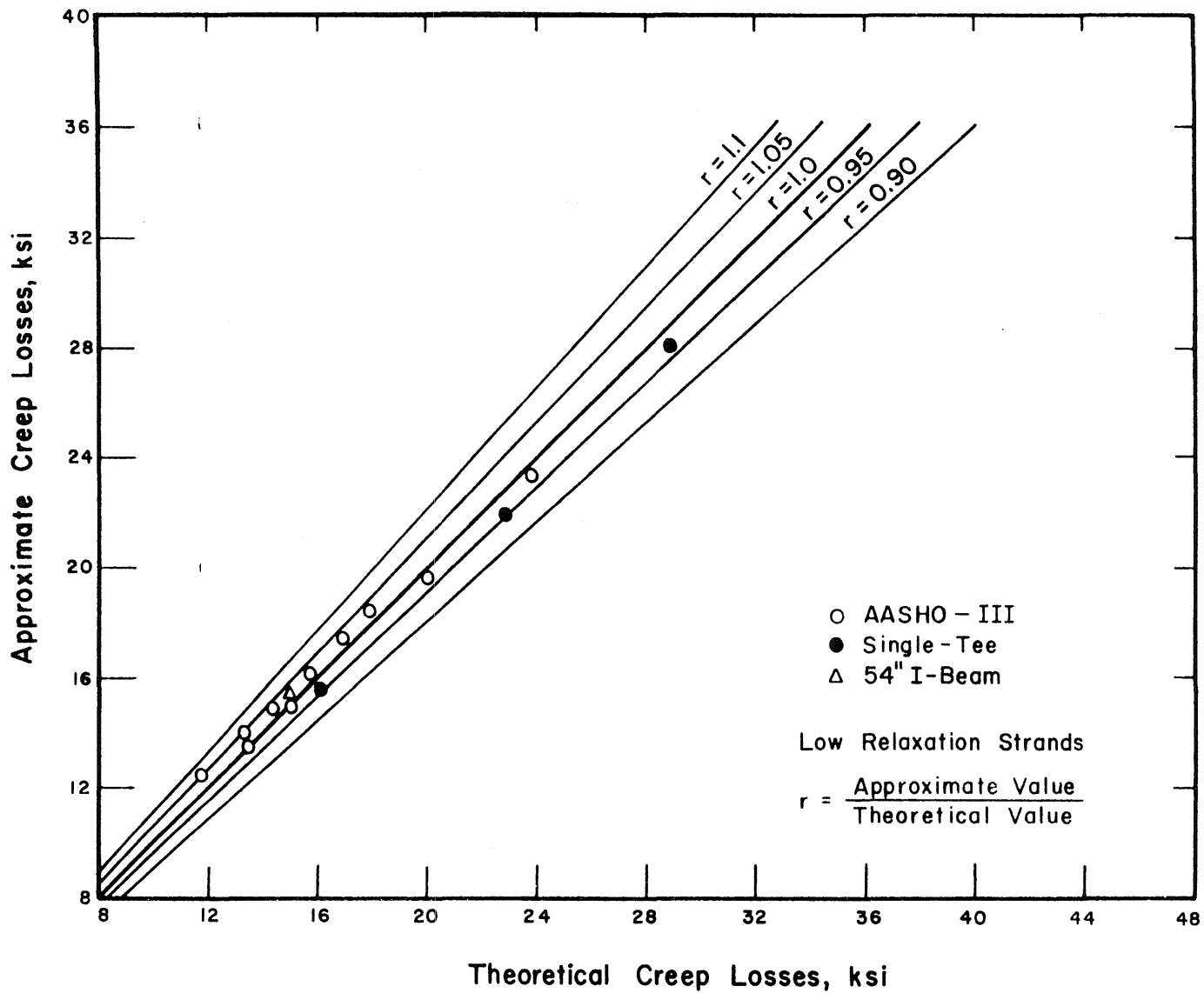


Fig. 5.5 Comparison of Creep Losses Calculated Using the Proposed Set of Loss Factors and the Theoretical Values, Low-Relaxation Strands

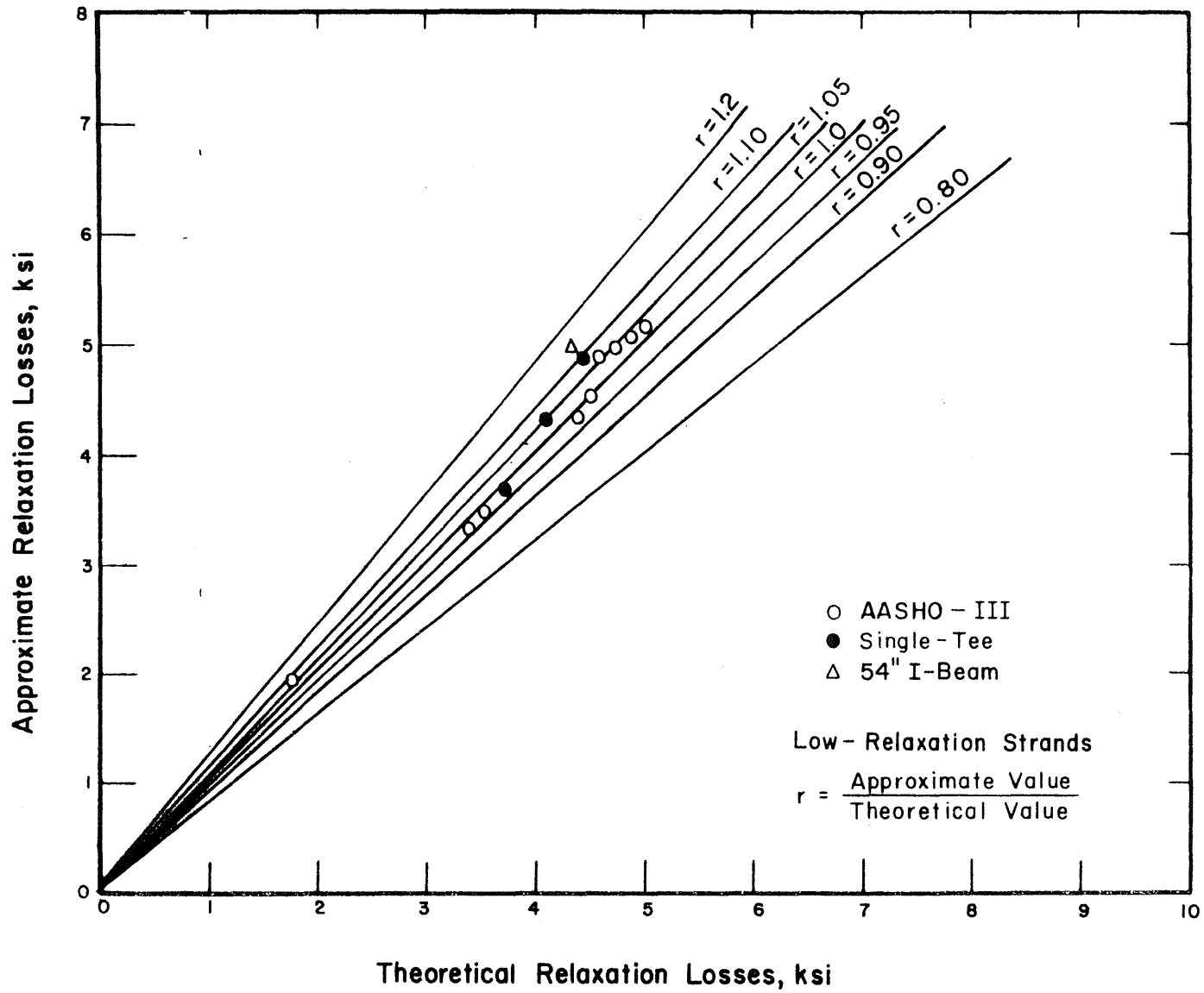


Fig. 5.6 Comparison of Relaxation Losses Calculated Using the Proposed Set of Loss Factors and the Theoretical Values, Low-Relaxation Strands

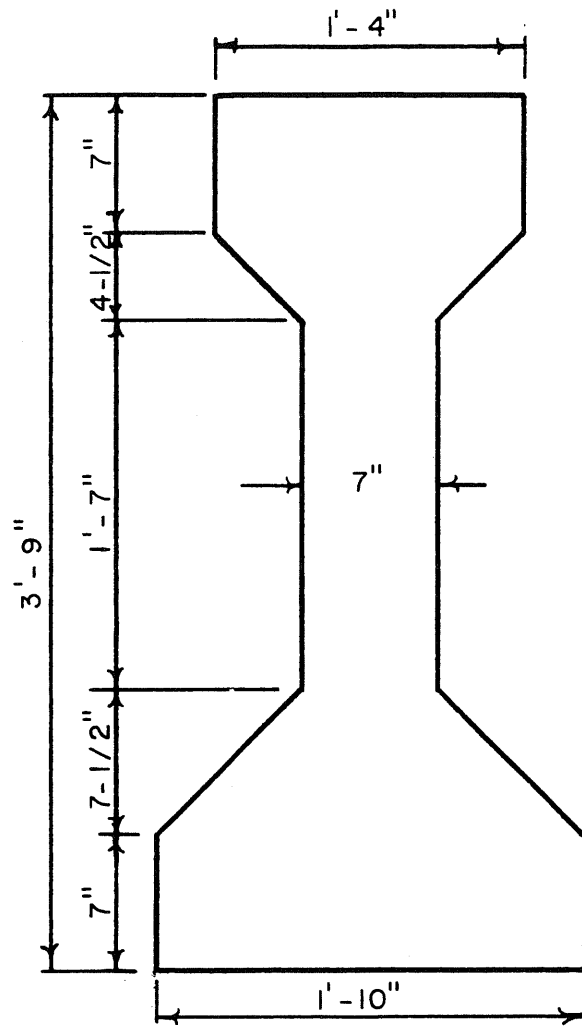
## APPENDIX A

## PRESTRESSED CONCRETE GIRDERS SELECTED IN THE STUDY

In this investigation typical precast prestressed concrete girders were selected for the study of the time-dependent prestress losses of composite and noncomposite prestress concrete girders.

In addition to the 42 and 48 in. Illinois standard girders used in the Douglas County, Jefferson County, and Champaign County bridges, four different types of sections were chosen for the analysis of simply supported prestressed girders.

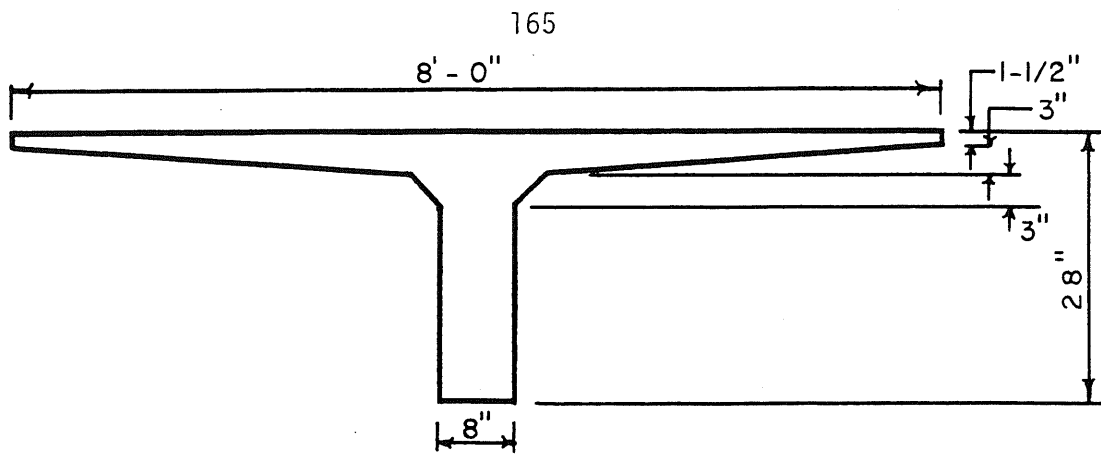
The additional girders considered were: AASHTO-Type III girder, a Single-Tee girder, Double-Tee girder, and an Illinois standard 54"-I beam. Cross sections properties of these girders, as well as spans used are given in Figs. A.1 to A.5. Area of prestressing steel and values of initial prestressing were taken as variables.



$$\begin{aligned}
 I &= 125390 \text{ in.}^4 \\
 A_c &= 560 \text{ in.}^2 \\
 e_{\text{end}} &= 10.27 \text{ in.} \\
 W_t &= 582 \text{ plf}
 \end{aligned}$$

$$\begin{aligned}
 h &= 45 \text{ in.} \\
 Y_b &= 20.27 \text{ in.} \\
 e_c &= 17.50 \text{ in.} \\
 \text{Span} &= 70 \text{ ft}
 \end{aligned}$$

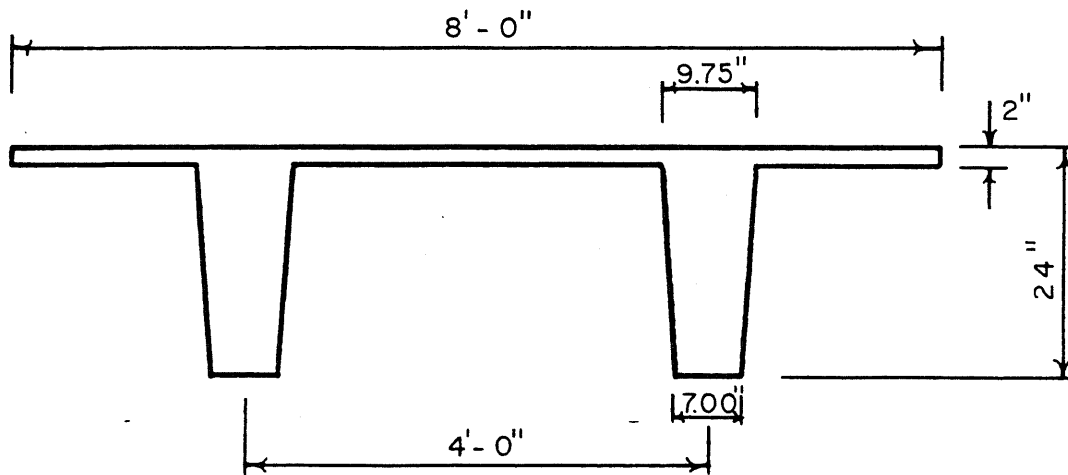
Fig. A.1 AASHTO-Type III Section



$I = 33649 \text{ in.}^4$   
 $A_c = 506 \text{ in.}^2$   
 $e_{\text{end}} = 7.46 \text{ in.}$   
 $W_t = 527 \text{ plf}$

$h = 28 \text{ in.}$   
 $Y_b = 20.79 \text{ in.}$   
 $e_c = 17.54 \text{ in.}$   
 $\text{Span} = 70 \text{ ft}$

Fig. A.2 Single-Tee Section--8ST28



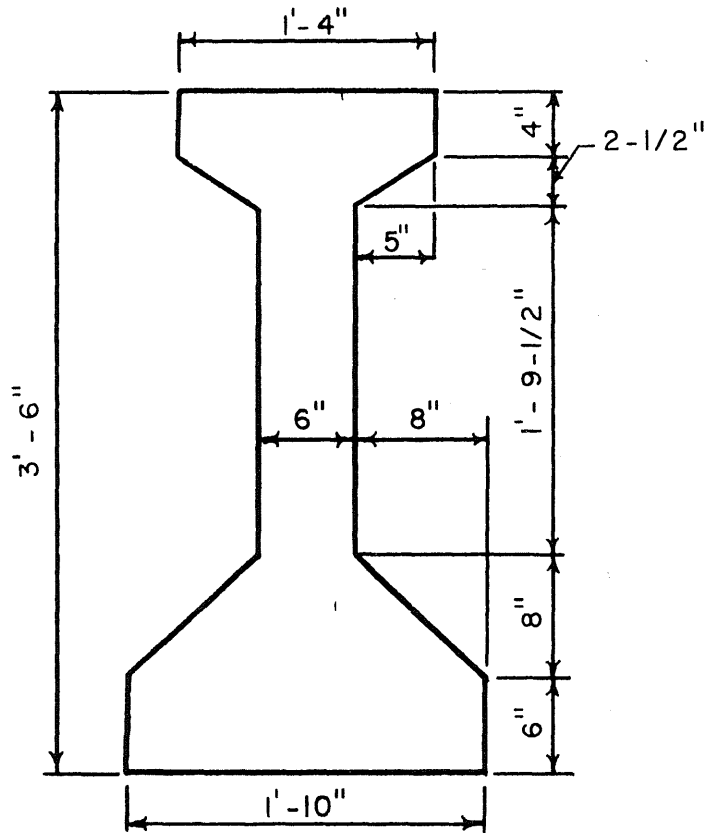
$I = 31192 \text{ in.}^4$   
 $A_c = 560 \text{ in.}^2$   
 $e_{\text{end}} = 6.51 \text{ in.}$   
 $W_t = 583 \text{ plf}$

$h = 24 \text{ in.}$   
 $Y_b = 15.51 \text{ in.}$   
 $e_c = 12.76 \text{ in.}$   
 $\text{Span} = 80 \text{ ft}$

Fig. A.3 Double-Tee Section--8DT24B

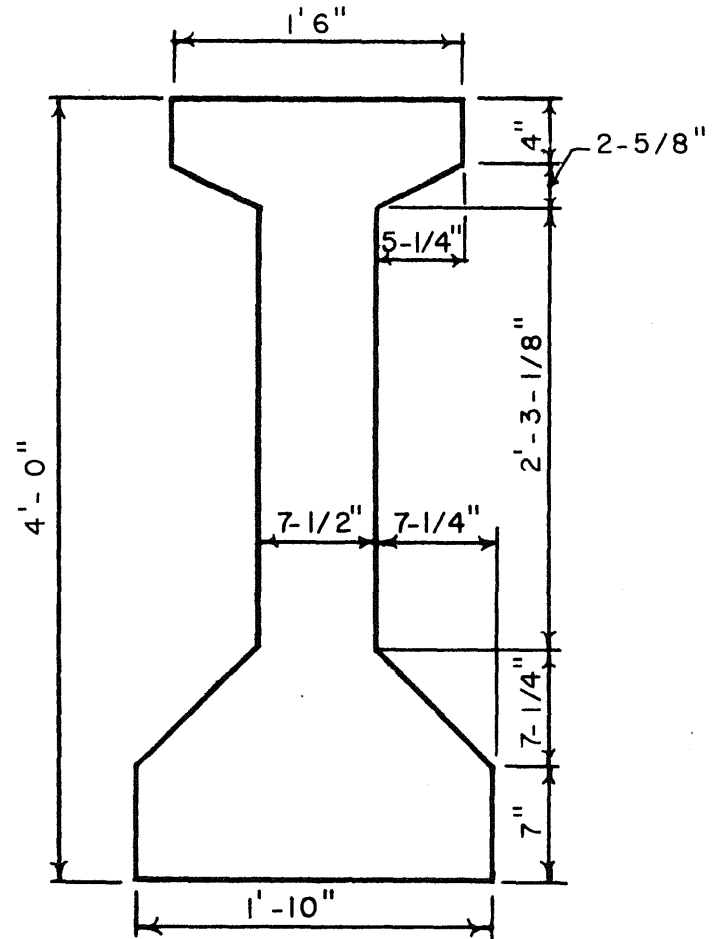
Douglas Co. And Jefferson Co. Girder

Champaign Co. Girder



$I = 90955.6 \text{ in.}^4$   
 $h = 42 \text{ in.}$   
 $A_c = 464.5 \text{ in.}^2$   
 $A_{st} = 2.613 \text{ in.}^2$   
 $W_t = 485 \text{ plf}$

$Y_b = 17.652 \text{ in.}$   
 $e_{end} = 3.15 \text{ in.}$   
 $e_c = 8.65 \text{ in.}$   
 $\text{Span} = 45.08 \text{ ft}$

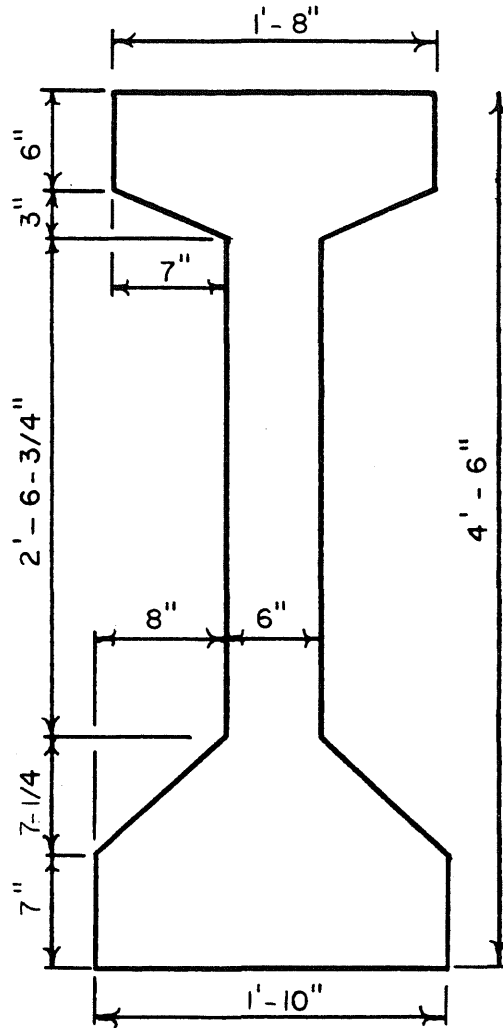


$I = 144117.1 \text{ in.}^4$   
 $h = 48 \text{ in.}$   
 $A_c = 569.8 \text{ in.}^2$   
 $A_{st} = 4.138 (4.356) \text{ in.}^2$   
 $W_t = 595 \text{ plf}$

$Y_b = 21.088 \text{ in.}$   
 $e_{end} = 6.94 (7.19) \text{ in.}$   
 $e_c = 16.14 (15.19) \text{ in.}$   
 $\text{Span} = 71.66 (71.16) \text{ ft}$

\* Numbers In ( ) Correspond To The Jefferson Co. Girder

Fig. A.4 Illinois Standard Cross Section for Precast Prestressed Concrete I-Beams, 42 and 48 in. Depths



$I = 213078 \text{ in.}^4$   
 $h = 54 \text{ in.}$   
 $A_c = 599 \text{ in.}$   
 $W_t = 624 \text{ plf}$

$Y_b = 24.97 \text{ in.}$   
 $e_{\text{end}} = 9.68 \text{ in.}$   
 $e_c = 17.91 \text{ in.}$   
 $\text{Span} = 92 \text{ ft}$

Fig. A.5 Illinois Standard 54 in.-I Beam

## APPENDIX B

## NOTATION

The nomenclature used in this work are defined where they first appear. A summary of the nomenclature used is given below:

$A_c$	area of beam concrete section
$A_{st}$	area of prestressing steel
$CR_c$	prestress losses due to creep of the concrete, in psi
$CR_s$	prestress losses due to relaxation of the steel, in psi
$D$	degree of hardening of the concrete at the moment of loading
$E_c$	Young's modulus of concrete at 28 days
$E_{ci}$	Young's modulus of concrete at the time of transfer of prestress
$E_{co}$	secant modulus of concrete at 28 days
$E_{st}$	Young's modulus of prestressing steel
$ES$	prestress losses due to elastic shortening of the concrete, in psi
$F$	influence of specimen size on shrinkage losses
$F_I$	influence of initial prestressing on relaxation losses (stress-relieved strands)
$F_{IL}$	influence of initial prestressing on relaxation losses (low-relaxation strands)



$F_R$	influence of steel yield stress on relaxation losses (stress-relieved strands)
$F_{RL}$	influence of steel yield stress on relaxation losses (low-relaxation strands)
$I$	moment of inertia of cross section of the beam concrete
$K$	influence of relative humidity and time of transfer of prestress on creep losses
$K_R$	influence of transfer of prestress on creep losses
$K_{RH}$	influence of relative humidity on creep losses
$K_b$	influence of composition of concrete mix on creep and shrinkage
$K_c$	influence of ambient relative humidity on creep
$K_d$	influence of age of the concrete at time of loading on creep
$K_e$	influence of specimen size on creep and shrinkage
$K_p$	influence of longitudinal reinforcement on shrinkage
$-K_t$	time-strain relationship for creep and shrinkage
$M_{DL}$	dead load moment of beam concrete
$P_i$	prestressing force just before transfer of prestress
$P_o$	prestressing force immediately after transfer of prestress
$R$	time from stressing to transfer, days

R.H.	ambient relative humidity, in percentage
SH	prestress losses due to shrinkage of the concrete, in psi
T°C	temperature in centigrades
T°F	temperature in fahrenheit
$d_m$	theoretical thickness of the member
e	eccentricity of prestressing strands
$e_c$	eccentricity of prestressing strands at midspan
$e_{end}$	eccentricity of prestressing strands at end of the span
$f_{cd}$	average concrete stress at the level of the center of gravity immediately after transfer of prestress and including the stress due to dead load of girder and deck
$f_{cds}$	change in concrete stress at the level of the center of gravity of the steel at the section considered due to dead load of the deck concrete and permanent formwork
$f_{cir}$	concrete stress at the level of the center of gravity of the prestressing steel immediately after transfer of prestress and including the stress due to dead load of girder
$f_{cr}$	average concrete stress at the level of the center of gravity of the prestressing steel immediately after transfer of prestress and including the stress due to dead load of girder
$f_s$	steel stress at time t

$f_{si}$	initial steel stress immediately after stressing
$f_y$	steel stress at an off-set strain of 0.001
$n$	$\frac{E_{st}}{E_c}$ , modular ratio
$p$	$\frac{A_{st}}{A_c}$ , percentage of longitudinal reinforcement
$r$	ratio of approximate to theoretical values
$t$	time after application of load
$y_b$	distance from bottom fiber to center of gravity of the section
$\Delta f_s$	total estimated prestress losses, in psi
$\Delta t$	number of days during which hardening has taken place at T°C
$\phi_t$	creep coefficient
$\epsilon_c$	influence of relative humidity on shrinkage
$\epsilon_{cr}(t)$	creep strain of concrete at time t
$\epsilon_{co}$	instantaneous elastic strain of the concrete due to the application of load at time $t_0$
$\epsilon_{sh}(t)$	shrinkage strain of concrete at time t
$\sigma_{co}$	constant stress the concrete is subjected to at time $t_0$

